

UNIVERSITE LOUIS PASTEUR
ECOLE DOCTORALE DES SCIENCES DE LA VIE ET DE LA SANTE

THESE

Présentée pour obtenir le grade de

DOCTEUR DE L'UNIVERSITE LOUIS PASTEUR – STRASBOURG I

Discipline : Sciences du Vivant – Aspects Moléculaires et Cellulaires de la Biologie

Spécialité : Immunologie

Par

Sébastien WIECKOWSKI

Synthetic CD40L mimetics: biological effects and potential applications in immunotherapy

Directeur de Thèse Prof. Dr. Sylvie FOURNEL
Co-directeur de Thèse Dr. Gilles GUICHARD

Soutenue publiquement le 30 mai 2007

Membres du jury :

Rapporteur interne	Prof. Dr. Jean-Louis PASQUALI
Rapporteur externe	Dr. Hugues LORTAT-JACOB
Rapporteur externe	Prof. Dr. Winfried WELS
Examineur	Dr. Jean-Yves BONNEFOY
Invité	Dr. Sylviane MULLER

Remerciements

Je tiens ici à exprimer ma sincère reconnaissance à toutes les personnes qui ont contribué à ce travail de thèse, réalisé au Laboratoire d'Immunologie et Chimie Thérapeutiques (UPR 9021).

Je remercie les membres de mon jury, le Professeur Jean-Louis Pasquali (Université de Strasbourg, Hôpital Civil), le Docteur Hugues Lortat-Jacob (Institut de Biologie Structurale, Grenoble), ainsi que le Docteur Jean-Yves Bonnefoy (Transgene, Strasbourg), d'avoir accepté de juger mon travail.

I am grateful to Professor Winfried Wels (Georg-Speyer-Haus, Frankfurt am Main) for accepting to evaluate this work.

Je remercie le Docteur Sylviane Muller, directrice de l'UPR 9021, de m'avoir accueilli dans son unité et d'avoir accepté de participer à mon jury.

Je tiens à exprimer mes remerciements au Professeur Sylvie Fournel, ma directrice de thèse, qui m'a supervisé avec beaucoup d'optimisme. Son enthousiasme pour la recherche, son appui constant et sa grande disponibilité m'ont apporté les meilleures conditions possible pour accomplir ce travail. Sylvie, tu as su me faire confiance, me donner beaucoup de liberté dans ce projet et me recadrer lorsque c'était nécessaire.

Je remercie le Docteur Gilles Guichard, mon co-directeur de thèse, de m'avoir continuellement motivé durant mon doctorat. Gilles, merci pour ta rigueur et ta précision qui m'ont beaucoup apporté.

Je remercie le Docteur Nathalie Trouche, sans qui le projet n'aurait pas été ce qu'il est.

Un grand merci au Docteur Johan Hoebcke, pour m'avoir initié à la résonance plasmonique de surface, mais aussi pour m'avoir montré sa vision de la recherche.

J'ai une pensée particulière pour mes anciens maîtres de stage, en particulier le Docteur Robert Feil grâce à qui tout a réellement commencé.

Merci à tous les collègues actuels et anciens de l'ICT pour leur gentillesse, leurs encouragements et leur aide. Travailler à vos côtés fut un réel plaisir. Un merci particulier à Hayet, Sara, Sylvie « CpG », Jürgen et Pierre.

Special thanks to Julien Beyrath for his careful reading of the manuscript.

Merci à toutes les personnes qui ont été impliquées dans ce projet, en particulier à Alberto Bianco, Olivier Chaloin et Hélène Dumortier.

Je remercie le Ministère de l'Éducation Nationale, de l'Enseignement Supérieur et de la Recherche, ainsi que la Fondation pour la Recherche Médicale pour leur support financier.

Je remercie ma famille, en particulier mes parents et ma p'tite frangine Steph, pour leur soutien sans faille. Maman, Papa, merci d'avoir cru en moi et de m'avoir aidé de tout votre possible dans mes projets. Je vous en serai éternellement reconnaissant.

Je termine ces remerciements en exprimant toute mon estime à ma compagne Béatrice, qui a su me soutenir au quotidien et supporter mes quelques variations d'humeur... Merci Béa pour avoir partagé avec moi tous les mauvais et surtout les bons moments durant ces années, et pour m'avoir continuellement encouragé. Je n'oublierai jamais combien tu t'es investie dans tout cela. Cette thèse est aussi un peu la tienne.

List of Headings

Abbreviations	vii
List of Figures.....	viii
List of Tables.....	ix

INTRODUCTION	1
---------------------------	----------

CHAPTER 1

BIOLOGICAL OUTCOMES OF THE CD40–CD40L INTERACTION

1.1 Discovery of CD40 (also named CDw40 and Bp50)	4
1.1.1 Identification of CD40	4
1.1.2 Cellular expression of CD40	4
1.2 Discovery of CD40–ligand (also named CD40L, CD154, gp39 and T-BAM)	6
1.2.1 Cloning of CD40L.....	6
1.2.2 Cellular expression of CD40L.....	7
1.3 Other proteins interact with CD40	9
1.4 CD40L binds to other receptors	9
1.5 Level of CD40 crosslinking is important for activation of biological responses.....	10
1.5.1 Engagement of CD40 with anti-CD40 Ab	10
1.5.2 Engagement of CD40 with CD40L	11
1.6 CD40 plays a central role in immune response	12
1.6.1 Discovery of the X–linked hyper IgM syndrome	12
1.6.2 Role of CD40 in B lymphocytes	12
1.6.2.1 <i>Effect of anti-CD40 mAb on B cell proliferation</i>	13
1.6.2.2 <i>CD40 engagement and B cell activation</i>	13
1.6.2.3 <i>CD40 is important for isotype switching</i>	14
1.6.2.4 <i>CD40 is important for rescue from apoptosis of mature B lymphocytes</i>	16
1.6.3 Role of CD40 in other immune cells.....	16
1.7 Function of CD40 in malignant cells.....	17

CHAPTER 2

CD40 AND CD40L: GENES AND PROTEINS

2.1 Characteristics of the CD40 protein sequence	19
2.1.1 The human sequence	19
2.1.2 The mouse sequence	20

List of Headings

2.2 Regulation of CD40 expression	21
2.2.1 Organization of the <i>CD40</i> gene	21
2.2.1.1 <i>The mouse gene</i>	21
2.2.1.2 <i>The human gene</i>	21
2.2.2 Transcriptional regulation of <i>CD40</i> expression.....	22
2.2.3 Post-transcriptional regulation of <i>CD40</i> expression	23
2.2.3.1 <i>Alternative splicing of the CD40 mRNA</i>	23
2.2.3.2 <i>Stability of the CD40 mRNA</i>	24
2.2.4 Post-translational regulation of CD40 expression	25
2.3 Characteristics of the CD40L protein sequence	26
2.3.1 The mouse sequence	26
2.3.2 The human sequence	27
2.4 Regulation of CD40L expression	28
2.4.1 Organization of the <i>CD40L</i> gene	28
2.4.2 Transcriptional regulation of <i>CD40L</i> expression	28
2.4.3 Post-transcriptional regulation of <i>CD40L</i> expression	30
2.4.4 Post-translational regulation of CD40L expression.....	30
2.5 Three-dimensional view of the CD40–CD40L interaction	32
2.5.1 The TNF/TNF-R superfamily	32
2.5.2 The TNF family proteins.....	36
2.5.3 The TNF-R family proteins.....	37
2.5.4 The three-dimensional structure of CD40L.....	39
2.5.5 Three-dimensional model of the CD40–CD40L interaction	40
2.5.5.1 <i>A three-dimensional model for CD40</i>	40
2.5.5.2 <i>Residues important for the CD40–CD40L interaction</i>	41
2.5.5.3 <i>Construction of a CD40–CD40L interaction model</i>	42
2.5.6 Usefulness of the three-dimensional model of the CD40–CD40L interaction.....	45

CHAPTER 3

CELL SIGNALING INITIATED FROM CD40

3.1 CD40 clustering and downstream signaling	46
3.1.1 Consequences of membrane receptor crosslinking in cell signaling	46
3.1.2 Minimal CD40 oligomerization requirement for activation of cell signaling	46
3.1.2.1 <i>Extracellular oligomerization</i>	46
3.1.2.2 <i>Intracellular oligomerization</i>	47
3.1.3 Structural mechanisms governing initiation of intracellular signals.....	48
3.2 Role of pre-ligand binding assembly domain in CD40	49
3.2.1 The PLAD domain	49

List of Headings

3.2.2 PLAD requirement for CD40 signaling.....	50
3.3 CD40 signaling is initiated within membrane rafts	51
3.3.1 Membrane rafts	51
3.3.2 CD40 is localized into lipid raft microdomains.....	52
3.3.3 Caveolae are implicated in CD40 signaling	52
3.3.4 Translocation of CD40 into lipid rafts	53
3.4 CD40–induced cell signaling	54
3.4.1 CD40–activated signaling pathways	54
3.4.1.1 Intermediates implicated in CD40 signaling.....	54
3.4.1.2 Common signaling pathways activated by CD40	55
3.4.2 Implication of TRAF adaptor molecules.....	56
3.4.2.1 CD40 signals through adaptor molecules.....	56
3.4.2.2 The TNF-R–associated factors	56
3.4.2.2.1 The TRAF family	56
3.4.2.2.2 TRAFs are located into lipid rafts	57
3.4.2.2.3 Regulation of TRAF functions.....	57
3.4.2.2.4 TRAF protein structure	58
3.4.2.3 The TRAF–CD40 interaction.....	59
3.4.2.3.1 TRAF–binding sites.....	59
3.4.2.3.2 CD40–mediated activation of TRAFs	60
3.4.2.3.3 The TRAF–CD40 interaction viewed at the three-dimensional level	61
3.4.2.4 TRAF–specific signaling	62
3.4.2.4.1 TRAF1	62
3.4.2.4.2 TRAF2.....	63
3.4.2.4.3 TRAF3	63
3.4.2.4.4 TRAF4	64
3.4.2.4.5 TRAF5.....	65
3.4.2.4.6 TRAF6.....	65
3.4.3 TRAF–independent CD40 signaling	66
Poster 1: summary of the signaling pathways engaged by CD40	67

CHAPTER 4

THE CD40–CD40L INTERACTION AS A TARGET FOR IMMUNOTHERAPY

4.1 Blockade of the CD40–CD40L interaction	70
4.1.1 CD40-based treatment of autoimmune diseases	71
4.1.1.1 Systemic Lupus Erythematosus.....	72
4.1.1.2 An anti-CD40L therapy for other autoimmune diseases?.....	74
4.1.2 Chronic inflammation	75
4.1.3 Transplantation	76
4.2 Boosting the immune response by activation of the CD40 signaling.....	77
4.2.1 Hyper-IgM syndrome and immunodeficiencies.....	77
4.2.2 Infections.....	78
4.2.3 Vaccination.....	80

List of Headings

4.2.4 Cancer	82
CHAPTER 5	85
C3-SYMMETRIC PEPTIDE SCAFFOLDS ARE FUNCTIONAL MIMETICS OF TRIMERIC CD40L <i>Nat Chem Biol 1, 377-382 (2005)</i> Fournel, S., Wieckowski, S. , Sun, W., Trouche, N., Dumortier, H., Bianco, A., Chaloin, O., Habib, M., Peter, J. C., Schneider, P., Vray, B., Toes, R. E., Offringa, R., Melief, C. J., Hoebeke, J., and Guichard, G.	
CHAPTER 6	109
SOLID-PHASE SYNTHESIS OF CD40L MIMETICS <i>Org Biomol Chem 4, 1461-1463 (2006)</i> Bianco, A., Fournel, S., Wieckowski, S. , Hoebeke, J., and Guichard, G.	
CHAPTER 7	119
SMALL TRIVALENT ARCHITECTURES MIMICKING HOMOTRIMERS OF THE TNF SUPERFAMILY MEMBER CD40L: DELINEATING THE RELATIONSHIP BETWEEN STRUCTURE AND EFFECTOR FUNCTION <i>(submitted to JACS)</i> Sun, W., Wieckowski, S. , Trouche, N., Chaloin, O., Briand, J.-P., Hoebeke, J., Fournel, S., and Guichard, G.	
CHAPTER 8	156
COOPERATIVITY IN THE INTERACTION OF SYNTHETIC CD40L MIMETICS WITH CD40 AND ITS IMPLICATION IN CELL SIGNALING <i>Biochemistry 46, 3482-3493 (2007)</i> Wieckowski, S. , Trouche, N., Chaloin, O., Guichard, G., Fournel, S., and Hoebeke, J.	
CHAPTER 9	177
CELL-SPECIFIC SIGNALING INDUCED BY SYNTHETIC CD40L MIMETICS IN MALIGNANT AND NORMAL CELLS <i>(in preparation)</i> Wieckowski, S. , Trouche, N., Guichard, G., and Fournel, S.	
CHAPTER 10	214
SMALL MOLECULE CD40L MIMETICS PROMOTE CONTROL OF PARASITEMIA AND ENHANCE T CELLS PRODUCING INTERFERON-γ DURING EXPERIMENTAL TRYPANOSOMA CRUZI INFECTION[†] <i>J Immunol 178, 6700-6704 (2007)</i> Habib, M., Rivas, M. N., Chamekh, M., Wieckowski, S. , Sun, W., Bianco, A., Trouche, N., Chaloin, O., Dumortier, H., Goldman, M., Guichard, G., Fournel, S., and Vray, B. [[†] collaboration]	
CONCLUSION AND PERSPECTIVES	220

Abbreviations

Ab	antibody	MEK	MAPK/ERK kinase
ADP	adenosine diphosphate	MHC	major histocompatibility complex
Ag	antigen	mini-CD40L	small synthetic CD40L mimetic
APC	antigen-presenting cells	mRNA	messenger RNA
ASM	acid sphingomyelinase	MW	molecular weight
bp	base pair	NF-AT	nuclear factor of activated T cells
BCR	B cell receptor	NF-κB	nuclear factor κB
C₃	three-fold axial	NIK	NF-κB-inducing kinase
C4BPα	alpha chain of C4b binding protein	N-ter	N-terminus
cAMP	cyclic adenosine monophosphate	ODN	oligodeoxynucleotide
CD40-B	anti-CD40-activated B cells	OmpC	outer membrane protein C
CD40-Ig	recombinant human CD40 coupled to human IgG1 Fc domain	PDB	Protein Data Bank
CRD	cysteine-rich domain	PHA	phyto-hemagglutinin
C-ter	C-terminus	PI	phosphoinositide
Da	Dalton	PI3K	phosphatidyl inositol-3 kinase
DC	dendritic cell	PKC	protein kinase C
DISC	death-inducing signaling complex	PLAD	pre-ligand binding assembly domain
dsDNA	double-strand DNA	PLCγ2	phospholipase Cy2
EC	extracellular	PMA	phorbol 12-myristate 13-acetate [also named 12-O-tetradecanoyl phorbol-13-acetate (TPA)]
EGR-1	early growth response-1	PBMC	peripheral blood mononuclear cells
EMSA	electrophoretic mobility shift assay	PNA	peptide nucleic acid
ERK	extracellular signal-regulated kinase	PTEN	phosphatase and tensin homolog deleted on chromosome 10
F(ab')₂	two Fab units linked by disulfide bridges	sCD40L	soluble CD40L
Fab	fragment antigen binding	scFv	single chain fragment variable
Fc	fragment crystallizable	SDS-PAGE	sodium dodecyl sulfate-polyacrylamide gel electrophoresis
GAS	gamma activated sequences	siIgM	surface IgM
GC	germinal center	SLE	systemic lupus erythematosus
HIGM	X-linked hyper IgM	SPR	surface plasmon resonance
HSP70	unrelated 70-kDa mycobacterial heat shock protein	STAT	signal transducer and activator of transcription
IC	intracytoplasmic	TACE	metalloprotease-disintegrin
IFN	interferon	T-BAM	T cell-B cell activating molecule
Ig	immunoglobulin	T_c	T cytotoxic
IκB	inhibitor of κB	TCR	T-cell receptor
IKK	IκB kinase	TGF	tumor growth factor
IL	interleukin	T_H	T helper
IP₃	inositol (1,4,5)-triphosphate	TM	transmembrane
IS	immune system	TNF	tumor necrosis factor
JAK3	Janus kinase 3	TNF-R	tumor necrosis factor receptor
kb	kilobase	TRAF	TNF-R-associated factor
LMP1	latent membrane protein 1	T_{reg}	regulatory T cells
LPS	lipopolysaccharide	UTR	untranslated region
LT	lymphotoxin		
mAb	monoclonal antibody		
MAPK	mitogen activated protein kinase		

List of Figures

Figure	Title	Page
Figure A	Design of mini-CD40Ls	3
Figure 1	Nucleic acid and predicted protein sequences of human CD40	19
Figure 2	Alignment of the protein sequences of mouse and human CD40	20
Figure 3	Organization of the mouse <i>CD40</i> gene	21
Figure 4	Organization of the human <i>CD40</i> gene	22
Figure 5	Potential putative cis-regulatory elements located within the human <i>CD40</i> gene promoter	23
Figure 6	Alternative splicing variants of the mouse <i>CD40</i> mRNA	24
Figure 7	Alignment of the protein sequences of human and mouse CD40L	27
Figure 8	Organization of the human <i>CD40L</i> gene	28
Figure 9	Putative cis-regulatory elements located within the human and mouse <i>CD40L</i> promoters	29
Figure 10	Interaction network between proteins of the TNF and TNF-R families	33
Figure 11	Structure of the TNF homology domain of human CD40L	36
Figure 12	Topology of the TNF homology domain of human CD40L	37
Figure 13	Three-dimensional structure of human TNF-R1	38
Figure 14	Structure of human CD40L	40
Figure 15	Three-dimensional model of human CD40	41
Figure 16	Residues implicated in the CD40–CD40L interaction	43
Figure 17	Residues involved in stabilization of the CD40–CD40L interaction	44
Figure 18	Summary of the residues implicated in the CD40–CD40L interaction	45
Figure 19	Implication of PLAD in TNF-R and CD40 signaling	50
Figure 20	CD40 reorganization into rafts is dependent on ASM	53
Figure 21	The TRAF family members	58
Figure 22	Three-dimensional structure of the human TRAF2's TRAF domain	59
Figure 23	Three-dimensional structure of the TRAF-C domain of human TRAF6 complexed with a peptide derived from the CD40 intracytoplasmic domain	61
Figure 24	Three-dimensional model of the TRAF2–CD40 interaction	62
Figure 25	JAK and TRAF binding motifs on the intracytoplasmic sequence of CD40	66
Figure 26	CD40L controls immune cell functions and inflammatory reaction	71
Figure 27	Molecular defects leading to hyper-IgM syndromes	78
Figure 28	CD40 Troy and Vaccibody	81

List of Tables

Table	Title	Page
Table 1	List of other CD40-expressing cells	5
Table 2	List of other CD40L-expressing cells	8
Table 3	General data on the TNF/TNF-R superfamily members	34
Table 4	Summary of phase 1 anti-CD40-targeted therapy studies	83

INTRODUCTION

INTRODUCTION

I.1 Overview of the immune system

The immune system (IS) is the defense system of our organism. It fights against pathogenic microorganisms and cancer, implying a broad range of cells and molecules that act in concert to eliminate or neutralize foreign agents. This process of immunity may be viewed as three subsequent steps: specific recognition of the disturbing agent, mounting of an effector response against it and generation of a memory response for long-term protection against the foreign organism or substance.

In vertebrates, two kinds of protection act in cooperation. Innate immunity constitutes the first line of defense against pathogens, and is provided by physical, chemical and cellular components. Adaptive immunity is characterized by three properties: specificity, diversity, and memory. Specificity is provided by antibodies (Ab) and T-cell receptors (TCR) that first interact with the antigen (Ag), directly or in the context of major histocompatibility complex (MHC), respectively. Exogenous antigens are internalized by antigen-presenting cells (APC) represented by dendritic cells (DCs), macrophages and B lymphocytes, processed and presented to CD4⁺ T helper (T_H) lymphocytes via class II MHC. Endogenous antigens are degraded in the cytosol of nucleated cells and presented to CD8⁺ cytotoxic T (T_C) lymphocytes via class I MHC. Crosstalk between the two modes of presentation has also been described. Nevertheless, interaction of T lymphocytes with Ag leads to their activation. Activated T_H cells secrete cytokines and express costimulatory molecules that regulate the overall IS, and activated T_C cells initiate cytotoxic response.

Mounting of immune response necessitates different specialized organs and tissues for selection, development and maturation of leucocytes (the primary lymphoid organs thymus and bone marrow), and their activation by Ag (secondary lymphoid organs including lymph nodes and spleen). Furthermore, it involves specialized cells including natural killer cells, phagocytic cells as neutrophils, and non-phagocytic as basophils and mast cells. Finally, the Ag is brought by APC from distant sites to secondary lymphoid organs via lymphatic system, and presented to T and B cells. Activated T and B cells and their products (cytokines and Ab) are then released into the circulation. The inflammatory process gathers all components of the IS to the site of infection. In some circumstances, parts of the IS may be defective, leading to inefficient protection against pathogens and cancer. Inversely, the IS may attack self-components of the organism if not properly controlled.

INTRODUCTION

I.2 The CD40–CD40L interaction

The CD40–CD40L interaction was shown to play a central role in development of both humoral and cellular immune responses. In fact, CD40–CD40L controls proliferation of B lymphocytes, production of Ab, isotype switching, germinal centers formation and generation of B memory response. Moreover, CD40 triggering on DCs activates them, leading to upregulation of costimulatory and MHC molecules, enhanced production of IL-12 cytokine, and efficient presentation of Ag to T lymphocytes (chapter 1).

CD40 belongs to the tumor necrosis factor (TNF)-receptor (TNF-R) family (chapter 2), and is constitutively expressed on B lymphocytes, dendritic cells and monocytes/macrophages. CD40L belongs to the TNF family, and is mainly expressed transiently on activated T lymphocytes. Proteins from the TNF-R/TNF superfamily assemble in a three-fold axial (C_3) symmetry, forming hexavalent complexes that are important for transduction of intracellular cell signaling (chapter 3).

Importance of the CD40–CD40L duet during immune responses has led many groups to use antibodies directed against these molecules as therapeutics, to either inhibit or activate the IS. For example, many authors have described that CD40 activation might lead to an enhanced anti-tumor immune response implying DCs. Furthermore, some data have demonstrated that triggering of the CD40 molecule expressed on tumor cells induces a direct inhibition of their proliferation, and sensitizes them to apoptosis. All these observations suggest that targeting of the CD40–CD40L interaction might be highly important for immunotherapy in diverse diseases (chapter 4).

I.3 The mini-CD40Ls

Research on synthetic multivalent molecules that could act as ligands in complex biological systems is an innovating field in medicinal chemistry. For example, dimeric peptides and small organic molecules have been shown to bind on and activate dimeric cytokine receptors.

On the basis of crystallographic data and directed mutagenesis experiments, we have developed fully synthetic molecules named mini-CD40Ls that mimic biological functions of homotrimeric CD40L. These molecules were built on synthetic C_3 platforms linked to

INTRODUCTION

residues essential for the interaction with CD40 via spacer arms of optimized length (Figure A).^a

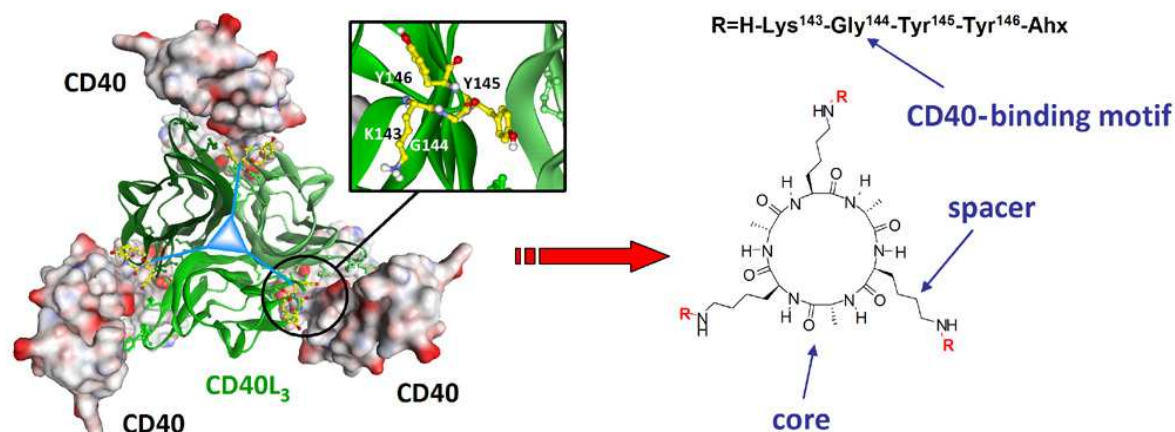


Figure A. Design of mini-CD40Ls. Small synthetic CD40L mimetics were constructed on the basis of known crystallographic data and directed mutagenesis studies (left). Residues important for the CD40–CD40L interaction (indicated in the inset) were used as CD40–binding motif, linked to a C₃ symmetric platform via spacer arms (right).

Data obtained with mini-CD40Ls in various molecular and cellular systems suggested for the first time that small synthetic molecules could act as functional CD40L mimetics (chapters 5 and 6). A complete structure–activity study was performed on mini-CD40Ls by varying the core structure, the spacer length and the CD40–binding peptide. We got detailed informations on their mechanisms of action and were able to optimize them (chapter 7). In particular, we found an interesting mini-CD40L mutant that has lost its cooperative effect in the interaction with CD40. Data obtained with mini-CD40Ls suggested that binding properties to CD40 are important for the biological effects (chapter 8). We then used mini-CD40Ls as valuable tool to dissect complex signaling pathways activated by CD40 in different cell systems (chapter 9). Finally, in collaboration with a team from Brussels, we demonstrated the application of our mini-CD40Ls in a murine model of experimental infection with *Trypanosoma cruzi*. Results demonstrated that mini-CD40Ls can induce an efficient T immune response *in vivo* (chapter 10).

^a Guichard G, Fournel S, Bianco A, Hoebeke J, Muller S. Nouvelles molécules multimériques : leur procédé de préparation et leur utilisation pour la préparation de médicaments. Brevet français 02/06631, déposant CNRS 2002-05-30; PCT/FR03/01613 2003-05-28; European Application Number 03756015.8, filed 2003-05-28.

Guichard G, Fournel S, Hoebeke J, Wieckowski S. New Multimeric Molecules, their preparation process and their use for the preparation of drugs. Brevet Français 04/13331, déposant CNRS 2004-12-15; U.S. Patent Application Number 60/525124, filed 2003-11-28.

Guichard G, Fournel S, Chaloin O, Trouche N, Wieckowski S, Hoebeke J. Novel multimeric CD40 ligands, method for preparing same and use thereof for preparing drugs. French Patent FR2879202, published 2006-06-16. International Publication Number WO002006064133 (2006-06-22).

CHAPTER 1

BIOLOGICAL OUTCOMES OF THE CD40–CD40L INTERACTION

CHAPTER 1

1.1 Discovery of CD40 (also named CDw40 and Bp50)

1.1.1 Identification of CD40

CD40 was first described by Koho and Paulie in 1984 when, in search for antibodies directed against the human urinary bladder carcinoma, they obtained an interesting hybridoma named S2C6, from which antibody showed not only a high specificity for the neoplastic urothelium, but also for B cell-derived malignant and transformed lymphocytes.¹ B cells, but not other normal cells, were stained with this monoclonal antibody (mAb), as seen by immunofluorescence. Immunoprecipitation experiments on protein extracts from the Burkitt's lymphoma cell line Raji have identified a unique Ag named Bp50, with a molecular weight (MW) of approximately 50 kDa.²

Human erythrocytes rosette-negative tonsil lymphocytes were also used as immunogen for the generation of another mAb directed against CD40 named G28-5.³ This antibody showed cellular reactivity similar to S2C6. That is why the Third International Workshop has formed a cluster group and designated the 50,000 Dalton Ag Bp50 as CDw40 in 1986, and three years later CD40.

1.1.2 Cellular expression of CD40

To get better insights on the specificity of the anti-CD40 mAb, Paulie and co-workers tested its reactivity against various cell lines of hematopoietic origin and various leukemia cells, and showed a complete restriction to B lineage cells, including many malignant B cells, and normal tonsil and spleen B lymphocytes.⁴ CD40 was initially detected on Bp35⁺ (CD20⁺) B cells in blood and tonsil, with higher expression level on tonsil B cells.³ In addition, CD40 expression was shown to be significantly enhanced on cultured B cells from Burkitt lymphomas, on Epstein-Barr virus-transformed lymphoblastoid cell lines, and on non-T acute lymphoblastic leukemia. These observations led to the proposal of CD40 function as a receptor for B cell growth factors.

¹ Koho, H, et al. (1984). Monoclonal antibodies to antigens associated with transitional cell carcinoma of the human urinary bladder. I. Determination of the selectivity of six antibodies by cell ELISA and immunofluorescence. *Cancer Immunol Immunother* 17, 165.

² Paulie, S, et al. (1984). Monoclonal antibodies to antigens associated with transitional cell carcinoma of the human urinary bladder. II. Identification of the cellular target structures by immunoprecipitation and SDS-PAGE analysis. *Cancer Immunol Immunother* 17, 173.

³ Clark, E A, et al. (1986). Activation of human B cells mediated through two distinct cell surface differentiation antigens, Bp35 and Bp50. *Proc Natl Acad Sci U S A* 83, 4494.

⁴ Paulie, S, et al. (1985). A p50 surface antigen restricted to human urinary bladder carcinomas and B lymphocytes. *Cancer Immunol Immunother* 20, 23.

CHAPTER 1

Uckun *et al.* have monitored the expression of CD40 during fetal B cell precursor proliferation and differentiation.⁵ CD40 expression begins after expression of CD10 and CD19 and prior to the expression of CD20, CD21, CD22, CD24, and surface immunoglobulin M (sIgM), and precedes immunoglobulin (Ig) heavy chain genes rearrangement. Furthermore, the majority of CD34⁺ hematopoietic cells from bone marrow and cord blood express CD40 transiently.⁶ Other groups have later described expression of CD40 on various other cells as detailed in Table 1.

Table 1. List of other CD40-expressing cells

Cells that express CD40	References
Interdigitating cells present in the T cell zones of secondary lymphoid tissues	Ling, et al. (1987). <i>Leucocyte Typing III</i> , 302.
Basal layer of epithelial sections and most epithelial cell lines	Young, et al. (1989). <i>Int J Cancer</i> 43 , 786.
Highly purified follicular dendritic cells	Schriever, et al. (1989). <i>J Exp Med</i> 169 , 2043.
Epidermal Langerhans cells	Romani, et al. (1989). <i>J Invest Dermatol</i> 93 , 600.
Dendritic cells	Freudenthal, et al. (1990). <i>Proc Natl Acad Sci U S A</i> 87 , 7698.
Basophils	Valent, et al. (1990). <i>Int Arch Allergy Appl Immunol</i> 91 , 198.
Monocytes/macrophages	Alderson, et al. (1993). <i>J Exp Med</i> 178 , 669; Vyth-Dreese, et al. (1995). <i>Eur J Immunol</i> 25 , 3023.
HLA-DR-negative epithelial cells, in majority keratinocytes	Peguet-Navarro, et al. (1995). <i>J Immunol</i> 155 , 4241.
Endothelial cells	Karmann, et al. (1995). <i>Proc Natl Acad Sci U S A</i> 92 , 4342.
Smooth muscle cells	Mach, et al. (1997). <i>Proc Natl Acad Sci U S A</i> 94 , 1931.
Microglia	Nguyen, et al. (1998). <i>Eur J Immunol</i> 28 , 2537.
Astrocytes in inflammatory context	Tan, et al. (1998). <i>J Immunol</i> 160 , 4271.
Hepatocytes	Afford, et al. (1999). <i>J Exp Med</i> 189 , 441.
Resting human platelets	Henn, et al. (2001). <i>Blood</i> 98 , 1047.

CD40 expression on vascular endothelial cells⁷ and on fibroblasts from a variety of tissues⁸ is upregulated in inflammatory contexts, suggesting that this receptor has an important role in vasculature and fibrosis. Cytokines such as interleukin (IL)-1, interferon (IFN)- γ and TNF- α induce a significant increase in CD40 expression from thymic epithelial cells of various origins.⁹

Pathological contexts may also lead to an elevated expression of CD40, as observed on peripheral blood and synovial fluid T cells of rheumatoid arthritis patients, but CD40

⁵ Uckun, F M, et al. (1990). Temporal association of CD40 antigen expression with discrete stages of human B-cell ontogeny and the efficacy of anti-CD40 immunotoxins against clonogenic B-lineage acute lymphoblastic leukemia as well as B-lineage non-Hodgkin's lymphoma cells. *Blood* **76**, 2449.

⁶ Saeland, S, et al. (1992). Distribution of surface-membrane molecules on bone marrow and cord blood CD34⁺ hematopoietic cells. *Exp Hematol* **20**, 24.

⁷ Hollenbaugh, D, et al. (1995). Expression of functional CD40 by vascular endothelial cells. *J Exp Med* **182**, 33.

⁸ Fries, K M, et al. (1995). CD40 expression by human fibroblasts. *Clin Immunol Immunopathol* **77**, 42; Kaufman, J, et al. (2001). Fibroblasts as sentinel cells: role of the CD40-CD40 ligand system in fibroblast activation and lung inflammation and fibrosis. *Chest* **120**, 53S.

⁹ Galy, A H, et al. (1992). CD40 is functionally expressed on human thymic epithelial cells. *J Immunol* **149**, 775.

CHAPTER 1

expression increase is not restricted to inflamed tissue.¹⁰ Detection of a functional CD40 on fibroblasts in female reproductive tissues indicates the implication of immune cells in reproductive physiology.¹¹ The constitutive expression of CD40 and its up-regulation by IFN γ on oral keratinocytes may be exploited for immune regulation and therapeutic use in oral disease.¹² Thus, the pleiotropic expression of CD40 on immune and non-immune cells places it at the interplay of complex networks of physiological regulations.

1.2 Discovery of CD40–ligand (also named CD40L, CD154, gp39 and T-BAM)

1.2.1 Cloning of CD40L

Brian *et al.* found that membranes isolated from an activated mouse T_H clone, were able to stimulate proliferation of unfractionated B cells, and that this effect was enhanced by the addition of the T_H line culture supernatant.¹³ In order to identify T cell surface molecules that mediate contact–dependent T helper function, Lederman *et al.* generated a mAb, designated 5c8, that inhibited the activation of B cell mediated by Jurkat D1.1 cells, a T cell leukemia clone that constitutively expressed contact–dependent helper effector function.¹⁴ This antibody was shown to immunoprecipitate a novel protein of approximately 30 kDa. No binding was observed on other cell lines such as T cell leukemia and B cell–derived cell lines. Only a subset of T cells, activated with the protein kinase C (PKC) inducer 12-O-tetradecanoyl phorbol-13-acetate (PMA) and phyto-hemagglutinin (PHA), was found to express the 5c8 Ag named T cell–B cell activating molecule (T-BAM), and later designated as CD40L.

A recombinant human CD40 coupled to a human IgG₁ Fc domain (CD40-Ig) has also been used as bait to catch CD40L. It was shown that both the soluble form of CD40 and CD40-Ig i) inhibited anti-CD40–induced proliferation of tonsil B cells activated with anti-IgM Ab, and IgE secretion by B cells following co-stimulation with anti-CD40 Ab and IL-4; and ii) significantly decreased the IL-4–induced IgE production by peripheral blood mononuclear cells (PBMC).¹⁵ The chimeric protein also inhibited T_H–dependent RNA synthesis in B cells, proliferation and IgM as well as IgG₁ productions, but only if added during the first 24 hours

¹⁰ Potocnik, A J, et al. (1990). Expression of activation antigens on T cells in rheumatoid arthritis patients. *Scand J Immunol* 31, 213.

¹¹ King, A E, et al. (2001). Cd40 expression in uterine tissues: a key regulator of cytokine expression by fibroblasts. *J Clin Endocrinol Metab* 86, 405.

¹² Dorrego, M V, et al. (2007). CD40 in human oral epithelia. *Oral Oncol* (doi:10.1016/j.oraloncology.2006.12.008).

¹³ Brian, A A. (1988). Stimulation of B-cell proliferation by membrane-associated molecules from activated T cells. *Proc Natl Acad Sci U S A* 85, 564.

¹⁴ Lederman, S, et al. (1992). Identification of a novel surface protein on activated CD4+ T cells that induces contact-dependent B cell differentiation (help). *J Exp Med* 175, 1091.

¹⁵ Fanslow, W C, et al. (1992). Soluble forms of CD40 inhibit biologic responses of human B cells. *J Immunol* 149, 655.

CHAPTER 1

of differentiation.¹⁶ Once again, only activated T_H1 cells were stained with CD40-Ig. Finally, a single-chain protein with MW \approx 32–39 kDa was immunoprecipitated,¹⁷ suggesting that the CD40-Ig construct and the 5c8 mAb recognize the same protein, the CD40–ligand. Armitage *et al.* first cloned and sequenced the mouse form of CD40L.¹⁸ When expressed at the membrane of fixed CV-1/EBNA cells, the transfection product of the CD40L coding region was able to induce B cell proliferation in the absence of co-stimulation, and the production of IgE in the presence of IL-4.

A probe corresponding to the coding region of the mouse CD40L was then used to clone the human form of CD40L from a stimulated peripheral blood T cell library. The CV-1/EBNA system used to test the functionality of the cloned ligands showed that both human and mouse forms induced proliferation of human B cells, which was amplified in the presence of IL-4. However, only the mouse CD40L was able to activate mouse B cells without co-stimulation.¹⁹

1.2.2 Cellular expression of CD40L

The authors showed by immunohistochemistry that CD40L expression is restricted to relatively small mononuclear cells in lymphoid but not in other tissues, including muscle, brain, kidney, intestine, ovary, uterus, testis, skin, lung, or liver.

CD40L–expressing cells are preferentially localized in the mantle zone and germinal center (GC) light zone of secondary follicles of all peripheral lymphoid tissues. They are restricted to CD3⁺,CD4⁺ T lymphocytes.²⁰ Moreover, CD40L–positive T cells and cytokine–producing cells were found in close proximity to antigen–specific, antibody–forming B cells in the spleen.²¹

¹⁶ Noelle, R J, et al. (1992). A 39-kDa protein on activated helper T cells binds CD40 and transduces the signal for cognate activation of B cells. *Proc Natl Acad Sci U S A* 89, 6550.

¹⁷ Hermann, P, et al. (1993). Expression of a 32-kDa ligand for the CD40 antigen on activated human T lymphocytes. *Eur J Immunol* 23, 961.

¹⁸ Armitage, R J, et al. (1992). Molecular and biological characterization of a mouse ligand for CD40. *Nature* 357, 80.

¹⁹ Spriggs, M K, et al. (1992). Recombinant human CD40 ligand stimulates B cell proliferation and immunoglobulin E secretion. *J Exp Med* 176, 1543.

²⁰ Lederman, S, et al. (1992). Molecular interactions mediating T-B lymphocyte collaboration in human lymphoid follicles. Roles of T cell-B-cell-activating molecule (5c8 antigen) and CD40 in contact-dependent help. *J Immunol* 149, 3817.

²¹ Van den Eertwegh, A J, et al. (1993). In vivo CD40-gp39 interactions are essential for thymus-dependent humoral immunity. I. In vivo expression of CD40 ligand, cytokines, and antibody production delineates sites of cognate T-B cell interactions. *J Exp Med* 178, 1555.

CHAPTER 1

CD40L was detectable 4 hours after stimulation with anti-CD3 Ab or PMA, with maximal expression at 8 to 16 hours, and significant expression was still detected after 36 h.¹⁹ A combination of PMA and anti-CD3 Ab induces a faster and higher expression of CD40L.

A small proportion of CD8⁺ T cells were also shown to express CD40L, in particular when stimulated with a combination of PMA and the calcium ionophore ionomycin. Moreover, the dim CD40 staining observed on total CD4⁺ cells upon activation with an anti-CD3 antibody was largely concentrated in the memory cell population, suggesting that the expression of T_H effector function may be regulated by the density of CD40L expression.²² Other authors have described a wider pattern of expression for CD40L than activated T cells, as summarized in Table 2.

Table 2. List of other CD40L-expressing cells

Cells that express CD40L	References
Activated B cells	Grammer, et al. (1995). <i>J Immunol</i> 154 , 4996.
Thymocytes	Foy, et al. (1995). <i>J Exp Med</i> 182 , 1377.
Mast cells and basophils	Gauchat, et al. (1993). <i>Nature</i> 365 , 340.
Eosinophils	Gauchat, et al. (1995). <i>Eur J Immunol</i> 25 , 863.
CD40-activated human blood dendritic cells	Pinchuk, et al. (1996). <i>J Immunol</i> 157 , 4363.
IL-2-activated natural killer (NK) cells	Carbone, et al. (1997). <i>J Exp Med</i> 185 , 2053.
Monocytes/macrophages	Mach, et al. (1997). <i>Proc Natl Acad Sci U S A</i> 94 , 1931.
Smooth muscle and vascular endothelial cells	Mach, et al. (1997). <i>Proc Natl Acad Sci U S A</i> 94 , 1931.
Activated platelets	Henn, et al. (1998). <i>Nature</i> 391 , 591.
Renal glomerular and tubular epithelial cells during chronic graft rejection	Gaweco, et al. (1999). <i>Kidney Int</i> 55 , 1543.
Human lung fibroblasts	Kaufman, et al. (2004). <i>J Immunol</i> 172 , 1862.
Astrocytes (upregulated during Alzheimer's disease)	Calingasan, et al. (2002). <i>Neurobiol Aging</i> 23 , 31.

A role for CD40L in mediating neurotoxic inflammation has been suggested. Engagement of microglia CD40 shifts activated microglia response away from phagocytosis and towards antigen presentation. This results in microglia ineffective in removal of amyloid beta-peptide and in an increase of pro-inflammatory cytokines production by T cells.²³

Recently, naive CD4⁺ T cells were shown to express CD40L, both at mRNA and protein levels.²⁴ CD40L expression level is down-regulated following encounter with CD40-expressing cells, but is still sufficient to influence autoantigen-engaged B cell survival. Finally, the constitutive expression of CD40L by naive T lymphocytes may also contribute to

²² Roy, M, et al. (1993). The regulation of the expression of gp39, the CD40 ligand, on normal and cloned CD4+ T cells. *J Immunol* **151**, 2497.

²³ Townsend, K P, et al. (2005). CD40 signaling regulates innate and adaptive activation of microglia in response to amyloid beta-peptide. *Eur J Immunol* **35**, 901.

²⁴ Lesley, R, et al. (2006). Naive CD4 T cells constitutively express CD40L and augment autoreactive B cell survival. *Proc Natl Acad Sci U S A* **103**, 10717.

CHAPTER 1

the homeostatic maintenance of regulatory T cells (T_{reg}) since $CD40^{-/-}$ and $CD40L^{-/-}$ mice display reduced numbers of $CD25^{+}, FoxP3^{+} T_{reg}$.²⁵

1.3 Other proteins interact with CD40

Surprisingly, CD40L is not the only protein that interacts with CD40. In 1995, a 23-kDa cell surface protein (p23), was co-precipitated with CD40 in malignant and normal B cell extracts.²⁶ Brodeur and co-workers showed that the alpha chain of the human complement regulator C4b binding protein (C4BP α) interacts with CD40 at a site distinct from the CD40L binding region on human B cells, and colocalizes with B cells in tonsil GC.²⁷ C4BP α induced B cells proliferation, expression of CD54 and CD86 and IL-4-dependent IgE production. Activation of B cell at sites of inflammation could be in part due to this interaction.

Recent data proposed another mechanism involving CD40L that accounts for the binding of C4BP to CD40.²⁸ In fact, the formation of stable high-molecular weight complexes between C4BP with soluble CD40L completely inhibits CD40-activation of human cholangiocytes.

The unrelated 70-kDa mycobacterial heat shock protein (HSP70) was also shown to bind CD40.²⁹ More precisely, human HSP70 in the adenosine diphosphate (ADP) state and in the presence of peptide substrate, binds to CD40-expressing cells and is internalized after activation of p38 mitogen activated protein kinase (MAPK) signaling. The strong affinity of CD40 for HSP70-ADP-peptide ensures the capture by macrophages and dendritic cells of peptide loaded HSP70 inside a necrotic tumor cell for example.³⁰

1.4 CD40L binds to other receptors

Initial studies on CD40- and CD40L-deficient mice have suggested that CD40L may bind to other receptors than CD40.³¹ Later, Andre and Prasad demonstrated that the specific interaction of soluble CD40L with the integrin $\alpha IIb\beta 3$ on platelets via a KGD integrin-

²⁵ Guiducci, C, et al. (2005). CD40/CD40L interaction regulates CD4+CD25+ T reg homeostasis through dendritic cell-produced IL-2. *Eur J Immunol* 35, 557.

²⁶ Morio, T, et al. (1995). Characterization of a 23-kDa protein associated with CD40. *Proc Natl Acad Sci U S A* 92, 11633.

²⁷ Brodeur, S R, et al. (2003). C4b-binding protein (C4BP) activates B cells through the CD40 receptor. *Immunity* 18, 837.

²⁸ Williams, K T, et al. (2007). C4b Binding Protein Binds to CD154 Preventing CD40 Mediated Cholangiocyte Apoptosis: A Novel Link between Complement and Epithelial Cell Survival. *PLoS ONE* 2, e159.

²⁹ Wang, Y, et al. (2001). CD40 is a cellular receptor mediating mycobacterial heat shock protein 70 stimulation of CC-chemokines. *Immunity* 15, 971.

³⁰ Becker, T, et al. (2002). CD40, an extracellular receptor for binding and uptake of Hsp70-peptide complexes. *J Cell Biol* 158, 1277.

³¹ Mehlhop, P D, et al. (2000). CD40L, but not CD40, is required for allergen-induced bronchial hyperresponsiveness in mice. *Am J Respir Cell Mol Biol* 23, 646.

CHAPTER 1

recognition motif induces outside-in signaling leading to platelets activation and stabilization of arterial thrombi.³² Recently, Léveillé *et al.* showed that soluble CD40L binds to inactive integrin $\alpha 5\beta 1$, inducing IL-8 gene expression subsequent to the activation of the ERK1/2 pathway.³³

It must be kept in mind that the CD40/CD40L system is not only essential for mounting a proper immune response, but is also involved in numerous other physiological compartments. Thus, we should be aware of the different signaling pathways induced in different cell types prior to intervention on the CD40-CD40L interaction for therapeutic purpose.

1.5 Level of CD40 crosslinking is important for activation of biological responses

1.5.1 Engagement of CD40 with anti-CD40 Ab

Anti-CD40 F(ab')₂ fragments were fully active, suggesting that the Fc domain is not required for effector function.³⁴ In comparison, F(ab) is significantly less potent, but efficiently inhibits proliferative response induced by intact antibody.³⁵ Since pre-activation of blood B lymphocytes leads to increases in CD40 expression, a relation between the density of CD40 molecules along the different stages of maturation of the B lymphocytes, and the differential responses induced by anti-CD40, could not be excluded.

Gordon *et al.* have used a second layer antibody to crosslink anti-CD40 Ab, and demonstrated higher levels of proliferation and RNA synthesis on resting B lymphocytes than with “monomeric” antibody.³⁶ The ultimate demonstration of the CD40 cross-linking theory came from Banchereau and co-workers. By using the CDw32 L mouse cell line transfected with the Fc- γ receptor for optimal crosslinking of anti-CD40 Ab, they obtained a long-term growth of normal human B cell in culture supplied with a combination of anti-CD40 and IL-4.³⁷ Crosslinking of anti-CD40 Ab by adsorption on the culture matrix failed to give any

³² Andre, P, et al. (2002). CD40L stabilizes arterial thrombi by a beta3 integrin--dependent mechanism. *Nat Med* 8, 247; Prasad, K S, et al. (2003). Soluble CD40 ligand induces beta3 integrin tyrosine phosphorylation and triggers platelet activation by outside-in signaling. *Proc Natl Acad Sci U S A* 100, 12367.

³³ Leveille, C, et al. (2006). CD40 ligand binds to alpha 5beta 1 integrin and triggers cell signaling. *J Biol Chem* 282, 5143.

³⁴ Ledbetter, J A, et al. (1987). Augmentation of normal and malignant B cell proliferation by monoclonal antibody to the B cell-specific antigen BP50 (CDW40). *J Immunol* 138, 788.

³⁵ Paulie, S, et al. (1989). The human B lymphocyte and carcinoma antigen, CDw40, is a phosphoprotein involved in growth signal transduction. *J Immunol* 142, 590.

³⁶ Gordon, J, et al. (1988). Resting B lymphocytes can be triggered directly through the CDw40 (Bp50) antigen. A comparison with IL-4-mediated signaling. *J Immunol* 140, 1425.

³⁷ Banchereau, J, et al. (1991). Long-term human B cell lines dependent on interleukin-4 and antibody to CD40. *Science* 251, 70.

CHAPTER 1

detectable proliferation. These results suggest that the fibroblasts have by themselves an important function and would mimic the follicular dendritic cells; the added cytokines would substitute for GC T cells.³⁸ Finally, anti-CD40 Ab was efficient in inhibiting the CD23 expression induced by the T helper D1.1 cell line on B cells, in contrast to the cross-linked anti-CD40 which becomes agonistic.³⁹

This has suggested that the only fully biologically active form of anti-CD40 is the cross-linked one, which mimics the membranous natural ligand, while the monomeric antibody has inhibitory properties. Thus, results obtained with agonistic mAbs should not be systematically extrapolated to the natural ligand.

1.5.2 Engagement of CD40 with CD40L

Most of the stimulatory effects observed with anti-CD40 antibodies corroborates with the use of the natural ligand.

Human tonsil B cell proliferation induced by human CD40L was significantly enhanced when IL-2, IL-4, or IL-10 were added to culture, and strongly suppressed by tumor growth factor (TGF)- β .⁴⁰ Interestingly, although IFN γ partially inhibited the action of CD40L alone, its effect was synergistic in the presence of IL-4. A soluble form of the mouse CD40L was engineered consisting of the entire extracellular domain of CD40L fused to the extracellular region of the mouse CD8- α chain. As shown by sodium dodecyl sulfate–polyacrylamide gel electrophoresis (SDS-PAGE) in non-reducing conditions, this fusion protein is produced in monomeric form, but also in trimer and higher molecular mass species.⁴¹ However, although it causes alone the increase in size of a small proportion of human B cells, it induces only modest proliferation of human and mouse B cells. Robust B cell proliferation was only observed in co-stimulation with anti-Ig.

Furthermore, in the absence of a costimulus, recombinant CD40L induces expression of CD25 and CD40L on resting T cells. It also induced proliferation and enhanced CD69

³⁸ Banchereau, J, et al. (1991). Growing human B lymphocytes in the CD40 system. *Nature* 353, 678.

³⁹ Lederman, S, et al. (1992). Molecular interactions mediating T-B lymphocyte collaboration in human lymphoid follicles. Roles of T cell-B-cell-activating molecule (5c8 antigen) and CD40 in contact-dependent help. *J Immunol* 149, 3817.

⁴⁰ Armitage, R J, et al. (1993). Human B cell proliferation and Ig secretion induced by recombinant CD40 ligand are modulated by soluble cytokines. *J Immunol* 150, 3671.

⁴¹ Lane, P, et al. (1993). Soluble CD40 ligand can replace the normal T cell-derived CD40 ligand signal to B cells in T cell-dependent activation. *J Exp Med* 177, 1209.

CHAPTER 1

expression following activation with PHA or anti-CD3 antibody, and secretion of IFN γ , TNF α and IL-2 from T cells co-cultured with a submitogenic concentration of PHA.⁴²

Finally, a soluble form of human CD40L with a MW of 18 kDa, as well as a 17-kDa fragment of the mouse form, were sufficient to bind to CD40, to induce tonsil B cell proliferation and differentiation in combination with IL-4, and to rescue GC B cells from apoptosis. Gel filtration and analytical ultracentrifugation indicated that the soluble CD40L was trimeric.⁴³

1.6 CD40 plays a central role in immune response

1.6.1 Discovery of the X-linked hyper IgM syndrome

The pivotal role of CD40–CD40L interaction in immune system was established by the finding that X-linked hyper IgM (HIGM) syndrome is due to mutations in the *CD40L* gene leading to abnormal expression from activated T cells.⁴⁴ The disease can also involve splicing defect (as seen in chapter 2), or expression of a defective protein containing amino acid substitutions.⁴⁵ Recent findings showed that mutations in the gene promoter could also cause the disease.⁴⁶ Missense mutations have also been proposed to give diverse detrimental effects in the CD40L protein, such as destabilization of the functional structure, loss of trimerization, and tendencies to aggregation.⁴⁷

This rare disorder is characterized by defective isotype switching and lack of somatic mutation, leading to very low or absent IgG and IgA, and increased IgM levels in sera that are responsible for recurrent infections.⁴⁸

1.6.2 Role of CD40 in B lymphocytes

⁴² Armitage, R J, et al. (1993). CD40 ligand is a T cell growth factor. *Eur J Immunol* 23, 2326.

⁴³ Mazzei, G J, et al. (1995). Recombinant soluble trimeric CD40 ligand is biologically active. *J Biol Chem* 270, 7025.

⁴⁴ Allen, R C, et al. (1993). CD40 ligand gene defects responsible for X-linked hyper-IgM syndrome. *Science* 259, 990;

DiSanto, J P, et al. (1993). CD40 ligand mutations in x-linked immunodeficiency with hyper-IgM. *Nature* 361, 541.

⁴⁵ Aruffo, A, et al. (1993). The CD40 ligand, gp39, is defective in activated T cells from patients with X-linked hyper-IgM syndrome. *Cell* 72, 291.

⁴⁶ van Hoeyveld, E, et al. (2007). Hyper-immunoglobulin M syndrome caused by a mutation in the promotor for CD40L. *Immunology* 120, 497.

⁴⁷ Thusberg, J, et al. (2007). The structural basis of hyper IgM deficiency - CD40L mutations. *Protein Eng Des Sel* 20, 133.

⁴⁸ Kroczek, R A, et al. (1994). Defective expression of CD40 ligand on T cells causes "X-linked immunodeficiency with hyper-IgM (HIGM1)". *Immunol Rev* 138, 39.

CHAPTER 1

1.6.2.1 Effect of anti-CD40 mAb on B cell proliferation

Anti-CD40 mAb markedly increased the proportion of human tonsil B cells, pre-activated with anti-Ig or anti-Bp35 Ab, entering G1 and S-phases and thus enhanced their proliferation.³ Thus, only stimulation of CD40 did not induce any significant effect, but acted as a co-stimulant for B cell activation and proliferation. Anti-CD22 antibodies further enhanced the proliferative response induced by anti-CD40 plus anti-CD20.⁴⁹

1.6.2.2 CD40 engagement and B cell activation

The complex events taking place during the activation of B lymphocytes in peripheral lymphoid organs, after the first MHC-II–peptide–TCR interaction between B and T cells have been extensively dissected in a number of studies.

Gordon *et al.* described the maintenance of resting B cell proliferation in culture by the synergistic sustenance of replication cycle by recombinant IL-4 and anti-CD40.⁵⁰ They further depicted the mechanisms of activation and noticed an enlargement of the resting tonsil B lymphocytes in contact with anti-CD40 Ab. Whereas the signal induced by CD40 conditions B cells to mitogenic signals, IL-4 up-regulates CD40 expression.^{36,51}

IL-4 was the only cytokine, from a panel of eleven, able to enhance anti-CD40-induced B cell proliferation.⁵² Since IL-4 alone did not drive B cells sufficiently far into cycle, it was postulated to act later in G1 to drive appropriately activated B lymphocytes to proliferate.⁵³ Furthermore, the constitutive expression of CD40 on human B cells is high, making possible that IL-4 induces a conformational change in CD40 leading to altered binding characteristics of CD40L and variations in its cellular effects.⁴⁰

An additional striking observation was the metabolic energy- and calcium-dependent strong homotypic aggregation in presence of the CD40 mAb.³⁶ This phenomenon was

⁴⁹ Pezzutto, A, et al. (1987). Amplification of human B cell activation by a monoclonal antibody to the B cell-specific antigen CD22, Bp 130/140. *J Immunol* 138, 98.

⁵⁰ Gordon, J, et al. (1987). Synergistic interaction between interleukin 4 and anti-Bp50 (CDw40) revealed in a novel B cell restimulation assay. *Eur J Immunol* 17, 1535.

⁵¹ Valle, A, et al. (1989). Activation of human B lymphocytes through CD40 and interleukin 4. *Eur J Immunol* 19, 1463.

⁵² Rousset, F, et al. (1991). Cytokine-induced proliferation and immunoglobulin production of human B lymphocytes triggered through their CD40 antigen. *J Exp Med* 173, 705.

⁵³ Clark, E A, et al. (1989). Activation of human B cells. Comparison of the signal transduced by IL-4 to four different competence signals. *J Immunol* 143, 3873.

CHAPTER 1

explained by the up-regulation of adhesion molecules CD54 (also named ICAM-1), and was dependent on the CD40 cytoplasmic domain.⁵⁴

Adhesion can be mediated independently of integrins, as shown on transformed B cell lines, but engages one or more tyrosine kinases.⁵⁵ Nevertheless, additional interaction molecules are involved in the T cell–B cell collaboration, since CD3–activated T cells from HIGM patients could induce CD25 expression on B cells.⁵⁶ Human tonsil interdigitating dendritic cells have been shown to interact with naive B cells within T cell area.⁵⁷ In fact, dendritic cells also play a direct role by providing signals to CD40-activated B cells leading to T–dependent enhanced proliferation and differentiation.⁵⁸ Nevertheless, anti-CD40–induced proliferation is independent on the change in intracellular Ca^{2+} concentration.⁵⁹

1.6.2.3 CD40 is important for isotype switching

IL-4 and anti-CD40 mAb are not only synergistic in induction of B cell proliferation and in induction of IgE synthesis by CD20⁺ cells and IgE⁻ cells (that have not been pre-activated *in vivo*), via the autocrine production of IL-6.⁶⁰ In fact, anti-CD40 mAb was shown to induce sIgM⁺ B cells to switch to IgG₄/IgG and IgE production in the presence of recombinant IL-4.

The mAb strongly enhances expression of germline epsilon and of productive epsilon transcript induced by IL-4,⁶¹ while suppressing IgG, IgM, and IgA synthesis.⁶² The switch junction of S μ to S ϵ was sequenced, and while direct, it did not show any duplication,

⁵⁴ Barrett, T B, et al. (1991). CD40 signaling activates CD11a/CD18 (LFA-1)-mediated adhesion in B cells. *J Immunol* 146, 1722.

⁵⁵ Kansas, G S, et al. (1991). Transmembrane signals generated through MHC class II, CD19, CD20, CD39, and CD40 antigens induce LFA-1-dependent and independent adhesion in human B cells through a tyrosine kinase-dependent pathway. *J Immunol* 147, 4094.

⁵⁶ Nishioka, Y, et al. (1994). The role of CD40-CD40 ligand interaction in human T cell-B cell collaboration. *J Immunol* 153, 1027.

⁵⁷ Bjorck, P, et al. (1997). Human interdigitating dendritic cells directly stimulate CD40-activated naive B cells. *Eur J Immunol* 27, 1266.

⁵⁸ Dubois, B, et al. (1997). Dendritic cells enhance growth and differentiation of CD40-activated B lymphocytes. *J Exp Med* 185, 941.

⁵⁹ Gruber, M F, et al. (1989). Anti-CD45 inhibition of human B cell proliferation depends on the nature of activation signals and the state of B cell activation. A study with anti-IgM and anti-CDw40 antibodies. *J Immunol* 142, 4144.

⁶⁰ Jabara, H H, et al. (1990). CD40 and IgE: synergism between anti-CD40 monoclonal antibody and interleukin 4 in the induction of IgE synthesis by highly purified human B cells. *J Exp Med* 172, 1861.

⁶¹ Gascan, H, et al. (1991). Anti-CD40 monoclonal antibodies or CD4⁺ T cell clones and IL-4 induce IgG₄ and IgE switching in purified human B cells via different signaling pathways. *J Immunol* 147, 8.

⁶² Zhang, K, et al. (1991). CD40 stimulation provides an IFN-gamma-independent and IL-4-dependent differentiation signal directly to human B cells for IgE production. *J Immunol* 146, 1836.

CHAPTER 1

deletion, insertion or extensive point mutation.⁶³ In contrast to proliferation, secretion of IgM, IgG and IgE by B cells does not require crosslinking by the CDw32 L cells.⁶⁴

Influence of various cytokines during isotype switching was studied, and it was shown for example that, IFN γ did not inhibit the production of IgE by cells stimulated with anti-CD40 and IL-4.⁵² Mast cells and basophils have been proposed to replace T cells, in conjunction with IL-4, for the induction of IgE production. Inhibition of IgE production by CD40-Ig indicates the involvement of CD40L. In addition, the finding that CD40L is expressed in mast cells upon induction by PMA and ionomycin, and is constitutive in basophils, suggest that isotype switching may also occur in peripheral organs such as the lung or the skin, respectively.⁶⁵

Finally, although the number and phenotype of T and B cells from a CD40^{-/-} chimeras were not altered, spleen cells from these animals failed to proliferate in response to soluble CD40L, and to secrete IgG₁ and IgE in response to CD40L in combination with IL-4.⁶⁶ B cells that lack CD40 undergo normal maturation, but memory B cell responses are absent after immunization with the T cell-dependent Ag keyhole limpet hemocyanin.

One more level of complexity is achieved with interdigitating dendritic cells, that not only play an important role in the B cell proliferation in GC, but also induce isotype switch towards IgA and IgG₁.⁶⁷ More recently, interdigitating dendritic cells were shown to suppress IgE production from CD40/IL4-stimulated B cells by direct contact, and to inhibit Ig class switch recombination through production of IFN γ and TGF β after activation by B lymphocytes.⁶⁸

Thus, CD40 expression on B cells is not required for their development, but plays an important role in B-cell activation, antibody responses to T-dependent antigens, isotype switching and formation of germinal centers.

⁶³ Shapira, S K, et al. (1992). Molecular analysis of the induction of immunoglobulin E synthesis in human B cells by interleukin 4 and engagement of CD40 antigen. *J Exp Med* 175, 289.

⁶⁴ Banchereau, J, et al. (1991). Growing human B lymphocytes in the CD40 system. *Nature* 353, 678.

⁶⁵ Gauchat, J F, et al. (1993). Induction of human IgE synthesis in B cells by mast cells and basophils. *Nature* 365, 340.

⁶⁶ Castigli, E, et al. (1994). CD40-deficient mice generated by recombination-activating gene-2-deficient blastocyst complementation. *Proc Natl Acad Sci U S A* 91, 12135.

⁶⁷ Dubois, B, et al. (1999). Dendritic cells directly modulate B cell growth and differentiation. *J Leukoc Biol* 66, 224.

⁶⁸ Obayashi, K, et al. (2007). Dendritic cells suppress IgE production in B cells. *Int Immunol* 19, 217.

CHAPTER 1

1.6.2.4 CD40 is important for rescue from apoptosis of mature B lymphocytes

Additional insight in mechanisms of antigen-driven selection in GC was gained with experiments involving negatively-selected GC B cells. Centroblasts spontaneously enter apoptosis in culture, and although polyspecific anti-Ig or anti-CD40 could delay cell death, significant survival was obtained only with the combined signals of B cell receptor (BCR) and CD40.⁶⁹ Apoptosis level of the human B cell line Ramos after engagement of IgM was reduced in the presence of anti-CD20 and anti-CD40 Abs.⁷⁰ This result supports the protective role of CD40 signal during this process.

To assess the molecular nature of the signal that inhibits Ig-mediated apoptosis during activation of mature B cells by Ags, Tsubata *et al.* have observed blockage of anti-IgM-induced growth inhibition of B lymphoma WEHI-231 co-stimulated by either human CD40L or anti-CD40 Ab.⁷¹ Finally, anti-mouse CD40 mAb was also effective in rescuing apoptosis of WEHI-231 and CH31 B lymphoma cells induced by soluble anti-IgM antibodies. In synergy with IL-4, it produces a vigorous proliferation of anti-IgM-preactivated normal splenic B cells.⁷² Further studies revealed that Bcl-2, Bcl-X_L, c-myc, and p53/p21⁷³ are implicated in the anti-apoptotic signal sent from CD40 to WEHI 231 mouse B lymphoma stimulated with anti-IgM. A similar effect was observed for the Bcl homolog A1, that is implicated in anti-apoptotic pathways engaged by CD40, as observed in the WEHI cells, in isolated human GC B cells and in human Ramos cell line.⁷⁴

In addition, CD40 can induce re-expression of telomerase activity in memory B cells, thereby contributing to an expanded lifespan of these cells.⁷⁵

1.6.3 Role of CD40 in other immune cells

In addition to these multiple roles in B cell, CD40 triggering at the surface of other APC enhances their survival, the Ag-presenting functions of dendritic cells (enhancement of MHC class II and accessory molecules levels, secretion of key cytokines including IL-12), as well as

⁶⁹ Liu, Y J, et al. (1989). Mechanism of antigen-driven selection in germinal centres. *Nature* 342, 929.

⁷⁰ Valentine, M A, et al. (1992). Rescue from anti-IgM-induced programmed cell death by the B cell surface proteins CD20 and CD40. *Eur J Immunol* 22, 3141.

⁷¹ Tsubata, T, et al. (1993). B-cell apoptosis induced by antigen receptor crosslinking is blocked by a T-cell signal through CD40. *Nature* 364, 645.

⁷² Santos-Argumedo, L, et al. (1994). Antibodies to mouse CD40 protect normal and malignant B cells from induced growth arrest. *Cell Immunol* 156, 272.

⁷³ Tsubata, T. (1999). Apoptosis of mature B cells. *Inter Rev Immunol* 18, 347.

⁷⁴ Craxton, A, et al. (1999). Signal transduction pathways that regulate the fate of B lymphocytes. *Adv Immunol* 73, 79.

⁷⁵ Hu, B T, et al. (1997). Telomerase is up-regulated in human germinal center B cells in vivo and can be re-expressed in memory B cells activated in vitro. *J Immunol* 159, 1068.

CHAPTER 1

antimicrobial and cytotoxic activities of macrophages (expression of pro-inflammatory molecules, cytokines and chemokines).⁷⁶

The fact that inducible CD40L expression is predominately restricted to activated T cells, and that activated T cells respond to CD40L, suggests that CD40L is involved in a T cell-dependent T cell activation process.⁷⁷ Help provided by CD4⁺ to CD8⁺ cell responses is thought to occur through APC activation via CD40.⁷⁸ Most recently, CD4⁺ T cells were shown to directly induce differentiation of CD8⁺ to memory cells through engagement of CD40 which is transiently expressed upon activation CD8⁺ cells.⁷⁹ Moreover, CD4⁺ memory T cells can survive and proliferate in the absence of CD40 signal, whereas primary CD4⁺ T cell expansion and effector cell differentiation are dependent on the CD40-CD40L interaction.⁸⁰

1.7 Function of CD40 in malignant cells

CD40 is expressed by normal immune cells but also by many malignant cells, in particular malignant B cells. While absent from pre-B cells of the acute lymphocytic leukemia type, CD40 was shown to be expressed in numerous progenitors or pre-B cells obtained by EBV transformation of B lymphocytes from fetal bone marrow. It is also present on cells of intermediate stages.⁴ The first observation of a potential effect of anti-CD40 Ab on malignant B cells was made by Ledbetter *et al.*⁸¹ In response to anti-CD40 Ab, some but not all lymphoma cells proliferate, possibly according to their stage of maturation. In contrast, no proliferative effect, with few exceptions, was observed on CD40-positive leukemia co-stimulated or not with PMA.⁸²

Beiske and coworkers enlarged the panel of neoplastic B cells tested against the anti-CD40, including follicle-center-cell lymphomas, chronic lymphatic B-cell leukemia and other cases of various histological types, and showed on some cells a total inhibition of

⁷⁶ van Kooten, C, et al. (2000). CD40-CD40 ligand. *J Leukoc Biol* 67, 2.

⁷⁷ Fanslow, W C, et al. (1994). Recombinant CD40 ligand exerts potent biologic effects on T cells. *J Immunol* 152, 4262.

⁷⁸ Schoenberger, S P, et al. (1998). T-cell help for cytotoxic T lymphocytes is mediated by CD40-CD40L interactions. *Nature* 393, 480; Bennett, S R, et al. (1998). Help for cytotoxic-T-cell responses is mediated by CD40 signalling. *Nature* 393, 478; Ridge, J P, et al. (1998). A conditioned dendritic cell can be a temporal bridge between a CD4+ T-helper and a T-killer cell. *Nature* 393, 474.

⁷⁹ Bourgeois, C, et al. (2002). A role for CD40 expression on CD8+ T cells in the generation of CD8+ T cell memory. *Science* 297, 2060.

⁸⁰ MacLeod, M, et al. (2006). CD4 memory T cells survive and proliferate but fail to differentiate in the absence of CD40. *J Exp Med* 203, 897.

⁸¹ Ledbetter, J A, et al. (1987). Augmentation of normal and malignant B cell proliferation by monoclonal antibody to the B cell-specific antigen BP50 (CDW40). *J Immunol* 138, 788.

⁸² Ghaderi, A A, et al. (1988). Stimulation of B-chronic lymphocytic leukemia populations by recombinant interleukin-4 and other defined growth-promoting agents. *Leukemia* 2, 165.

CHAPTER 1

proliferation and no proliferation if co-stimulated with PMA.⁸³ These variable responses to anti-CD40 along the neoplastic B-cell subsets were not correlated with the density of CD40 at the membrane since this was similar in responder and non-responder groups, but were directed by distinct signaling pathways.

As seen by electron microscopy on the human Burkitt lymphoma cell line Daudi, CD40 was rapidly internalized via coated pits and directed to endocytic compartments, what could be a mechanism of regulation of the CD40 signaling in some cells.⁸⁴ Such a receptor-bound ligand internalization was observed for soluble TNF on human monocytes.⁸⁵

Although an anti-mouse CD40 antiserum induces proliferation of B cells in the presence of costimulators and rescues WEHI 231 cells from apoptosis induced by anti-IgM, it also suppresses *in vitro* growth of several B lineage malignancies. In contrast, no effect was observed on CD40-negative thymoma.⁸⁶ In human cells, anti-CD40 mAb also appeared to directly inhibit proliferation of variety of human Burkitt lymphoma cell lines, with level of inhibition directly linked to the degree of crosslinking. These effects contrast with proliferation induced after engagement of CD40 on non-neoplastic B cells.⁸⁷ Furthermore, membranous form of CD40L specifically induces expression of CD95 (also named Fas) on multiple Burkitt's lymphoma B cell lines, thus conferring sensitivity to Fas-mediated death signals.⁸⁸

Potentiality to use CD40-mediated direct anti-proliferative effect on malignant cells, in parallel to the induction of a strong immune response will be discussed in chapter 4.

⁸³ Beiske, K, et al. (1988). Triggering of neoplastic B cells via surface IgM and the cell surface antigens CD20 and CDw40. Responses differ from normal blood B cells and are restricted to certain morphologic subsets. *Int J Cancer* 42, 521.

⁸⁴ Press, O W, et al. (1989). Endocytosis and degradation of monoclonal antibodies targeting human B-cell malignancies. *Cancer Res* 49, 4906.

⁸⁵ Imamura, K, et al. (1987). Expression of tumor necrosis factor receptors on human monocytes and internalization of receptor bound ligand. *J Immunol* 139, 2989.

⁸⁶ Heath, A W, et al. (1993). Antibodies to mouse CD40 stimulate normal B lymphocytes but inhibit proliferation of B lymphoma cells. *Cell Immunol* 152, 468.

⁸⁷ Funakoshi, S, et al. (1994). Inhibition of human B-cell lymphoma growth by CD40 stimulation. *Blood* 83, 2787.

⁸⁸ Schattner, E J, et al. (1996). CD4+ T-cell induction of Fas-mediated apoptosis in Burkitt's lymphoma B cells. *Blood* 88, 1375.

CHAPTER 2

CD40 AND CD40L: GENES AND PROTEINS

CHAPTER 2

2.1 Characteristics of the CD40 protein sequence

2.1.1 The human sequence

The human *CD40* cDNA was isolated from the human Burkitt lymphoma Raji line library.¹ The open reading frame of its sequence contains 831 base pairs (bp) from which the translated product was predicted to be composed of 277 amino acids. The first 20 residues, predominantly hydrophobic, compose the signal peptide. The remaining sequence has the characteristics of a type I membrane glycoprotein with a predicted MW of 28,300 Da. The extracellular domain consists of 193 residues, which include 22 cysteines and two potential N-linked glycosylation sites; the transmembrane region contains 22 hydrophobic residues; and the cytoplasmic region is made of 62 amino acids (Figure 1).

```
1  GCCTCGCTCGGCGCCAGCTGGTCTGCCGCCTGGTCTCACCTCGCCATGTTTCTCTCCCTCTCCAGTGCCTCTCGGGCTGCTTGTCTGACCGTGTCCATCCAGAACCCCACTG
1  M V R L P L Q C Y L W G C L L T A V H P E P P T A
121  CATGCAGAGAAAAACAGTACCTAATAAACAGTCACTGCTGTTCTTTGTGCCAACCAGGACAGAAAC TGGTGAAGTACTGCACAGAGTTTCACTGAAACGGAATGCCCTTCCCTTCCGGTGA
20  C R E K Q Y L I N S Q C C S L C Q P G Q K L V S D C T E F T E T E C L P C G E S
241  GCGAATTCCTAGACACCTGGAAACAGAGACACACACTGCCACCAAGCAAAATACCTGACCCCAACCTAGGGCTTCGGGTCCAGCAGAAGGGCCACTCAGAAACAGACACCATCTGCACCT
66  E F L D T W H R E T H C H Q H K Y C D P N L G L R V Q Q K G T S E T D T I C T C
361  GTGAAGAAGCGCTGCCACTGTACAGTGAAGGCTGTGAGAGCTGTGTCCTGCACCCTCATGCTCGCCCGCTTTGGGGTCAAGCAGATTGCTACAGGGGTTTCTGATACCATCTGCCACC
106  E E G W H C T S E A C E S C Y L H R S C S P G F G Y K Q I A T G V S D T I C E P
481  CCTGCCAGTCCGGTCTCTCCAATGTGTCATCTGCTTTCCAAAAATGTCACCTTGGACAAAGCTGTGAGACCAAAAGACCTGGTTGTGCAACAGCCAGGCACAACAAAGACTGATGTTG
146  C P V G F F S N V S S A F E K C H P W T S C E T K D L V Y Q Q A G T N K T D V Y
801  TCTGTGGTCCCAAGGATCGGCTGAGAGCCCTGGTGGTGTATCCCCATCATCTTCGGATCCTGTTTGCATCCTCTTGGTCTGGTCTTTATCAAAAAGGTGGCCAAGAAAGCCAAACCAATA
186  C G P Q D R L R A L V V I P I I F G I L F A I L L V L V F I K K V A K K P T N K
721  AAGCCCAACCCCAAGCAGGAACCCAGGAGATCAATTTCCCGACATCTCTGCGCTCCCAACACTGCTGCTCCAGTGCAGGAGACTTTACATGGATGCCAACCGGTACCCAGGGAG
226  A P H P K Q E P Q E I N F P D D L P G S N T A A P V Q E T L H G C Q P V T Q E D
841  ATGCCAAAGAGAGTCCGATCTCAGTGCAGGAGAGACAGTGAAGCTGCACCCACCAAGGAGTGTGGCCACGTGGGCAAAACAGGACAGTTGGCCAGAGAGCTGGTCTGCTGTCAGGGGT
266  G K E S R I S V Q E R Q
981  GCAGGCAGAAAGCGGGAGCTATGCCCAAGTCAAGTCCAGCCCTC
```

Figure 1. Nucleic acid (upper line) and predicted protein (lower line) sequences of human CD40. The transmembrane domain is indicated with “*”, and potential N-linked glycosylation sites are marked by “CHO”, under the protein sequence.¹

Under SDS-PAGE, the CD40 MW was estimated at 47 kDa. Anomalies during the gel migration when run at different polyacrylamide concentrations, as well as post-translational modifications, might explain the difference with calculated MW.² Interestingly, CD40 was also found as a dimer in non-reducing conditions, and a few trimers and tetramers were formed from purified monomers. Moreover, a 4 kDa–smaller band was described as a proteolytic cleavage product, and CD40 was shown to be sensible to glycopeptidase F. By sequencing the 30 amino terminal residues, Braesch-Andersen *et al.* not only confirmed the sequence of the predicted mature CD40, but also showed existence of conservative and destructive substitutions in different cell types.

¹ Stamenkovic, I, et al. (1989). A B-lymphocyte activation molecule related to the nerve growth factor receptor and induced by cytokines in carcinomas. *Embo J* 8, 1403.

² Braesch-Andersen, S, et al. (1989). Biochemical characteristics and partial amino acid sequence of the receptor-like human B cell and carcinoma antigen CDw40. *J Immunol* 142, 562.

CHAPTER 2

Finally, alignment of the CD40 sequence with the first domain of the low-density lipoprotein receptor allowed the decomposition of the extracellular region into 4 subdomains of approximately 40 residues, and into serine/threonine stretches of variable length preceding the transmembrane domain.

2.1.2 The mouse sequence

Mouse *CD40* cDNA was cloned later from B lymphocytes stimulated with lipopolysaccharide (LPS) and IL-4, and its sequence share some characteristics in common with the human form. It encodes a 305-residues typical type I integral membrane protein, with a hydrophobic leader sequence of 21 residues, followed by a 172-amino acids cysteine-rich extracellular domain, a 22 residues transmembrane domain and a 91 residues intracellular domain.³ The MW of the mature form was calculated at 31.4 kDa. Only one potential N-glycosylation site appears in the mouse form. The extracellular domains of the two species share 62% identity, with the 22 cysteines conserved, and 78% identity within the cytoplasmic domain. The last 32 residues of the human form are identical to the mouse form, but the later was predicted to contain an additional 28-residues sequence (Figure 2). To date, genomic DNA sequencing of the mouse *CD40* have revealed a 52 bp insertion upstream the TGA codon leading to a sequence longer than expected, what was corrected on Figure 2.

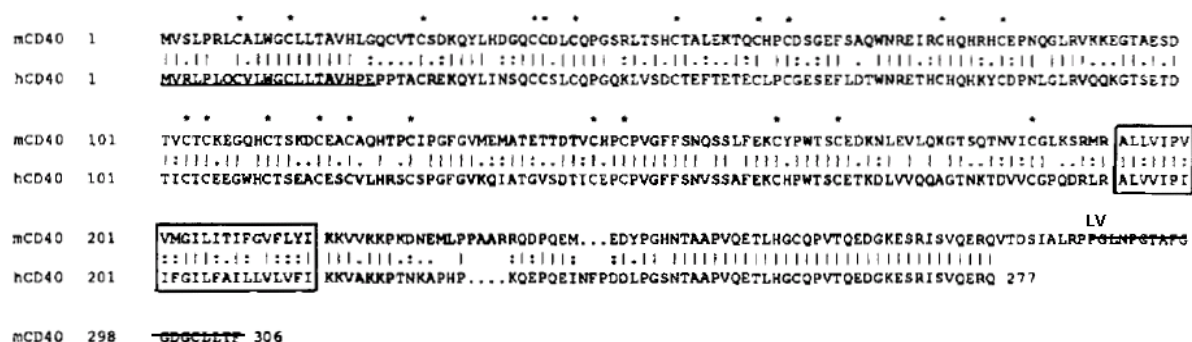


Figure 2. Alignment of the protein sequences of mouse (*mCD40*) and human (*hCD40*) CD40. The signal peptide of the human sequence is underlined, and the transmembrane domains are enclosed. The mouse sequence was corrected accordingly to the final sequence.² Cysteyl residues are marked with “*”. Residues identical in both forms are marked with “|”, similar residues with “:”, and homologous residues with “.”.

³ Torres, R M, et al. (1992). Differential increase of an alternatively polyadenylated mRNA species of mouse CD40 upon B lymphocyte activation. *J Immunol* 148, 620.

CHAPTER 2

Multiple alignment of the mouse CD40 revealed four putative domains that share a high degree of similarity with the extracellular domains of the human CD40 and with the human TNF and NGF receptors, the mouse 4-1BB, and the rat OX40.⁴

2.2 Regulation of CD40 expression

2.2.1 Organization of the *CD40* gene

2.2.1.1 The mouse gene

A mouse cDNA probe was used to isolate the complete *CD40* mouse gene from a BALB/c mouse liver genomic library.⁴ Comparison of the genomic DNA sequence with the cDNA sequence revealed a genomic organization within 9 exons along 16.3 kb (Figure 3).

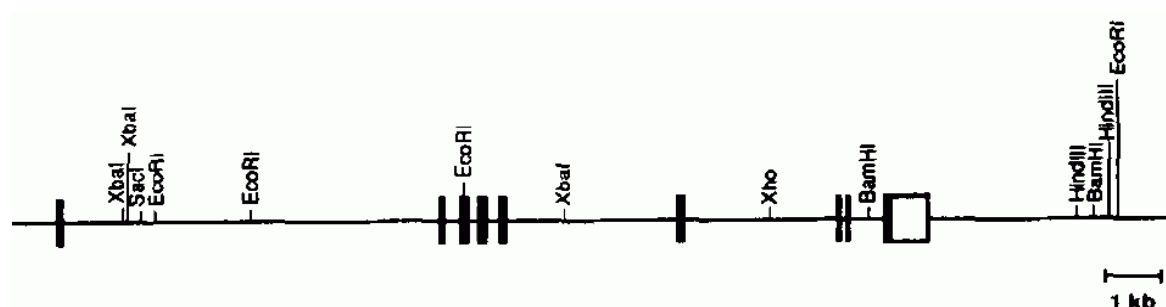


Figure 3. Organization of the mouse *CD40* gene. Exons are represented by black bars, and the 3' UTR is shown as an open box. Some restriction sites are indicated.⁴

Exon 1 contains the signal peptide, and certainly much more of the 5' untranslated region (UTR), since the start site of transcription was not identified. Exons 2 to 6 code for the N-terminal (N-ter) extracellular domain, exon 7 for the transmembrane domain, and exons 8 and 9 for the intracytoplasmic domain.

The mouse *CD40* gene was located on chromosome 2, more precisely at 2H3.⁵

2.2.1.2 The human gene

The human *CD40* was located to 20q11-q13 by in situ hybridization,⁵ more precisely along 20q12-q13.2. Tone *et al.* have sequenced all the exon/intron junction sequences of the human *CD40* gene and showed that it contains 9 exons distributed as in the mouse form (Figure 4).⁶

⁴ Grimaldi, J C, et al. (1992). Genomic structure and chromosomal mapping of the mouse CD40 gene. *J Immunol* 149, 3921.

⁵ Lafage-Pochitaloff, M, et al. (1994). Localization of the human CD40 gene to chromosome 20, bands q12-q13.2. *Leukemia* 8, 1172.

⁶ Tone, M, et al. (2001). Regulation of CD40 function by its isoforms generated through alternative splicing. *Proc Natl Acad Sci U S A* 98, 1751.

CHAPTER 2

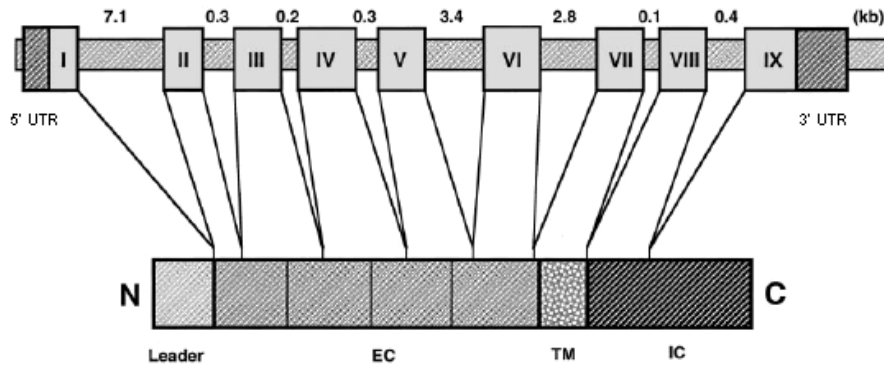


Figure 4. Organization of the human *CD40* gene. Exons are represented by gray boxes numbered, from 5' UTR to 3' UTR in Latin numbers. Lengths between adjacent exons are indicated above each intron. The resulting protein is shown beyond, with implication of the coding sequence of each exon in intracytoplasmic (IC), transmembrane (TM), or extracellular (EC) domains.⁷

2.2.2 Transcriptional regulation of *CD40* expression

Sequencing of the *CD40* promoter indicated the presence of a conserved AP-4 site and two Sp1 sites on both human and mouse genes.⁸ Neither TATA nor CAAT boxes have been described, but high frequency of CpG dinucleotides, which are known to be involved in epigenetic regulations in numerous genes, are present in the promoter. Nevertheless, evidences suggested that *CD40* is not imprinted in mouse or in human.⁹

Several cytokines have been shown to regulate transcription of *CD40*. *CD40* expression is upregulated by IFN γ on endothelial cells, whose activation is important for recruitment and extravasation of circulating immune cells at sites of inflammation.¹⁰ IFN γ and TNF α synergistically upregulates *CD40* transcription in rat vascular smooth muscle cells via the NF- κ B, RelA and STAT-1 pathways.¹¹ IFN γ also upregulated *CD40* in mouse macrophage and microglia cell lines via STAT-1 α . Putative cis-regulatory elements within the human *CD40* promoter were first determined in silico (Figure 5).

⁷ van Kooten, C, et al. (2000). CD40-CD40 ligand. *J Leukoc Biol* 67, 2.

⁸ Rudert, F, et al. (1995). Identification of a silencer, enhancer, and basal promoter region in the human CD95 (Fas/APO-1) gene. *DNA Cell Biol* 14, 931.

⁹ Williamson, C M, et al. (1995). Thirteen genes (Cebpb, E2f1, Tcf4, Cyp24, Pck1, Acra4, Edn3, Kcnb1, Mc3r, Ntsr, Cd40, Plcg1 and Rcad) that probably lie in the distal imprinting region of mouse chromosome 2 are not monoallelically expressed. *Genet Res* 65, 83.

¹⁰ Yellin, M J, et al. (1995). Functional interactions of T cells with endothelial cells: the role of CD40L-CD40-mediated signals. *J Exp Med* 182, 1857.

¹¹ Krzesz, R, et al. (1999). Cytokine-inducible CD40 gene expression in vascular smooth muscle cells is mediated by nuclear factor kappaB and signal transducer and activation of transcription-1. *FEBS Lett* 453, 191.

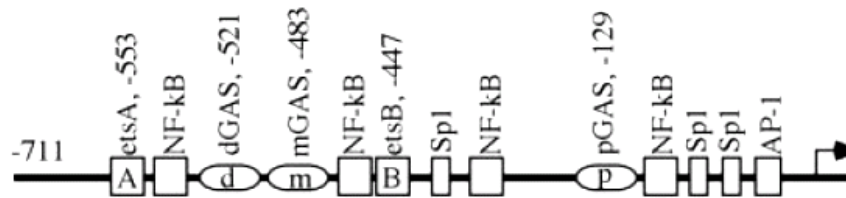


Figure 5. Potential putative cis-regulatory elements located within the human *CD40* gene promoter. Potential binding sites for diverse transcription factors were determined with MatInspector.¹² Transcription start site is represented by the arrow. Location of some elements is indicated respective to the transcription start site.

Deletion constructs, promoter mutagenesis and reporter assays as well as electrophoretic mobility shift assay (EMSA) in a mouse macrophage cell line confirmed that optimal IFN γ -induced *CD40* promoter activity requires the distal (d), proximal (p) and middle (m) gamma activated sequences (GAS), as well as etsA and etsB elements (Figure 5) in an optimal spatial orientation.¹³ Furthermore, various cytokines and LPS are involved in the complex regulation of *CD40* expression. For example, IL-4 antagonizes the IFN γ -induced *CD40* transcription via STAT-6, which binds and blocks the dGAS and pGAS sites.¹⁴

Unexpectedly, the human T cell leukemia virus type I Tax protein was shown to induce *CD40* gene expression on T cell lines via the NF- κ B pathway and implicates the proximal NF- κ B element (Figure 5).¹⁵ Since the *CD40* pathway is fully functional in T cell, engagement of *CD40* on T cells by *CD40L* synergizes with suboptimal levels of Tax to activate NF- κ B.

Concerning the mouse gene promoter, two Sp1 elements are located close to the transcription start site. They act cooperatively for the basal expression of *CD40*, and are necessary for a proper LPS-induced upregulation of *CD40* expression mediated by p65 NF- κ B, although phosphorylation of the Sp1 protein reduces its binding to the promoter.¹⁶

2.2.3 Post-transcriptional regulation of *CD40* expression

2.2.3.1 Alternative splicing of the *CD40* mRNA

Expression of the mouse *CD40* was shown to be regulated at the post-transcriptional level through the production of 5 alternative splicing variants (Figure 6).⁶

¹² Quandt, K, et al. (1995). MatInd and MatInspector: new fast and versatile tools for detection of consensus matches in nucleotide sequence data. *Nucleic Acids Res* 23, 4878.

¹³ Nguyen, V T, et al. (2000). Involvement of STAT-1 and ets family members in interferon-gamma induction of *CD40* transcription in microglia/macrophages. *J Biol Chem* 275, 23674.

¹⁴ Nguyen, V T, et al. (2000). IL-4-activated STAT-6 inhibits IFN-gamma-induced *CD40* gene expression in macrophages/microglia. *J Immunol* 165, 6235.

¹⁵ Harhaj, E W, et al. (2005). Human T cell leukemia virus type I Tax activates *CD40* gene expression via the NF-kappa B pathway. *Virology* 333, 145.

¹⁶ Tone, M, et al. (2002). The role of Sp1 and NF-kappa B in regulating *CD40* gene expression. *J Biol Chem* 277, 8890.

CHAPTER 2

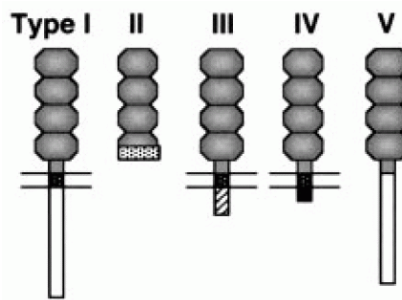


Figure 6. Alternative splicing variants of the mouse *CD40* mRNA. The five variants are schematized with cysteine-rich domains (CRD) in gray, transmembrane (hydrophobic) domain in black and intracytoplasmic domain in white or hashed.⁶

Some of these mRNA isoforms are expressed in specific tissues or in response to various stimuli. Type I is the predominant and fully functional form. Type III and IV should act as dominant negative and inhibit type I protein signaling. Type II, which expression is inducible by LPS in macrophages and dendritic cells, reduces the protein level of type I isoform by increasing its degradation. The function of the type V isoform was not investigated, but such a form should be released by the cell in a soluble form and act as a decoy receptor.

For the human *CD40*, type I and II isoform homologues were found in the human Burkitt lymphoma cell line Raji. An additional type III which lacks the fourth cysteine-rich domain, and a type IV consisting of the 21 first residues, were described in these cells. Since type II isoform is highly conserved in human and mouse sequences, it could also act as a negative regulator of type I protein expression in human cell (Figure 6).⁶

2.2.3.2 Stability of the *CD40* mRNA

Two alternative polyadenylation AAUAAA consensus sequences were detected in exon 9 within the large 3' UTR of the mouse *CD40* mRNA (Figure 3). Activation of B lymphocytes with various inducers result in the differential expression of two mRNA species.³ The use of downstream polyadenylation signal would include the AU-rich 3' UTR, sequence that has been associated with mRNA instability. Activation of mouse B cells with anti-IgM in the presence of IL-4 resulted in the upregulation of the shorter mRNA species that is more stable. Another example comes from the TGF β -dependent suppression of the IFN γ -induced *CD40* gene expression in mouse microglia.¹⁷ It was proposed that TGF β signaling reduces the

¹⁷ Nguyen, V T, et al. (1998). Post-transcriptional inhibition of *CD40* gene expression in microglia by transforming growth factor-beta. *Eur J Immunol* 28, 2537.

CHAPTER 2

half-life of *CD40* mRNA, probably by inhibiting IFN γ -induced stabilization of AU-rich element binding protein, or directly induces destabilization of the protein.

In contrast, human *CD40* mRNA was detected as a unique 1.5-kb species,¹ what avoids such a transcriptional regulation.

2.2.4 Post-translational regulation of CD40 expression

Finally, numerous evidences show that CD40 expression is regulated at a post-translational level. The human leukocyte serine protease elastase is released by polymorphonuclear leukocytes during acute inflammatory reactions against bacterial infection. This proteolytic enzyme was shown to reduce the expression of CD40 on human skin, lung and gingival fibroblasts, what resulted in the downregulation of CD40L-induced IL-8 and MCP-1 productions. Thus, elastase has a feedback action during the inflammatory processes.¹⁸ Furthermore, the house dust mite *Dematophagoides pteronyssinus* group 1 allergen cysteine-protease was not only described to induce cleavage of CD25 on T cells, but also induced cleavage of CD40 from the DC surface.¹⁹ CD40 downregulation leads to suppression of IL-12 production in response to CD40L, what directs the differentiation of naive CD4⁺ T cells towards T_H2, and favors IgE production. As observed by van Kooten *et al.*, downregulation of CD40L mRNA in activated T cells cultured with B cells is regulated through the release of soluble CD40 from B cells,²⁰ what was associated with a decreased level of the membranous form. These two phenomena might represent a possible CD40-dependent regulation of B cell activation.²¹

The release of soluble CD40 from B lymphocytes was recently shown to result from the shedding of the transmembrane receptor by the metalloprotease-disintegrin TNF α converting enzyme (TACE).²¹ TACE was first demonstrated to be responsible for the proteolytic release of TNF-receptor 1 (TNF-R1) and TNF-R2.²² Although TNF-R2 can be produced as a biologically active soluble receptor by alternative splicing during pathological

¹⁸ Nemoto, E, et al. (2002). Disruption of CD40/CD40 ligand interaction with cleavage of CD40 on human gingival fibroblasts by human leukocyte elastase resulting in down-regulation of chemokine production. *J Leukoc Biol* 72, 538.

¹⁹ Ghaemmaghami, A M, et al. (2002). The proteolytic activity of the major dust mite allergen Der p 1 conditions dendritic cells to produce less interleukin-12: allergen-induced Th2 bias determined at the dendritic cell level. *Clin Exp Allergy* 32, 1468.

²⁰ van Kooten, C, et al. (1994). B cells regulate expression of CD40 ligand on activated T cells by lowering the mRNA level and through the release of soluble CD40. *Eur J Immunol* 24, 787.

²¹ Contin, C, et al. (2003). Membrane-anchored CD40 is processed by the tumor necrosis factor-alpha-converting enzyme. Implications for CD40 signaling. *J Biol Chem* 278, 32801.

²² Reddy, P, et al. (2000). Functional analysis of the domain structure of tumor necrosis factor-alpha converting enzyme. *J Biol Chem* 275, 14608.

CHAPTER 2

conditions,²³ soluble forms of TNF receptors are derived from the same transcripts which encode the cell surface forms.²⁴ Soluble TNF-Rs were shown to bind to TNF and to inhibit its bioactivity by competing with cell surface TNF-Rs for free ligand. But at lower concentrations, they have a stabilizing function of the trimeric structure of TNF, prolonging its half-life and serving as a slow release reservoir when TNF levels diminish.²⁵

No more work has been achieved on the regulation of *CD40* expression by alternative splicing, but an application in downregulation of CD40 signaling has emerged by the use of peptide nucleic acid (PNA) antisense inhibitors which bind to the 3' end of the exon 6 splice junction of mouse *CD40* (Figure 3). PNAs induce the skip from exon 5 to exon 7, leading to an mRNA lacking the transmembrane coding domain and generate a premature stop codon.²⁶ Since the second splicing form transcript accumulated, the functional receptor protein level was downregulated in a dose- and time-dependent manner, and signal could be longer initiated.

2.3 Characteristics of the CD40L protein sequence

2.3.1 The mouse sequence

The mouse *CD40L* cDNA was isolated from a mouse thymoma cell line and was shown to be expressed as a single band 2-kb mRNA upon activation of T-helper cell lines.²⁷ The MW of the encoded protein was estimated at 33 kDa, a little higher than the predicted 29.4 kDa, suggesting that the extracellular Asn-Val-Thr potential N-glycosylation site (Figure 7) is effectively used. The open reading frame contains 780 bp coding for 260 amino acids. CD40L is a type II transmembrane glycoprotein in which the amino-terminal 22 residues are followed by a 24-amino-acids stretch of hydrophobic residues which functions as the transmembrane domain. The remaining C-terminus 214 residues consist of the putative extracellular domain which contains 4 cysteines (Figure 7).

²³ Lainez, B, et al. (2004). Identification and characterization of a novel spliced variant that encodes human soluble tumor necrosis factor receptor 2. *Int Immunol* 16, 169.

²⁴ Nophar, Y, et al. (1990). Soluble forms of tumor necrosis factor receptors (TNF-Rs). The cDNA for the type I TNF-R, cloned using amino acid sequence data of its soluble form, encodes both the cell surface and a soluble form of the receptor. *Embo J* 9, 3269.

²⁵ Aderka, D, et al. (1992). Stabilization of the bioactivity of tumor necrosis factor by its soluble receptors. *J Exp Med* 175, 323.

²⁶ Siwkowski, A M, et al. (2004). Identification and functional validation of PNAs that inhibit mouse CD40 expression by redirection of splicing. *Nucleic Acids Res* 32, 2695.

²⁷ Armitage, R J, et al. (1992). Molecular and biological characterization of a mouse ligand for CD40. *Nature* 357, 80.

CHAPTER 2

```

          10      20      30      40      50      60
hCD40L MIETYNQTS PRSAATGLPI SMKIFMYLLTVFLITQMIGSALFAVYLRRLDKIEDERNLH
      ..... : : : : : : : : : : : : : : : : : : : : : : : : : : : : : :
mCD40L MIETYSQSPRSVATGLPASMKIFMYLLTVFLITQMIGSVLFAVYLRRLDKVEEEVNLH
          10      20      30      40      50      60

          70      80      90      100     110     120
hCD40L EDFVFMKTIQRCNTGERSLSLLNCEEIKSQFEGFVKDIMLNKEETKKENSFEMQKGDQNP
      ..... : : : : : : : : : : : : : : : : : : : : : : : : : : : : : :
mCD40L EDFVFIKCLKRCNKGEGLSLLNCEEMRRQFEDLVKDITLNKEE-KKENSFEMQRGDEDP
          70      80      90      100     110

          130     140     150     160     170     180
hCD40L QIAAHVISEASSKTTSVLQWAEKGYTMSNNLVTLENGKQLTVKRQGLYYIYAQVTFCSN
      ..... : : : : : : : : : : : : : : : : : : : : : : : : : : : : : :
mCD40L QIAAHVVSEANSNAASVLQWAKKGYTMKSNLVMLENGKQLTVKREGLYYVYTQVTFCSN
          120     130     140     150     160     170

          190     200     210     220     230     240
hCD40L REASSQAPFIASLCLKSPGRFERILLRAANTHSSAKPCGQSIHLGGVFELQPGASVFN
      .. : : : : : : : : : : : : : : : : : : : : : : : : : : : : : :
mCD40L REPSSQRPFIVGLWLKPSGSRERILLKAANTHSSSQLCEQQSVHLGGVFELQAGASVFN
          180     190     200     210     220     230

          250     260
hCD40L VTDP SQVSHGTGFTSFGLLKL
      .. : : : : : : : : : :
mCD40L VTEASQVIHRVGFSSFGLLKL
          240     250     260

```

Figure 7. Alignment of the protein sequences of human (hCD40L) and mouse (mCD40L) CD40L. The transmembrane domains are enclosed. Residues identical in both forms are marked with “:”, and homologous residues with “.”.^{27,28}

2.3.2 The human sequence

The human *CD40L* was cloned some months later by different groups from activated T cells.²⁸ Its cDNA encodes a \approx 33–36 kDa type II membrane glycoprotein of 261 amino acids highly similar to the mouse CD40L with 82.8% identity in the cDNA sequence and 77.4% identity in the protein sequence. The human CD40L contains 5 cysteines (Figure 7), and it consists of a C-terminal extracellular domain of 215 residues, a 24-amino acid transmembrane domain, and an N-terminal cytoplasmic tail of 22 residues (Figure 7).

As in the mouse protein, a potential glycosylation exists in the extracellular domain at position 240–242, and was confirmed later in biochemical studies and analysis of crystallography data.²⁹

²⁸ Graf, D, et al. (1992). Cloning of TRAP, a ligand for CD40 on human T cells. *Eur J Immunol* 22, 3191; Hollenbaugh, D, et al. (1992). The human T cell antigen gp39, a member of the TNF gene family, is a ligand for the CD40 receptor: expression of a soluble form of gp39 with B cell co-stimulatory activity. *Embo J* 11, 4313.

²⁹ Karpusas, M, et al. (1995). 2 A crystal structure of an extracellular fragment of human CD40 ligand. *Structure* 3, 1031.

CHAPTER 2

2.4 Regulation of CD40L expression

2.4.1 Organization of the *CD40L* gene

Location of the human *CD40L* gene in the Xq26.3-Xq27.1 region,²⁸ where X-linked hyper-IgM syndrome has been mapped, has offered explanations for the disorder, as shown in Chapter 1. The mouse gene lies in the proximal region of the mouse X chromosome, and is linked to *HPRT*.³⁰

The human gene consists of 5 exons and 4 intervening introns (Figure 8),³¹ similarly to the mouse form.³² The first exon contains the intracellular, transmembrane domains, and the first 6 residues of the extracellular region, the remainder being encoded by exons 2–5 (Figure 8). The last exon codes for the 125-residue C-terminus.

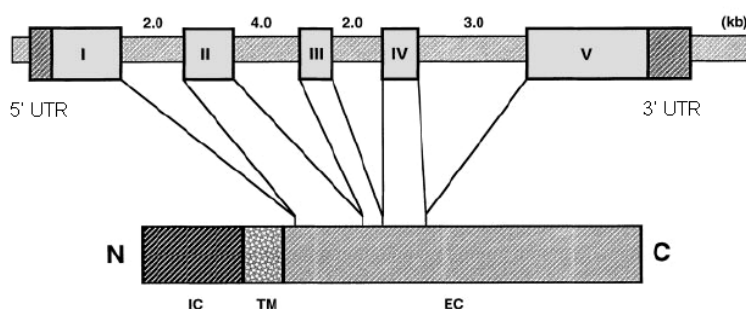


Figure 8. Organization of the human *CD40L* gene. Exons are represented by gray boxes numbered, from 5' UTR to 3' UTR in Latin numbers. Lengths between adjacent exons are indicated above each intron. The resulting protein is shown beyond, with implication in intracytoplasmic (IC), transmembrane (TM), or extracellular (EC) domains of the coding sequence of each exon.⁷

2.4.2 Transcriptional regulation of *CD40L* expression

As for *CD40*, *CD40L* expression is regulated at transcriptional, post-transcriptional and post-translational levels. Schubert *et al.* showed that two nuclear factor of activated T cells (NF-AT) binding sites in the 5' flank region of the human *CD40L* gene (Figure 9) contribute substantially and independently to the promoter function in activated T cells.³³ In addition to NF-AT, NF- κ B regulates *CD40L* expression in activated primary human T lymphocytes.³⁴ Constitutive interaction between NF- κ B c-Rel and NF-ATc1 proteins at the *CD40L* promoter leads to the synergistic activation of *CD40L* expression in aggressive B-cell lymphoma, raising

³⁰ Allen, R C, et al. (1993). CD40 ligand gene defects responsible for X-linked hyper-IgM syndrome. *Science* 259, 990.

³¹ Villa, A, et al. (1994). Organization of the human *CD40L* gene: implications for molecular defects in X chromosome-linked hyper-IgM syndrome and prenatal diagnosis. *Proc Natl Acad Sci U S A* 91, 2110.

³² Tsitsikov, E N, et al. (1994). Structure of the mouse *CD40* ligand gene. *Mol Immunol* 31, 895.

³³ Schubert, L A, et al. (1995). The human gp39 promoter. Two distinct nuclear factors of activated T cell protein-binding elements contribute independently to transcriptional activation. *J Biol Chem* 270, 29624.

³⁴ Srahna, M, et al. (2001). NF-kappaB is involved in the regulation of CD154 (CD40 ligand) expression in primary human T cells. *Clin Exp Immunol* 125, 229.

CHAPTER 2

a possible mechanism for autonomous neoplastic B-cell growth.³⁵ Furthermore, both calcineurin and calcium/calmodulin-dependent kinase IV was shown to be implicated and to act synergistically in the calcium-dependent activation of CD40L gene expression.³⁶ The mouse promoter contains four putative NF-AT-like motifs (Figure 9) that recruit two members of the NF-AT family, forming in the presence of the nuclear component AP-1 (itself composed of the Fos and Jun proteins) a transcriptionally active complex.³⁷

Of interest, the 3'-flanking segment of the human *CD40L* gene contains NF- κ B/Rel binding site in an open chromatin configuration region to which binds p50. This element acts as an orientation-independent enhancer of the *CD40L* transcription.³⁸ Further experimental data demonstrated that the *CD40L* gene is under the regulation of many more elements, including CD28 response element,³⁹ the AT-hook transcription factor ANKA,⁴⁰ early growth response-1 (EGR-1),⁴¹ and the Mit consensus E-boxes recognized by TFE3 and TFEB (Figure 9).⁴² Recently, a new NF-AT recognition motif was found by phylogenetic analysis on primates, dog and cow promoter sequences (Figure 9).⁴³ In this study, some of the transcription binding elements have been found across all the 22 mammals tested, while others are specific to particular orders of mammals.

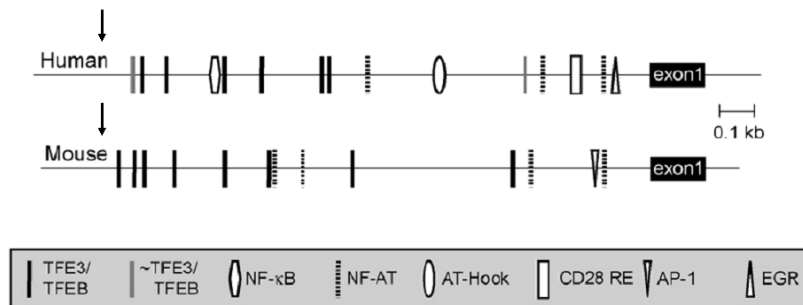


Figure 9. Putative cis-regulatory elements located within the human and mouse *CD40L* promoters. Binding sites for diverse transcription factors within the human (upper) and mouse (lower) promoter are represented respectively to the symbol indicated under. The novel NF-AT recognition site is represented by the arrow.⁴³

³⁵ Pham, L V, et al. (2005). Constitutive NF-kappaB and NFAT activation in aggressive B-cell lymphomas synergistically activates the CD154 gene and maintains lymphoma cell survival. *Blood* 106, 3940.

³⁶ Lobo, F M, et al. (1999). Calcium-dependent activation of TNF family gene expression by Ca²⁺/calmodulin kinase type IV/Gr and calcineurin. *J Immunol* 162, 2057.

³⁷ Tsytsykova, A V, et al. (1996). The CD40L promoter contains nuclear factor of activated T cells-binding motifs which require AP-1 binding for activation of transcription. *J Biol Chem* 271, 3763.

³⁸ Schubert, L A, et al. (2002). A T cell-specific enhancer of the human CD40 ligand gene. *J Biol Chem* 277, 7386.

³⁹ Parra, E, et al. (2001). Identification of a CD28 response element in the CD40 ligand promoter. *J Immunol* 166, 2437.

⁴⁰ Siddiq, A, et al. (2001). Regulation of CD40 and CD40 ligand by the AT-hook transcription factor ANKA. *Nature* 410, 383.

⁴¹ Lindgren, H, et al. (2001). Regulation of transcriptional activity of the mouse CD40 ligand promoter in response to signals through TCR and the costimulatory molecules CD28 and CD2. *J Immunol* 166, 4578; Cron, R Q, et al. (2006). Early growth response-1 is required for CD154 transcription. *J Immunol* 176, 811.

⁴² Huan, C, et al. (2006). Transcription factors TFE3 and TFEB are critical for CD40 ligand expression and thymus-dependent humoral immunity. *Nat Immunol* 7, 1082.

⁴³ Steiper, M E, et al. (2006). Phylogenetic analysis of the promoter region of the CD40L gene in primates and other mammals. *Infect Genet Evol* (doi:10.1016/j.meegid.2006.12.004).

2.4.3 Post-transcriptional regulation of *CD40L* expression

Post-transcriptional modulation of *CD40L* expression primarily involves mRNA stability. Extensive activation of T cells with anti-CD3 mAb induced stabilization of the *CD40L* transcript in parallel to a graded decrease in its expression.⁴⁴ This contrast with its rapid upregulation and destabilization in response to early T cell activation. Human endothelial cells also induce stabilization of *CD40L* mRNA in PMA-activated T cells through a CD58-dependent mechanism.⁴⁵

The 3' non-coding region of the *CD40L* gene contains AUUUA motifs.⁴⁶ Non-AU-rich elements were also shown to be involved in the stabilization of *CD40L* mRNA. For example, a p25 RNA binding protein binds to these distinct cis-acting regions unless stimulation of T cells with PMA and/or ionomycin.⁴⁷

2.4.4 Post-translational regulation of *CD40L* expression

A second potential translation start site was suggested at position 61. It was located just before the transmembrane domain (Figures 7 and 8), raising the possibility of the generation of a secreted form, with the hydrophobic region serving as a signal peptide. Besides the lack of a consensus Kozak sequence and the absence of evidence for alternatively spliced forms or for use of alternate transcription start site,⁴⁸ Northern blot analysis of activated T cells revealed a major *CD40L* mRNA species of 1.8–2.1 kb.²⁸

In fact, a 31-kDa form lacking the cytoplasmic tail, which sequence begins at Met21, and found in hetero-multimeric *CD40L* complexes at the cell surface of human T cells, was thought to be processed by proteolysis during delivery at the membrane.⁴⁹ Soluble form of *CD40L* (s*CD40L*) was observed in culture supernatants from T cells activated *in vitro*,²⁰ and in the serum of patients with B cell lymphoma,⁵⁰ acute coronary syndrome unstable angina,⁵¹

⁴⁴ Ford, G S, et al. (1999). Regulation of CD154 (CD40 ligand) mRNA stability during T cell activation. *J Immunol* 162, 4037.

⁴⁵ Murakami, K, et al. (1999). Human endothelial cells augment early CD40 ligand expression in activated CD4+ T cells through LFA-3-mediated stabilization of mRNA. *J Immunol* 163, 2667.

⁴⁶ Gauchat, J F, et al. (1993). Human CD40-ligand: molecular cloning, cellular distribution and regulation of expression by factors controlling IgE production. *FEBS Lett* 315, 259.

⁴⁷ Rigby, W F, et al. (1999). Characterization of RNA binding proteins associated with CD40 ligand (CD154) mRNA turnover in human T lymphocytes. *J Immunol* 163, 4199.

⁴⁸ Graf, D, et al. (1995). A soluble form of TRAP (CD40 ligand) is rapidly released after T cell activation. *Eur J Immunol* 25, 1749.

⁴⁹ Hsu, Y M, et al. (1997). Heteromultimeric complexes of CD40 ligand are present on the cell surface of human T lymphocytes. *J Biol Chem* 272, 911.

⁵⁰ Younes, A, et al. (1998). Elevated levels of biologically active soluble CD40 ligand in the serum of patients with chronic lymphocytic leukaemia. *Br J Haematol* 100, 135.

CHAPTER 2

hypercholesterolemia,⁵² inflammatory bowel disease,⁵³ systemic lupus erythematosus (SLE),⁵⁴ and also during atherosclerosis.⁵⁵ This is frequently associated with platelet activation. Recently, significantly higher levels of sCD40L were detected in both cerebrospinal fluid and plasma from HIV-1–infected patients impaired with HIV-1–associated dementia than in non–impaired counterparts, and were shown to act in synergy with Tat in the release of TNF α from monocytes.⁵⁶

Some data suggest that soluble, but still biologically active, 15 to 18–kDa CD40L is cleaved inside microsomes at Met113–Gln114, and lacks the transmembrane domain.⁵⁷ Other groups have demonstrated the implication of the Zn²⁺–dependent metalloproteinase ADAM-10, which can act at least partially at the cell surface.⁵⁸ We can imagine the generation of sCD40L from a fraction of membrane–bound CD40L internalized subsequent to receptor–mediated endocytosis.⁵⁹ Finally, the 18–kDa soluble form was found in cell surface hetero-multimeric complexes with the 33–kDa CD40L and the form lacking the cytoplasmic domain. This suggests that a proteolytic process of the trimeric full length CD40L has occurred during its transport to the plasma membrane.⁴⁹ Other forms of downregulation of CD40L expression include capping and receptor-mediated endocytosis mediated by CD40,⁶⁰ and blocking by soluble CD40.⁶¹

⁵¹ Aukrust, P, et al. (1999). Enhanced levels of soluble and membrane-bound CD40 ligand in patients with unstable angina. Possible reflection of T lymphocyte and platelet involvement in the pathogenesis of acute coronary syndromes. *Circulation* 100, 614.

⁵² Cipollone, F, et al. (2002). Association between enhanced soluble CD40L and prothrombotic state in hypercholesterolemia: effects of statin therapy. *Circulation* 106, 399.

⁵³ Danese, S, et al. (2003). Activated platelets are the source of elevated levels of soluble CD40 ligand in the circulation of inflammatory bowel disease patients. *Gut* 52, 1435.

⁵⁴ Vakkalanka, R K, et al. (1999). Elevated levels and functional capacity of soluble CD40 ligand in systemic lupus erythematosus sera. *Arthritis Rheum* 42, 871; Kato, K, et al. (1999). The soluble CD40 ligand sCD154 in systemic lupus erythematosus. *J Clin Invest* 104, 947.

⁵⁵ Vishnevetsky, D, et al. (2004). CD40 ligand: a novel target in the fight against cardiovascular disease. *Ann Pharmacother* 38, 1500.

⁵⁶ Sui, Z, et al. (2007). Functional Synergy between CD40 Ligand and HIV-1 Tat Contributes to Inflammation: Implications in HIV Type 1 Dementia. *J Immunol* 178, 3226.

⁵⁷ Pietravalle, F, et al. (1996). Human native soluble CD40L is a biologically active trimer, processed inside microsomes. *J Biol Chem* 271, 5965; Ludewig, B, et al. (1996). Induction, regulation, and function of soluble TRAP (CD40 ligand) during interaction of primary CD4+ CD45RA+ T cells with dendritic cells. *Eur J Immunol* 26, 3137.

⁵⁸ Matthies, K M, et al. (2006). Differential regulation of soluble and membrane CD40L proteins in T cells. *Cell Immunol* 241, 47.

⁵⁹ Kiessling, L L, et al. (1998). Transforming the cell surface through proteolysis. *Chem Biol* 5, R49.

⁶⁰ Yellin, M J, et al. (1994). CD40 molecules induce down-modulation and endocytosis of T cell surface T cell-B cell activating molecule/CD40-L. Potential role in regulating helper effector function. *J Immunol* 152, 598.

⁶¹ Grammer, A C, et al. (1995). The CD40 ligand expressed by human B cells costimulates B cell responses. *J Immunol* 154, 4996.

CHAPTER 2

2.5 Three-dimensional view of the CD40–CD40L interaction

2.5.1 The TNF/TNF-R superfamily

Decades earlier was discovered TNF α , a cytokine that is toxic for neoplastic cell lines but not for mouse embryo cultures.⁶² In parallel, the non-specifically toxic lymphotoxin (LT), also named LT α or TNF β , was described to be released by activated lymphocytes.⁶³ When cDNA of these two proteins were cloned,⁶⁴ they were shown to be similar, and thus were the first classified members of the TNF family. This family is now composed of 19 different ligands, encoded by 18 genes, which interact with 29 different receptors (Figure 10), classified in the TNF-R family.⁶⁵ A comprehensive survey of ligand-receptor interactions and cross-species reactivity within human and mouse TNF and TNF-R families was recently achieved.⁶⁶ The system used 293T cells expressing the extracellular domain of each receptor, which was anchored to the membrane via a glycosylated phosphatidylinositol link, and soluble fusion ligands comprising the extracellular domain hexamerized by an Fc portion of human IgG₁. All the tested interactions were strictly specific, although a weak interaction between human TNF and mouse TNF-R2 has been detected after oligomerization of the ligand. Some ligand/receptor pairs were shown to be partially species-specific. For example, the mouse CD40L recognized both human and mouse receptors, but the mouse CD40 was not recognized by the human CD40L. Finally, some TNF-Rs were not bound by any known TNF ligands, suggesting that other members of the TNF family remain to be identified.

Additional general informations are shown in Table 3 derived from the extensive work of Locksley *et al.* who have summarized the structure, function and gene locations of all the TNF/TNF-R superfamily members.⁶⁷

⁶² Carswell, E A, et al. (1975). An endotoxin-induced serum factor that causes necrosis of tumors. *Proc Natl Acad Sci U S A* 72, 3666.

⁶³ Granger, G A, et al. (1968). Lymphocyte in vitro cytotoxicity: mechanisms of immune and non-immune small lymphocyte mediated target L cell destruction. *J Immunol* 101, 111.

⁶⁴ Pennica, D, et al. (1984). Human tumour necrosis factor: precursor structure, expression and homology to lymphotoxin. *Nature* 312, 724; Gray, P W, et al. (1984). Cloning and expression of cDNA for human lymphotoxin, a lymphokine with tumour necrosis activity. *Nature* 312, 721.

⁶⁵ Bodmer, J L, et al. (2002). The molecular architecture of the TNF superfamily. *Trends Biochem Sci* 27, 19.

⁶⁶ Bossen, C, et al. (2006). Interactions of tumor necrosis factor (TNF) and TNF receptor family members in the mouse and human. *J Biol Chem* 281, 13964.

⁶⁷ Locksley, R M, et al. (2001). The TNF and TNF receptor superfamilies: integrating mammalian biology. *Cell* 104, 487.

CHAPTER 2

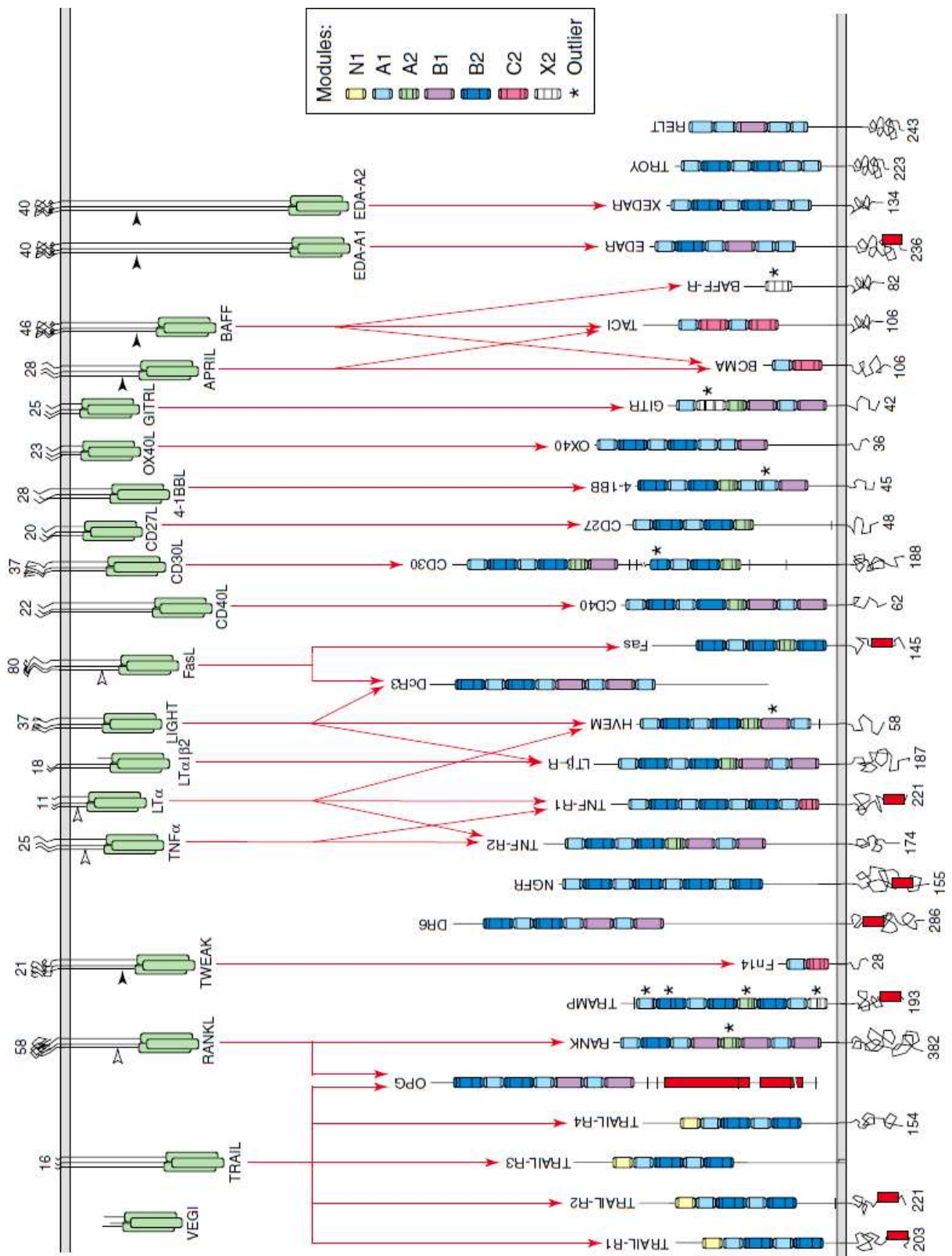


Figure 10. Interaction network between proteins of the TNF and TNF-R families.

Effective interactions are represented by a red arrow. Module composition of the extracellular domains is schematized for each TNF-R family members and will be discussed later. See text for detailed informations.⁶⁵

CHAPTER 2

Table 3. General data on the TNF/TNF-R superfamily members⁶⁷

Standardized	Other Names	Accession	Human Chromosome	Mouse Chromosome	Phenotypes associated with mutations	Additional functional observations
Receptor						
NGFR	TNFRSF16 p75	M14764	17q21-q22	11, 55.6 cM	Defective sensory neuron innervation; impaired heat sensitivity	
Troy	TNFRSF19 Taj	AF167555	13q12.11-12.3	14		Expressed in hair follicles and epithelium; the mouse gene is located near the waved coat locus.
EDAR		AF130988	2q11-q13	10, 29.0 cM	Hypohydrotic ectodermal dysplasia – abnormal tooth, hair and sweat gland formation	
XEDAR	EDA-A2R		AF298812	X		Likely role in skin, hair and tooth formation
CD40	TNFRSF5 p50, Bp50	X60592	20q12-q13.2	2, 97.0 cM	Defective Ig class switching and GC formation causing immunodeficiency	
DcR3	TNFRSF6B	AF104419	20q13			Secreted decoy receptor for FasL with possible role in tumor evasion
FAS	TNFRSF6 CD95, APO-1, APT1	M67454	10q24.1	19, 23.0 cM	Impaired activation-induced T cell death; lymphoproliferation; autoimmunity (ALPS)	
OX40	TNFRSF4 CD134, ACT35, TXGP1L	X75962	1p36	4, 79.4 cM	Defective T cell responses	
AITR	TNFRSF18 GITR	AF125304	1p36.3	4		Glucocorticoid-induced; inhibits T cell receptor-dependent apoptosis
CD30	TNFRSF8 Ki-1, D1S166E	M83554	1p36	4, 75.5 cM		Marker of Reed-Stemberg cells in Hodgkin's disease
HveA	TNFRSF14 HVEM, ATAR, TR2, LIGHTR	U70321	1p36.3-p36.2			Probable role in T cell proliferation and receptor for herpes simplex virus
4-1BB	TNFRSF9 CD137, ILA	L12964	1p36	4, 75.5 cM		Probable role in T cell responses
TNFR2	TNFRSF1B CD120b, p75, TNFR, TNFR80, TNF-R-II	M32315	1p36.3-p36.2	4, 75.5 cM	Increased sensitivity to bacterial pathogens; decreased sensitivity to LPS; reduced antigen-induced T cell apoptosis	
DR3	TNFRSF12 TRAMP, WSL-1, LARD, WSL-LR, DDR3, TR3, APO-3	U72763	1p36.2			A linked, partially duplicated copy of the gene encodes a potential decoy receptor
CD27	TNFRSF7 Tp55, S152	M63928	12p13	6, 60.35 cM	Defective T cell responses	
TNFR1	TNFRSF1A CD120a p55-R, TNFR, TNFR60 TNF-R-I	M75866	12p13.2	6, 60.55 cM	Impaired clearance of bacterial pathogens; resistance to LPS; LN present; defective GC formation; defective PP formation	
LT β R	TNFRSF3 TNFR2-RP, TNFCR, TNF-R-III	L04270	12p13	6, 60.4 cM	Absence of LN, PP; defective GC formation	
RANK	TNFRSF11A TRANCE-R	AF018253	18q22.1		Osteopetrosis; absence of osteoclasts; absence of lymph nodes; PP present; abnormal B cell development	Required for lactating mammary gland development
TACI	CAML interactor		AF023614	17p11	11	Probable role in B cell responses
BCMA	TNFRSF17 BCM	Z29574	16p13.1			Probable role in B cell responses
DR6	TR7	NM_014452	6p21.1-12.2			

(...)

CHAPTER 2

Table 3 (continued). General data on the TNF/TNF-R superfamily members⁶⁷

OPG	TNFRSF11B	OCIF, TR1 osteoprotegerin	U94332	8Q24		Osteoporosis; arterial calcification
DR4	TNFRSF10A	Apo2, TRAILR-1	U90875	8p21		Probable inducer of lymphocyte death and activation
DR5	TNFRSF10B	KILLER, TRICK2A, TRAIL-R2, TRICKB	AF012628	8p22-p21		Probable inducer of lymphocyte death and activation
DcR1	TNFRSF10C	TRAILR3, LIT, TRID	AF012536	8p22-p21		GPI-linked decoy receptor—interferes with TRAIL signaling
DcR2	TNFRSF10D	TRUNDD TRAILR4	AF029761	8p21		Transmembrane decoy receptor—interferes with TRAIL signaling
Ligand						
EDA		EDA1	NM_001399	Xq12-q13.1	X, 37.0 cM	Hypohydrotic ectodermal dysplasia – abnormal tooth, hair and sweat gland formation
CD40L	TNFSF5	IMD3, HIGM1, TRAP, CD154, gp39	X67878	Xq26	X, 18.0 cM	Defective T cell and IgG responses; hyper IgM syndrome
FasL	TNFSF6	APT1LG1	U11821	1q23	1, 85.0 cM	Impaired activation-induced T cell death; lymphoproliferation; autoimmunity; ALPS
OX40L	TNFSF4	gp34 TXGP1	D90224	1q25	1, 84.9 cM	Defective T cell responses
AITRL	TNFSF18	TL6, hGITRL	AF125303	1q23		Inhibits T cell receptor-dependent apoptosis
CD30L	TNFSF8		L09753	9q33	4, 32.2 cM	Possible role in malignant lymphocyte disorders
VEGI	TNFSF15	TL1	AF039390			Potential vascular endothelial cell growth inhibitor
LIGHT	TNFSF14	LT ₁ , HVEM-L	AF036581	19 (probable)	17	
4-1BBL	TNFSF9		U03398	19p13.3	17	Defective T cell responses
CD27L	TNFSF7	CD70	L08096	19p13	17, 20.0 cM	
LT _α	TNFSF1	TNFB, LT	X01393	6p21.3	17, 19.06 cM	Absence of LN and PP; disorganized splenic microarchitecture; defective GC formation
TNF	TNFSF2	tumor necrosis factor; cachectin, TNFA, DIF	X01394	6p21.3	17, 19.06	LN present; defective GC formation; increased susceptibility to microbial pathogens
LT _β	TNFSF3	TNFC, p33	L11015	6p21.3	17, 19.061	Absence of peripheral LN and PP; presence of mesenteric and some cervical LN; defective GC formation
TWEAK	TNFSF12	DR3L APO3L	AF030099	17p13	11?	Potential role in monocyte and NK cell cytotoxicity
APRIL	TNFSF13		NM_003808	17p13.1	11?	Probable role in B cell responses
BLYS	TNFSF13B	BAFF, THANK, TALL1	AF132600	13q32-34		Probable role in B cell responses
RANKL	TNFSF11	TRANCE, OPGL, ODF	AF013171	13q14	14, 45.0	Osteopetrosis; absence of osteoclasts; absence of lymph nodes; PP present; normal splenic architecture; abnormal B cell and T cell development
TRAIL	TNFSF10	Apo-2L TL2	U37518	3q26		

2.5.2 The TNF family proteins

TNF family members are type II transmembrane proteins with intracellular N-ter and extracellular C-terminus region (C-ter). Active TNF ligands form non-covalent C_3 symmetric homotrimers at the cell surface. LT is an exception as it can form both the $LT\alpha_2\beta_1$ and $LT\alpha_1\beta_2$ hetero-trimers.⁶⁸

They are characterized by a conserved C-ter domain named TNF homology domain (THD), composed of a 150-amino acid long conserved sequence framework of aromatic and hydrophobic residues, as shown in the three-dimensional structure of the extracellular domain of CD40L on Figure 11.⁶⁹

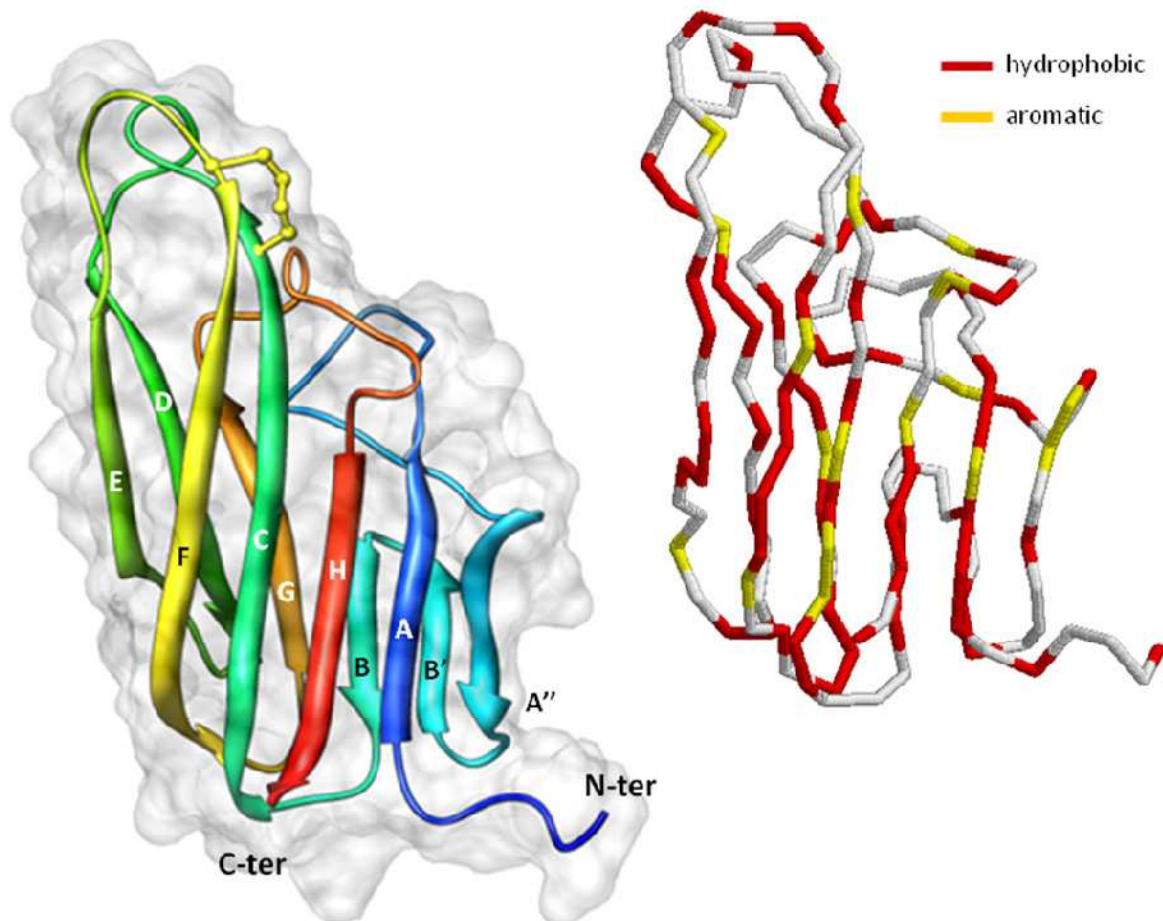


Figure 11. Structure of the TNF homology domain of human CD40L. Representations of the three-dimensional structure of the human CD40L extracellular domain (PDB code 1ALY). Cartoons drawing (left) indicates position of the ten β -strands, from the N-ter colored in blue (strand A), to the C-ter colored in red (strand H). Backbone drawing (right) indicates positions of hydrophobic (red) and aromatic (yellow) residues. The two representations are viewed from the same side.

⁶⁸ Browning, J L, et al. (1995). Characterization of surface lymphotoxin forms. Use of specific monoclonal antibodies and soluble receptors. *J Immunol* 154, 33.

⁶⁹ Karpusas, M, et al. (1995). 2 A crystal structure of an extracellular fragment of human CD40 ligand. *Structure* 3, 1031.

CHAPTER 2

The THDs are β -sandwich structures containing two stacked β -sheets, each composed of five anti-parallel strands that adopt a classical “jelly-roll” or Greek key topology (Figure 12).⁷⁰

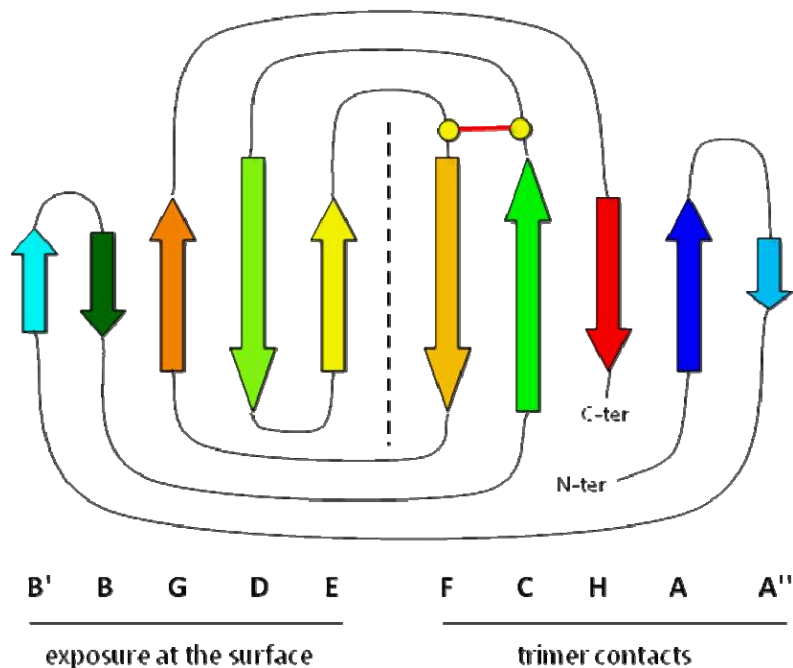


Figure 12. Topology of the TNF homology domain of human CD40L. Representation of the “jelly-roll” or Greek key topology of the human CD40L extracellular domain determined from its three-dimensional structure (Figure 11). β -strands are represented by arrows, from the N-ter (blue) to the C-ter (red), and named from A to H. The structural functions of the sheets are indicated. The disulfide bond is indicated as a red link between two cysteines represented by two yellow points.

The inner sheet, composed of the strands A, A'', H, C and F, is involved in contacts between monomers. The outer sheet, composed of the strands B, B', D, E and G, is exposed at the surface (Figure 12). One edge of each monomer, constituted of the strands E and F, interacts with the hydrophobic inner sheet of its neighbor resulting in a very stable trimer. As in TNF, FasL, LIGHT, VEGI, CD30L and CD27L, CD40L contains a single disulfide bond between the CD and EF loops that stabilizes the monomer. Some variability exists among members of the TNF family, as the disulfide bond location, or the presence of Zn^{2+} ion in the TRAIL structure. Nevertheless, interaction of TNF proteins with their cognate receptors is conferred by residues in the outer sheet.

2.5.3 The TNF-R family proteins

Receptors of the TNF-R family are primarily type I transmembrane proteins, with an extracellular N-ter and an intracellular C-ter. BCMA, TACI, BAFFR and XEDAR are lacking a

⁷⁰ Jones, E Y, et al. (1989). Structure of tumour necrosis factor. *Nature* 338, 225; Eck, M J, et al. (1989). The structure of tumor necrosis factor-alpha at 2.6 Å resolution. Implications for receptor binding. *J Biol Chem* 264, 17595.

CHAPTER 2

signal peptide, that is why they are termed type III transmembrane proteins. TRAIL-R3 is anchored by a covalently linked C-terminal glycolipid. OPG and DcR3 lack a transmembrane-interacting domain and are mainly secreted. In contrast, CD30, CD40, TNF-R1 and TNF-R2 can be processed under regulations to soluble forms by proteolytic cleavage or alternative splicing.

Primary sequence comparisons within the extracellular domain of TNF-Rs have defined the presence of cysteine-rich domains (CRD). These motifs are pseudo-repeats that contain six cysteines engaged in three disulfide bonds, as seen in the three-dimensional structure of soluble TNF-R1 (Figure 13).⁷¹

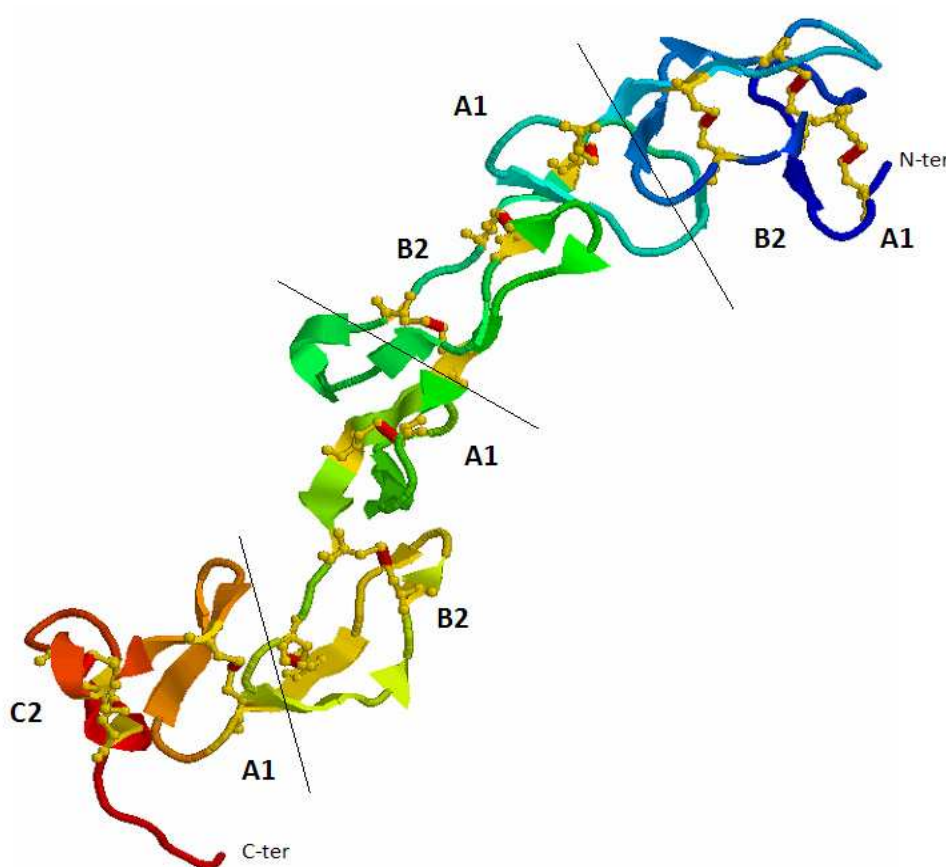


Figure 13. Three-dimensional structure of human TNF-R1. Cartoon representation of the human TNF-R1 extracellular domain (PDB code 1EXT). Disulfide bonds are represented in ballsticks. CRD modules are indicated.

The repeated and regular arrangement of CRDs confers to the receptor an elongated and stable shape (Figure 13). Each module type is designated by a letter and the number of disulfide bridges it contains (Figure 10). For example, A1 modules are 12–27 residues long, consisting of three short β -strands linked by turns, and a single disulfide bridge connecting strands 1 and 3. That yields a characteristic C-shaped structure. A2 modules contain a

⁷¹ Naismith, J H, et al. (1996). Seeing double: crystal structures of the type I TNF receptor. *J Mol Recognit* 9, 113.

CHAPTER 2

second disulfide bridge. B modules are 21–24 amino acids long and comprise three anti-parallel strands adopting a “paper-clip” S-shaped fold. Other modules exist but are less usual as the C2 module retrieved in soluble TNF-R1, the N terminal N2 module in TRAIL, and the non-structurally defined module X2 in TRAMP, GITR and BAFFR (Figure 10).

A typical CRD is composed of A1–B2, as in the structure of soluble TNF-R1 (Figure 13). Different other pairs of modules give the specificity to each receptor. All of them play distinct structural roles in the architecture of the domains.⁷²

2.5.4 The three-dimensional structure of CD40L

CD40L crystal structure was the third structure of the family resolved after TNF α and LT α . Before that, three-dimensional models of the extracellular regions of mouse⁷³ and human CD40L⁷⁴ have been constructed based on the similarity in primary structures between the CD40L and TNFs, with the known three-dimensional structure of TNF α used as a template.⁷⁰ These models were useful to analyze the location of CD40L mutations found in HIGM patients.⁷⁵

The human form is a 33-kDa transmembrane glycoprotein with a typical globular C-terminus extracellular THD of 25 Å × 30 Å × 50 Å dimensions, linked to the transmembrane domain by 65 residues. With respect to the TNF family, three monomers were shown to associate with a C₃ symmetry in a truncated pyramid shape. High homology within sequences of the β -sheets with TNF α , LT α , TRAIL, APRIL and BAFF was found, but significant variations in loops AA'', CD and EF that are implicated in the interaction with their cognate receptors.⁶⁹

Association between the monomers is mainly due to the tight interaction of two triads formed by the three Tyr170 and three His224 (Figure 14). These residues are located on β -strands C and F respectively on each monomer, along the three-fold axis, which is approximately parallel to the β -strands of each subunit, at the center of the homotrimer.

⁷² Naismith, J H, et al. (1998). Modularity in the TNF-receptor family. *Trends Biochem Sci* 23, 74.

⁷³ Peitsch, M C, et al. (1993). A 3-D model for the CD40 ligand predicts that it is a compact trimer similar to the tumor necrosis factors. *Int Immunol* 5, 233.

⁷⁴ Bajorath, J, et al. (1993). Knowledge-based model building of proteins: concepts and examples. *Protein Sci* 2, 1798.

⁷⁵ Aruffo, A, et al. (1993). The CD40 ligand, gp39, is defective in activated T cells from patients with X-linked hyper-IgM syndrome. *Cell* 72, 291.

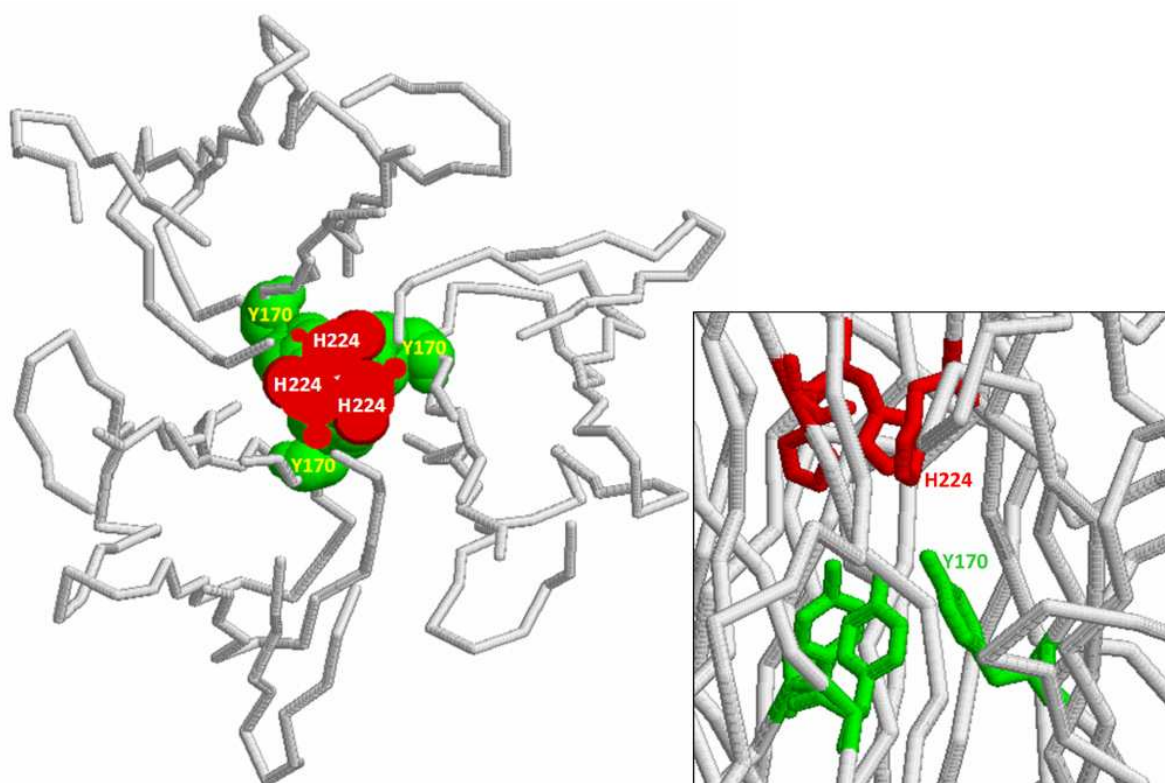


Figure 14. Structure of human CD40L. Backbone representations of the human CD40L extracellular domain (PDB code 1ALY) viewed from the top, from protein surface to cell membrane, in slab mode (left). Residues implicated in stabilization of the trimer protein are represented in spacefill. View from the side (right) where the same residues are drawn in sticks. His224 are colored in red, Tyr170 in green.

2.5.5 Three-dimensional model of the CD40–CD40L interaction

2.5.5.1 A three-dimensional model for CD40

Yet, no experimental structure of CD40 has been reported, but Bajorath constructed a detailed three-dimensional structure-based model of the TNFR-homologous extracellular region of human CD40. The crystal structure of the human TNF-R extracellular domain complexed with the human TNF β ⁷⁶ was used initially as a template to predict a preliminary model of the CD40 extracellular region.⁷⁷ Since a more accurate structure of unligated TNF-R is available, Bajorath *et al.* proposed an extended and refined model of the CD40 extracellular region with improved energies (Figure 15).⁷⁸

⁷⁶ Banner, D W, et al. (1993). Crystal structure of the soluble human 55 kd TNF receptor-human TNF beta complex: implications for TNF receptor activation. *Cell* 73, 431.

⁷⁷ Bajorath, J, et al. (1995). Analysis of gp39/CD40 interactions using molecular models and site-directed mutagenesis. *Biochemistry* 34, 9884.

⁷⁸ Bajorath, J, et al. (1997). Construction and analysis of a detailed three-dimensional model of the ligand binding domain of the human B cell receptor CD40. *Proteins* 27, 59.

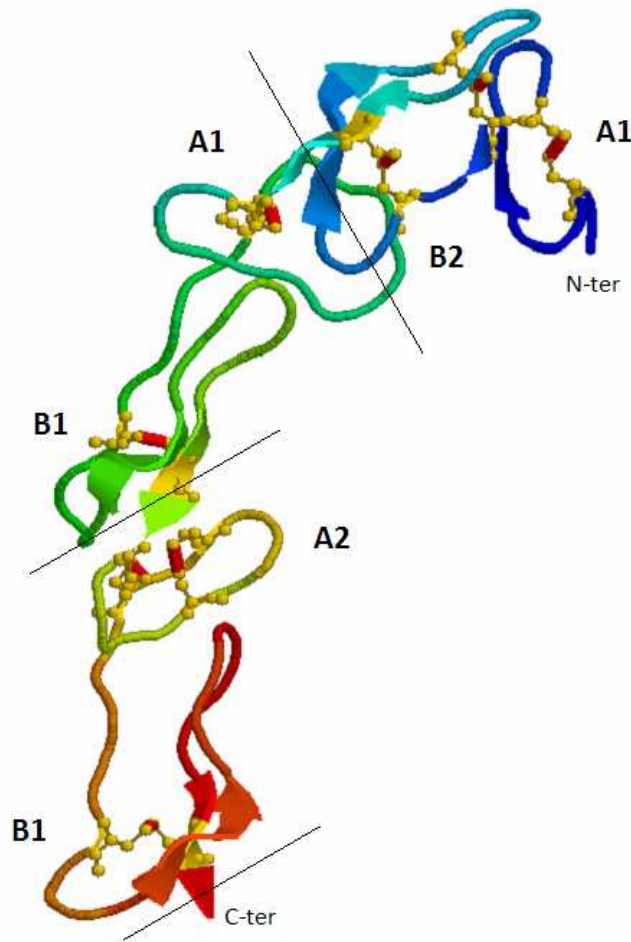


Figure 15. Three-dimensional model of human CD40. Cartoon representation of the three-dimensional model proposed for human CD40 extracellular domain (PDB code 1CDF).⁷⁸ Disulfide bonds are drawn in ballsticks. CRD modules are delineated.

Only three CRDs are shown on this model, the last C-ter CRD, composed of A1–B1, was omitted to avoid inaccuracies in the domain-domain orientation predictions.

2.5.5.2 Residues important for the CD40–CD40L interaction

Before any X-ray structure was obtained, a structure-based alignment of CD40L with TNF β allowed the preliminary identification of seven residues in the extracellular domain of CD40 and nine residues in CD40L which may be involved in CD40–CD40L interaction. Each of these residues was mutated, and soluble CD40 and CD40L mutants tested in various binding experiments. In this manner, CD40 residues Tyr82, Asp84 and Asn86 were demonstrated to be critical for CD40L binding. CD40 mutants Arg73 to Ala (Arg73-Ala) and Ser113-Ala have shown reduced binding in some assays suggesting a contribution of residues Arg73 and Ser113 in the CD40–CD40L interaction. CD40L mutants Lys143-Ala and Tyr145-Ala bound

CHAPTER 2

significantly less to CD40. Interestingly, N-glycosylation on CD40L does not appear to contribute to the interaction with CD40.⁷⁹

Extended mutagenesis experiments based on the molecular modeling of the CD40–CD40L complex have led to the identification of additional residues in CD40L (Tyr146, Arg203 and Gln220) and CD40 (Glu74, and Glu117) that contribute to the CD40–CD40L interaction. Thus two loop regions, Lys143 to Tyr146 in CD40L and Tyr82 to Asn86 in CD40, have been identified as “hot spots” for this interaction. Interestingly, mutation of Tyr145 to Phe in CD40L led to a fully functional CD40L mutant, suggesting that only the size of residue 145 is important for binding. The CD40 mutant Tyr82-Phe failed to interact with CD40L, indicating that the absence of the hydroxyl group on CD40 residue Tyr82 is sufficient to abrogate severely its interaction with CD40L. Finally, when looking at the CD40L molecular model, residues implicated in the CD40–CD40L interaction are located in distinct clusters suggesting that residues of two adjacent CD40L monomers are involved in the formation of the CD40 binding site (Figures 16–18).⁷⁹

2.5.5.3 Construction of a CD40–CD40L interaction model

Residues predicted to be important during the CD40–CD40L interaction were confirmed by Singh *et al.* who have generated a three-dimensional model of the CD40–CD40L complex (Figure 16). They used the known X-ray structure of the extracellular region of CD40L together with a model of CD40 based upon an alternative modular alignment of the TNF-R family as proposed by Naismith and Sprang.⁷²

All residue contacts involve domains 2 and 3 from CD40 (residues Ser65, Glu66, Thr70, Arg73, Glu74, His76, Cys77, His78, Gln79, Lys81, Tyr82, Asp84, Asn86, Thr112, Glu114, Ala115 and Glu117) with two subunits of the CD40L trimer (Ile127, Ser128, Glu129, Glu142, Lys143, Gly144, Tyr145, Tyr146, Cys178, Arg200, Phe201, Cys218, Gln220, Ser248, His249, Gly250, Thr251 and Gly252, and Ser185, Gln186, Ala187, Arg203 and Arg207 from the second symmetry related subunit) (Figure 16).

⁷⁹ Bajorath, J, et al. (1995). Identification of residues on CD40 and its ligand which are critical for the receptor-ligand interaction. *Biochemistry* 34, 1833.

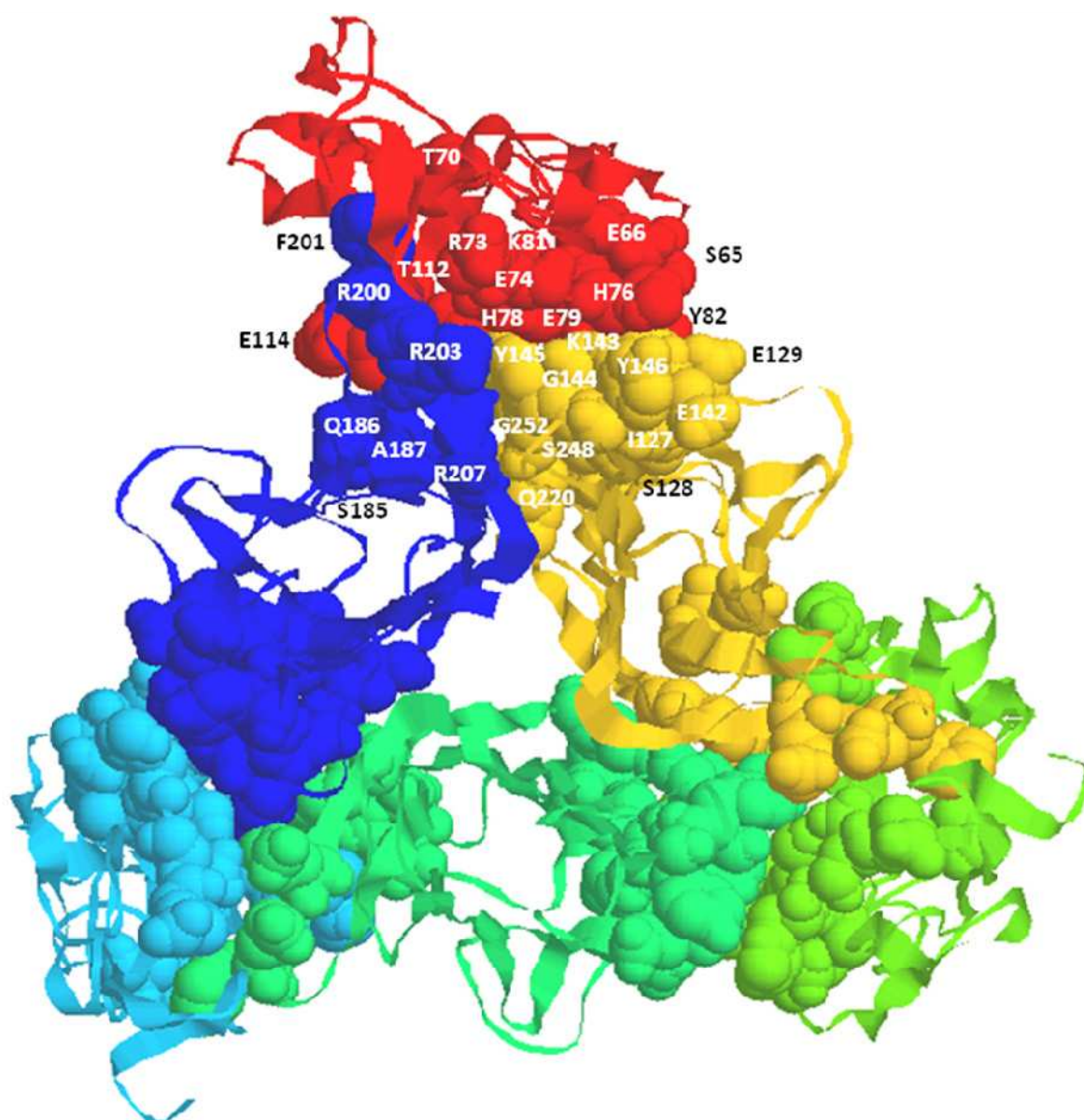


Figure 16. Residues implicated in the CD40–CD40L interaction. Ribbon/spacefill mixed representations of the CD40–CD40L interaction model, as proposed by Singh *et al.* (see text below; PDB file kindly provided from Dr. J. Singh).⁸⁰ Residues from CD40 (red, light blue and light green chains) and from CD40L (orange, dark blue and green chains) shown to be important for the interaction are represented as spacefill and named in one-letter code.

Contacts between basic and acidic residues include Glu74–Arg200, Glu74–Arg203, and with a separation distance greater than 5 Å Glu66–Lys143, Asp84–Arg207 and Glu117–Arg207 were calculated to stabilize the receptor–ligand complex (Figures 17 and 18).

⁸⁰ Singh, J, et al. (1998). The role of polar interactions in the molecular recognition of CD40L with its receptor CD40. *Protein Sci* 7, 1124.

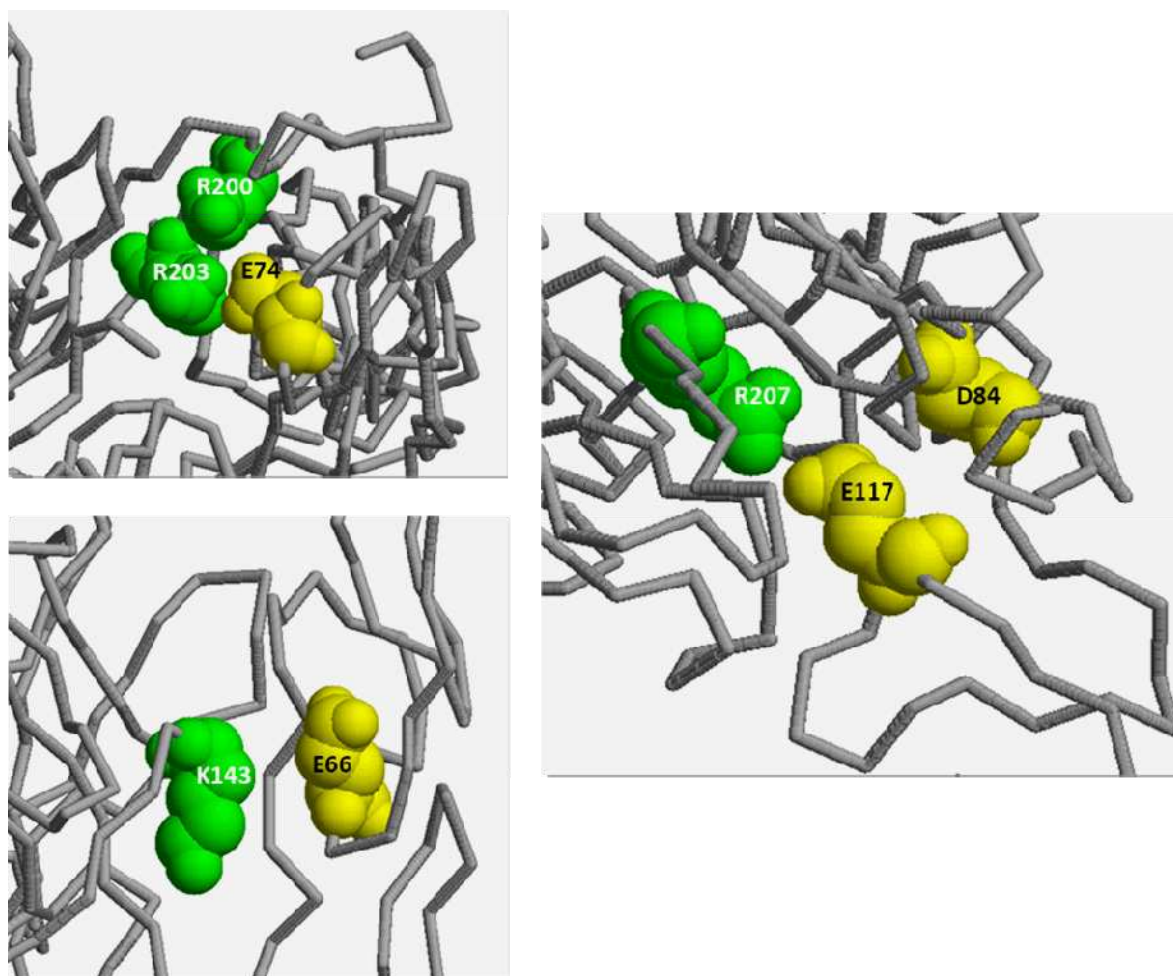


Figure 17. Residues involved in stabilization of the CD40–CD40L interaction. Backbone representations of the CD40–CD40L interaction model, as proposed by Singh *et al.* (PDB file kindly provided from Dr. J. Singh).⁸⁰ CD40 residues are colored in yellow, and CD40L residues are colored in green. The three views were obtained from the same model.

Further mutagenesis and binding studies indicated that the polar character of residues Lys143, Arg203 and Arg207 in CD40L is crucial for binding to CD40. Although Lys143-Arg mutation is tolerated, inversion of charge at this position by mutation to Glu not only abrogates the binding of CD40L to CD40, but also affects the integrity of the CD40L structure. Interestingly, mutation of Arg207 to Asn or Gln was tolerated suggesting that charge at this position is not crucial. But experimental identification of the residues essential for the binding of CD40L to its cognate receptor is still under wait for the accession of more detailed structural data at the atomic resolution.

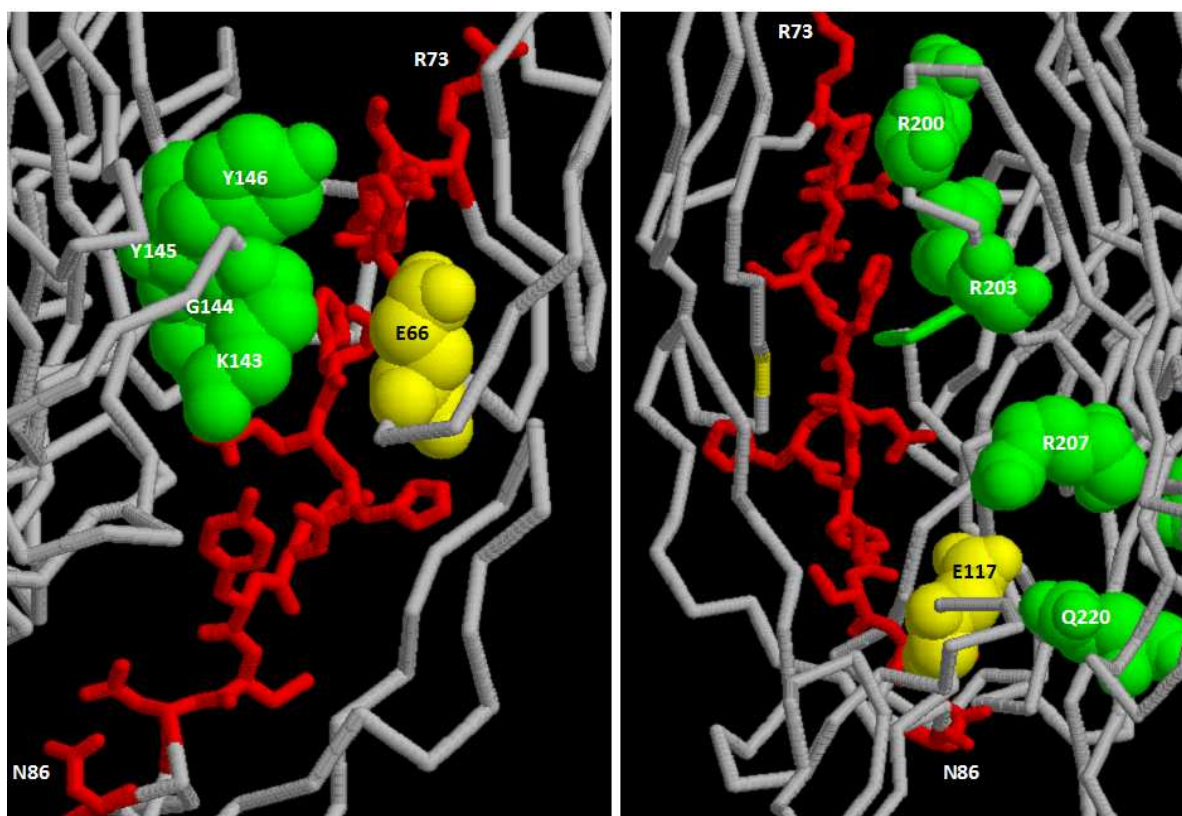


Figure 18. Summary of the residues implicated in the CD40–CD40L interaction. Mixed representations of the CD40–CD40L interaction model, as proposed by Singh *et al.* (PDB file kindly provided from Dr. J. Singh).⁸⁰ CD40 residues are colored in yellow, and CD40L residues in green. The left and right views are opposite.

2.5.6 Usefulness of the three-dimensional model of the CD40–CD40L interaction

Data detailed above were used to design a fusion protein consisting of CD40L Trp140 to Ser149 strand (WAEKGYTMS) inserted in the fifth external loop of the outer membrane protein C (OmpC) from *Salmonella typhi*.⁸¹ This construct has retained the capacity to form trimers, and specifically binds to CD40 as seen by enzyme-linked immunosorbent assay (ELISA) and immunofluorescence on human Raji B cell lymphoma. Although it failed to activate B cells in the presence of IL-4, it induced expression of MHC-II, CD23 and CD80 molecules on Raji cells, suggesting that CD40L residues Trp140 to Ser149 are important for biological activity in the context of the OmpC.

This study demonstrated the importance of structural information and site-directed mutagenesis data for the design of agonistic molecules mimicking the natural CD40L.

⁸¹ Vega, M I, et al. (2003). A *Salmonella typhi* OmpC fusion protein expressing the CD154 Trp140-Ser149 amino acid strand binds CD40 and activates a lymphoma B-cell line. *Immunology* 110, 206.

CHAPTER 3

CELL SIGNALING INITIATED FROM CD40

CHAPTER 3

3.1 CD40 clustering and downstream signaling

3.1.1 Consequences of membrane receptor crosslinking in cell signaling

As shown in chapter 1, CD40 crosslinking on B cell is a prerequisite for their activation. Anti-CD40 mAb F(ab) fragments are less active, and non-crosslinked anti-CD40 mAb can induce B cell proliferation only in the presence of a costimulus. Moreover, soluble CD40L in trimeric form activates B cell potently in the presence of costimuli, whereas membrane form is directly mitogenic. These results confirmed preceding observations showing requirement of CD40 aggregation for optimal signaling.¹ Importantly, CD40L clustering on T cells, upon initial contact with its cognate receptor, is required for aggregation of CD40 on B lymphocytes.²

Bjorck *et al.* proposed that both CD40 crosslink degree and efficiency might determine strength of the cell signaling.³ This crosslinking requirement has also been observed with other members of the TNF-R family. For example, Fas signaling requires hexameric FasL for organization of the death-inducing signaling complex (DISC), in which receptor oligomerization increases its avidity for FasL, and the efficient induction of apoptosis.⁴

3.1.2 Minimal CD40 oligomerization requirement for activation of cell signaling

3.1.2.1 Extracellular oligomerization

Although monomeric CD40L is unable to induce B cell proliferation, it binds to CD40, upregulates expression of class II molecules,⁵ and promotes rescue of B cells from apoptosis.⁶ This suggests that the receptor crosslinking level necessary for the initiation of some responses might vary among type and differentiation stage of a cell.⁷ This is consistent

¹ Paulie, S, et al. (1989). The human B lymphocyte and carcinoma antigen, CDw40, is a phosphoprotein involved in growth signal transduction. *J Immunol* 142, 590.

² Grassme, H, et al. (2002). Clustering of CD40 ligand is required to form a functional contact with CD40. *J Biol Chem* 277, 30289.

³ Bjorck, P, et al. (1994). Antibodies to distinct epitopes on the CD40 molecule co-operate in stimulation and can be used for the detection of soluble CD40. *Immunology* 83, 430.

⁴ Holler, N, et al. (2003). Two adjacent trimeric Fas ligands are required for Fas signaling and formation of a death-inducing signaling complex. *Mol Cell Biol* 23, 1428.

⁵ Fanslow, W C, et al. (1994). Structural characteristics of CD40 ligand that determine biological function. *Semin Immunol* 6, 267.

⁶ Pound, J D, et al. (1999). Minimal cross-linking and epitope requirements for CD40-dependent suppression of apoptosis contrast with those for promotion of the cell cycle and homotypic adhesions in human B cells. *Int Immunol* 11, 11.

⁷ van Kooten, C, et al. (2000). CD40-CD40 ligand. *J Leukoc Biol* 67, 2.

CHAPTER 3

with observation that, at levels higher than 5×10^5 of CD40 molecules in a transfected cell, the NF- κ B pathway is activated in the absence of CD40L.⁸

Moreover, hexameric and dodecameric forms of CD40L were shown to be more potent than the trimeric form in induction of B cell proliferation and expression of costimulatory molecules,^{4,9} although these two forms induced similar level of MHC II molecule expression. In contrast, trimeric and hexameric CD40L were shown to activate similar levels of NF- κ B and p38 pathways in CD40-transfected cells.¹⁰ Surprisingly, aggregated anti-CD40 mAb as well as soluble trimeric CD40L were unable to mediate IL-6 production in B cells, in contrast to membrane-bound CD40L.¹¹ Thus, insufficient CD40 crosslinking could not explain entirely the non-activity of anti-CD40 mAb.

In the case of CD95, apoptosis is induced by agonistic mAb as efficiently as by natural ligand. Since CD95 microaggregation is induced by agonistic mAb but not by CD95L, receptor clustering is not a prerequisite for initiation of cell death.¹² This suggests that CD40 aggregation could not account alone for the differences in cell signaling activated by diverse stimuli.

3.1.2.2 Intracellular oligomerization

During transfection experiments, dimeric construct of the CD40 cytoplasmic domain was shown to be sufficient for activation of the NF- κ B pathway, although trimerization generated a stronger signal.¹³ Targeting of trimeric domain to the membrane by meristoylation provided maximal activation of NF- κ B. Accordingly, disulfide-linked CD40/CD40 homodimers¹⁴ were observed in CD40-transfected and EBV-positive cells, and their levels rapidly increased upon CD40 oligomerization by either trimeric CD40L or crosslinked anti-CD40 mAb.¹⁵ Interestingly, CD40/CD40 dimer formation was demonstrated

⁸ Kaykas, A, et al. (2001). CD40 and LMP-1 both signal from lipid rafts but LMP-1 assembles a distinct, more efficient signaling complex. *Embo J* 20, 2641.

⁹ Haswell, L E, et al. (2001). Analysis of the oligomeric requirement for signaling by CD40 using soluble multimeric forms of its ligand, CD154. *Eur J Immunol* 31, 3094.

¹⁰ Pullen, S S, et al. (1999). High-affinity interactions of tumor necrosis factor receptor-associated factors (TRAFs) and CD40 require TRAF trimerization and CD40 multimerization. *Biochemistry* 38, 10168.

¹¹ Baccam, M, et al. (1999). Membrane-bound CD154, but not CD40-specific antibody, mediates NF- κ B-independent IL-6 production in B cells. *Eur J Immunol* 29, 3855.

¹² Legembre, P, et al. (2003). Cutting edge: SDS-stable Fas microaggregates: an early event of Fas activation occurring with agonistic anti-Fas antibody but not with Fas ligand. *J Immunol* 171, 5659.

¹³ Werneburg, B G, et al. (2001). Molecular characterization of CD40 signaling intermediates. *J Biol Chem* 276, 43334.

¹⁴ Braesch-Andersen, S, et al. (1989). Biochemical characteristics and partial amino acid sequence of the receptor-like human B cell and carcinoma antigen CDw40. *J Immunol* 142, 562.

¹⁵ Reyes-Moreno, C, et al. (2004). CD40/CD40 homodimers are required for CD40-induced phosphatidylinositol 3-kinase-dependent expression of B7.2 by human B lymphocytes. *J Biol Chem* 279, 7799.

CHAPTER 3

to be critical for some but not all cellular events. It could thus serve as initiator for rapid extension of CD40 oligomerization, bringing receptor molecules into close proximity with one another, what is needed for certain biological functions.

3.1.3 Structural mechanisms governing initiation of intracellular signals

Different anti-CD40 mAbs were tested for competitive binding on B cells in the presence of soluble trimeric CD40L. Whereas all of them promoted B cell rescue from apoptosis, indicating that this phenomenon does not depend on the CD40 epitope, only those competing for the CD40L binding site induced homotypic adhesions.⁶ Furthermore, mAbs that poorly inhibited CD40L binding to CD40 synergized with soluble CD40L-induced B cell proliferation in the absence of costimulus. Similarly, non-competing mAbs were shown to synergize with soluble trimeric CD40L for promoting CD23 expression and IgE production in human B cells.¹⁶ Additional data indicated that a monomeric scFv derived from the anti-CD40 mAb G28-5 is a potent agonist, able to crosslink the receptor at the membrane, and cooperates with soluble natural CD40L.¹⁷ Moreover, epitope specificity of these scFv has an important role in defining the functional properties of the receptor.¹⁸ All these observations suggest the existence of some allosteric movements and cooperativity between the different epitopes, in which formation of CD40-complex induced by the binding of the first ligand may influence the binding of subsequent molecules. This might ultimately lead to an enhanced binding of CD40L and/or stabilization of the CD40-CD40L complex.

Surface plasmon resonance experiments confirmed the correlation between the ability of anti-CD40 mAbs to compete with CD40L for binding to CD40 and cellular activation. More importantly, these experiments also demonstrated the absence of relation between high affinity of the mAbs and their activation potential.¹⁹ Thus, signaling pathways activated downstream CD40 are also determined by the manner CD40 is ligated.

Only the natural CD40-ligand, both in the membrane and soluble forms, may strictly provide the epitopes required for changes of the CD40 conformation that are necessary for the engagement of dedicated pathways. This cannot be fully imitated by the binding of anti-

¹⁶ Challa, A, et al. (1999). Epitope-dependent synergism and antagonism between CD40 antibodies and soluble CD40 ligand for the regulation of CD23 expression and IgE synthesis in human B cells. *Allergy* 54, 576.

¹⁷ Ledbetter, J A, et al. (1997). Agonistic activity of a CD40-specific single-chain Fv constructed from the variable regions of mAb G28-5. *Crit Rev Immunol* 17, 427.

¹⁸ Ellmark, P, et al. (2002). Modulation of the CD40-CD40 ligand interaction using human anti-CD40 single-chain antibody fragments obtained from the n-CoDeR phage display library. *Immunology* 106, 456.

¹⁹ Malmberg Hager, A C, et al. (2003). Affinity and epitope profiling of mouse anti-CD40 monoclonal antibodies. *Scand J Immunol* 57, 517.

CHAPTER 3

CD40 antibody. In contrast, Ellmark *et al.* showed that the extracellular domains of human CD40 are actually not essential for rescue of IgM-induced B cell line apoptosis.²⁰ Finally, the precise mechanisms of oligomerization and molecular activation of CD40 at the cell membrane upon its ligation remain to be elucidated.

3.2 Role of pre-ligand binding assembly domain in CD40

3.2.1 The PLAD domain

It has been observed that some members of the TNF-R family assemble constitutively in the absence of their cognate ligand. Papoff and coworkers first demonstrated that ligand-independent oligomerization of CD95 depends on the most distal extracellular domain CRD1 but not on the death domain (Figure 19A).²¹ Whereas soluble form of the receptor homo-oligomerizes, and hetero-oligomerizes with the membranous form, it is not the case for a truncated form lacking the 42 N-ter residues that compose most of the CRD1. Capacity to interact with CD95L and to initiate signaling when overexpressed at the membrane was conserved by this truncated form. Finally, a soluble truncated form of CD95 made of the 49 N-ter amino-acids is necessary and sufficient to mediate oligomerization of the receptor.

Similarly, TNF-R1 and R2 self-associate in the absence of TNF α , as seen by fluorescence resonance energy transfer on living cells.²² The putative N-ter functional domain that mediates ligand-independent receptor association was named pre-ligand binding assembly domain (PLAD). The PLAD is responsible for preformed receptor oligomerization prior to ligand binding, what is not sufficient for initiation of intracellular signals, but is necessary for the interaction with the cognate ligand (Figure 19A,B). Recently, TNF-R PLAD was targeted in the treatment of inflammation.²³ A soluble construct of TNF-R1 PLAD was demonstrated to bind to the receptor (Figure 19C), to potently inhibit effects of TNF α and consequently, to ameliorate inflammatory arthritis in various experimental mouse models by blocking TNF α -induced NF- κ B activation, expression of RANK and RANKL, and osteoclast differentiation.

²⁰ Ellmark, P, et al. (2003). Pre-assembly of the extracellular domains of CD40 is not necessary for rescue of mouse B cells from anti-immunoglobulin M-induced apoptosis. *Immunology* 108, 452.

²¹ Papoff, G, et al. (1999). Identification and characterization of a ligand-independent oligomerization domain in the extracellular region of the CD95 death receptor. *J Biol Chem* 274, 38241.

²² Chan, F K, et al. (2000). A domain in TNF receptors that mediates ligand-independent receptor assembly and signaling. *Science* 288, 2351.

²³ Deng, G M, et al. (2005). Amelioration of inflammatory arthritis by targeting the pre-ligand assembly domain of tumor necrosis factor receptors. *Nat Med* 11, 1066.

CHAPTER 3

These observations give explanations for the resistance of lymphocytes from patients with autoimmune lymphoproliferative syndrome to Fas-induced apoptosis.²⁴ Receptor molecules mutated in either the ligand-binding domain or in the death domain, still oligomerize with wild-type receptor, forming mixed trimers. These defective molecules thus dominantly interfere with apoptosis induced by CD95L, but not with apoptosis mediated by agonistic anti-CD95 mAb.

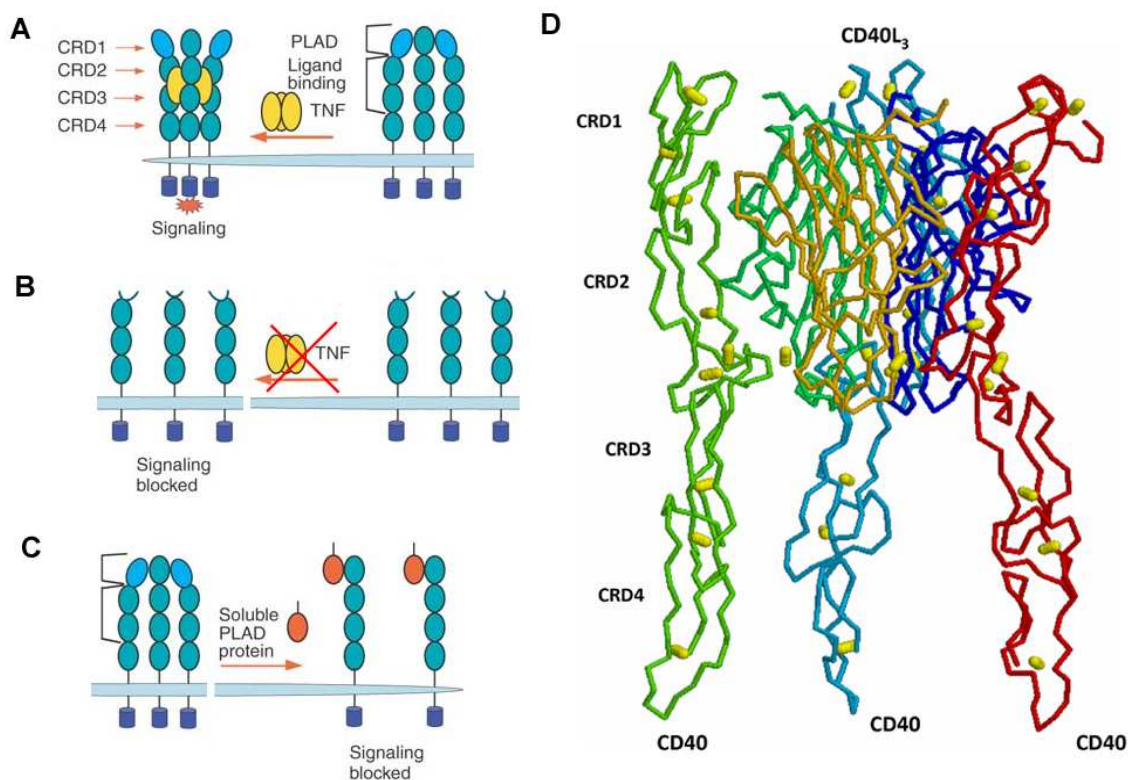


Figure 19. Implication of PLAD in TNF-R and CD40 signaling. PLAD is necessary for pre-formed trimer upon ligation (A). Mutated PLAD prevents binding of TNF to the receptor (B). Soluble PLAD protein dominantly interferes with TNF-R signaling (C). Figures 19A,B,C are adapted from Deng *et al.*²³ CD40 PLAD may be located in CRD1 as seen on the CD40-CD40L interaction model (D). CD40 backbone chains are colored in red, light green and light blue, cysteines are represented by yellow balls.

3.2.2 PLAD requirement for CD40 signaling

Although the complete mechanism of CD40-induced signaling is not fully understood, the simplest ligand-induced oligomerization model is not sufficient to explain initiation of downstream pathways. Increase in the avidity of the receptor-ligand interaction and/or change in the membrane arrangement of the receptor that allow binding of adaptor molecules and activation upon ligation of the receptor, are certainly implicated.

CD40, as well as TRAIL-R1 (DR4), were also shown to specifically pre-associate at the membrane in the absence of ligand.²³ This confirmed earlier observations of the CD40

²⁴ Siegel, R M, et al. (2000). Fas preassociation required for apoptosis signaling and dominant inhibition by pathogenic mutations. *Science* 288, 2354.

CHAPTER 3

oligomeric state in unstimulated cells.¹⁴ Malmborg Hager and Ellmark have further studied the ligand-independent oligomerization of CD40.¹⁹ They showed that CD40L binding to its receptor requires the CRD1 of CD40, where PLAD might be located based on homology studies (chapter 2), although this domain does not contain any of the residues important for CD40L ligation (Figure 19D).

Moreover, CD40 signaling was shown to be independent of the CRD1, since ligation of engineered CD40 proteins lacking part of their extracellular domains, by a peptide tag is sufficient to rescue anti-IgM-induced apoptosis of WEHI cells.²⁰

3.3 CD40 signaling is initiated within membrane rafts

3.3.1 Membrane rafts

The outer leaf plasma membrane of many cell types contains microdomains of approximately 50 nm of diameter, named lipid or membrane rafts. These microdomains structures move within the fluid bilayer and constitute functional platforms for the formation of signalosomes.²⁵ They are enriched in sphingolipids and cholesterol that self-aggregate and segregate from bulk unsaturated glycerophospholipids, forming a thick liquid-ordered phase. This resists to solubilization in non-ionic detergent, but can be isolated from low density fractions after buoyancy in a discontinuous sucrose gradient. Similar cholesterol-rich rafts exist in the inner leaflet of the plasma membrane, but their composition and function is not yet well known.²⁶

These microdomains have been described as essential structural platforms for a variety of functions. For example, lipid rafts have been shown to be crucial for T cell apoptosis mediated by Fas following TCR stimulation.²⁷ Modulation of TNF-R family protein location into lipid rafts may dynamically regulate the efficiency and outcomes of signaling by these receptors.

²⁵ Simons, K, et al. (1997). Functional rafts in cell membranes. *Nature* 387, 569.

²⁶ Hayashi, M, et al. (2006). Detection of cholesterol-rich microdomains in the inner leaflet of the plasma membrane. *Biochem Biophys Res Commun* 351, 713.

²⁷ Muppidi, J R, et al. (2004). Ligand-independent redistribution of Fas (CD95) into lipid rafts mediates clonotypic T cell death. *Nat Immunol* 5, 182.

CHAPTER 3

3.3.2 CD40 is localized into lipid raft microdomains

Ligand-independent pre-associated CD95 complexes were preferentially found within lipid rafts.²⁷ Similarly, Hostager *et al.* have shown that a significant level of CD40 is constitutively localized in these lipid microdomains in unstimulated mouse B cell line.²⁸ Similarly, CD40 engagement induces the nearly complete translocation of CD40 from detergent-soluble to detergent-insoluble fractions of plasma membrane, and this independently of downstream signaling molecules. Same observations have been reported on human DCs, in which integrity and reorganization of membranes rafts is required for engagement of signaling from CD40.²⁹ Although Malapati and co-workers described that CD40 functions outside the lipid rafts during BCR signaling in murine B lymphoma,³⁰ most of the authors gave consistent data showing that co-engagement of BCR and CD40 brings their signaling complexes into close proximity within rafts microdomains, allowing crosstalk between them.³¹ CD40L colocalized with CD40 within membrane rafts in unstimulated non-Hodgkin's lymphoma B cells,³² what was thought to be responsible for the constitutive activation of NF- κ B and autonomous cell growth in B cell lymphomas (chapter 2).

Targeting of CD40 C-ter signaling domain to lipid rafts and artificial trimerization were shown to synergistically initiate cell signaling, suggesting that both localization within lipid rafts and trimerization of the receptor are important for activation of CD40-induced signaling.⁸ Finally, one can suggest that binding of CD40L may induce a conformational change in the CD40 transmembrane domain, allowing it to interact with ceramide of the membrane rafts,³³ linking allosteric movements engaged by CD40L to location within lipid rafts.

3.3.3 Caveolae are implicated in CD40 signaling

Caveolae are lipid rafts structures coated with caveolin that form invaginations of the plasma membrane. In contrast to coated-pits, these domains are not constitutively

²⁸ Hostager, B S, et al. (2000). Recruitment of CD40 and tumor necrosis factor receptor-associated factors 2 and 3 to membrane microdomains during CD40 signaling. *J Biol Chem* 275, 15392.

²⁹ Vidalain, P O, et al. (2000). CD40 signaling in human dendritic cells is initiated within membrane rafts. *EMBO J* 19, 3304.

³⁰ Malapati, S, et al. (2001). The influence of CD40 on the association of the B cell antigen receptor with lipid rafts in mature and immature cells. *Eur J Immunol* 31, 3789.

³¹ Haxhinasto, S A, et al. (2004). Synergistic B cell activation by CD40 and the B cell antigen receptor: role of B lymphocyte antigen receptor-mediated kinase activation and tumor necrosis factor receptor-associated factor regulation. *J Biol Chem* 279, 2575.

³² Pham, L V, et al. (2002). A CD40 Signalosome anchored in lipid rafts leads to constitutive activation of NF-kappaB and autonomous cell growth in B cell lymphomas. *Immunity* 16, 37.

³³ Bollinger, C R, et al. (2005). Ceramide-enriched membrane domains. *Biochim Biophys Acta* 1746, 284.

CHAPTER 3

internalized.²⁵ CD40 was detected in caveolae together with some key signaling intermediates in unstimulated human renal proximal tubule cells.³⁴ CD40 engagement induces its dissociation as well as the dissociation of signaling partners from this structure, what is necessary for induction of downstream pathways.

3.3.4 Translocation of CD40 into lipid rafts

CD40 clustering was shown to be dependent on acid sphingomyelinase (ASM) translocation from intracellular stores onto the outer leaflet of the cell membrane,³⁵ in the same manner as CD95.³⁶ Primary stimulation via CD40 induced activation and membrane translocation of ASM which then colocalizes with the receptor and mediates release of ceramide. ASM accumulates in preexisting sphingolipid-rich rafts and triggers the formation of larger ceramide-enriched platforms, bringing together receptor and signaling molecules into close contact. Moreover, CD40-clustering causes stabilization of the ligand-receptor interaction leading to sustained signaling (Figure 20).³⁷ Mechanisms of ASM activation are still poorly understood. Caspases have been proposed to mediate upstream events initiating by CD95.³⁸ Recently, PKC δ was shown to activate ASM.³⁹

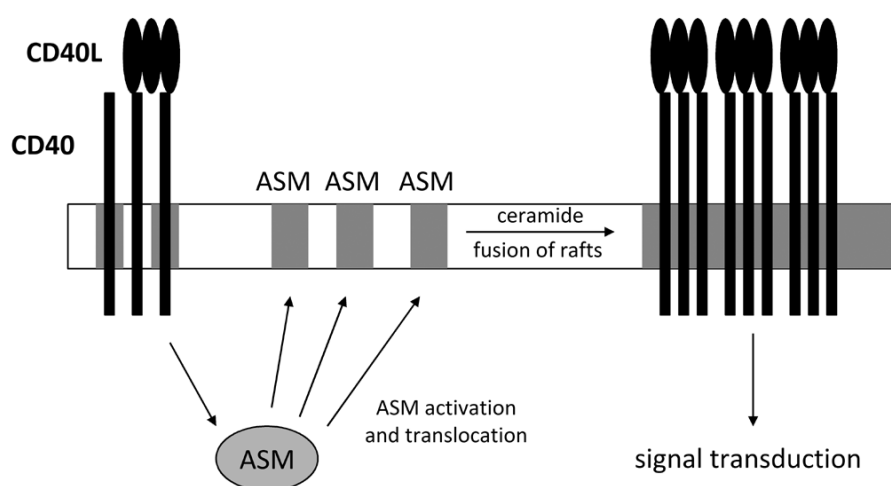


Figure 20. CD40 reorganization into rafts is dependent on ASM. Primary CD40 triggering with its cognate ligand induces activation and translocation of ASM to the plasma membrane (left). ASM thus induces fusion of rafts microdomains and oligomerization of CD40 molecules. This step is essential for CD40L-induced cell signal transduction. This scheme can be viewed with CD40 and CD40L inverted (see text below).

³⁴ Li, H, et al. (2004). Functional caveolae are a prerequisite for CD40 signaling in human renal proximal tubule cells. *Am J Physiol Renal Physiol* 286, F711.

³⁵ Grassme, H, et al. (2002). Ceramide-rich membrane rafts mediate CD40 clustering. *J Immunol* 168, 298.

³⁶ Grassme, H, et al. (2001). Molecular mechanisms of ceramide-mediated CD95 clustering. *Biochem Biophys Res Commun* 284, 1016.

³⁷ Gulbins, E, et al. (2002). Ceramide and cell death receptor clustering. *Biochim Biophys Acta* 1585, 139.

³⁸ Brenner, B, et al. (1998). Fas/CD95/Apo-I activates the acidic sphingomyelinase via caspases. *Cell Death Differ* 5, 29.

³⁹ Zeidan, Y H, et al. (2007). Activation of Acid Sphingomyelinase by Protein Kinase C δ -mediated Phosphorylation. *J Biol Chem* 282, 11549.

CHAPTER 3

In addition to primary activation of ASM from CD40, pre-clustering of CD40L is required for CD40 aggregation.² As for CD40 (Figure 20), CD40L ligation was shown to induce ASM activation and translocation to the membrane, leading to clustering of CD40L in ceramide-rich rafts.

3.4 CD40-induced cell signaling

3.4.1 CD40-activated signaling pathways

3.4.1.1 Intermediates implicated in CD40 signaling

Although CD40 phosphorylation was observed in B cells,⁴⁰ no receptor-autophosphorylation activity was detectable.¹ CD40 phosphorylation, that was enhanced in PMA-activated human tonsil B cells, involves serine and/or threonine since no tyrosine residue is present in the cytoplasmic domain (Chapter 2, Figure 1).⁴¹

Triggering of CD40 was shown to induce rapid serine and threonine phosphorylation on various proteins.⁴² It was also linked to protein tyrosine kinase/protein phosphatase activities.⁴³ In contrast to signals transduced through sIg,⁴⁴ CD40-induced tyrosine phosphorylation does not depend on activation of PKC, or on calmodulin- and calcineurin-dependent kinases,⁴⁵ but is important for stimulation of phosphoinositide (PI) turnover. Cell activation state also greatly influences CD40-induced events downstream the receptor, as seen for example in germinal center B cells where CD40 is coupled to functional protein tyrosine kinase but not the phosphatidylinositol signaling pathway.⁴⁶

⁴⁰ Clark, E A, et al. (1990). Association between IL-6 and CD40 signaling. IL-6 induces phosphorylation of CD40 receptors. *J Immunol* 145, 1400; Inui, S, et al. (1990). Identification of the intracytoplasmic region essential for signal transduction through a B cell activation molecule, CD40. *Eur J Immunol* 20, 1747.

⁴¹ Stamenkovic, I, et al. (1989). A B-lymphocyte activation molecule related to the nerve growth factor receptor and induced by cytokines in carcinomas. *Embo J* 8, 1403.

⁴² Einfeld, D A, et al. (1988). Molecular cloning of the human B cell CD20 receptor predicts a hydrophobic protein with multiple transmembrane domains. *EMBO J* 7, 711.

⁴³ Uckun, F M, et al. (1991). Stimulation of protein tyrosine phosphorylation, phosphoinositide turnover, and multiple previously unidentified serine/threonine-specific protein kinases by the Pan-B-cell receptor CD40/Bp50 at discrete developmental stages of human B-cell ontogeny. *J Biol Chem* 266, 17478.

⁴⁴ Lane, P J, et al. (1991). The role of tyrosine phosphorylation in signal transduction through surface Ig in human B cells. Inhibition of tyrosine phosphorylation prevents intracellular calcium release. *J Immunol* 146, 715.

⁴⁵ Kansas, G S, et al. (1991). Transmembrane signals generated through MHC class II, CD19, CD20, CD39, and CD40 antigens induce LFA-1-dependent and independent adhesion in human B cells through a tyrosine kinase-dependent pathway. *J Immunol* 147, 4094.

⁴⁶ Knox, K A, et al. (1993). Protein tyrosine phosphorylation is mandatory for CD40-mediated rescue of germinal center B cells from apoptosis. *Eur J Immunol* 23, 2578.

CHAPTER 3

3.4.1.2 Common signaling pathways activated by CD40

Protein tyrosine phosphatases are also implicated in the early events of CD40 signaling in human B cells, and are for example involved in the regulation of protein tyrosine kinases Lyn, Fyn and Syk,⁴⁷ as well as others PTKs.⁴⁵ Janus kinase 3 (JAK3), phosphatidylinositol-3 kinase (PI3K), phospholipase C γ 2 (PLC γ 2) are also implicated in CD40 signaling. Second messengers like IP₃, calcium as well as cyclic adenosine monophosphate (cAMP) have also been detected following CD40 activation.

T cell-dependent B cell stimulation is associated with NF- κ B induction via the CD40–CD40L interaction, independently of PKC-mediated signaling,⁴⁸ but dependent on both protein tyrosine kinase-dependent pathways and the redox equilibrium of the cell.⁴⁹ Noteworthy, engagement of CD40 on human Daudi cells by both whole anti-CD40 and F(ab')₂ fragments led to the same level of NF- κ B activation.

Numerous additional studies have described various signaling pathways engaged by CD40 that are summarized at the end of this chapter as exhaustively as possible from the current literature (Poster 1). Signaling pathways described in the most studied cell systems were included. I have paid attention on the cell-type in which pathways have been described. Although many pathways have been found in more than one cell-type, some others are cell-type-specific. Key intermediates that might contribute to CD40-signaling were also added. Due to high complexity and heterogeneity of the systems used, with sometimes controversial results, these pathways are not discussed here. The reader is invited to refer to corresponding references for detailed data since description of all these pathways is not the purpose of the thesis. Nevertheless, this figure underlines that activation of CD40 engages many common signaling pathways, and other remain certainly to be discovered. Targeting CD40 to induce one desired signal in one selective cell type is thus far from being realistic for the moment.

⁴⁷ Faris, M, et al. (1994). CD40 signaling pathway: anti-CD40 monoclonal antibody induces rapid dephosphorylation and phosphorylation of tyrosine-phosphorylated proteins including protein tyrosine kinase Lyn, Fyn, and Syk and the appearance of a 28-kD tyrosine phosphorylated protein. *J Exp Med* 179, 1923.

⁴⁸ Lalmanach-Girard, A C, et al. (1993). T cell-dependent induction of NF-kappa B in B cells. *J Exp Med* 177, 1215.

⁴⁹ Berberich, I, et al. (1994). Cross-linking CD40 on B cells rapidly activates nuclear factor-kappa B. *J Immunol* 153, 4357.

CHAPTER 3

3.4.2 Implication of TRAF adaptor molecules

3.4.2.1 CD40 signals through adaptor molecules

CD40 cytoplasmic domain is relatively small (Figure 1, chapter 2) and does not exhibit intrinsic enzymatic capacity. In contrast to some of the TNF-R family members, like Fas and TNF-R1 which contain an 80-residues death domain involved in caspase-mediated induction of apoptosis,⁵⁰ CD40 does not present obvious signaling motifs in the cytoplasmic domain. Nevertheless, the cytoplasmic region around Thr234 was shown to be essential in the signal transduced through CD40.⁵¹ Thus, external CD40 stimuli are transduced upon reorganization of the receptor and other different intermediate molecules under the membrane.

3.4.2.2 The TNF-R-associated factors

3.4.2.2.1 The TRAF family

The most important intracellular signaling proteins that interact with CD40, as well as with many members of the TNF-R family, are the TNF-R-associated factors (TRAFs). These adapter proteins are constituted of 409 to 567 amino acids and have no intrinsic enzymatic activity. The TRAF family is a phylogenetically conserved group of scaffold proteins that link receptors of the TNF-R and Toll/IL-1 family to signaling cascades.⁵² To date, six different members have been identified in mammals, two in *Drosophila* and one in *Caenorhabditis elegans* (Figure 21).⁵³ A homologous protein designated TRAF7 was recently identified. It is involved in apoptosis, and mediates TNF α -induced activation of p38, JNK pathways and regulation of NF- κ B and AP-1 via MEKK3.⁵⁴ But its implication in other TNF-R pathways has not been reported for the moment.

Interestingly, the main Epstein-Barr virus oncogenic latent membrane protein 1 (LMP1) was shown to mimic a constitutive CD40 that lacks an extracellular ligand. LMP1 interacts with TRAFs 2, 3, 5 and 6 and continuously initiates NF- κ B, JNK/AP-1, p38 and PI3K

⁵⁰ Yuan, W, et al. (1997). Programmed cell death in human ovary is a function of follicle and corpus luteum status. *J Clin Endocrinol Metab* 82, 3148.

⁵¹ Inui, S, et al. (1990). Identification of the intracytoplasmic region essential for signal transduction through a B cell activation molecule, CD40. *Eur J Immunol* 20, 1747.

⁵² Bradley, J R, et al. (2001). Tumor necrosis factor receptor-associated factors (TRAFs). *Oncogene* 20, 6482.

⁵³ Wajant, H, et al. (2001). The TNF-receptor-associated factor family: scaffold molecules for cytokine receptors, kinases and their regulators. *Cell Signal* 13, 389.

⁵⁴ Xu, L G, et al. (2004). TRAF7 potentiates MEKK3-induced AP1 and CHOP activation and induces apoptosis. *J Biol Chem* 279, 17278; Bouwmeester, T, et al. (2004). A physical and functional map of the human TNF-alpha/NF-kappa B signal transduction pathway. *Nat Cell Biol* 6, 97.

CHAPTER 3

pathways.⁵⁵ Although differences exist between pathways activated by CD40 and LMP1, CD40–induced cell signaling may be influenced by LMP1.⁵⁶

3.4.2.2 TRAFs are located into lipid rafts

Interestingly, TRAFs 2 and 3 were shown to be recruited into membrane rafts subsequently to CD40 activation.⁵⁸ Signals induced from other receptors can either positively or negatively influence TRAFs recruitment to the signalosome.⁵⁷ Duration and strength of TRAF2–dependent signaling was shown to be regulated by degradation of TRAF2 that is directed by CD40–induced ubiquitination.⁵⁸ Finally, TRAFs compartmentalization within rafts was shown to occur subsequently to their CD40–mediated recruitment at the membrane. Stabilization of the receptor signaling complex, and positioning of all signaling partners into vicinity, ultimately form the signalosome.²

3.4.2.3 Regulation of TRAF functions

Expression of TRAF members is regulated in a cell–specific manner at the transcriptional level.⁵⁵ Post-transcriptional modulation also occurs, since different spliced forms of TRAF2 were reported.⁵⁹ Finally, post–translational down–regulation of TRAF2 by CD40-mediated degradation/depletion has been observed,²⁸ as well as TRAF3 stabilization, what leads to its upregulation in urothelial cell CD40L–stimulated carcinoma.⁶⁰ TRAF2 also plays an important role in the activation–induced degradation of TRAF3.⁶¹ TRAF1 was shown to redistribute TRAF2 and CD40 from raft microdomains to detergent–soluble fractions, and to protect TRAF2 from CD40–mediated degradation.⁶² Relative intracellular abundance of TRAF proteins, as well as their interplay, play a critical role in modulation of biological responses induced through them.

⁵⁵ Ardila-Osorio, H, et al. (2005). TRAF interactions with raft-like buoyant complexes, better than TRAF rates of degradation, differentiate signaling by CD40 and EBV latent membrane protein 1. *Int J Cancer* 113, 267.

⁵⁶ Wu, S, et al. (2005). LMP1 protein from the Epstein-Barr virus is a structural CD40 decoy in B lymphocytes for binding to TRAF3. *J Biol Chem* 280, 33620.

⁵⁷ Kuhne, M R, et al. (1997). Assembly and regulation of the CD40 receptor complex in human B cells. *J Exp Med* 186, 337.

⁵⁸ Brown, K D, et al. (2002). Regulation of TRAF2 signaling by self-induced degradation. *J Biol Chem* 277, 19433.

⁵⁹ Brink, R, et al. (1998). Tumor necrosis factor receptor (TNFR)-associated factor 2A (TRAF2A), a TRAF2 splice variant with an extended RING finger domain that inhibits TNFR2-mediated NF-kappaB activation. *J Biol Chem* 273, 4129.

⁶⁰ Georgopoulos, N T, et al. (2006). A novel mechanism of CD40-induced apoptosis of carcinoma cells involving TRAF3 and JNK/AP-1 activation. *Cell Death Differ* 13, 1789.

⁶¹ Hostager, B S, et al. (2003). Tumor necrosis factor receptor-associated factor 2 (TRAF2)-deficient B lymphocytes reveal novel roles for TRAF2 in CD40 signaling. *J Biol Chem* 278, 45382.

⁶² Arron, J R, et al. (2002). Regulation of the subcellular localization of tumor necrosis factor receptor-associated factor (TRAF)2 by TRAF1 reveals mechanisms of TRAF2 signaling. *J Exp Med* 196, 923.

3.4.2.2.4 TRAF protein structure

All members of the TRAF family have a conserved C-terminal domain named the TRAF domain, itself subdivided into a highly homologous C-ter region termed TRAF-C and a region termed TRAF-N (Figure 21). The TRAF-N region possesses a coiled-coil domain and is involved in the interactions of TRAF molecules with other proteins found in the TRAF-receptor complex.⁶³ The TRAF-C region is critical for the interaction of TRAFs with the cytoplasmic domain of their respective receptors.⁶⁴ However, the TRAF-N also contributes to these associations.

All TRAF proteins except TRAF1 have an N-terminal RING finger, and all possess one (TRAF1) or several (TRAF2-6) zinc fingers (Figure 21). These structural motifs are important in promoting downstream signaling.⁶⁰ Moreover, zinc coordination by cysteine in RING and zinc finger motifs is essential for DNA binding. Although the N-terminal half of TRAF2 has been shown to translocate into the nucleus and to transactivate gene transcription in transfected cells,⁶⁵ whether or not TRAFs directly regulate gene transcription *in vivo* remains uncertain. Concerning TRAF7, except for N-terminal RING and zinc finger domains, it differs from the other members in the C-ter region that contains WD40 repeats and not the TRAF domain (Figure 21).

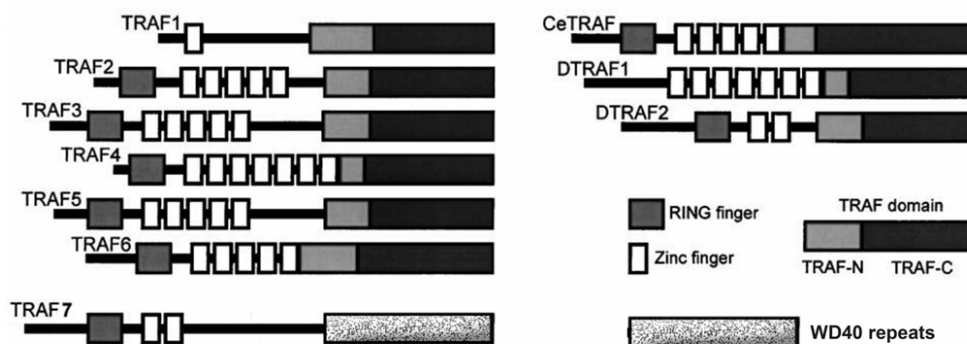


Figure 21. The TRAF family members. Schematic representation of the TRAF family proteins and their functional domains. Figure is adapted from Wajant *et al.*⁵³

TRAFs 3 and 5 have an additional isoleucine zipper motif between the most C-terminal zinc finger and the TRAF domain that can mediate homo- and heteromultimerization of these proteins.⁶⁶ In contrast, TRAFs 1 and 2 homo- and hetero-oligomerize through the

⁶³ Rothe, M, et al. (1995). The TNFR2-TRAF signaling complex contains two novel proteins related to baculoviral inhibitor of apoptosis proteins. *Cell* 83, 1243.

⁶⁴ Cheng, G, et al. (1995). Involvement of CRAF1, a relative of TRAF, in CD40 signaling. *Science* 267, 1494.

⁶⁵ Min, W, et al. (1998). The N-terminal domains target TNF receptor-associated factor-2 to the nucleus and display transcriptional regulatory activity. *J Immunol* 161, 319.

⁶⁶ Wajant, H, et al. (1999). TNF receptor associated factors in cytokine signaling. *Cytokine Growth Factor Rev* 10, 15.

CHAPTER 3

TRAF-C domain.⁶⁷ Crystal structures of TRAF2's TRAF domain indicate that TRAF-C forms an eight-strand antiparallel β -sandwich structure and TRAF-N forms a single α -helix (Figure 24).⁶⁸ Three TRAF2 molecules spontaneously multimerize through their TRAF domains to form a mushroom like trimer, in which TRAF-N assemble around a flexible triple helical coiled-coil, and the TRAF-C form a unique edge (Figure 22).

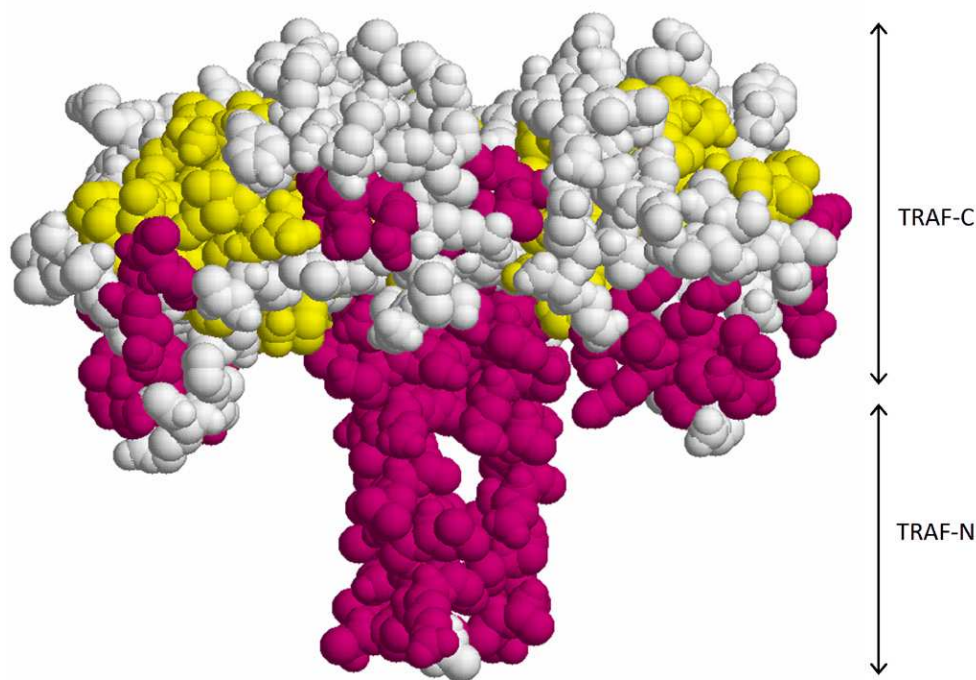


Figure 22. Three-dimensional structure of the human TRAF2's TRAF domain. Spacefill representation of TRAF domain of TRAF2 assembled in trimer. TRAF-C domain (residues 356-501) and part of the TRAF-N domain (residues 272-355) are shown. Residues composing β -strands are colored in yellow, and those composing α -helices are colored in pink (PDB code 1QSC).⁶⁸

3.4.2.3 The TRAF-CD40 interaction

3.4.2.3.1 TRAF-binding sites

TRAF-CD40 interaction is mediated by specific sites on both proteins. Earlier studies have demonstrated that TRAF6 binds to the membrane-proximal linear motif ²³¹QEPQEINF²³⁸ of the CD40 intracytoplasmic domain (Figure 25).⁶⁹ A distinct binding site was described for TRAFs 1, 2, 3 and 5, which interact either directly or indirectly with CD40.⁷⁰ This motif was mapped on residues ²⁵⁰PVQET²⁵⁴ (Figure 25).⁷² Further findings suggested

⁶⁷ Pullen, S S, et al. (1998). CD40-tumor necrosis factor receptor-associated factor (TRAF) interactions: regulation of CD40 signaling through multiple TRAF binding sites and TRAF hetero-oligomerization. *Biochemistry* 37, 11836.

⁶⁸ Park, Y C, et al. (1999). Structural basis for self-association and receptor recognition of human TRAF2. *Nature* 398, 533.

⁶⁹ Ishida, T, et al. (1996). Identification of TRAF6, a novel tumor necrosis factor receptor-associated factor protein that mediates signaling from an amino-terminal domain of the CD40 cytoplasmic region. *J Biol Chem* 271, 28745.

⁷⁰ Ishida, T K, et al. (1996). TRAF5, a novel tumor necrosis factor receptor-associated factor family protein, mediates CD40 signaling. *Proc Natl Acad Sci U S A* 93, 9437.

CHAPTER 3

that TRAF2 and TRAF3 recognize distinct residues within the PVQET motif.⁷¹ Since both TRAF2 and TRAF3 have been immunoprecipitated with an anti-CD40 mAb in human B cells, the simultaneous recruitment of both TRAF proteins to CD40 is possible.⁶⁰ Recently, a second functional TRAF2 binding site was identified at the C-terminal end of CD40, that consists on the ²⁷²SVQE²⁷⁵ motif (Figure 25).⁷²

Nevertheless, these TRAF binding sites have distinct contributions. Indeed, in primary DCs TRAFs 2, 3, 5 and 6 all contribute to DC maturation, but only TRAF6 is essential for activation of p38 and JNK pathways and production of IL-12 p40.⁷³ Furthermore, different TRAF proteins might be implicated in distinct signaling pathways at different stages of the B cell development, as suggested for TRAF6 which plays a crucial role in affinity maturation and long-lived plasma cell,⁷⁴ whereas TRAF2 and 3 are essential for class switching.⁷⁵

Interestingly, overexpression of the I-TRAF/TANK protein, which contains a PXQXT motif,⁷⁶ inhibited NF- κ B activation induced by overexpression of TRAF2. In contrast, its expression in small amounts enhanced TRAF2-induced NF- κ B signaling, suggesting that I-TRAF/TANK might not only act as an inhibitor of TRAFs, but also serve as a scaffolding adaptor linking TRAFs with important downstream partners.⁷⁷

3.4.2.3.2 CD40-mediated activation of TRAFs

TRAFs 1, 2, 3 and 5 have similar specificity of binding to TNF-Rs.⁷⁸ Moreover, a unique motif derived from the cytoplasmic domain of CD40 was shown to bind to both TRAF2 and TRAF3. These observations have led to the questions of specificity and modulation of each TRAF function during CD40 signaling. CD40 cytoplasmic fusion protein binds to TRAF2 and TRAF3 with a low affinity, as measured by surface plasmon resonance.¹⁰ No binding was detected to TRAF1 and TRAF6. Importantly, TRAF trimerization was required for high-affinity

⁷¹ Leo, E, et al. (1999). Differential requirements for tumor necrosis factor receptor-associated factor family proteins in CD40-mediated induction of NF- κ B and Jun N-terminal kinase activation. *J Biol Chem* 274, 22414.

⁷² Lu, L F, et al. (2003). CD40 signaling through a newly identified tumor necrosis factor receptor-associated factor 2 (TRAF2) binding site. *J Biol Chem* 278, 45414.

⁷³ Mackey, M F, et al. (2003). Distinct contributions of different CD40 TRAF binding sites to CD154-induced dendritic cell maturation and IL-12 secretion. *Eur J Immunol* 33, 779.

⁷⁴ Ahonen, C, et al. (2002). The CD40-TRAF6 axis controls affinity maturation and the generation of long-lived plasma cells. *Nat Immunol* 3, 451.

⁷⁵ Jabara, H, et al. (2002). The binding site for TRAF2 and TRAF3 but not for TRAF6 is essential for CD40-mediated immunoglobulin class switching. *Immunity* 17, 265.

⁷⁶ Rothe, M, et al. (1996). I-TRAF is a novel TRAF-interacting protein that regulates TRAF-mediated signal transduction. *Proc Natl Acad Sci U S A* 93, 8241.

⁷⁷ Chin, A I, et al. (1999). TANK potentiates tumor necrosis factor receptor-associated factor-mediated c-Jun N-terminal kinase/stress-activated protein kinase activation through the germinal center kinase pathway. *Mol Cell Biol* 19, 6665.

⁷⁸ Ye, H, et al. (1999). The structural basis for the recognition of diverse receptor sequences by TRAF2. *Mol Cell* 4, 321.

CHAPTER 3

interaction with CD40, what supports a model for an avidity-driven formation of the signalosome. Finally, TRAF proteins have specific affinity for CD40, and they require distinct level of oligomerization to stabilize their interaction with the receptor. These observations define a rational basis for the particular functions of TRAFs during CD40 signaling.

Activation of TRAF molecules certainly occurs via their post-translational modification, since BCR engagement alone or in combination with anti-CD40 mAb has been shown to enhance the phosphorylation of TRAF2.³¹ The accepted scenario for TRAFs is that TRAF proteins remain in the cytoplasm until activation of the receptor. Then, TRAFs are recruited to the membrane, activated in the signalosome and released into the cytoplasm for propagation of the signal by interacting with numerous kinases and adaptor/regulators in various signaling pathways.⁷⁹

3.4.2.3.3 The TRAF-CD40 interaction viewed at the three-dimensional level

Structural data from crystal of the TRAF domain of TRAF6 complexed with a peptide derived from the cytoplasmic domain of CD40 indicated that the linear sequence of CD40 bind to a surface groove on TRAF-C in an extended conformation (Figure 23).⁸⁰ The proline side-chain is fully buried into the binding pocket, orienting all other CD40 residues for optimal contact with the edge of the β -sandwich structure (Figure 23).

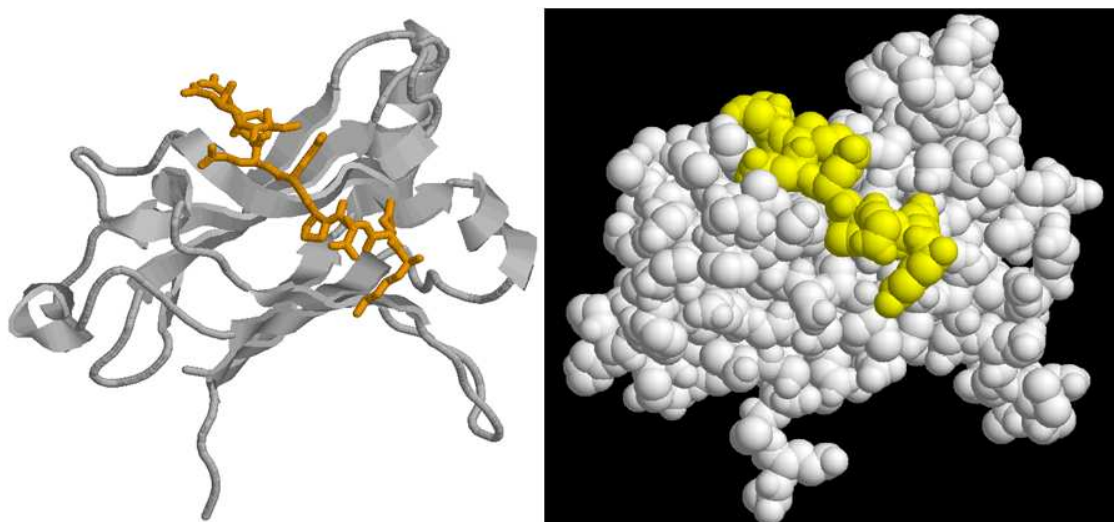


Figure 23. Three-dimensional structure of the TRAF-C domain of human TRAF6 complexed with a peptide derived from the CD40 intracytoplasmic domain. The same view of TRAF-C domain of TRAF6 complex with the CD40 fragment ²³⁰KQEPQEIDF²³⁸, that contains the Asn237-Asp mutation for an enhanced interaction affinity, represented in cartoon (left) and spacefill (right). CD40 peptide is represented in orange sticks (left) or yellow spacefill (right) (PDB code 1LB6).

⁷⁹ Wajant, H, et al. (2001). The TNF-receptor-associated factor family: scaffold molecules for cytokine receptors, kinases and their regulators. *Cell Signal* 13, 389.

⁸⁰ Ye, H, et al. (2002). Distinct molecular mechanism for initiating TRAF6 signalling. *Nature* 418, 443.

TRAF2 recognition peptide bound to TRAF2 in a similar manner than TRAF6 recognition motif bound to TRAF6, apart from some variation in direction of the motif that may alter conformation of other TRAFs and thereby influence their binding to the cytoplasmic domain of CD40. Each CD40 fragment associates with one monomer of TRAF2 (Figure 24A).⁸¹ Most importantly, ligand-induced trimerization of the receptor and self-association of TRAF molecules lead to the formation of intracellular signaling complexes with C_3 symmetry with the TRAF-N domain pointing toward the cytoplasm (Figure 24B).⁸² CD40L geometry is thus transduced to TRAF adaptor molecules inside the cell.

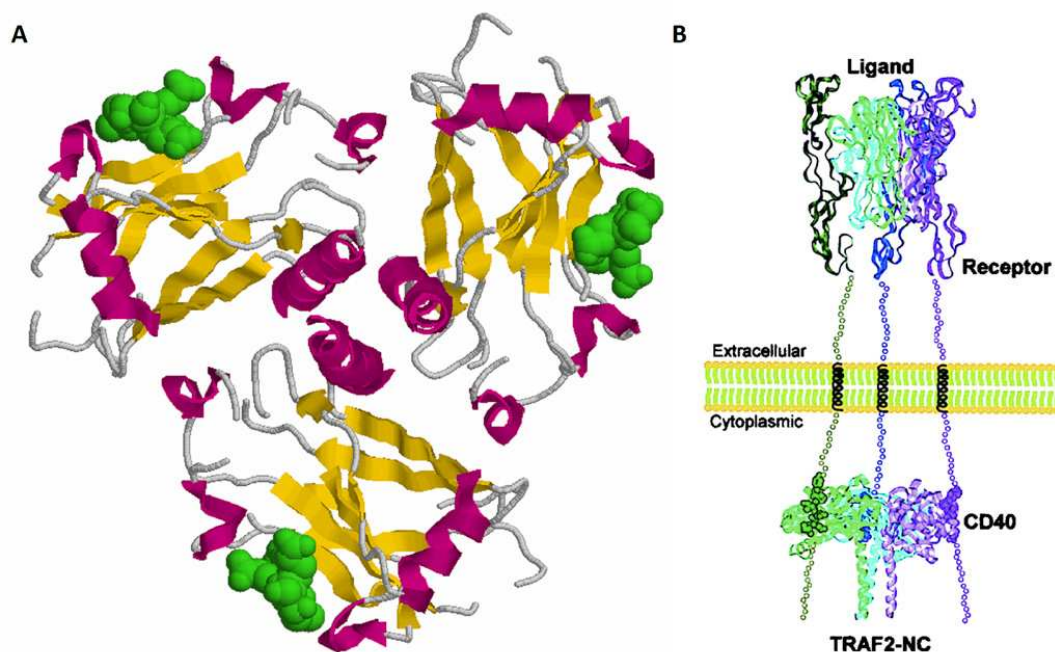


Figure 24. Three-dimensional model of the TRAF2–CD40 interaction. (A) Same structure as in Figure 22, represented in cartoons. The TRAF2-binding peptides Ac-²⁵⁰YPIQET²⁵⁵-NH₂ derived from CD40 are represented in green spacefill. Three-fold symmetry axis is perpendicular to the plan, with TRAF-N domain helices in the center pointing toward the reader. (B) Model of CD40/TRAF2 complex induced by ligand/receptor interaction as suggested by McWhirter and coworkers (PDB code 1QSC).⁸¹

3.4.2.4 TRAF-specific signaling

3.4.2.4.1 TRAF1

TRAF1 interacts only weakly with CD40 in the absence of TRAF2, and cooperates with TRAF2 to enhance some CD40-induced pathways.⁸³ It was also proposed that the stoichiometry of each protein in TRAF1–TRAF2 complexes determine their ability to engage

⁸¹ McWhirter, S M, et al. (1999). Crystallographic analysis of CD40 recognition and signaling by human TRAF2. *Proc Natl Acad Sci U S A* 96, 8408.

⁸² Chung, J Y, et al. (2002). All TRAFs are not created equal: common and distinct molecular mechanisms of TRAF-mediated signal transduction. *J Cell Sci* 115, 679.

⁸³ Xie, P, et al. (2006). Cooperation between TNF receptor-associated factors 1 and 2 in CD40 signaling. *J Immunol* 176, 5388.

CHAPTER 3

signaling downstream CD40.⁸⁴ Although TRAF1 has been shown to associate with a number of cytoplasmic molecules implicated in NF- κ B and JNK activation, its complex role in regulation of apoptotic signals is not fully understood.

3.4.2.4.2 TRAF2

TRAF2 was linked to the NF- κ B and AP-1 pathways,⁸⁵ and transfection of full-length TRAF2 cells led to an enhanced activation of NF- κ B in untreated epithelial cells.⁶³ NF- κ B-inducing kinase (NIK) was shown to mediate TRAF2-dependent NF- κ B activation from the LT- β receptor and to interact with TRAFs 1, 3, 5 and 6.⁸⁶ Several other molecules that influence TRAF2-mediated NF- κ B activation have also been described.⁸⁷ More recently, the MAP3K8 Tpl/COT1 was shown to be recruited to the CD40 receptor complex via its interaction with TRAF2 and TRAF6, resulting in activation of inhibitor of κ B (I κ B) kinase (IKK) and subsequent induction of NF- κ B.⁸⁸ TRAF2 can also interact with MEKK1 (also named MAP3K), and TNF-R1 activation was shown to enhance the TRAF2-MEKK1 interaction, thereby activating MAPK pathways.⁸⁹ Experiments with TRAF2^{-/-} mice confirmed that TRAF2 is an essential mediator of JNK activation.⁹⁰

Interestingly, TRAFs were also shown to interact with cell structure-related proteins. For example, caveolin-1 was shown to interact with TRAF2, targeting it to lipid rafts.⁹¹

3.4.2.4.3 TRAF3

TRAF3 overexpression was shown to block the TRAF2-dependent NF- κ B induction.⁶³ Furthermore, a dominant negative form of TRAF3, in which the ring finger was deleted, inhibited CD40-induced upregulation of CD23 in human B lymphoma, probably by displacing TRAF2 from the receptor.⁹² In fact, TRAF3 is not necessary for the induction of antibody

⁸⁴ Fotin-Mleczek, M, et al. (2004). Tumor necrosis factor receptor-associated factor (TRAF) 1 regulates CD40-induced TRAF2-mediated NF-kappaB activation. *J Biol Chem* 279, 677.

⁸⁵ Bradley, J R, et al. (2001). Tumor necrosis factor receptor-associated factors (TRAFs). *Oncogene* 20, 6482.

⁸⁶ Luftig, M A, et al. (2001). Effects of the NIK aly mutation on NF-kappaB activation by the Epstein-Barr virus latent infection membrane protein, lymphotoxin beta receptor, and CD40. *J Biol Chem* 276, 14602.

⁸⁷ Song, H Y, et al. (1996). The tumor necrosis factor-inducible zinc finger protein A20 interacts with TRAF1/TRAF2 and inhibits NF-kappaB activation. *Proc Natl Acad Sci U S A* 93, 6721.

⁸⁸ Chan, H, et al. (2005). TRAF-dependent association of protein kinase Tpl2/COT1 (MAP3K8) with CD40. *Biochem Biophys Res Commun* 328, 198.

⁸⁹ Baud, V, et al. (1999). Signaling by proinflammatory cytokines: oligomerization of TRAF2 and TRAF6 is sufficient for JNK and IKK activation and target gene induction via an amino-terminal effector domain. *Genes Dev* 13, 1297.

⁹⁰ Yeh, W C, et al. (1997). Early lethality, functional NF-kappaB activation, and increased sensitivity to TNF-induced cell death in TRAF2-deficient mice. *Immunity* 7, 715.

⁹¹ Feng, X, et al. (2001). Caveolin-1 associates with TRAF2 to form a complex that is recruited to tumor necrosis factor receptors. *J Biol Chem* 276, 8341.

⁹² Cheng, G, et al. (1995). Involvement of CRAF1, a relative of TRAF, in CD40 signaling. *Science* 267, 1494.

CHAPTER 3

secretion,⁹³ and B cells from TRAF3-deficient mice upregulated CD23 and proliferated normally in response to CD40L.⁹⁴ However, isotype switching in response to T-dependent antigens is defective, suggesting that TRAF3 is not required for CD40 signaling, but is important in T-dependent immune responses.

Recently, association between TRAF3 and TRAF2 was reported.⁹⁵ This interaction involves the TRAF-C domain of TRAF3 and zinc-finger regions of TRAF2. TRAF3/TRAF2 hetero-trimerization inhibits the TRAF2-induced NF- κ B pathway, but not the activation of AP-1. TRAF3 was also shown to regulate both the classical (p50/RelA) and alternative (p52/RelB)⁹⁶ NF- κ B pathways induced from TRAFs 2/5.⁹⁷ An important role for TRAF3 in CD40-mediated apoptosis of cancer cell was described recently, through activation of the JNK/AP-1 pathway and activation of caspase 9.⁶⁰

Interestingly, recruitment of TRAF3 to microtubule network was shown to occur via MIP-T3 which specifically interacts with TRAF3 through the TRAF-N.⁹⁸ TRAF3 was also shown associated with a component of the nuclear pore central plug.⁹⁹

3.4.2.4.4 TRAF4

TRAF4 was shown to be expressed in breast carcinoma but not in normal tissues, and localized predominantly to the nucleus,¹⁰⁰ and is overexpressed in human carcinomas, suggesting that TRAF4 has an oncogenic role.¹⁰¹ To date, no data have described implication of TRAF4 in CD40 signaling, although a CD40-TRAF4 could be detected *in vitro*.¹⁰² Nevertheless, TRAF4 mediates TNF signaling and inhibits Fas-mediated apoptosis of HEK

⁹³ Hostager, B S, et al. (1999). Cutting edge: contrasting roles of TNF receptor-associated factor 2 (TRAF2) and TRAF3 in CD40-activated B lymphocyte differentiation. *J Immunol* 162, 6307.

⁹⁴ Xu, Y, et al. (1996). Targeted disruption of TRAF3 leads to postnatal lethality and defective T-dependent immune responses. *Immunity* 5, 407.

⁹⁵ He, L, et al. (2004). TRAF3 forms heterotrimers with TRAF2 and modulates its ability to mediate NF- κ B activation. *J Biol Chem* 279, 55855.

⁹⁶ Dejardin, E. (2006). The alternative NF- κ B pathway from biochemistry to biology: pitfalls and promises for future drug development. *Biochem Pharmacol* 72, 1161.

⁹⁷ Hauer, J, et al. (2005). TNF receptor (TNFR)-associated factor (TRAF) 3 serves as an inhibitor of TRAF2/5-mediated activation of the noncanonical NF- κ B pathway by TRAF-binding TNFRs. *Proc Natl Acad Sci U S A* 102, 2874.

⁹⁸ Ling, L, et al. (2000). MIP-T3, a novel protein linking tumor necrosis factor receptor-associated factor 3 to the microtubule network. *J Biol Chem* 275, 23852.

⁹⁹ Gamper, C, et al. (2000). TRAF-3 interacts with p62 nucleoporin, a component of the nuclear pore central plug that binds classical NLS-containing import complexes. *Mol Immunol* 37, 73.

¹⁰⁰ Regnier, C H, et al. (1995). Presence of a new conserved domain in CART1, a novel member of the tumor necrosis factor receptor-associated protein family, which is expressed in breast carcinoma. *J Biol Chem* 270, 25715.

¹⁰¹ Camilleri-Broet, S, et al. (2007). TRAF4 overexpression is a common characteristic of human carcinomas. *Oncogene* 26, 142.

¹⁰² Roy, N, et al. (1997). The c-IAP-1 and c-IAP-2 proteins are direct inhibitors of specific caspases. *Embo J* 16, 6914.

CHAPTER 3

cells when overexpressed.¹⁰³ Furthermore, TRAF4 enhances GITR-induced NF- κ B activation, modulating suppressive functions of T_{reg} cells.¹⁰⁴

3.4.2.4.5 TRAF5

TRAF5 involvement in CD40 signaling was provided by cells from TRAF5^{-/-} mice in which receptor-mediated lymphocyte activation was substantially impaired but which displayed normal CD40-mediated NF- κ B and JNK activation.¹⁰⁵ This suggests that TRAF5 compensation mechanisms might be efficient to some extent. TRAF5 self-associates in the cytoplasm of HeLa cells,⁹⁴ and interacts with either CD40 directly⁷⁰ or via heterotrimerization with TRAF3.⁶⁷ The latter case was suggested to explain why CD40-induced NF- κ B mediated by TRAF5 was enhanced in the presence of TRAF3.¹⁰⁶ Finally, like TRAF2, TRAF5 is important for the NF- κ B activation via both the classical and alternative pathways which is regulated by TRAF3.⁹⁶

3.4.2.4.6 TRAF6

TRAF6 is implicated in CD40-mediated IKK and NF- κ B activation in monocyte/macrophage.¹⁰⁷ TRAF6 is also implicated in CD40 signaling in B cell and is required for the production of inflammatory cytokines through the engagement of Src/ERK1/2 pathway.¹⁰⁸ This is consistent with earlier observations that transfection of TRAF6 into 293 cells activated NF- κ B pathway, such as with TRAF2 and TRAF5.⁶⁹ Recently, TRAF6 was shown to induce apoptosis through interaction with caspase and its activation by a RING domain-dependent mechanism.¹⁰⁹ Interestingly, Benson *et al.* showed that CD40 can protect B cells from CD95-mediated apoptosis by inhibiting caspase activation via TRAF6 and the PI3K/Akt pathway.¹¹⁰

¹⁰³ Fleckenstein, D S, et al. (2003). Tumor necrosis factor receptor-associated factor (TRAF) 4 is a new binding partner for the p70S6 serine/threonine kinase. *Leuk Res* 27, 687.

¹⁰⁴ Esparza, E M, et al. (2004). TRAF4 functions as an intermediate of GITR-induced NF-kappaB activation. *Cell Mol Life Sci* 61, 3087.

¹⁰⁵ Nakano, H, et al. (1999). Targeted disruption of Traf5 gene causes defects in CD40- and CD27-mediated lymphocyte activation. *Proc Natl Acad Sci U S A* 96, 9803.

¹⁰⁶ Leo, E, et al. (1999). Differential requirements for tumor necrosis factor receptor-associated factor family proteins in CD40-mediated induction of NF-kappaB and Jun N-terminal kinase activation. *J Biol Chem* 274, 22414.

¹⁰⁷ Mukundan, L, et al. (2005). TNF receptor-associated factor 6 is an essential mediator of CD40-activated proinflammatory pathways in monocytes and macrophages. *J Immunol* 174, 1081.

¹⁰⁸ Lomaga, M A, et al. (1999). TRAF6 deficiency results in osteopetrosis and defective interleukin-1, CD40, and LPS signaling. *Genes Dev* 13, 1015.

¹⁰⁹ He, L, et al. (2006). TRAF6 regulates cell fate decisions by inducing caspase 8-dependent apoptosis and the activation of NF-kappaB. *J Biol Chem* 281, 11235.

¹¹⁰ Benson, R J, et al. (2006). Rapid CD40-mediated rescue from CD95-induced apoptosis requires TNFR-associated factor-6 and PI3K. *Eur J Immunol* 36, 2535.

3.4.3 TRAF-independent CD40 signaling

Janus kinase 3 (JAK3) pathway seems to be important for CD40-mediated activation of monocytes¹¹¹ and dendritic cells,¹¹² but not of B cells.¹¹³ JAK3 has been shown to interact with a proline motif in the intracellular region of CD40, through two identified JAK binding-motifs (Figure 25).¹¹⁴ JAK3 is phosphorylated following CD40 ligation, resulting in the phosphorylation of STAT-3, STAT-5 α and STAT-6. Numerous CD40-induced pathways have been described, but some of them were neither associated to TRAF nor to JAK3 (Poster 1).

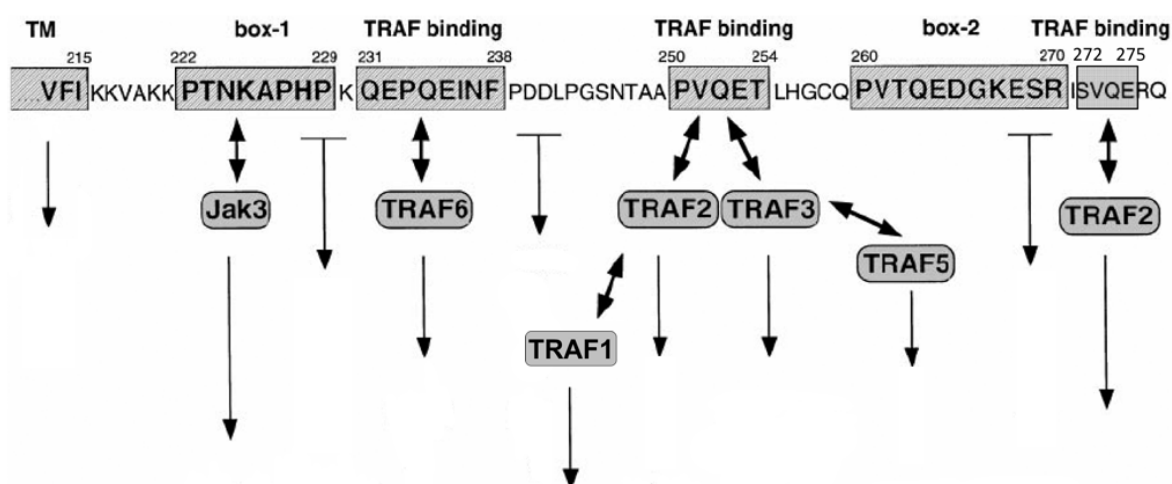


Figure 25. JAK and TRAF binding motifs on the intracytoplasmic sequence of CD40. JAK3 (box-1 and box-2) as well as TRAF (TRAF binding) binding motifs are indicated on the intracytoplasmic domain sequence of CD40. Some other pathways were shown to be initiated apart from these motifs. Figure is adapted from van Kooten *et al.*⁷

¹¹¹ Revy, P, et al. (1999). Activation of the Janus kinase 3-STAT5a pathway after CD40 triggering of human monocytes but not of resting B cells. *J Immunol* 163, 787.

¹¹² Saemann, M D, et al. (2002). CD40 triggered human monocyte-derived dendritic cells convert to tolerogenic dendritic cells when JAK3 activity is inhibited. *Transplant Proc* 34, 1407.

¹¹³ Jabara, H H, et al. (1998). Role of JAK3 in CD40-mediated signaling. *Blood* 92, 2435.

¹¹⁴ Hanissian, S H, et al. (1997). Jak3 is associated with CD40 and is critical for CD40 induction of gene expression in B cells. *Immunity* 6, 379.

CHAPTER 3

References related to Poster 1

- [1] Ren et al. (1994). Signal transduction via CD40 involves activation of lyn kinase and phosphatidylinositol-3-kinase, and phosphorylation of phospholipase C gamma 2. *J Exp Med* 179, 673.
- [2] Faris et al. (1994). CD40 signaling pathway: anti-CD40 monoclonal antibody induces rapid dephosphorylation and phosphorylation of tyrosine-phosphorylated proteins including protein tyrosine kinase Lyn, Fyn, and Syk and the appearance of a 28-kD tyrosine phosphorylated protein. *J Exp Med* 179, 1923.
- [3] Berberich et al. (1994). Cross-linking CD40 on B cells rapidly activates nuclear factor-kappa B. *J Immunol* 153, 4357.
- [4] Uckun et al. (1991). Stimulation of protein tyrosine phosphorylation, phosphoinositide turnover, and multiple previously unidentified serine/threonine-specific protein kinases by the Pan-B-cell receptor CD40/Bp50 at discrete developmental stages of human B-cell ontogeny. *J Biol Chem* 266, 17478.
- [5] Hanissian et al. (1997). Jak3 is associated with CD40 and is critical for CD40 induction of gene expression in B cells. *Immunity* 6, 379.
- [6] Davies et al. (2005). NF-kappaB overrides the apoptotic program of TNF receptor 1 but not CD40 in carcinoma cells. *Cell Signal* 17, 729.
- [7] Vidalain et al. (2000). CD40 signaling in human dendritic cells is initiated within membrane rafts. *Embo J* 19, 3304.
- [8] Garceau et al. (2000). Lineage-restricted function of nuclear factor kappaB-inducing kinase (NIK) in transducing signals via CD40. *J Exp Med* 191, 381.
- [9] Craxton et al. (1998). p38 MAPK is required for CD40-induced gene expression and proliferation in B lymphocytes. *J Immunol* 161, 3225.
- [10] Aicher et al. (1999). Differential role for p38 mitogen-activated protein kinase in regulating CD40-induced gene expression in dendritic cells and B cells. *J Immunol* 163, 5786.
- [11] Berberich et al. (1996). Cross-linking CD40 on B cells preferentially induces stress-activated protein kinases rather than mitogen-activated protein kinases. *Embo J* 15, 92.
- [12] Suttles et al. (1999). CD40 signaling of monocyte inflammatory cytokine synthesis through an ERK1/2-dependent pathway. A target of interleukin (il)-4 and il-10 anti-inflammatory action. *J Biol Chem* 274, 5835.
- [13] Li et al. (1996). CD40 ligation results in protein kinase C-independent activation of ERK and JNK in resting murine splenic B cells. *J Immunol* 157, 1440.
- [14] Arron et al. (2001). A positive regulatory role for Cbl family proteins in tumor necrosis factor-related activation-induced cytokine (trance) and CD40L-mediated Akt activation. *J Biol Chem* 276, 30011.
- [15] Yu et al. (2004). The role of the p38 mitogen-activated protein kinase, extracellular signal-regulated kinase, and phosphoinositide-3-OH kinase signal transduction pathways in CD40 ligand-induced dendritic cell activation and expansion of virus-specific CD8+ T cell memory responses. *J Immunol* 172, 6047.
- [16] Pearson et al. (2001). CD40-mediated signaling in monocytic cells: up-regulation of tumor necrosis factor receptor-associated factor mRNAs and activation of mitogen-activated protein kinase signaling pathways. *Int Immunol* 13, 273.
- [17] Trompouki et al. (2003). CYLD is a deubiquitinating enzyme that negatively regulates NF-kappaB activation by TNFR family members. *Nature* 424, 793.
- [18] Chen et al. (2006). Internalization of CD40 regulates its signal transduction in vascular endothelial cells. *Biochem Biophys Res Commun* 345, 106.
- [19] Flaxenburg et al. (2004). The CD40-induced signaling pathway in endothelial cells resulting in the overexpression of vascular endothelial growth factor involves Ras and phosphatidylinositol 3-kinase. *J Immunol* 172, 7503.
- [20] Deregibus et al. (2003). CD40-dependent activation of phosphatidylinositol 3-kinase/Akt pathway mediates endothelial cell survival and in vitro angiogenesis. *J Biol Chem* 278, 18008.

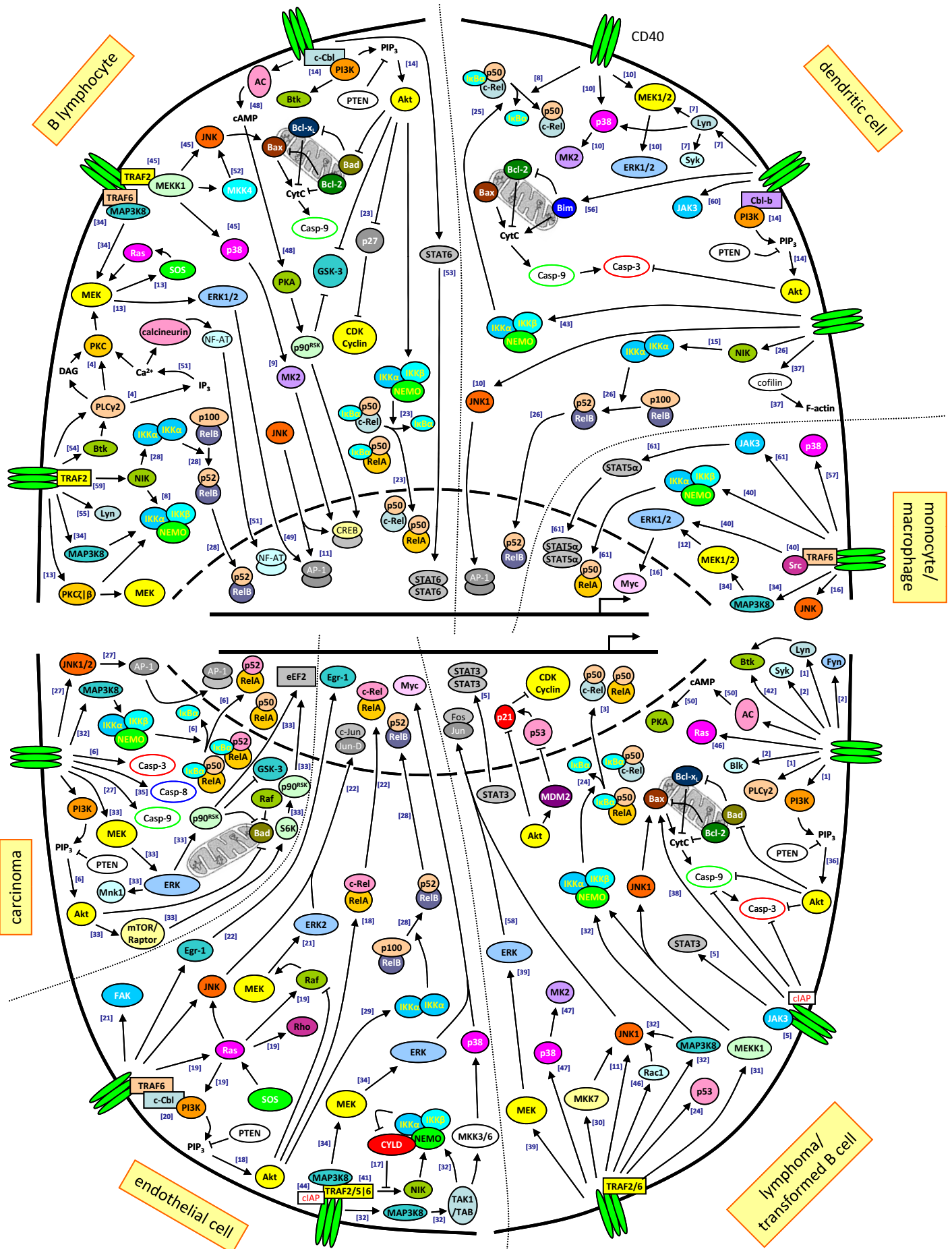
CHAPTER 3

- [21] Reyes et al. (2002). Adhesion of B cell lines to endothelial cells from human lymphoid tissue modulates tyrosine phosphorylation and endothelial cell activation. *J Immunol* 169, 5881.
- [22] Bavendiek et al. (2002). Induction of tissue factor expression in human endothelial cells by CD40 ligand is mediated via activator protein 1, nuclear factor kappa B, and Egr-1. *J Biol Chem* 277, 25032.
- [23] Andjelic et al. (2000). Phosphatidylinositol 3-kinase and NF-kappa B/Rel are at the divergence of CD40-mediated proliferation and survival pathways. *J Immunol* 165, 3860.
- [24] Hollmann et al. (2002). CD40-mediated apoptosis in murine B-lymphoma lines containing mutated p53. *Exp Cell Res* 280, 201.
- [25] Ouaz et al. (2002). Dendritic cell development and survival require distinct NF-kappaB subunits. *Immunity* 16, 257.
- [26] Yanagawa et al. (2006). Distinct regulation of CD40-mediated interleukin-6 and interleukin-12 productions via mitogen-activated protein kinase and nuclear factor kappaB-inducing kinase in mature dendritic cells. *Immunology* 117, 526.
- [27] Georgopoulos et al. (2006). A novel mechanism of CD40-induced apoptosis of carcinoma cells involving TRAF3 and JNK/AP-1 activation. *Cell Death Differ* 13, 1789.
- [28] Coope et al. (2002). CD40 regulates the processing of NF-kappaB2 p100 to p52. *Embo J* 21, 5375.
- [29] Gustin et al. (2006). Akt regulates basal and induced processing of NF-kappaB2 (p100) to p52. *J Biol Chem* 281, 16473.
- [30] Foltz et al. (1998). Human mitogen-activated protein kinase kinase 7 (MKK7) is a highly conserved c-Jun N-terminal kinase/stress-activated protein kinase (JNK/SAPK) activated by environmental stresses and physiological stimuli. *J Biol Chem* 273, 9344.
- [31] Sakata et al. (1995). Selective activation of c-Jun kinase mitogen-activated protein kinase by CD40 on human B cells. *J Biol Chem* 270, 30823.
- [32] Chan et al. (2005). TRAF-dependent association of protein kinase Tpl2/COT1 (MAP3K8) with CD40. *Biochem Biophys Res Commun* 328, 198.
- [33] Davies et al. (2004). Inhibition of phosphatidylinositol 3-kinase- and ERK MAPK-regulated protein synthesis reveals the pro-apoptotic properties of CD40 ligation in carcinoma cells. *J Biol Chem* 279, 1010.
- [34] Eliopoulos et al. (2003). Tpl2 transduces CD40 and TNF signals that activate ERK and regulates IgE induction by CD40. *Embo J* 22, 3855.
- [35] Eliopoulos et al. (2000). CD40 induces apoptosis in carcinoma cells through activation of cytotoxic ligands of the tumor necrosis factor superfamily. *Mol Cell Biol* 20, 5503.
- [36] Georgakis et al. (2006). Inhibition of the phosphatidylinositol-3 kinase/Akt promotes G1 cell cycle arrest and apoptosis in Hodgkin lymphoma. *Br J Haematol* 132, 503.
- [37] Verdijk et al. (2004). Morphological changes during dendritic cell maturation correlate with cofilin activation and translocation to the cell membrane. *Eur J Immunol* 34, 156.
- [38] Szocinski et al. (2002). Activation-induced cell death of aggressive histology lymphomas by CD40 stimulation: induction of bax. *Blood* 100, 217.
- [39] Hollmann et al. (2006). Constitutive activation of extracellular signal-regulated kinase predisposes diffuse large B-cell lymphoma cell lines to CD40-mediated cell death. *Cancer Res* 66, 3550.
- [40] Mukundan et al. (2005). TNF receptor-associated factor 6 is an essential mediator of CD40-activated proinflammatory pathways in monocytes and macrophages. *J Immunol* 174, 1081.
- [41] Hauer et al. (2005). TNF receptor (TNFR)-associated factor (TRAF) 3 serves as an inhibitor of TRAF2/5-mediated activation of the noncanonical NF-kappaB pathway by TRAF-binding TNFRs. *Proc Natl Acad Sci U S A* 102, 2874.
- [42] Brunner et al. (2002). Bruton's tyrosine kinase is activated upon CD40 stimulation in human B lymphocytes. *Immunobiology* 206, 432.
- [43] Mackey et al. (2003). Distinct contributions of different CD40 TRAF binding sites to CD154-induced dendritic cell maturation and IL-12 secretion. *Eur J Immunol* 33, 779.
- [44] Werneburg et al. (2001). Molecular characterization of CD40 signaling intermediates. *J Biol Chem* 276, 43334.

CHAPTER 3

- [45] Gallagher et al. (2007). Kinase MEKK1 is required for CD40-dependent activation of the kinases Jnk and p38, germinal center formation, B cell proliferation and antibody production. *Nat Immunol* 8, 57.
- [46] Gulbins et al. (1996). Activation of the Ras signaling pathway by the CD40 receptor. *J Immunol* 157, 2844.
- [47] Sutherland et al. (1996). Differential activation of the ERK, JNK, and p38 mitogen-activated protein kinases by CD40 and the B cell antigen receptor. *J Immunol* 157, 3381.
- [48] Kato et al. (1994). Mechanisms of T cell contact-dependent B cell activation. *J Immunol* 152, 2130.
- [49] Huo et al. (1996). Isolation and characterization of murine fra-1: induction mediated by CD40 and surface Ig is protein kinase C dependent. *J Immunol* 157, 3812.
- [50] Goldstein et al. (1997). Cyclic-AMP modulates downstream events in CD40-mediated signal transduction, but inhibition of protein kinase A has no direct effect on CD40 signaling. *J Immunol* 159, 5871.
- [51] Klaus et al. (1994). Properties of mouse CD40. Ligation of CD40 activates B cells via a Ca(++)-dependent, FK506-sensitive pathway. *Eur J Immunol* 24, 3229.
- [52] Nishina et al. (1997). Impaired CD28-mediated interleukin 2 production and proliferation in stress kinase SAPK/ERK1 kinase (SEK1)/mitogen-activated protein kinase kinase 4 (MKK4)-deficient T lymphocytes. *J Exp Med* 186, 941.
- [53] Karras et al. (1997). Induction of STAT protein signaling through the CD40 receptor in B lymphocytes: distinct STAT activation following surface Ig and CD40 receptor engagement. *J Immunol* 159, 4350.
- [54] Goldstein et al. (1996). Induction of costimulatory molecules B7-1 and B7-2 in murine B cells. the CBA/N mouse reveals a role for Bruton's tyrosine kinase in CD40-mediated B7 induction. *Mol Immunol* 33, 541.
- [55] Wang et al. (1996). Altered antigen receptor signaling and impaired Fas-mediated apoptosis of B cells in Lyn-deficient mice. *J Exp Med* 184, 831.
- [56] Chen et al. (2007). Deficiency of Bim in dendritic cells contributes to over-activation of lymphocytes and autoimmunity. *Blood* (blood-2006-11-056424v1).
- [57] Mathur et al. (2004). Reciprocal CD40 signals through p38MAPK and ERK-1/2 induce counteracting immune responses. *Nat Med* 10, 540.
- [58] Shirakata et al. (1999). Distinct subcellular localization and substrate specificity of extracellular signal-regulated kinase in B cells upon stimulation with IgM and CD40. *J Immunol* 163, 6589.
- [59] Nguyen et al. (1999). TRAF2 deficiency results in hyperactivity of certain TNFR1 signals and impairment of CD40-mediated responses. *Immunity* 11, 379.
- [60] Saemann et al. (2002). CD40 triggered human monocyte-derived dendritic cells convert to tolerogenic dendritic cells when JAK3 activity is inhibited. *Transplant Proc* 34, 1407.
- [61] Revy et al. (1999). Activation of the Janus kinase 3-STAT5a pathway after CD40 triggering of human monocytes but not of resting B cells. *J Immunol* 163, 787.

Poster 1: summary of the signaling pathways engaged by CD40



CHAPTER 4

THE CD40–CD40L INTERACTION AS A TARGET FOR IMMUNOTHERAPY

CHAPTER 4

The CD40–CD40L interaction has a central role in both adaptive and cellular immune responses, making it a promising target for immunotherapy. Such non-specific immunomodulation implies suppression of immune response, as in autoimmune diseases, inflammatory conditions and transplantation, as well as activation or enhancement of immune responses against infections and cancer, and in an immunodeficiency context.¹ Here, we discuss the different approaches used for treating these diseases.

4.1 Blockade of the CD40–CD40L interaction

As described in the chapter 1, CD40L is mainly expressed transiently on activated CD4⁺ helper T cells subsequent to recognition of MHC–peptide complexes.² CD40L promotes B cell rescue from apoptosis, proliferation, differentiation into germinal center cells, up-regulation of costimulatory and activation molecules, Ig isotype switching, selection and maturation into memory cells.³ In addition, CD40L triggers CD40 at the surface of other APC including dendritic cells and monocytes/macrophages. It enhances survival of these cells, antigen presenting functions of dendritic cells, and antimicrobial and cytotoxic activities of macrophages. Finally, priming of CD8⁺ cytotoxic T lymphocytes generally requires help provided by CD4⁺, and the CD40–CD40L interaction was shown to be essential in the CTL priming via activated DCs.⁴ Thus, CD40L also controls T cell functions and inflammatory reactions (Figure 26).

Furthermore, CD40 was detected on a wide range of non-hematopoietic cells, including endothelial cells, epithelial cells and fibroblasts, and is expressed in higher levels in various pathological contexts.³ In these cells, CD40L induces inflammatory responses by inducing their proliferation, up-regulation of adhesion molecules, production of cytokines and chemokines leading to migration and extravasation of leukocytes to sites of inflammation, and fibrosis.⁵ The fact that not only CD4⁺ T cells but also endothelial cells,

¹ Schonbeck, U, et al. (2001). The CD40/CD154 receptor/ligand dyad. *Cell Mol Life Sci* 58, 4.

² Lederman, S, et al. (1992). Identification of a novel surface protein on activated CD4⁺ T cells that induces contact-dependent B cell differentiation (help). *J Exp Med* 175, 1091.

³ van Kooten, C, et al. (2000). CD40-CD40 ligand. *J Leukoc Biol* 67, 2.

⁴ Bennett, S R, et al. (1998). Help for cytotoxic-T-cell responses is mediated by CD40 signalling. *Nature* 393, 478;

Schoenberger, S P, et al. (1998). T-cell help for cytotoxic T lymphocytes is mediated by CD40-CD40L interactions. *Nature* 393, 480.

⁵ Kaufman, J, et al. (2001). Fibroblasts as sentinel cells: role of the CD40-CD40 ligand system in fibroblast activation and lung inflammation and fibrosis. *Chest* 120, 53S; Yellin, M J, et al. (1995). Functional interactions of T cells with endothelial cells: the role of CD40L-CD40-mediated signals. *J Exp Med* 182, 1857.

CHAPTER 4

fibroblasts and platelets have been reported to express CD40L, suggests that non-immune cells could be involved in the sustenance of inflammation.⁶

The central role of CD40 signaling in both humoral and cellular immune responses provides an interesting target to decrease abnormal immune response against self-antigen (autoimmunity) and chronic inflammation.

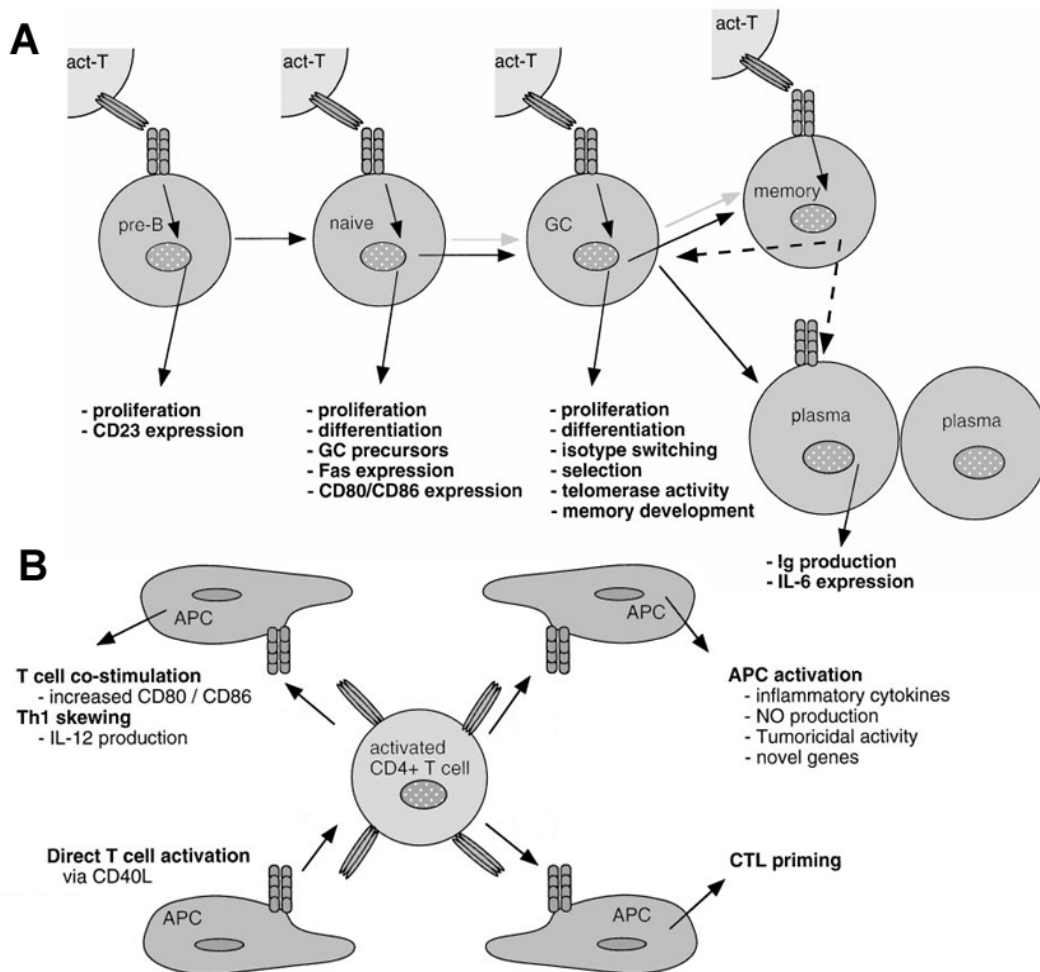


Figure 26. CD40L controls immune cell functions and inflammatory reaction. CD40L controls B cell development, from pre-B to memory and plasma cells via naïve and germinal center (GC) stages (A), as well as T cell and APC functions (B). Figure was derived from van Kooten and coworkers.³

4.1.1 CD40-based treatment of autoimmune diseases

A potential role of CD40–CD40L interaction has been established in several autoimmune diseases,⁷ such as SLE-like syndromes,⁸ rheumatoid arthritis (RA),⁹ experimental autoimmune encephalomyelitis¹⁰ and multiple sclerosis (MS).¹¹

⁶ Henn, V, et al. (1998). CD40 ligand on activated platelets triggers an inflammatory reaction of endothelial cells. *Nature* 391, 591; Kaufman, J, et al. (2004). Expression of CD154 (CD40 ligand) by human lung fibroblasts: differential regulation by IFN-gamma and IL-13, and implications for fibrosis. *J Immunol* 172, 1862; Mach, F, et al. (1997). Functional CD40 ligand is expressed on human vascular endothelial cells, smooth muscle cells, and macrophages: implications for CD40-CD40 ligand signaling in atherosclerosis. *Proc Natl Acad Sci U S A* 94, 1931.

CHAPTER 4

CD40 signaling has furthermore been associated with early events in the development of insulin-dependent diabetes mellitus as seen in non-obese diabetic (NOD) mice,¹² Sjogren's syndrome,¹³ inflammatory bowel disease,¹⁴ and systemic sclerosis,¹⁵ among other diseases.

4.1.1.1 Systemic Lupus Erythematosus

SLE is characterized by abnormal B cell activation and differentiation to memory and plasma cell effectors producing pathogenic IgG autoantibodies of high avidity directed against nuclear antigens, phospholipids and cell surface molecules.¹⁶ These autoantibodies are responsible for clotting, haemolytic anaemia, thrombocytopenia and leukopenia associated with the disease. The most important outcome, leading to the formation of immune complex in glomerulonephritis, arthritis, serositis and vasculitis, is induced by anti-DNA autoantibodies.¹⁷ Since i) CD40L has been shown to be hyper-expressed in lymphocytes from lupus prone mice¹⁸ and from active SLE patient,¹⁹ and ii) IgG production requires class switching, anti-CD40L antibodies have emerged as interesting tools for treatment of SLE.

Anti-CD40L mAbs delayed and reduced the incidence of lupus nephritis when administered to pre-nephritic mice.¹⁸ They significantly prolonged survival of mice with established lupus nephritis by inhibiting the initiation of GC reactions,²⁰ reducing severity of nephritis and decreasing associated inflammation, sclerosis/fibrosis and vasculitis.²¹ Thanks

⁷ Datta, S K, et al. (1997). CD40-CD40 ligand interaction in autoimmune disease. *Arthritis Rheum* 40, 1735.

⁸ Ma, J, et al. (1996). Autoimmune lpr/lpr mice deficient in CD40 ligand: spontaneous Ig class switching with dichotomy of autoantibody responses. *J Immunol* 157, 417.

⁹ Durie, F H, et al. (1994). Collagen-induced arthritis as a model of rheumatoid arthritis. *Clin Immunol Immunopathol* 73, 11.

¹⁰ Grewal, I S, et al. (1996). Requirement for CD40 ligand in costimulation induction, T cell activation, and experimental allergic encephalomyelitis. *Science* 273, 1864.

¹¹ Gerritse, K, et al. (1996). CD40-CD40 ligand interactions in experimental allergic encephalomyelitis and multiple sclerosis. *Proc Natl Acad Sci U S A* 93, 2499.

¹² Balasa, B, et al. (1997). CD40 ligand-CD40 interactions are necessary for the initiation of insulinitis and diabetes in nonobese diabetic mice. *J Immunol* 159, 4620.

¹³ Nakamura, H, et al. (1999). Expression of CD40/CD40 ligand and Bcl-2 family proteins in labial salivary glands of patients with Sjogren's syndrome. *Lab Invest* 79, 261.

¹⁴ Liu, Z, et al. (1999). Hyperexpression of CD40 ligand (CD154) in inflammatory bowel disease and its contribution to pathogenic cytokine production. *J Immunol* 163, 4049.

¹⁵ Allamore, Y, et al. (2005). Increased plasma soluble CD40 ligand concentrations in systemic sclerosis and association with pulmonary arterial hypertension and digital ulcers. *Ann Rheum Dis* 64, 481.

¹⁶ Cabral, A R, et al. (1998). Autoantibodies in systemic lupus erythematosus. *Curr Opin Rheumatol* 10, 409.

¹⁷ Spronk, P E, et al. (1996). Anti-dsDNA production coincides with concurrent B and T cell activation during development of active disease in systemic lupus erythematosus (SLE). *Clin Exp Immunol* 104, 446.

¹⁸ Mohan, C, et al. (1995). Interaction between CD40 and its ligand gp39 in the development of mouse lupus nephritis. *J Immunol* 154, 1470.

¹⁹ Devi, B S, et al. (1998). Peripheral blood lymphocytes in SLE--hyperexpression of CD154 on T and B lymphocytes and increased number of double negative T cells. *J Autoimmun* 11, 471.

²⁰ Luzina, I G, et al. (2001). Spontaneous formation of germinal centers in autoimmune mice. *J Leukoc Biol* 70, 578.

²¹ Kalled, S L, et al. (1998). Anti-CD40 ligand antibody treatment of SNF1 mice with established nephritis: preservation of kidney function. *J Immunol* 160, 2158.

CHAPTER 4

to reversible immunosuppressive effect of anti-CD40L therapy, mounting of immune responses could be regained after completion of the treatment.²²

Clinical trials have been initiated to evaluate the safety and efficacy of anti-human CD40L humanized mAbs in patients with autoimmune diseases including SLE, idiopathic thrombocytopenic purpura and multiple sclerosis.²³ Encouraging results have been obtained in an open-label study on SLE patients which showed reductions in disease activity indices and levels of anti-dsDNA producing cells after a well tolerated brief period of treatment.²⁴ However, clinical trials of anti-CD40L mAbs have been halted because of thromboembolic complications,²⁵ despite significant immunomodulatory effects of the anti-CD40L treatment.²⁶

A recent study established the association of autoantibody directed against CD40L produced in SLE patients with thrombocytopenia but not thromboembolism.²⁷ As described in chapter 1, CD40L binds to other cell surface molecules than CD40. The complex role of CD40L in the mechanisms of thromboembolism and thrombocytopenia is still speculative. Nevertheless, the promising rituximab (anti-human CD20 mAb) treatment of SLE by depletion of B cells has shown rapid improvement in clinical manifestations, correlated with downregulation of CD40 and CD80 expression on CD19⁺ B lymphocytes²⁸ and downregulation of CD40L expression on CD4⁺ T cells,²⁹ thus reinforcing the importance of the CD40–CD40L interaction in disease progression.

²² Early, G S, et al. (1996). Anti-CD40 ligand antibody treatment prevents the development of lupus-like nephritis in a subset of New Zealand black x New Zealand white mice. Response correlates with the absence of an anti-antibody response. *J Immunol* 157, 3159.

²³ Dumont, F J. (2002). IDEC-131. IDEC/Eisai. *Curr Opin Investig Drugs* 3, 725; Kuwana, M, et al. (2004). Effect of a single injection of humanized anti-CD154 monoclonal antibody on the platelet-specific autoimmune response in patients with immune thrombocytopenic purpura. *Blood* 103, 1229.

²⁴ Davis, J C, Jr., et al. (2001). Phase I clinical trial of a monoclonal antibody against CD40-ligand (IDEC-131) in patients with systemic lupus erythematosus. *J Rheumatol* 28, 95; Huang, W, et al. (2002). The effect of anti-CD40 ligand antibody on B cells in human systemic lupus erythematosus. *Arthritis Rheum* 46, 1554.

²⁵ Kawai, T, et al. (2000). Thromboembolic complications after treatment with monoclonal antibody against CD40 ligand. *Nat Med* 6, 114.

²⁶ Boumpas, D T, et al. (2003). A short course of BG9588 (anti-CD40 ligand antibody) improves serologic activity and decreases hematuria in patients with proliferative lupus glomerulonephritis. *Arthritis Rheum* 48, 719.

²⁷ Nakamura, M, et al. (2006). Autoantibody to CD40 ligand in systemic lupus erythematosus: association with thrombocytopenia but not thromboembolism. *Rheumatology* 45, 150.

²⁸ Tokunaga, M, et al. (2005). Down-regulation of CD40 and CD80 on B cells in patients with life-threatening systemic lupus erythematosus after successful treatment with rituximab. *Rheumatology* 44, 176.

²⁹ Sfikakis, P P, et al. (2005). Remission of proliferative lupus nephritis following B cell depletion therapy is preceded by down-regulation of the T cell costimulatory molecule CD40 ligand: an open-label trial. *Arthritis Rheum* 52, 501.

4.1.1.2 An anti-CD40L therapy for other autoimmune diseases?

Stimulating results were obtained by administration anti-CD40L mAb in diverse autoimmune disease animal models. For example, such a treatment led to ameliorations in a mouse model of autoimmune haemolytic anaemia,³⁰ in the experimental autoimmune glomerulonephritis model of Goodpasture's disease in rat,³¹ in mouse experimental autoimmune thyroiditis, a model of the Hashimoto's thyroiditis,³² in experimental autoimmune myasthenia gravis, the rat model for the human myasthenia gravis disease,³³ and in hapten-induced colitis in mice, model that mimics some aspects of the Crohn's disease in humans.³⁴

Both anti-CD40L Ab and a CD40-IgG construct were found to be effective in inhibition of the CD40-CD40L interaction, and reduced the incidence of a murine Graves' disease model.³⁵ Anti-CD40L mAb treatment succeeded in collagen-induced arthritis in mice, a model of rheumatoid arthritis, by disrupting joint inflammation and subsequent bone erosion, and reducing serum antibody titers to collagen. Moreover, an original strategy was developed to attenuate antigen-induced arthritis with the use of a decoy oligodeoxynucleotide neutralizing the transcription factor STAT-1, which is implicated, at least in part, in the IFN γ -mediated expression of CD40 on macrophages (see chapter 2) and synovial fibroblasts.³⁶

These results suggest that the blockade of CD40-CD40L interaction remains a good strategy for the treatment of autoimmune diseases, but more specific and safer alternatives to anti-CD40L are needed. Noteworthy, some peptides have recently been described to inhibit the CD40-CD40L interaction.³⁷

³⁰ Sadlack, B, et al. (1995). Generalized autoimmune disease in interleukin-2-deficient mice is triggered by an uncontrolled activation and proliferation of CD4+ T cells. *Eur J Immunol* 25, 3053.

³¹ Reynolds, J, et al. (2004). Blockade of the CD154-CD40 costimulatory pathway prevents the development of experimental autoimmune glomerulonephritis. *Kidney Int* 66, 1444.

³² Carayanniotis, G, et al. (1997). Suppression of mouse thyroiditis via blockade of the CD40-CD40L interaction. *Immunology* 90, 421.

³³ Im, S H, et al. (2001). Blockade of CD40 ligand suppresses chronic experimental myasthenia gravis by down-regulation of Th1 differentiation and up-regulation of CTLA-4. *J Immunol* 166, 6893.

³⁴ Stuber, E, et al. (1996). Blocking the CD40L-CD40 interaction in vivo specifically prevents the priming of T helper 1 cells through the inhibition of interleukin 12 secretion. *J Exp Med* 183, 693.

³⁵ Chen, C R, et al. (2006). Blockade of costimulation between T cells and antigen-presenting cells: an approach to suppress mouse Graves' disease induced using thyrotropin receptor-expressing adenovirus. *Thyroid* 16, 427.

³⁶ Huckel, M, et al. (2006). Attenuation of mouse antigen-induced arthritis by treatment with a decoy oligodeoxynucleotide inhibiting signal transducer and activator of transcription-1 (STAT-1). *Arthritis Res Ther* 8, R17.

³⁷ Kitagawa, M, et al. (2005). Identification of three novel peptides that inhibit CD40-CD154 interaction. *Mod Rheumatol* 15, 423.

CHAPTER 4

4.1.2 Chronic inflammation

Apart from autoimmune diseases, chronic inflammatory responses result from persistent infections and many diseases. It may culminate in the interference with normal tissue function and destruction of the tissue if not controlled properly. In atherosclerosis, where cell-mediated immunity contributes to the development of vessel wall lesion, the CD40–CD40L interaction was thought to be important since both macrophages and CD4⁺ T cells were detected in the injured endothelium.³⁸ Treatment with anti-CD40L mAb reduced the initiation and early phases of atherosclerosis,³⁹ limited lesion progression and reduced the macrophage and lipid content of atheroma in hypercholesterolemic mice.⁴⁰ Moreover, enhanced levels of soluble and membrane-bound CD40L were detected in patients with unstable angina,⁴¹ supporting the implication of T lymphocytes and/or platelets in the pathogenesis of acute coronary syndromes. Thus, CD40L is an interesting target for treatment of these cardiovascular diseases.⁴²

The CD40/CD40L duet is also implicated in lung disorders. Administration of a soluble CD40L construct was found to induce pulmonary inflammatory reactions in CD40^{+/+} but not CD40^{-/-} mice.⁴³ Treatment with anti-CD40L mAb was efficient in preventing pulmonary inflammation and fibrosis consequent to oxygen-induced acute respiratory distress syndrome,⁴⁴ and radiation-induced pulmonary toxicity.⁴⁵

Of importance, a study demonstrated that continuous activation of Langerhans cells by CD40L in the skin not only leads to chronic inflammatory dermatitis, but also to the development of systemic autoimmunity.⁴⁶ This suggests that, the frontier between tolerance and autoimmunity could be easily broken through chronic inflammation mediated by CD40L.

³⁸ Schmitz, G, et al. (1998). T-lymphocytes and monocytes in atherogenesis. *Herz* 23, 168.

³⁹ Mach, F, et al. (1998). Reduction of atherosclerosis in mice by inhibition of CD40 signalling. *Nature* 394, 200.

⁴⁰ Schonbeck, U, et al. (2000). Inhibition of CD40 signaling limits evolution of established atherosclerosis in mice. *Proc Natl Acad Sci U S A* 97, 7458.

⁴¹ Aukrust, P, et al. (1999). Enhanced levels of soluble and membrane-bound CD40 ligand in patients with unstable angina. Possible reflection of T lymphocyte and platelet involvement in the pathogenesis of acute coronary syndromes. *Circulation* 100, 614.

⁴² Vishnevetsky, D, et al. (2004). CD40 ligand: a novel target in the fight against cardiovascular disease. *Ann Pharmacother* 38, 1500.

⁴³ Wiley, J A, et al. (1997). Exogenous CD40 ligand induces a pulmonary inflammation response. *J Immunol* 158, 2932.

⁴⁴ Adawi, A, et al. (1998). Disruption of the CD40-CD40 ligand system prevents an oxygen-induced respiratory distress syndrome. *Am J Pathol* 152, 651.

⁴⁵ Adawi, A, et al. (1998). Blockade of CD40-CD40 ligand interactions protects against radiation-induced pulmonary inflammation and fibrosis. *Clin Immunol Immunopathol* 89, 222.

⁴⁶ Mehling, A, et al. (2001). Overexpression of CD40 ligand in mouse epidermis results in chronic skin inflammation and systemic autoimmunity. *J Exp Med* 194, 615.

CHAPTER 4

4.1.3 Transplantation

Because CD40–CD40L interaction can prohibit tolerance, inhibition of CD40 activation has been investigated to prolong the survival of experimentally transplanted organs. Furthermore, expression of CD40L was shown to correlate with rejection in human cardiac allografts.⁴⁷ Anti-CD40L mAbs have been used successfully in mice to prevent allograft rejection of pancreatic islets,⁴⁸ heart,⁴⁹ skin transplants,⁵⁰ and bone marrow transplants⁵¹ as well as in associated graft-versus-host disease,⁵² by inhibiting alloimmune responses.⁵³ Long-term acceptance of xenogeneic rat-to-mouse cardiac and skin grafts, as well as prolonged survival of pig-to-mouse skin xenograft, was obtained when co-administrated with soluble CTLA4 which inhibits the CD28–B7 interaction.⁵⁴ Similar results have been described for skin and cardiac allografts.⁵⁵ Importantly, anti-CD40L treatment showed beneficial effects in a rhesus monkey model of kidney allotransplantation⁵⁶ and primary skin transplantation.⁵⁷

Alternatively, targeting CD40 with an anti-CD40 mAb, which has been shown to possess antagonistic properties,⁵⁸ also successfully extended the survival of renal allograft in primate model.⁵⁹ So far, the first clinical attempt using humanized anti-CD40L mAb in human

⁴⁷ Reul, R M, et al. (1997). CD40 and CD40 ligand (CD154) are coexpressed on microvessels in vivo in human cardiac allograft rejection. *Transplantation* 64, 1765.

⁴⁸ Parker, D C, et al. (1995). Survival of mouse pancreatic islet allografts in recipients treated with allogeneic small lymphocytes and antibody to CD40 ligand. *Proc Natl Acad Sci U S A* 92, 9560.

⁴⁹ Larsen, C P, et al. (1996). CD40-gp39 interactions play a critical role during allograft rejection. Suppression of allograft rejection by blockade of the CD40-gp39 pathway. *Transplantation* 61, 4.

⁵⁰ Markees, T G, et al. (1997). Prolonged survival of mouse skin allografts in recipients treated with donor splenocytes and antibody to CD40 ligand. *Transplantation* 64, 329.

⁵¹ Blazar, B R, et al. (1997). Blockade of CD40 ligand-CD40 interaction impairs CD4+ T cell-mediated alloreactivity by inhibiting mature donor T cell expansion and function after bone marrow transplantation. *J Immunol* 158, 29.

⁵² Durie, F H, et al. (1994). Antibody to the ligand of CD40, gp39, blocks the occurrence of the acute and chronic forms of graft-vs-host disease. *J Clin Invest* 94, 1333.

⁵³ Larsen, C P, et al. (1997). The CD40 pathway in allograft rejection, acceptance, and tolerance. *Curr Opin Immunol* 9, 641.

⁵⁴ Elwood, E T, et al. (1998). Prolonged acceptance of concordant and discordant xenografts with combined CD40 and CD28 pathway blockade. *Transplantation* 65, 1422.

⁵⁵ Larsen, C P, et al. (1996). Long-term acceptance of skin and cardiac allografts after blocking CD40 and CD28 pathways. *Nature* 381, 434.

⁵⁶ Kirk, A D, et al. (1999). Treatment with humanized monoclonal antibody against CD154 prevents acute renal allograft rejection in nonhuman primates. *Nat Med* 5, 686.

⁵⁷ Elster, E A, et al. (2001). Treatment with the humanized CD154-specific monoclonal antibody, hu5C8, prevents acute rejection of primary skin allografts in nonhuman primates. *Transplantation* 72, 1473.

⁵⁸ Adams, A B, et al. (2005). Development of a chimeric anti-CD40 monoclonal antibody that synergizes with LEA29Y to prolong islet allograft survival. *J Immunol* 174, 542.

⁵⁹ Pearson, T C, et al. (2002). Anti-CD40 therapy extends renal allograft survival in rhesus macaques. *Transplantation* 74, 933.

CHAPTER 4

organ transplantation failed to show efficacy,⁶⁰ but efforts are pursued in various models to demonstrate the efficiency of blocking CD40–CD40L interaction in graft acceptance.⁶¹

Evidences for the therapeutic potential of anti-CD40L administration in all these animal models are encouraging, but possible applications to humans are far from being granted because of manifest limitations shown by first clinical trials. Moreover, controversial data support immunosuppressive mechanisms for anti-CD40L by not only a simple blockade of the CD40–CD40L interaction⁶² but also an Fc–dependent destruction of activated T cells.⁶³ The discovery of refined inhibitors of the CD40–CD40L interaction would undoubtedly offer a pivotal solution for a broad range of diseases.

4.2 Boosting the immune response by activation of the CD40 signaling

4.2.1 Hyper-IgM syndrome and immunodeficiencies

As described in chapter 1, the primary proof for the essential role of the CD40–CD40L in mounting humoral immune response came from the observations that alterations in the *CD40L* gene lead to the X-linked immunodeficiency hyper-IgM syndrome.⁶⁴ Similar immunodeficiency was observed in patients with B lymphocytes defective in CD40–mediated signaling.⁶⁵ These clinical observations are in accordance with symptoms developed by CD40–⁶⁶ and CD40L–deficient mice.⁶⁷ We better know now that hyper-IgM syndromes might ensue from different origins, as reflected by complex mechanisms that govern the antibody maturation (Figure 27).⁶⁸

⁶⁰ Elster, E A, et al. (2004). The road to tolerance: renal transplant tolerance induction in nonhuman primate studies and clinical trials. *Transpl Immunol* 13, 87.

⁶¹ Brown, D L, et al. (2006). Short-term anti-CD40 ligand costimulatory blockade induces tolerance to peripheral nerve allografts, resulting in improved skeletal muscle function. *Plast Reconstr Surg* 117, 2250; Jochum, C, et al. (2007). CD154 blockade and donor-specific transfusions in DLA-identical marrow transplantation in dogs conditioned with 1-Gy total body irradiation. *Biol Blood Marrow Transplant* 13, 164.

⁶² Ferrant, J L, et al. (2004). The contribution of Fc effector mechanisms in the efficacy of anti-CD154 immunotherapy depends on the nature of the immune challenge. *Int Immunol* 16, 1583.

⁶³ Monk, N J, et al. (2003). Fc-dependent depletion of activated T cells occurs through CD40L-specific antibody rather than costimulation blockade. *Nat Med* 9, 1275; Waldmann, H. (2003). The new immunosuppression: just kill the T cell. *Nat Med* 9, 1259.

⁶⁴ Kroczek, R A, et al. (1994). Defective expression of CD40 ligand on T cells causes "X-linked immunodeficiency with hyper-IgM (HIGM1)". *Immunol Rev* 138, 39.

⁶⁵ Durandy, A, et al. (1997). Abnormal CD40-mediated activation pathway in B lymphocytes from patients with hyper-IgM syndrome and normal CD40 ligand expression. *J Immunol* 158, 2576.

⁶⁶ Kawabe, T, et al. (1994). The immune responses in CD40-deficient mice: impaired immunoglobulin class switching and germinal center formation. *Immunity* 1, 167.

⁶⁷ Renshaw, B R, et al. (1994). Humoral immune responses in CD40 ligand-deficient mice. *J Exp Med* 180, 1889.

⁶⁸ Durandy, A, et al. (2006). Hyper-IgM syndromes. *Curr Opin Rheumatol* 18, 369.

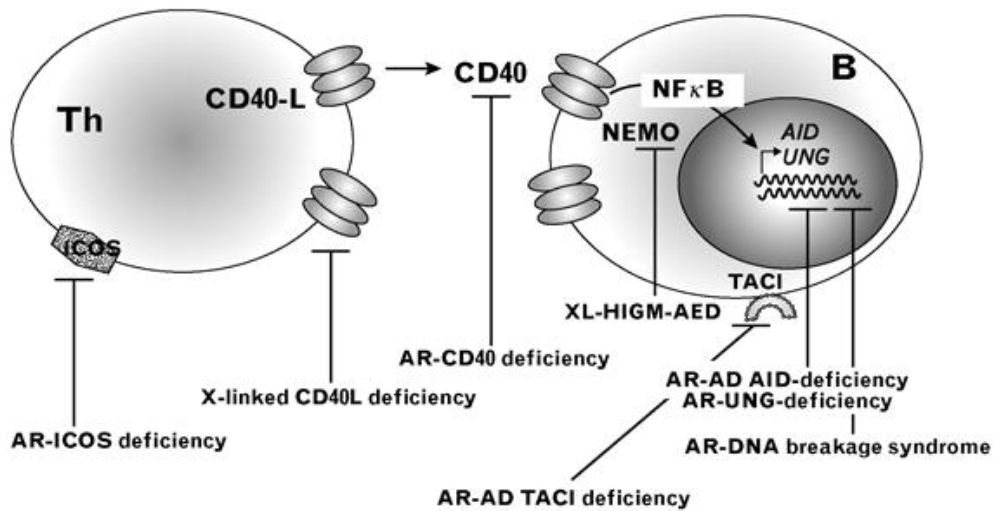


Figure 27. Molecular defects leading to hyper-IgM syndromes. Abnormalities in the partners of the CD40 signaling and associated HIGM syndromes are indicated.⁶⁸

Interestingly, evidence for the association of CD40/CD154 dysfunction with rheumatoid arthritis has been provided by studies linking the HIGM syndrome with increased incidences of this autoimmune disease.⁶⁹

Treatment of *Pneumocystis carinii* infection, an opportunistic infection to which hyper-IgM or HIV-positive patient have shown increased susceptibility, in SCID mice with a recombinant soluble trimeric CD40L protein was unfortunately ineffective.⁷⁰

To date, only a genetic repair of the CD40L gene defect by trans-splicing resulted in the correction of the disease in a mouse model.⁷¹ In view of this result, it could be envisaged to develop more potent drugs that activate CD40 signaling, for treating appropriate cases of HIGM and common variable immunodeficiency.⁷²

4.2.2 Infections

Implication of the CD40–CD40L interaction in infectious diseases came from early observation that susceptibility of human T cell lines to both the human and simian immunodeficiency virus correlates with expression of CD40,⁷³ but not CD40L. Furthermore,

⁶⁹ Sibilia, J, et al. (1996). Hyper-IgM syndrome associated with rheumatoid arthritis: report of RA in a patient with primary impaired CD40 pathway. *Br J Rheumatol* 35, 282.

⁷⁰ Vestereng, V H, et al. (2001). Recombinant CD40 ligand administration does not decrease intensity of *Pneumocystis carinii* infection in scid mice. *J Eukaryot Microbiol Suppl*, 153S.

⁷¹ Tahara, M, et al. (2004). Trans-splicing repair of CD40 ligand deficiency results in naturally regulated correction of a mouse model of hyper-IgM X-linked immunodeficiency. *Nat Med* 10, 835.

⁷² Farrington, M, et al. (1994). CD40 ligand expression is defective in a subset of patients with common variable immunodeficiency. *Proc Natl Acad Sci U S A* 91, 1099.

⁷³ Agy, M B, et al. (1991). Viral and cellular gene expression in CD4+ human lymphoid cell lines infected by the simian immunodeficiency virus, SIV/Mne. *Virology* 183, 170.

CHAPTER 4

experiments in CD40L-deficient mice have demonstrated that CD40-CD40L interaction is required for a strong antiviral humoral immune response, and suggested a role for CD40L in the establishment and maintenance of CD8⁺ CTL memory.⁷⁴

The capacity of CD40L to mediate antiviral activities was suggested from experiments with vaccinia viruses expressing CD40L, which showed controlled replication in mice, even in the absence of T or B cells.⁷⁵ Finally, a soluble trimeric CD40L protein was efficient in suppressing HIV replication in DCs and transmission to CD4⁺ cells by both CC-chemokine-dependent and independent mechanisms leading to inhibition of the viral reverse transcription activity.⁷⁶ Although of potential interest, administration of CD40 agonists in human during viral infection is not necessarily beneficial. For example, infection of DCs with dengue virus was enhanced in the presence of membranous CD40L, due to a decrease in antiviral mediator levels and prevention for infected DCs to enter apoptosis after their maturation.⁷⁷

In addition to extracellular, intravesicular and intracytoplasmic, viral and bacterial infections,⁷⁸ activating CD40 has been shown to be also attractive for the treatment of protozoan infections. Experiments in CD40L- and CD40-deficient mice have demonstrated the pivotal role of the CD40-CD40L interaction in cell-mediated immune response to *Leishmania major*, notably through the polarization of the immune response toward T_H1.⁷⁹ The susceptible T_H2 response to the parasite naturally initiated in BALB/c mice could be reversed toward the efficient T_H1 type by administration of an agonistic anti-CD40 mAb.⁸⁰ In a comparable manner, PBMC from patients with HIGM syndrome acquired the capacity to produce remarkable amounts of the type 1 cytokine IL-12 in response to *Toxoplasma gondii* when incubated with soluble trimeric CD40L.⁸¹ Finally, CD40L-transfected fibroblasts, as well as activating anti-CD40 mAb, were effective in reducing parasitemia and mortality of mice

⁷⁴ Borrow, P, et al. (1996). CD40L-deficient mice show deficits in antiviral immunity and have an impaired memory CD8⁺ CTL response. *J Exp Med* 183, 2129.

⁷⁵ Ruby, J, et al. (1995). CD40 ligand has potent antiviral activity. *Nat Med* 1, 437.

⁷⁶ McDyer, J F, et al. (1999). Differential effects of CD40 ligand/trimer stimulation on the ability of dendritic cells to replicate and transmit HIV infection: evidence for CC-chemokine-dependent and -independent mechanisms. *J Immunol* 162, 3711.

⁷⁷ Sun, P, et al. (2006). CD40 ligand enhances dengue viral infection of dendritic cells: a possible mechanism for T cell-mediated immunopathology. *J Immunol* 177, 6497.

⁷⁸ Grewal, I S, et al. (1997). The CD40-CD154 system in anti-infective host defense. *Curr Opin Immunol* 9, 491.

⁷⁹ Campbell, K A, et al. (1996). CD40 ligand is required for protective cell-mediated immunity to *Leishmania major*. *Immunity* 4, 283; Kamanaka, M, et al. (1996). Protective role of CD40 in *Leishmania major* infection at two distinct phases of cell-mediated immunity. *Immunity* 4, 275.

⁸⁰ Ferlin, W G, et al. (1998). The induction of a protective response in *Leishmania major*-infected BALB/c mice with anti-CD40 mAb. *Eur J Immunol* 28, 525.

⁸¹ Subauste, C S, et al. (1999). CD40-CD40 ligand interaction is central to cell-mediated immunity against *Toxoplasma gondii*: patients with hyper IgM syndrome have a defective type 1 immune response that can be restored by soluble CD40 ligand trimer. *J Immunol* 162, 6690.

CHAPTER 4

inoculated with *Trypanizoma cruzi*, the effect being mediated by IL-12, IFN γ and TNF α , and dependent on the production of nitric oxide.⁸² An original concept was recently described, in which the CD40L molecule was expressed by the parasite itself. This recombinant CD40L-transfected strain led to lower virulence induced higher IFN γ production when injected into mice, and survival of inoculated mice.⁸³ Furthermore, surviving mice resisted a challenge infection with wild type strain, thereby confirming the vaccine adjuvant capacity of CD40L.

Nevertheless, depending on the infectious context, CD40-CD40L interaction is implicated in initiation of appropriately polarized helper responses, as seen with CD40-deficient DC primed with soluble egg antigen from *Schistosoma mansoni* that failed to induce the inherent T_H2 response.⁸⁴ CD40 agonists could be used to correct the T_H balance toward the appropriate immune response.

4.2.3 Vaccination

Because of its capacity to increase effector responses and to generate memory responses against diverse pathogens, CD40L has been proposed as a potent adjuvant for vaccination. Early studies have demonstrated that vaccinia-infected anti-CD40-activated human B (CD40-B) cells could be used as efficient antigen presenting cells to stimulate a memory virus-specific CD8 response.⁸⁵ In the same way, the insect cell line Schneider 2 expressing CD40L in a non-baculovirus system was effective in enhancing antigen presentation of the MHC-I cytomegalovirus pp65 peptide loaded on B cells.⁸⁶ Similarly, a protective T_H1 response was obtained by administration to mice of low-immunogenic heat-killed *Listeria monocytogenes* in the presence of agonistic anti-CD40 mAb.⁸⁷

These results were reinforced by observations that human B cells activated by anti-CD40 express molecules important for homing to secondary lymphoid organs and attracting

⁸² Chaussabel, D, et al. (1999). CD40 ligation prevents *Trypanosoma cruzi* infection through interleukin-12 upregulation. *Infect Immun* 67, 1929.

⁸³ Chamekh, M, et al. (2005). Transfection of *Trypanosoma cruzi* with host CD40 ligand results in improved control of parasite infection. *Infect Immun* 73, 6552.

⁸⁴ MacDonald, A S, et al. (2002). Cutting edge: Th2 response induction by dendritic cells: a role for CD40. *J Immunol* 168, 537.

⁸⁵ Khanna, R, et al. (1993). Presentation of endogenous viral peptide epitopes by anti-CD40 stimulated human B cells following recombinant vaccinia infection. *J Immunol Methods* 164, 41.

⁸⁶ Yoon, S H, et al. (2005). Activation of B cells using Schneider 2 cells expressing CD40 ligand for the enhancement of antigen presentation in vitro. *Exp Mol Med* 37, 567.

⁸⁷ Rolph, M S, et al. (2001). CD40 signaling converts a minimally immunogenic antigen into a potent vaccine against the intracellular pathogen *Listeria monocytogenes*. *J Immunol* 166, 5115.

CHAPTER 4

T cells.⁸⁸ To reduce toxicity induced by high doses of antibody, Barr *et al.* have chemically attached herpes virus glycoprotein D antigen to an anti-CD40 mAb and demonstrated an efficient adjuvant effect at low doses of conjugate.⁸⁹ More recently, an antigenic peptide was inserted in the C region of an anti-CD40 antibody or presented in a homodimer composed of anti-CD40 scFv and antigenic unit (Figure 28).⁹⁰ Such constructs efficiently deliver antigen to DCs while inducing their maturation.

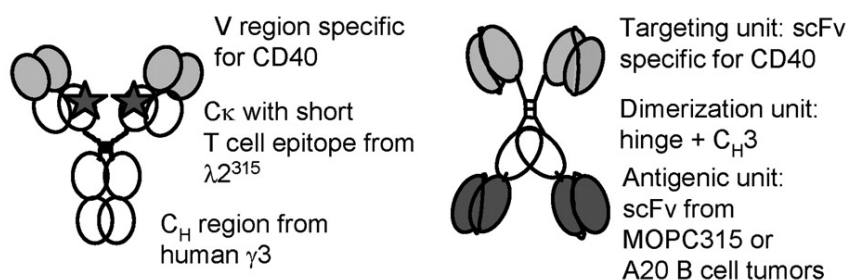


Figure 28. CD40 Troy and Vaccibody. Insertion of antigenic peptide (T cell epitope) in the constant (C $_H$) domain of an anti-CD40 mAb in a troybody (left), or combination of an antigenic peptide with anti-CD40 scFv as a vaccibody (right).⁹⁰

Besides anti-CD40 mAb, other adjuvant molecules have been used to stimulate the CD40 signaling, such as multimeric soluble CD40L,⁹¹ HSP70 or C4BP as reviewed recently.⁹²

These data suggest that co-administration of CD40 activators might be useful for development of novel vaccine formulations. In the future, the most promising application of such a formulation will certainly be therapeutic tumor vaccination. In this regard, vaccination with a peptide encoding a minimal CD8 epitope associated with CD40 activation has shown efficacy in converting tolerance to strong cytotoxic response priming what permitted to control a tumor challenge.⁹³ Adenovirus particles carrying the genetic code for tumor-associated antigens were targeted to DC by decorating viral vectors with anti-CD40 antibodies.⁹⁴ In addition to a more specific delivery of the tumor antigens, these constructs also triggered CD40 on the targeted DCs, thus activating them. Although DCs are an

⁸⁸ von Bergwelt-Baildon, M, et al. (2005). CD40-activated B-cells express full 'lymph node homing triad' and induce T-cell chemotaxis: potential as cellular adjuvants. *Blood*.

⁸⁹ Barr, T A, et al. (2003). A potent adjuvant effect of CD40 antibody attached to antigen. *Immunology* 109, 87.

⁹⁰ Schjetne, K W, et al. (2007). Delivery of Antigen to CD40 Induces Protective Immune Responses against Tumors. *J Immunol* 178, 4169.

⁹¹ Stone, G W, et al. (2006). Macaque multimeric soluble CD40 ligand and GITR ligand constructs are immunostimulatory molecules in vitro. *Clin Vaccine Immunol* 13, 1223.

⁹² Kornbluth, R S, et al. (2006). Immunostimulatory combinations: designing the next generation of vaccine adjuvants. *J Leukoc Biol* 80, 1084.

⁹³ Diehl, L, et al. (1999). CD40 activation in vivo overcomes peptide-induced peripheral cytotoxic T-lymphocyte tolerance and augments anti-tumor vaccine efficacy. *Nat Med* 5, 774.

⁹⁴ de Gruijl, T D, et al. (2002). Prolonged maturation and enhanced transduction of dendritic cells migrated from human skin explants after in situ delivery of CD40-targeted adenoviral vectors. *J Immunol* 169, 5322.

CHAPTER 4

attractive target for increasing immune response against tumors,⁹⁵ knowledge of their complex biology is still not understood enough to envisage controlled therapeutic manipulations. CD40–B cells have been described as homogeneously activated APCs that can be obtained in larger quantities and higher qualities than DCs. Thus, CD40–B cells should be envisioned as interesting alternative antigen–presenting cells for cellular vaccines.⁹⁶

4.2.4 Cancer

Tumor cells evade the immune system, thus activation of CD40 could redirect the immune responses towards the malignancy, either by boosting effector cells and/or by enhancing expression of MHC and costimulatory molecules on tumor cells.⁹⁷ In addition, triggering CD40 expressed on malignant cells, including non-hematopoietic cancer cells, has been shown to induce direct cytotoxicity, albeit in a cell type–dependent manner as seen in chapter 1. Conversely, blockade of the CD40–CD40L interaction in chronic lymphocytic leukemia has been shown to be beneficial.⁹⁸ However, cell signaling induced from CD40 ligation and leading to apoptosis or progression of malignant cells remains obscure. Early studies have demonstrated the efficiency of anti-CD40 mAb-based immunotherapy of cancer in mice,⁹⁹ of CD40L–transduced tumor,¹⁰⁰ and of administration of recombinant CD40L.¹⁰¹

Another way for activating CD40 *in vivo* was the use of attenuated *Salmonella typhimurium* as a vehicle in oral genetic immunization for expression of human CD40L.¹⁰² Anti-CD40 mAb therapy also triggered cytotoxic response and treated CD40–negative malignancies,¹⁰³ either by activating DCs and/or directly activating differentiation of CD8⁺ T

⁹⁵ Banchereau, J, et al. (2005). Dendritic cells as therapeutic vaccines against cancer. *Nat Rev Immunol* 5, 296.

⁹⁶ Schultze, J L, et al. (2004). DCs and CD40-activated B cells: current and future avenues to cellular cancer immunotherapy. *Trends Immunol* 25, 659.

⁹⁷ Costello, R T, et al. (1999). What is the real role of CD40 in cancer immunotherapy? *Immunol Today* 20, 488.

⁹⁸ Younes, A, et al. (1998). Elevated levels of biologically active soluble CD40 ligand in the serum of patients with chronic lymphocytic leukaemia. *Br J Haematol* 100, 135.

⁹⁹ Francisco, J A, et al. (2000). Agonistic properties and in vivo antitumor activity of the anti-CD40 antibody SGN-14. *Cancer Res* 60, 3225; French, R R, et al. (1999). CD40 antibody evokes a cytotoxic T-cell response that eradicates lymphoma and bypasses T-cell help. *Nat Med* 5, 548; Funakoshi, S, et al. (1994). Inhibition of human B-cell lymphoma growth by CD40 stimulation. *Blood* 83, 2787.

¹⁰⁰ Briones, J, et al. (2002). In vivo antitumor effect of CD40L-transduced tumor cells as a vaccine for B-cell lymphoma. *Cancer Res* 62, 3195; Fujita, N, et al. (2001). CD40 ligand promotes priming of fully potent antitumor CD4(+) T cells in draining lymph nodes in the presence of apoptotic tumor cells. *J Immunol* 167, 5678.

¹⁰¹ Vonderheide, R H, et al. (2001). Phase I study of recombinant human CD40 ligand in cancer patients. *J Clin Oncol* 19, 3280.

¹⁰² Urashima, M, et al. (2000). An oral CD40 ligand gene therapy against lymphoma using attenuated *Salmonella typhimurium*. *Blood* 95, 1258.

¹⁰³ Tutt, A L, et al. (2002). T cell immunity to lymphoma following treatment with anti-CD40 monoclonal antibody. *J Immunol* 168, 2720; van Mierlo, G J, et al. (2002). CD40 stimulation leads to effective therapy of CD40(-) tumors through induction of strong systemic cytotoxic T lymphocyte immunity. *Proc Natl Acad Sci U S A* 99, 5561.

CHAPTER 4

lymphocytes, or sensitizing tumor cells to other anti-cancer agents.¹⁰⁴ Furthermore, CD40L gene transfer into tumor cells could induce direct tumoricidal activity of host alveolar macrophages.¹⁰⁵

Recently, the humanized agonistic anti-CD40 mAb SNG-40, was evaluated for a clinical application in multiple myeloma treatment.¹⁰⁶ Authors depicted favorable effects such as the upregulation of Fas/FasL, TRAIL and TNF α that all lower malignant cells survival. In parallel, inhibition of malignant cells proliferation by reduction of soluble CD40L-induced signaling and IL-6 secretion was observed.¹⁰⁷ A recent paper summarized the encouraging results obtained in other phase 1 studies of CD40-targeted therapy in cancer patients with various malignancies and different formulations (Table 4).¹⁰⁸

Table 4. Summary of phase 1 anti-CD40-targeted therapy studies¹⁰⁸

Drug	Formulation	CD40 signaling	Patient population	Clinical trial findings
Recombinant CD40L	Recombinant human trimer	Agonist	Solid tumors or NHL ($n = 32$)	<ul style="list-style-type: none"> • Increased AST/ALT • Injection site reactions • 2 PR
CP-870,893	Fully human IgG2 mAb	Agonist	Solid tumors ($n = 29$)	<ul style="list-style-type: none"> • CRS • 4 PR
SGN-40	Humanized IgG1 mAb	Weak agonist	NHL ($n = 29$; ongoing) Multiple myeloma ($n = 23$; ongoing)	<ul style="list-style-type: none"> • CRS • 4 PR, 1 CR • CRS • 4 patients with decreases in M-protein
HCD 122	Fully human IgG1 mAb	Antagonist	CLL and multiple myeloma	
CD40L-expressing CLL cells	Adenovirus gene therapy	Agonist	CLL ($n = 11$)	<ul style="list-style-type: none"> • Flu-like symptoms • Reductions in tumor burden
Leukemia cells with CD40L and IL-2 – expressing fibroblasts	Adenovirus gene therapy	Agonist	Acute or lymphoblastic leukemia in remission ($n = 10$)	<ul style="list-style-type: none"> • Well tolerated • 9 patients disease-free at median follow-up of 41 mo

Abbreviations: AST, aspartate aminotransferase; ALT, alanine aminotransferase; NHL, non-Hodgkin's lymphoma; PR, partial response; CR, complete response; CRS, cytokine release syndrome; CLL, chronic lymphocytic leukemia.

¹⁰⁴ Eliopoulos, A G, et al. (2004). The role of the CD40 pathway in the pathogenesis and treatment of cancer. *Curr Opin Pharmacol* 4, 360.

¹⁰⁵ Imaizumi, K, et al. (1999). Enhancement of tumoricidal activity of alveolar macrophages via CD40-CD40 ligand interaction. *Am J Physiol* 277, L49.

¹⁰⁶ Tai, Y T, et al. (2004). Mechanisms by which SGN-40, a humanized anti-CD40 antibody, induces cytotoxicity in human multiple myeloma cells: clinical implications. *Cancer Res* 64, 2846.

¹⁰⁷ Law, C L, et al. (2005). Preclinical antilymphoma activity of a humanized anti-CD40 monoclonal antibody, SGN-40. *Cancer Res* 65, 8331.

¹⁰⁸ Vonderheide, R H. (2007). Prospect of targeting the CD40 pathway for cancer therapy. *Clin Cancer Res* 13, 1083.

CHAPTER 4

In conclusion, tumor therapy with CD40 agonists may be an efficient strategy for treating cancer, by both the simultaneous stimulation of immune responses and direct anti-proliferative effect. The challenge will be to activate the CD40 pathway safely, that is by avoiding high doses of agonistic mAb, use of retroviral vectors or combination with irradiation.¹⁰⁹ To this end, a combination antibody-based therapy was recently proposed.¹¹⁰ It combines the induction of tumor cell apoptosis by agonist anti-TRAIL DR5 mAb, and the triggering of CD8⁺ cells by activation through CD40 and CD137 with respective agonist antibodies.

A variety of combinations including recombinant proteins, in particular from the TNF superfamily,¹¹¹ or cytokines can be imagined.¹¹² Nevertheless, CD40 activation has recently been shown to promote neovascularization in a tumor-prone transgenic mouse model.¹¹³ Thus, complete description of the complex roles of CD40–CD40L interaction in different cells during tumorigenesis would be a prerequisite to the proposal of new tools for treating cancer.

¹⁰⁹ Honeychurch, J, et al. (2003). Anti-CD40 monoclonal antibody therapy in combination with irradiation results in a CD8 T-cell-dependent immunity to B-cell lymphoma. *Blood* 102, 1449.

¹¹⁰ Uno, T, et al. (2006). Eradication of established tumors in mice by a combination antibody-based therapy. *Nat Med* 12, 693.

¹¹¹ Tamada, K, et al. (2006). Renewed interest in cancer immunotherapy with the tumor necrosis factor superfamily molecules. *Cancer Immunol Immunother*, 55, 355.

¹¹² Cretney, E, et al. (2007). Cancer: novel therapeutic strategies that exploit the TNF-related apoptosis-inducing ligand (TRAIL)/TRAIL receptor pathway. *Int J Biochem Cell Biol* 39, 280.

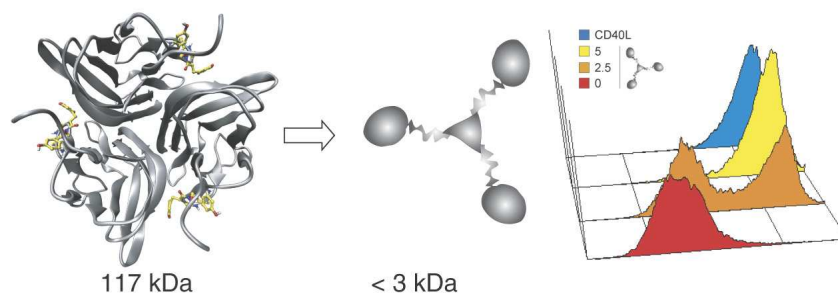
¹¹³ Chiodoni, C, et al. (2006). Triggering CD40 on endothelial cells contributes to tumor growth. *J Exp Med* 203, 2441.

CHAPTER 5

C3-SYMMETRIC PEPTIDE SCAFFOLDS ARE FUNCTIONAL MIMETICS OF TRIMERIC CD40L

Nat Chem Biol 1, 377-382 (2005)

Fournel, S.*, **Wieckowski, S.***, Sun, W., Trouche, N., Dumortier, H., Bianco, A., Chaloin, O., Habib, M., Peter, J. C., Schneider, P., Vray, B., Toes, R. E., Offringa, R., Melief, C. J., Hoebeke, J., and Guichard, G. [* equal contribution]



CHAPTER 5

CD40-based immunotherapy is a promising way to fight various diseases. Anti-CD40 mAbs, membrane-bound CD40L and soluble CD40L have provided important hope for treatment of infections and cancer. Development of new CD40 agonists would be of great interest. In particular, small synthetic molecules with high chemical stability, amenable to large-scale production, and devoid of side effects would be valuable tools.

Here, we described the design of small synthetic molecules with C_3 symmetry that can mimic soluble CD40L homotrimers. Based on crystallographic data and results from site-directed mutagenesis experiments, we chose the CD40-binding peptide Lys¹⁴³-Gly-Tyr-Tyr¹⁴⁶ and linked it via spacer arms to a synthetic core platform of three-fold symmetry. These molecules, named mini-CD40Ls, efficiently bound to CD40 and inhibited binding of recombinant CD40L to CD40, as assessed by surface plasmon resonance. Furthermore, mini-CD40Ls were fully biologically active, as they induced apoptosis of human lymphoma cell lines, and maturation of a mouse dendritic cell line. Mini-CD40Ls also activated the NF- κ B pathway and induced expression of *IL12 p40* gene. We used a biotinylated form of mini-CD40L to show by confocal microscopy its colocalization with CD40 at the plasma membrane. Interestingly, an Ala-scan study on the CD40-binding peptide suggested that all the residues, except the glycine, are important for function of mini-CD40Ls. Finally, we demonstrated a proliferation of mouse B cells induced synergistically by mini-CD40L and agonistic anti-CD40 mAb, suggesting that the C_3 symmetry of the CD40L mimetics is necessary, but not sufficient for certain biological functions.

For the first time, we have described the concept of C_3 symmetric small CD40 agonist molecules. We proved that such molecules are fully functional and reproduce, to some extent, the biological effects induced by natural CD40L. These results have paved the way for application of mini-CD40Ls in various systems. Moreover, this strategy could be extended to other members of the TNF family.

C3-symmetric peptide scaffolds are functional mimetics of trimeric CD40L

Sylvie FOURNEL, Sébastien WIECKOWSKI, Weimin SUN, Nathalie TROUCHE, Hélène DUMORTIER, Alberto BIANCO, Olivier CHALOIN, Mohammed HABIB, Jean-Christophe PETER, Pascal SCHNEIDER, Bernard VRAY, René E. TOES, Rienk OFFRINGA CORNELIS, JM MELIEF, Johan HOEBEKE & Gilles GUICHARD

Nature chemical biology, 2005, Vol. 1, Pages 377 - 382

Pages 86-91 :

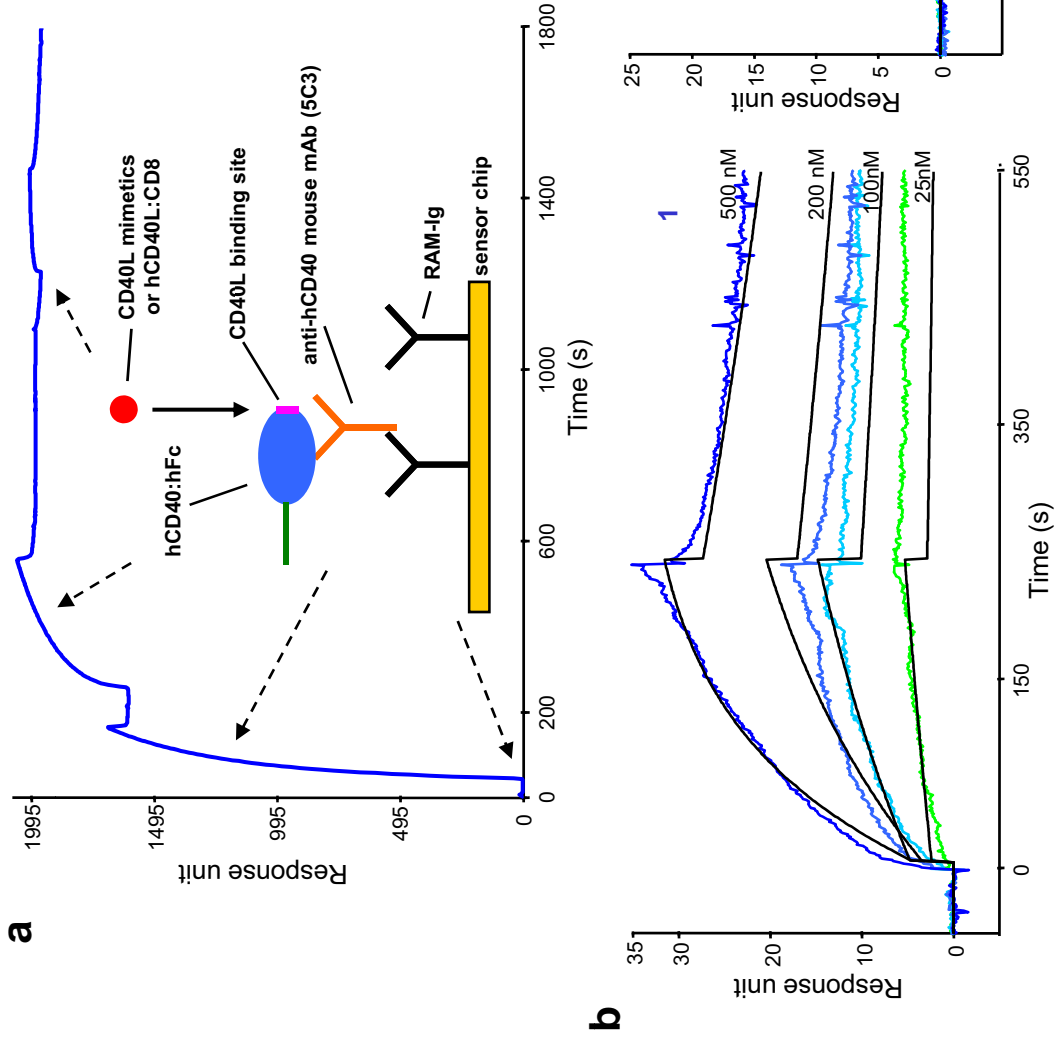
La publication présentée ici dans la thèse est soumise à des droits détenus par un éditeur commercial.

Pour les utilisateurs ULP, il est possible de consulter cette publication sur le site de l'éditeur :

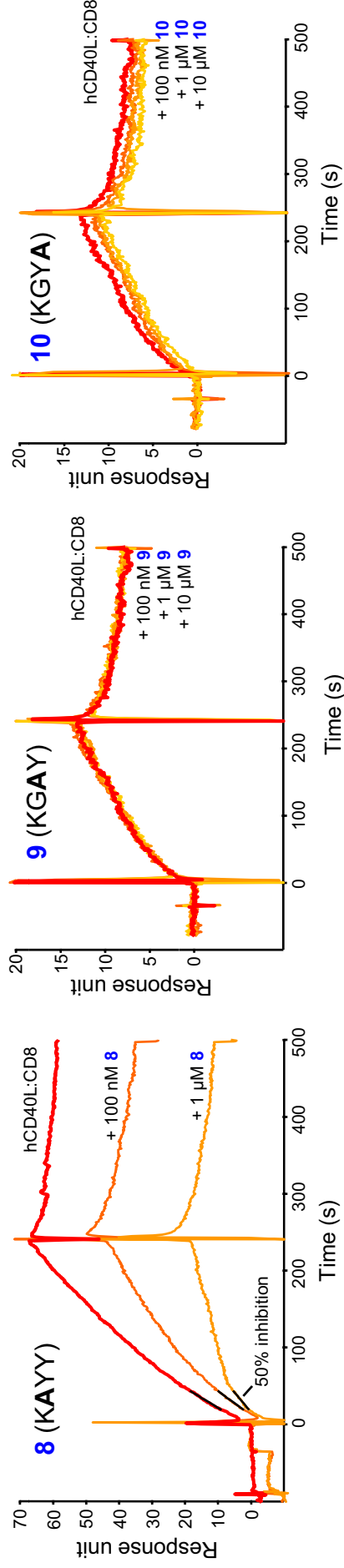
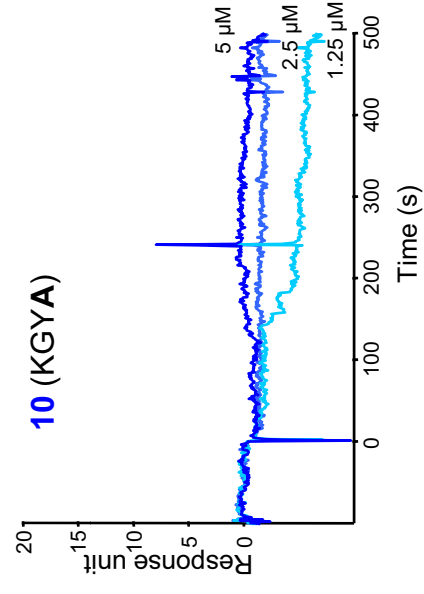
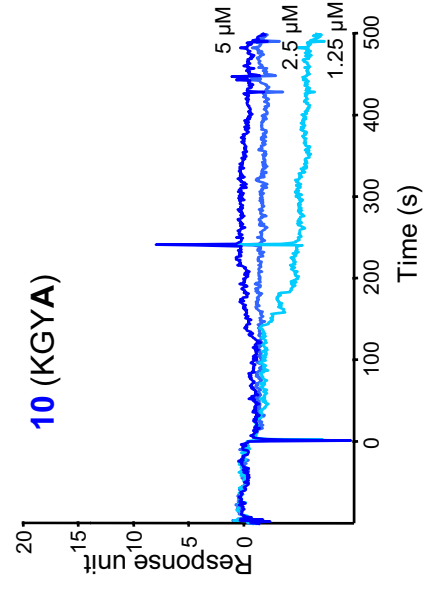
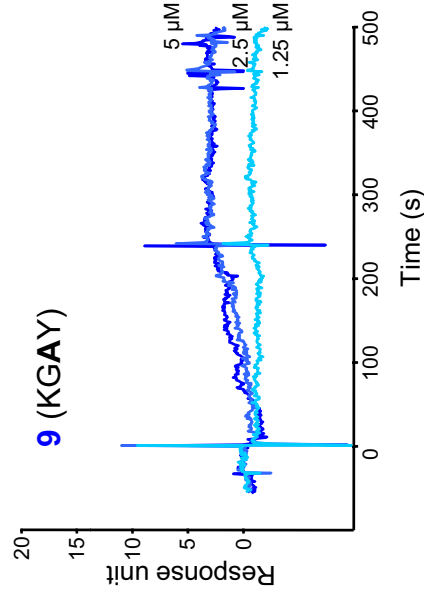
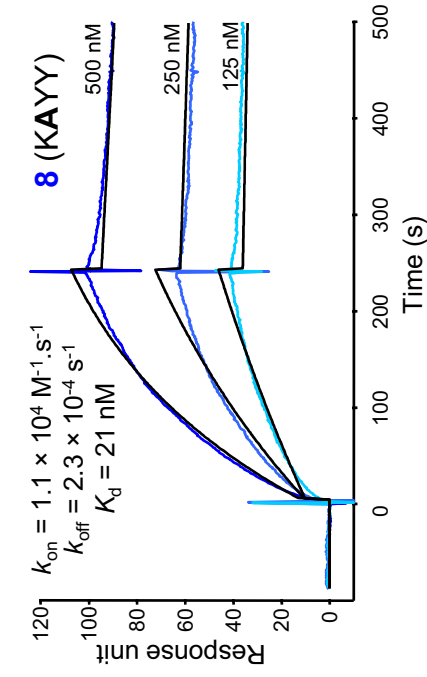
<http://dx.doi.org/10.1038/nchembio746>

La version imprimée de cette thèse peut être consultée à la bibliothèque ou dans un autre établissement via une demande de prêt entre bibliothèques (PEB) auprès de nos services :

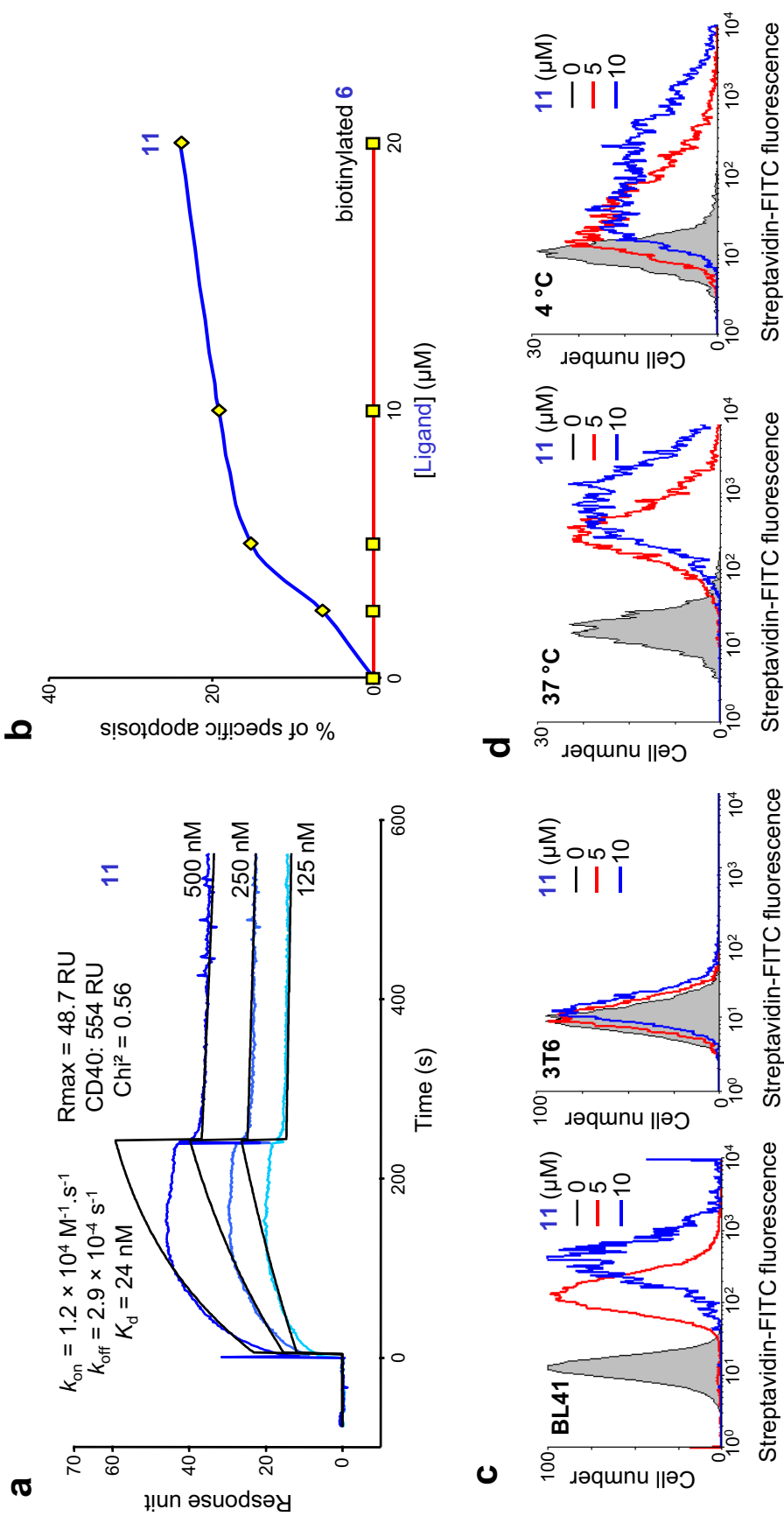
<http://www-sicd.u-strasbg.fr/services/peb/>



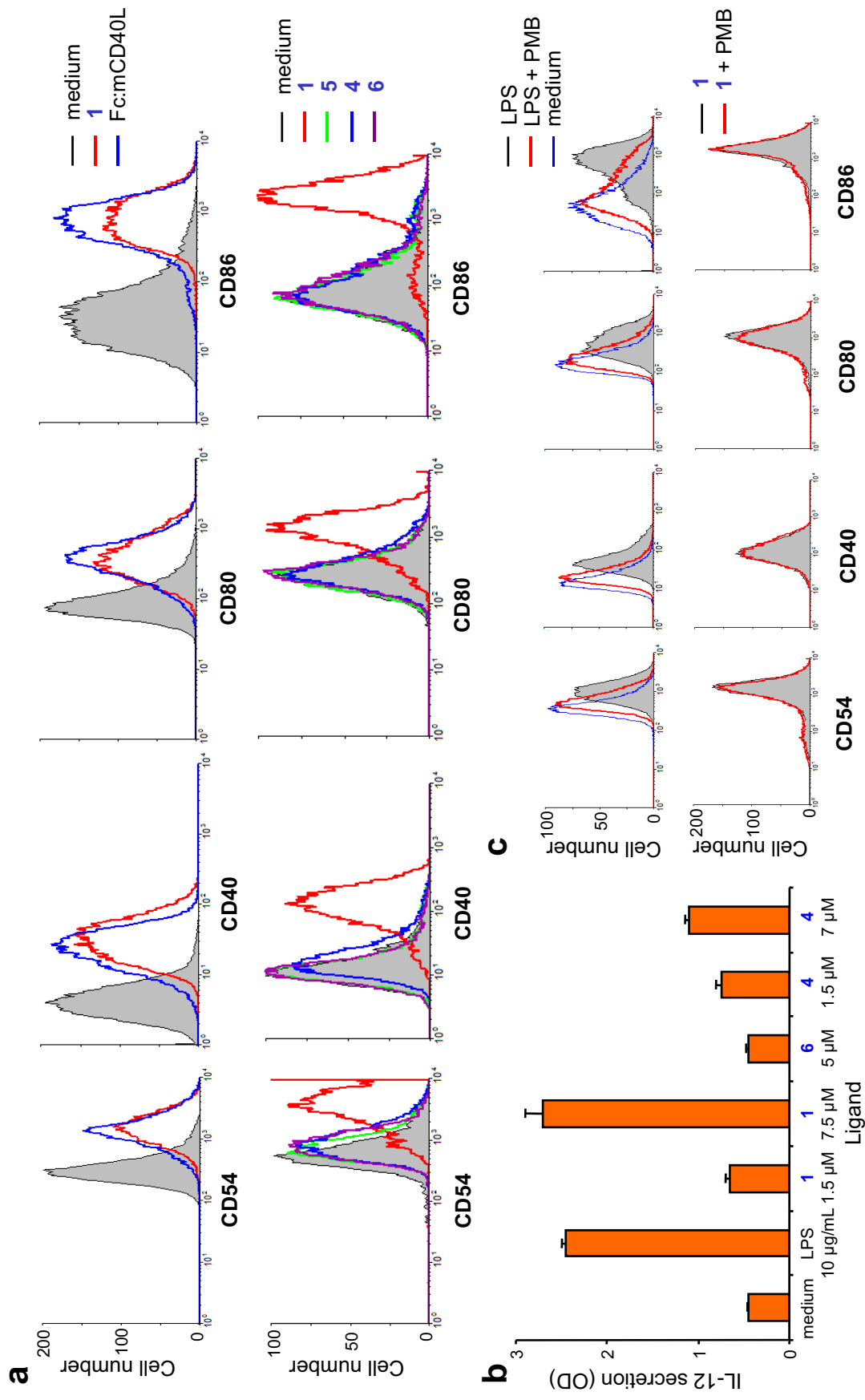
Supplementary Figure 1. Binding of anti-human CD40 mAb 5C3 to CD40 does not prevent subsequent binding of **1** or hCD40L:CD8 as seen by SPR experiments. **(a)** Global sensorgram and schematic representation of the binding of a mouse anti-human CD40 mAb (10 $\mu\text{g}/\text{mL}$) to a rabbit anti-mouse Ig (RAM-Ig) coated chip followed by the binding of hCD40:hFc (10 $\mu\text{g}/\text{mL}$) and subsequent binding of ligand **1** at 500 nM. **(b)** Kinetics data obtained from **1** (left) and hCD40L:CD8 (right) binding. Affinity constants were comparable to those derived from direct assays (data not shown).

a**b**

Supplementary Figure 2. Scanning single amino acid substitutions within the CD40 binding motif of **1**. **(a)** Inhibition of CD40-binding by SPR (upper panels). **8** (Gly144 \rightarrow Ala), **9** (Tyr145 \rightarrow Ala), **10** (Tyr146 \rightarrow Ala) were tested for their capacity to inhibit the binding of soluble hCD40L:CD8 to CD40. **(b)** Direct binding to CD40 by SPR (lower panels). Tendency of Ligand **7** (Lys143 \rightarrow Gly) to aggregate under SPR conditions precluded further analyses of SPR data.



Supplementary Figure 3. Compound **11**, a biotinylated analog of ligand **2** binds to CD40, induces lymphoma apoptosis and interacts with membrane-associated CD40 molecule. **(a)** Direct binding of **11** to CD40 as measured by SPR. **(b)** Induction of apoptosis (16 h) by **11** in human B-lymphoma cell line BL41 analyzed by the decrease in uptake of DiOC₆(3). Biotinylated ligand **6** was used as a control. **(c)** Specific staining of CD40-positive cells (BL41) by **11** detected with streptavidin-FITC as measured by flow cytometry (left). 3T6 fibroblasts were used as a CD40-negative control cells (right). **(d)** Staining of BL41 cells by **11** at 37 °C (left) or 4 °C (right).



Supplementary Figure 4. Maturation of the murine dendritic cell line D1 by CD40L mimetics (**a**) CD40L mimetic **1** as well as Fc:mCD40L induce maturation of the mouse dendritic cell line D1 (upper panel). **4**, **5** and **6** did not induce maturation of D1 cells (lower panel). Expression of maturation markers was measured by flow cytometry after 48 h of treatment with **1** (8 μ M), Fc:mCD40L (1.25 μ g/mL) or other ligands at 10 μ M. (**b**) IL-12 secretion measured in cell culture supernatants after 48 h treatment with **1**, **6** and **4**. LPS is used as positive control. (**c**) Expression of maturation markers after 48 h treatment with LPS at 10 μ g/mL (upper panel) or **1** at 10 μ M (lower panel) with or without the LPS inhibitor polymyxin B (PMB).

Supplementary Table 1. Summary of inhibition experiments and measured kinetic values for the interaction of the different ligands with CD40. The data were evaluated by the indicated binding model which are further schematized. Data for **5** were not calculable as this molecule forms aggregates on the chip; data for **4** and **6** were not calculable as binding was not detectable. Overall k_{off} were determined as the mean of the all the dissociation k_{obs} . Overall $K_d = \text{Overall } k_{\text{off}} / k_{\text{on1}}$.

ligand	Inhibition		
	hCD40L:CD8 Rmax (RU)	CD40 (RU)	IC50 (nM)
1	94	625	78
2	76	625	50
3	75	790	9900
4	50	890	no inhibition
5	47	440	no inhibition
6	94	690	no inhibition
hCD40L:CD8	-	-	-

ligand	Direct binding (1:1 Langmuir binding model)					
	CD40 (RU)	k_{on} (1/M.s)	k_{off} (1/s)	K_d (nM)	Rmax (RU)	Chi2
1	465	7.3E+03	4.7E-04	64.4	36.3	1.83
2	495	6.1E+03	8.8E-04	145	37.2	1.17
3	470	1.4E+02	2.1E-05	153	179	0.51
hCD40L:CD8	460	1.4E+04	7.9E-04	58	150	2.93

ligand	Direct binding (trivalent binding model)										
	CD40 (RU)	k_{on1} (1/M.s)	k_{off1} (1/s)	k_{on2} (1/RU.s)	k_{off2} (1/s)	k_{on3} (1/RU.s)	k_{off3} (1/s)	K_d1 (nM)	Overall k_{off} (1/s)	Overall K_d (nM)	Chi2
1	465	6.0E+03	5.7E-04	1.3E-03	1.2E-01	4.5E-03	3.5E-02	95	3.54E-04	59.5	1.34
2	495	5.7E+03	9.8E-04	5.7E-04	1.4E-01	6.1E-03	4.2E-02	174	6.90E-04	121.9	0.97
3	470	1.4E+02	2.5E-03	2.5E-03	1.6E-03	1.5E-07	1.3E-03	17860	1.30E-03	9286	0.77
hCD40L:CD8	460	9.4E+03	1.3E-03	4.1E-04	5.8E-02	5.0E-06	3.1E-05	138	7.60E-04	80.7	1.76

ligand

4 N.D.

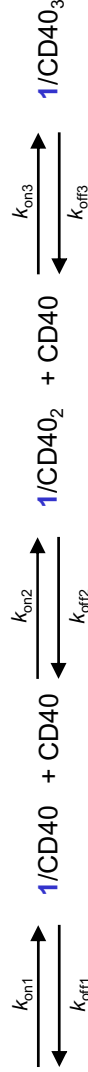
5 aggregates

6 N.D.

1:1 Langmuir binding model:



trivalent binding model:



$$K_d1 = k_{\text{off1}}/k_{\text{on1}}$$

C_3 -symmetric peptide scaffolds are functional mimetics of trimeric CD40L

Sylvie Fournel,^{1,6} Sébastien Wieckowski,^{1,6} Weimin Sun,^{1,5,7} Nathalie Trouche,^{1,7} Hélène Dumortier,¹ Alberto Bianco,¹ Olivier Chaloin,¹ Mohammed Habib,² Jean-Christophe Peter,¹ Pascal Schneider,³ Bernard Vray,² René E. Toes,⁴ Rienk Offringa,⁴ Cornelis J. M. Melief,⁴ Johan Hoebeke,¹ and Gilles Guichard¹

Supplementary Methods

I- Chemistry procedures

General. Thin layer chromatography (TLC) was performed on silica gel 60 F254 (Merck) with detection by UV light and charring with 1% w/w ninhydrin in ethanol followed by heating. Flash column chromatography was carried out on silica gel (0.063-0.200 nm). HPLC analysis was performed on a Nucleosil C₁₈ column (5 μ m, 4.6 x 150 mm) by using a linear gradient of A (0.1% TFA in H₂O) and B (0.08% TFA in CH₃CN) at a flow rate of 1.2 mL/min with UV detection at 214 nm. Mass spectra have been recorded using a MALDI-TOF apparatus (BRUKER Protein-TOF). NMR Spectra were recorded on a Bruker DRX500 MHz. The fully protected pentapeptides Boc-Lys(Boc)-Gly-Tyr(OtBu)-Tyr(OtBu)-Ahx-OH (**20**), Boc-Gly-Gly-Tyr(OtBu)-Tyr(OtBu)-Ahx-OH (**21**), Boc-Lys(Boc)-Ala-Tyr(OtBu)-Tyr(OtBu)-Ahx-OH (**22**), Boc-Lys(Boc)-Gly-Ala-Tyr(OtBu)-Ahx-OH (**23**), and Boc-Lys(Boc)-Gly-Tyr(OtBu)-Ala-Ahx-OH (**24**), were synthesized on a 2-chlorotriyl chloride resin by standard solid phase procedures¹.

Synthesis of ligand 1 and cyclopeptide core structure 5.

Z-Lys(Boc)-D-Ala-OMe (12). Z-Lys(Boc)-OH (5.99 g; 15.75 mmol) was dissolved in DMF (50 mL) containing HCl·H₂N-D-Ala-OMe (2.09 g; 15 mmol), BOP (6.96 g; 15.75 mmol) and DIEA (7.6 mL, 45 mmol) was added to this solution. The reaction mixture was stirred for 2 hours at room temperature. Then, an aqueous saturated sodium bicarbonate solution (500 mL) was added under stirring followed by ethyl acetate (200 mL). The organic layer was washed with aqueous saturated sodium bicarbonate solution (2 x 100 mL), water, (2 x 100 mL), 1 M potassium hydrogen sulphate aqueous solution (2 x 100 mL), water, brine (1 x 100 mL), dried over sodium sulphate and then concentrated *in vacuo* to yield crude **12** (6.85 g; yield 98%); white solid; HPLC *t*_R 9.3 min (linear gradient, 30-100% B, 20 min). The purity of the crude peptide was >97% (determined by C₁₈ RP-HPLC).

Z-D-Ala-Lys(Boc)-D-Ala-OMe (13). Crude dipeptide **12** (4.66 g; 10 mmol) was dissolved in MeOH (100 mL) with HCl (10 mmol) at room temperature and hydrogenated in the presence of a 10% Pd/C catalyst. After 3 hours, the catalyst was removed by filtration and the filtrate

concentrated *in vacuo* to yield the HCl salt (3.71 g, yield 100%) as a white solid. The HCl salt (3.68 g; 10 mmol) was dissolved in DMF (20 mL) containing Z-D-Ala-OH (2.34 g; 10.5 mmol) and BOP (4.64 g; 10.5 mmol). DIEA (3.4 mL; 20 mmol) was added to this solution and the reaction mixture was stirred for 4 hours at room temperature. Then, an aqueous saturated sodium bicarbonate solution (500 mL) was added under stirring followed by ethyl acetate (200 mL). The organic layer was washed with aqueous saturated sodium bicarbonate solution (2 x 100 mL), water, (2 x 100 mL), 1 M potassium hydrogen sulphate aqueous solution (2 x 100 mL), water, brine (1 x 100 mL), dried over sodium sulphate and then concentrated *in vacuo* to yield **13** (5.2 g, yield 97%); white solid; HPLC t_R 8.9 min (linear gradient, 30-100% B, 20 min). The purity of the crude peptide was 88% (determined by C₁₈ RP-HPLC).

Z-Lys(Boc)-D-Ala-Lys(Boc)-D-Ala-OMe (14). Crude compound **13** (5.1g; 9.5 mmol) was dissolved in MeOH (100 mL) with HCl (9.5 mmol) at room temperature and hydrogenated in the presence of a 10% Pd/C catalyst. After 3 hours, the catalyst was removed by filtration and the filtrate concentrated *in vacuo*. The expected HCl salt was precipitated in ether and dried *in vacuo* over KOH. Yield: 100% (4.2 g). The HCl salt (4.2 g; 9.5 mmol) was dissolved in DMF (20 mL) containing Z-Lys(Boc)-OH (3.8 g; 10.5 mmol), BOP (4.42g; 10 mmol). DIEA (4.2 mL; 25 mmol) was added to this solution and the reaction mixture was stirred overnight at room temperature. Then, an aqueous saturated sodium bicarbonate solution (500 mL) was added under stirring followed by ethyl acetate (200 mL). The organic layer was washed with aqueous saturated sodium bicarbonate solution (2 x 100 mL), water, (2 x 100 mL), 1 M potassium hydrogen sulphate aqueous solution (2 x 100 mL), water, brine (1 x 100 mL), dried over sodium sulphate and then concentrated *in vacuo* to leave a residue that solidified upon trituration in hexane. It was collected, washed with hexane, diisopropylether and dried *in vacuo* over KOH to give **14** (6.8 g, yield 93%); white solid; HPLC t_R 10.9 min (linear gradient, 30-100% B, 20 min). The purity of the crude peptide was 90% (determined by C₁₈ RP-HPLC).

Z-D-Ala-Lys(Boc)-D-Ala-Lys(Boc)-D-Ala-OMe (15). Crude compound **14** (6.8 g; 8.9 mmol) was dissolved in MeOH (100 mL) with HCl (8.9 mmol) at room temperature and hydrogenated in the presence of a 10% Pd/C catalyst. After 3 hours, the catalyst was removed by filtration and the filtrate concentrated *in vacuo* to yield a white solid. Yield: 91% (5.4 g). The HCl salt (5.4 g; 8.1 mmol) was dissolved in DMF (25 mL) containing Z-D-Ala-OH (1.9 g; 8.5 mmol), BOP (3.8 g; 8.5 mmol). DIEA (3 mL; 17.8 mmol) was added to this solution and the reaction mixture was

stirred for 6 hours at room temperature. Then, an aqueous saturated sodium bicarbonate solution (500 mL) was added under stirring followed by ethyl acetate (200 mL). The organic layer was washed with aqueous saturated sodium bicarbonate solution (2 x 100 mL), water, (2 x 100 mL), 1 M potassium hydrogen sulphate aqueous solution (2 x 100 mL), water, brine (1 x 100 mL), dried over sodium sulphate and then concentrated *in vacuo* to leave a residue that solidified upon trituration in hexane. It was collected, washed with hexane, diisopropylether and dried *in vacuo* over KOH to give **15** (5.3 g, yield 78%); white solid; HPLC t_R 10.67 min (linear gradient, 30-100% B, 20 min). The purity of the crude peptide was 77% (determined by C₁₈ RP-HPLC).

Z-Lys(Boc)-D-Ala-Lys(Boc)-D-Ala-Lys(Boc)-D-Ala-OMe (16). Compound **15** (5.3 g; 6.3 mmol) was dissolved in MeOH (100 mL) with HCl (6.3 mmol) at room temperature and hydrogenated in the presence of a 10% Pd/C catalyst. After 5 hours, the catalyst was removed by filtration and the filtrate concentrated *in vacuo*. The expected HCl salt was precipitated in ether and dried *in vacuo* over KOH. Yield: 91% (4.7 g). The HCl salt (4.7 g; 5.5 mmol) was dissolved in DMF (20 mL) containing Z-Lys(Boc)-OH (2.2 g, 5.8 mmol), BOP (2.56 g; 5.8 mmol). DIEA (1.9 mL; 11 mmol) was added to this solution and the reaction mixture was stirred overnight at room temperature. Then, an aqueous saturated sodium bicarbonate solution (500 mL) was added under stirring followed by ethyl acetate (200 mL). The organic layer was washed with aqueous saturated sodium bicarbonate solution (2 x 100 mL), water, (2 x 100 mL), 1 M potassium hydrogen sulphate aqueous solution (2 x 100 mL), water, brine (1 x 100 mL), dried over sodium sulphate and then concentrated *in vacuo* to leave a residue that solidified upon trituration in hexane. It was collected, washed with hexane, diisopropylether and dried *in vacuo* over KOH to give crude **16** (5.3 g, yield: 90%); white solid; HPLC t_R 12.26 min (linear gradient, 30-100% B, 20 min). The purity of the crude peptide was 60% (determined by C₁₈ RP-HPLC).

Z-Lys(Boc)-D-Ala-Lys(Boc)-D-Ala-Lys(Boc)-D-Ala-OH (17). Crude Compound **16** (5.3 g; 4.9 mmol) was dissolved in acetone (20 mL) and 1 N NaOH (5.9 mL) was added at 0°C. The reaction mixture was maintained at 0°C for 1 hour before it was allowed to warm to room temperature. After 6 hours, the reaction mixture was concentrated *in vacuo*. Then, ethyl acetate (100 mL) was added under stirring followed by 1 N potassium hydrogen sulphate aqueous solution (2 x 100 mL), water, brine (1 x 100 mL), dried over sodium sulphate and then concentrated *in vacuo* to leave a residue that solidified upon trituration in diisopropylether. It was collected, washed with diisopropylether and dried *in vacuo* over KOH. The crude product was purified by flash column

chromatography (CHCl₃/MeOH/AcOH, 120:10:5) to yield pure **17** (2.3 g, yield: 44%); white solid; HPLC t_R 11.28 min (linear gradient, 30-100% B, 20 min).

H-Lys(Boc)-D-Ala-Lys(Boc)-D-Ala-Lys(Boc)-D-Ala-OH (18). Compound **17** (1.53 g; 1.46 mmol) was dissolved in MeOH (10 mL) at room temperature and hydrogenated in the presence of a 10% Pd/C catalyst. After 4 hours, the catalyst was removed by filtration and the filtrate concentrated *in vacuo*. The expected HCl salt was precipitated in diisopropylether and dried *in vacuo* over KOH (1.17 g, yield: 88%); HPLC t_R 16.9 min (linear gradient, 5-65% B, 20 min). The purity of the crude peptide was 70% (determined by C₁₈ RP-HPLC).

Cyclo-[(Lys(Boc)-D-Ala-)]₃ (19). Crude compound **18** (800 mg; 0.87 mmol) was dissolved in DMF (80 mL) at room temperature containing EDC·HCl (201 mg; 1.05 mmol), HOBt (142 mg; 1.05 mmol) and DIEA (373 mL; 2.19 mmol) was added to this solution. The reaction mixture was stirred 2 days at room temperature and the reaction mixture was concentrated *in vacuo*. A saturated sodium bicarbonate solution (100 mL) was added under stirring, followed by ethyl acetate (100 mL). The organic layer was washed with a saturated sodium bicarbonate solution (2 x 100 mL), followed by 1 N potassium hydrogen sulphate aqueous solution (2 x 100 mL), water, brine (1 x 100 mL), dried over sodium sulphate and then concentrated *in vacuo* to give crude **19** (780 mg, quant. yield); white solid; MS (MALDI-TOF) calcd for C₄₂H₇₅N₉O₁₂ : (m/z) 897.55. Found: [M+Na]⁺ = 919.88, [M+K]⁺ = 936.02.

Cyclo-[(Lys-D-Ala-)]₃ (5). Compound **19** (650 mg; 0.76 mmol) was dissolved in TFA (6 mL) for 1 hour at room temperature. The mixture amine was concentrated *in vacuo*. The expected amine was precipitated in ether (50 mL). It was collected, washed with ether and dried *in vacuo* to give crude **5** (700 mg, yield: 98%); HPLC t_R 16.84 min (linear gradient, 5-65% B, 20 min); MS (MALDI-TOF) calcd for C₂₇H₅₁N₉O₆ : (m/z) 597.40. Found: [M+H]⁺ = 598.50.

Ligand 1. Compound **5** (37 mg; 39 μmol) was dissolved in DMF (1.5 mL) at room temperature containing pentapeptide Boc-Lys(Boc)-Gly-Tyr(OtBu)-Tyr(OtBu)-Ahx-OH (**20**) (124 mg; 129 μmol), BOP (57 mg; 129 μmol), and DIEA (120 μl) was added to this solution. The reaction mixture was stirred 2 days at room temperature and then concentrated *in vacuo*. A saturated sodium bicarbonate solution (10 mL) was added under stirring. The precipitate was washed with a

saturated sodium bicarbonate solution (2 x 10 mL), followed by 1 N potassium hydrogen sulphate aqueous solution (2 x 10 mL), water, brine (1 x 10 mL), hexane (2 x 5 mL) and dried *in vacuo*. Yield: 100% (140 mg). The crude protected ligand (140 mg; 39 μ mol) was deprotected with trifluoroacetic acid (2 mL). After 2 hours at room temperature, the trifluoroacetic acid was removed *in vacuo* by co-evaporation with hexane. The expected TFA salt was precipitated in ether, collected, washed with ether and dried *in vacuo* over KOH. To give crude **1** (110 mg, yield: 100%). Purification by semi-preparative C₁₈ RP-HPLC followed by lyophilization gave pure **1** (30 mg, 27% yield and >99% purity); HPLC t_R 10.98 min (linear gradient, 5-65% B, 20 min); Table with ¹H chemical shifts for ligand **1** are given in **Supplementary Fig.5**; MS (MALDI-TOF) calcd for C₁₂₃H₁₈₃N₂₇O₂₇: (m/z) 2470.38. Found: [M+H]⁺ = 2471.83, [M+Na]⁺ = 2493.82, [M+K]⁺ = 2509.81.

Alanine/Glycine scanning

Ligand 7. The synthesis of **7** was performed with the pentapeptide Boc-Gly-Gly-Tyr(OtBu)-Tyr(OtBu)-Ahx-OH (**21**, 29.8 mg) and compound **5** (10.8 mg) according to procedure described for ligand **1**. The purity of the crude ligand was 27% (determined by C₁₈ RP-HPLC). Purification by semipreparative C₁₈ RP-HPLC gave pure **7** (yield = 2.5 mg, 9% and >99 % purity). HPLC t_R 11.90 min (linear gradient, 5-65% B, 20 min); MS (MALDI-TOF) calcd for C₁₁₁H₁₅₆N₂₄O₂₇ : 2258.6. Found : [M+H]⁺ = 2260.08, [M+Na]⁺ = 2282.05, [M+K]⁺ = 2298.02.

Ligand 8. The synthesis of **8** was performed with the pentapeptide Boc-Lys(Boc)-Ala-Tyr(OtBu)-Tyr(OtBu)-Ahx-OH (**22**, 34 mg) and compound **5** (10 mg) according to procedure described for ligand **1**. The purity of the crude ligand was 41% (determined by C₁₈ RP-HPLC). Purification by semipreparative C₁₈ RP-HPLC gave pure **8** (yield = 4 mg, 15% and >99 % purity). HPLC t_R 11.21 min (linear gradient, 5-65% B, 20 min); MS (MALDI-TOF) calcd for C₁₂₆H₁₈₉N₂₇O₂₇ : 2514.05. Found : [M+H]⁺ = 2515.40, [M+Na]⁺ = 2537.35 , [M+K]⁺ = 2553.43.

Ligand 9. The synthesis of **9** was performed with pentapeptide Boc-Lys(Boc)-Gly-Ala-Tyr(OtBu)-Ahx-OH (**23**, 28.42 mg) and compound **5** (10 mg) according to the procedure described for ligand **1**. The purity of the crude ligand was 50% (determined by C₁₈ RP-HPLC). Purification by semipreparative C₁₈ RP-HPLC gave pure **9** (yield = 4 mg, 15% and >99 %

purity). HPLC t_R 10.27 min (linear gradient, 5-65% B, 20 min); MS (MALDI-TOF) calcd for $C_{105}H_{171}N_{27}O_{24}$: 2195.67. Found : $[M+H]^+ = 2196.57$, $[M+Na]^+ = 2218.55$, $[M+K]^+ = 2234.55$.

Ligand 10. The synthesis of **10** was performed with pentapeptide Boc-Lys(Boc)-Gly-Tyr(OtBu)-Ala-Ahx-OH (**19**, 28.42 mg) and compound **5** (10 mg) according to the procedure described for ligand **1**. The purity of the crude ligand was 54% (determined by C_{18} RP-HPLC). Purification by semipreparative C_{18} RP-HPLC gave pure **10** (yield = 4 mg, 15% and >99 % purity). HPLC t_R 10.24 min (linear gradient, 5-65% B, 20 min); MS (MALDI-TOF) calcd for $C_{105}H_{171}N_{27}O_{24}$: 2195.67. Found : $[M+H]^+ = 2196.45$, $[M+Na]^+ = 2218.46$, $[M+K]^+ = 2234.45$.

II- Biological procedures

Cells and reagents. BL41 and Raji cells have been characterized as human Burkitt lymphomas, Jurkat cells as human T-cell leukemia, A20 as mouse B-cell lymphoma and 3T6 as mouse Swiss Albino embryo fibroblast cell line. D1 cells have been described as a MHC class II–positive growth factor–dependent immature DC, derived from adult mice spleen². Supernatant (SN) from NIH/3T3 fibroblast cells which produced mouse recombinant GM-CSF was collected from confluent cultures. SN generally contains 10–20 ng/mL mouse GM-CSF. Soluble human CD40:mIg fusion protein (extracellular (193 residues) domain of human CD40 fused to mouse IgG2a Fc (233 residues)), hCD40L:mCD8 (extracellular (213 residues) domain of human CD40L fused to the extracellular domain (167 residues) of mouse CD8 α) and human TRAILR1:hFc were from Ancell corporation (Bayport, MN). Human TNFR1:hFc was from Sigma-Aldrich (Saint-Louis, MO). Recombinant soluble hFc:mCD40L was produced in CHO cells as previously described for Fc-EDA³ using amino acids 115-260 of mouse CD40L. Recombinant hTNFR2:hFc, hLT β R:hFc, hEDAR:hFc, mBCMA:hFc were produced as described for hTRAILR2:hFc⁴. Another soluble hCD40:hFc was purchased from Oncogene (Calbiochem, San Diego, USA). The purified mouse anti-human CD40 mAb 5C3 and the purified anti-mouse CD40 3/23 were purchased from Pharmingen (San Jose, CA) as well as the fluorescein isothiocyanate (FITC)-conjugated streptavidin (SAv), R-phycoerythrin (PE) anti-mouse CD54, PE anti-mouse CD80, PE anti-mouse CD86, FITC anti-mouse CD40 (clone 3/23) and FITC-anti-IA^b/IE^b. Polyclonal

rabbit anti-I κ B α (antiserum) and monoclonal mouse anti-actin (C4) antibodies were purchased from Pharmingen. The Alexa Fluor[®] 488 (AF 488) labelled goat anti-mouse IgG (γ 1) (GAM) and Alexa Fluor[®] 546 (AF 546) labelled SA ν were purchased from Molecular Probes (Eugene, Oregon, USA). Peroxydase labelled GAM and goat anti-rabbit (GAR) antibodies as well as the Enhanced-Chemiluminescent reagent detection for Western blotting were purchased from Amersham.

Effect of anti-CD40 antibody on CD40L and CD40L mimetics binding by SPR. hCD40:hFc recombinant protein (Oncogene, La Jolla, CA) and the LG11-2 control protein were injected on a chip covered with the mouse anti-human CD40 antibody before injecting hCD40L:CD8 fusion protein or CD40L mimetics. The BIAevaluation 4.1 software was used to analyze the selective binding responses. Sensorgrams from the control flow cell with LG11-2 were subtracted from sensorgrams obtained with captured hCD40:hFc to yield selective binding responses (see **Supplementary Fig. 1**).

Measurement of apoptosis. To analyze apoptosis by annexin V/PI labelling⁵, cells were resuspended in 100 μ L of annexin V binding buffer (10 mM Hepes pH 7.4, 140 mM NaCl, 2.5 mM CaCl₂) containing 5 μ L of annexin V-FITC (Pharmingen) and 10 μ L of propidium iodide (PI) (Molecular Probes) at 10 μ g/mL and incubated at room temperature in the dark. After 20 min, 400 μ L of annexin V binding buffer were added and cells were analyzed by flow cytometry. To analyze apoptosis by the 3,3'-dihexyloxacarbocyanine iodide (DiOC₆(3)) (Interchim, Montluçon, France) uptake⁶, approximately 1×10^6 cells washed in PBS were resuspended in 300 μ L of PBS containing 40 nM DiOC₆(3) and incubated at 37°C for 30 min. Cells were then directly analyzed by flow cytometry.

DAPI (4',6-diamidino-2-phenylindole) staining of the cells nuclei. After two washes in PBS, cells were fixed in methanol for 5 min at room temperature before being dried. They were then incubated with 500 μ L of DAPI (Molecular Probes) at 0.5 μ g/mL in PBS for 30 min at room temperature in the dark. After two washes in PBS, cells were mounted in ready to use Fluorescent Mounting Medium (DakoCytomation, Carpinteria, CA) before analysis under epifluorescent microscope (Olympus BX51) using the DAPI narrow-band cube (360-370 nm excitation filter and 420-460 nm emission filter).

Staining for flow cytometry analysis. Cells were washed in PBS containing 2% FBS and then incubated at 4°C for 20 min with the various antibodies used at a concentration recommended by the manufacturer. After two washes in PBS-2% FBS, cells were analyzed by flow cytometry. For staining with the biotinylated compound **11**, cells were washed in PBS containing 1% bovine serum albumin (BSA) (Roche, Indianapolis, IN) and first incubated 20 min at the indicated temperature with the compound **11** diluted in PBS-1% BSA at the indicated concentrations. After washing, cells were incubated with FITC-SAv at 1 µg/mL at 4°C for 15 min before another wash and subsequent analysis by flow cytometry. In the case of 3T6 fibroblasts, cells were first let grow and adhere at 5×10^5 cells/mL for 24 hours before staining *in situ* using the previous conditions. Cells were analyzed with a FACSCalibur[®]. At least 25,000 events were acquired for each experiment using the CellQuest 3.3 software (Becton Dickinson, Pont de Claix, France) and the data were processed with the WinMDI 2.8 freeware (Joseph Trotter, Scripps Research Institute, <http://facs.scripps.edu/software.html>).

Colocalization analysis by confocal microscopy. Burkitt lymphoma cells (1×10^6) were washed with PBA (PBS containing 1% (w/v) BSA and 15 mM NaN₃) and incubated with indicated concentration of biotinylated compound **11** at 37°C for 10 min. Cells were then washed with cold PBA and incubated with the anti-human CD40 5C3 mAb at 5 µg/mL in PBA on ice for 15 min. After three washes with cold PBS, cells were incubated with SAv-AF 546 at 1 µg/mL and GAM-AF 488 at 2 µg/mL in PBS on ice for 10 min. After two washes with cold PBS, cells were resuspended in ready to use Fluorescent Mounting Medium (DakoCytomation) before analysis by confocal microscopy. Imaging data were collected using an inverted Zeiss LSM 510 Meta confocal laser scanning microscope (Zeiss, Jena, Germany). To avoid cross-talk, a multi-track configuration was used consisting of i) a track set allowing excitation at 488 nm (Ar-ion laser) and emission at wavelengths within the 505-530 nm band after deflection by a NFT 545 Secondary Dichroic Beam Splitter, and ii) a track set allowing excitation at 543 nm (HeNe laser) and emission at wavelengths greater than 560 nm after transmission by the NFT 545 Secondary Dichroic Beam Splitter. Data were processed with the ImageJ 1.33u freeware (Wayne Rasband, National Institutes of Health, <http://rsb.info.nih.gov/ij/>), LSM Reader 3.2d plugin (Patrick Pirrotte, Yannick Krempf and Jérôme Mutterer, Institute for Molecular Biology of Plants, Strasbourg, France) and Colocalization_Finder 1.0 plugin (C. Laummonerie and J. Mutterer). Data generated from the latter plugin were processed with Microsoft Excel 10 for computation of colocalization coefficients.⁷

Western blotting. Total cellular extracts were prepared by incubation in lysis buffer (20 mM Tris-HCl pH 6.8, 150 mM NaCl, 10% glycerol, 1% Triton X-100, 0.1% sodium dodecyl sulfate (SDS), 5 mM EDTA, 1 mM sodium orthovanadate, protease inhibitor cocktail (Sigma, St Louis, MO)) for 30 min on ice. Lysates were clarified by centrifugation at 10,000 g for 20 min at 4°C and quantified for total protein concentration with the bicinchoninic acid assay (BCA, Pierce, Rockford, IL). 20 µg of total cellular proteins were separated by 10% SDS-polyacrylamide gel electrophoresis and transferred to nitrocellulose membrane. The membrane was saturated with Tris-buffered saline (TBS) containing 0.5% (w/v) Tween 20 (TBS-T) and 5% (w/v) non-fat milk (TBS-T/milk) for 1 h at room temperature and then incubated with the anti-IκBα or anti-actin antibody at 1/2,000 in TBS-T/milk overnight at 4°C. After 3 washes with TBS-T at room temperature, membrane was incubated with GAM or GAR (for anti-actin and anti-IκBα respectively) (Amersham) 1/5,000 in TBS-T/milk at room temperature for 1 h. After 3 washes with TBS-T, membrane was incubated with ECL reagent (Amersham) and relative signal intensity of each band quantified by densitometry with the ImageJ 1.33u freeware (Gel Analyzer tool) after scanning of the radiography.

Comparative reverse transcription (RT)-polymerase chain reaction (PCR). Expression of the *IL-12 p40* messenger RNA (mRNA) was evaluated by comparative RT-PCR as already described.⁸ 2 µg of total RNA isolated from D1 cells using TriReagent-LS (Molecular Research Center, Inc., Cincinnati, OH) were converted to cDNA with Moloney-Murine Leukemia Virus Reverse Transcriptase (Sigma) according to the manufacturer's instructions. The primers used to amplify *IL-12 p40* cDNA were:

the forward primer 5' - GGA AGC ACG GCA GCA GAA TA - 3'; and the reverse one 5' - AAC TTG AGG GAG AAG TAG GAA TGG - 3'.⁹

As a constant probe, the cDNA sequence of the housekeeping gene *glyceraldehyde phosphate dehydrogenase (Gapdh)* was also amplified as a constant probe using the following primers:

the forward primer 5' - CGT CCC GTA GAC AAA ATG GTG - 3'; and the reverse one 5' - GTG GAT GCA GGG ATG ATG TTC - 3'.

The sizes of the amplified products were 180 bp for *IL-12 p40* and 642 pb for *Gapdh*. A thermal cycle of 30 s at 94°C, 45 s at 56°C, and 45 s at 74°C was used for 24 to 30 times for *IL-12 p40* and 16 to 22 for *Gapdh* using the Taq DNA polymerase (Promega, Madison, WI) according to the manufacturer's instructions. Five µL of each amplicon were taken from the exponential phase

of the PCR (checked in each test) and analyzed by electrophoresis on a 1% agarose gel in a 10 mM sodium-borate, 2 mM EDTA and 2 µg/mL ethidium bromide buffer. Imaging data of the ethidium bromide stained amplified products were obtained with the ChemiDoc XRS system (Biorad) using the Quantity One software. The relative intensity of each band was then quantified by densitometry with the ImageJ 1.33u freeware (Gel Analyzer tool).

ELISA for IL-12 measurements. IL-12 secretion was evaluated by sandwich ELISA using commercial antibodies from PharMingen and polyvinyl plates (Falcon, Oxnard, CA; reference 3912). It was tested in supernatants collected at 48h.

Statistical analysis. The Student's t-test was used to analyze the results.

Références

- 1- Houben-Weyl Methods of Organic Chemistry Vol. E22a: Synthesis of Peptides and peptidomimetics, M. Goodman, Felix, A., Moroder, L., Toniolo, C, Eds. (Georg Thieme verlag, Stuttgart, 2002)
- 2- Winzler, C. *et al.* Maturation stages of mouse dendritic cells in growth factor-dependent long-term cultures. *J. Exp. Med.* **185**, 317-28 (1997)
- 3- Gaide O., Schneider P. Permanent correction of an inherited ectodermal dysplasia with recombinant EDA. *Nature Medicine* **9**, 614-618 (2003)
- 4- Schneider P., Production of recombinant TRAIL and TRAIL receptor: Fc chimeric proteins. *Methods Enzymol.* **322**, 325-345 (2000)
- 5- Koopman G. *et al.*. Annexin V for flow cytometric detection of phosphatidylserine expression on B cells undergoing apoptosis. *Blood* **84**,1415-1420 (1994)
- 6- Macho, A. *et al.* Mitochondrial dysfunctions in circulating T lymphocytes from human immunodeficiency virus-1 carriers. *Blood* **86**, 2481-2487 (1995)
- 7- Manders, E.E.M., Verbeek, F.J., Aten J.A. Measurement of co-localisation of objects in dual-colour confocal images. *J. Microscopy* **169**, 375 (1993)
- 8- Freiss G., Puech C., Vignon F. Extinction of Insulin-like Growth Factor-1 mitogenic signaling by antiestrogen-stimulated Fas-Associated Protein Tyrosine Phosphatase-1 in human breast cancer cells. *Mol. Endo.* **12**, 568-579 (1998)
- 9- Overbergh L., Valckx D., Waer M., Mathieu C. Quantification of murine cytokine mRNAs using Real Time Quantitative Reverse Transcriptase PCR. *Cytokine* **11**, 305-312 (1999)

CHAPTER 6

SOLID-PHASE SYNTHESIS OF CD40L MIMETICS

Org Biomol Chem 4, 1461-1463 (2006)

Bianco, A., Fournel, S., **Wieckowski, S.**, Hoebeke, J., and Guichard, G.

CHAPTER 6

Synthesis of mini-CD40Ls in solution highly restricts the combinatorial scope of synthesis and could not permit their easy chemical modulations. We described here synthesis of mini-CD40Ls based on a solid-support chemistry. Interestingly, a dimeric form of mini-CD40L, which was involuntarily generated during the process, was isolated and tested.

The described solid-phase synthesis of mini-CD40L was successful. Molecule generated in this way was produced in high yield and purity. Moreover, it was fully functional as shown by surface plasmon resonance experiment and apoptosis assay. Such a chemical strategy would have a direct application in production of combinatorial trimeric molecules, in order to fish unknown targets for example. Interestingly, a synthesis side-product, identified as a dimeric form of mini-CD40L, was isolated. We tested its activity and showed that it is less efficient than the normal trimeric mini-CD40L in inhibiting the binding of recombinant CD40L to CD40. Moreover, this dimeric mini-CD40L induced significantly less apoptosis of B lymphoma cells than did the trimeric form.

We have described here a handy strategy for synthesis of mini-CD40Ls. Modification of the CD40-binding motif by combinatorial chemistry is now conceptually possible. These results also confirmed the requirement of the C_3 symmetry in mini-CD40Ls for their biological functions.

Solid-phase synthesis of CD40L mimetics

Alberto BIANCO, Sylvie FOURNEL, Sébastien WIECKOWSKI, Johan HOEBEKE and Gilles GUICHARD

Organic and biomolecular chemistry, 2006, Vol. 4, Pages 1461 - 1463

Pages 110-112 :

La publication présentée ici dans la thèse est soumise à des droits détenus par un éditeur commercial.

Pour les utilisateurs ULP, il est possible de consulter cette publication sur le site de l'éditeur :

<http://dx.doi.org/10.1039/b601528j>

La version imprimée de cette thèse peut être consultée à la bibliothèque ou dans un autre établissement via une demande de prêt entre bibliothèques (PEB) auprès de nos services :

<http://www-sicd.u-strasbg.fr/services/peb/>

Solid-phase synthesis of CD40L mimetics

**Alberto Bianco,* Sylvie Fournel, Sébastien Wieckowski, Johan Hoebeke, and
Gilles Guichard***

*Institut de Biologie Moléculaire et Cellulaire, UPR 9021 CNRS, Immunologie et Chimie
Thérapeutiques, 15 Rue René Descartes, 67084 Strasbourg, France. Fax: 33 388 610680;
Tel: 33 388 417088; E-mail: A.Bianco@ibmc.u-strasbg.fr; G.Guichard@ibmc.u-strasbg.fr*

Electronic Supplementary Information

General

All reagents and solvents were obtained from commercial suppliers and used without further purification. 2-(3,5-Dimethoxy-4-formylphenoxy)ethyl polystyrene resin (0.62 mmol/g) was obtained from Novabiochem (Läufelfingen, Switzerland). Wang resin and amino acids were purchased from NeomPS (Strasbourg, France). Peptides were synthesised manually on 5 ml fritted syringes or on a semi-automated synthesiser working under nitrogen flow.¹ Peptide H-Lys-Gly-Tyr-Tyr-Ahx-OH **4** was synthesised on a Wang resin using standard solid-phase procedures.² RP-HPLC analyses were carried out on a Macherey-Nagel C₁₈ column (5 µm, 150 × 4.6 mm) using a linear gradient of A: 0.1% TFA in water and B: 0.08% TFA in acetonitrile, 5-65% B in 20 min at 1.2 mL/min flow rate. Chromatograms were recorded on a Varian ProStar 330 photodiode array detector. RP-HPLC purifications were carried out on a Macherey-Nagel C₁₈ column (7 µm, 250 × 10 mm) using a linear gradient of A: 0.1% TFA in water and B: 0.08% TFA in acetonitrile, 5-65% B in 30 min at 6.0 mL/min flow rate. Chromatograms were recorded at 230 nm. MALDI-tof mass analysis was performed on a linear Protein-tof Bruker instrument using α-cyano-4-hydroxycinnamic as a matrix.

Abbreviations

Symbols and abbreviations for amino acids and peptides are in accord with the recommendations of the IUPAC-IUB Commission on Nomenclature (*J. Biol. Chem.* 1972, 247, 977). Other abbreviations used are: AcOH, acetic acid; Boc, *tert*-butyloxycarbonyl; Bop, benzotriazole-1-yl-oxy-tris-(dimethylimino)-phosphonium hexafluorophosphate; *t*Bu, *tert*-butyl; DBU, 1,8-diazabicyclo[5,4,0]undecen-7-ene; DIC, diisopropylethylcarbodiimide; DEA, diethylamine, DIEA, diisopropylethylamine; DMAP, 4-dimethylaminopyridine; EDC×HCl, N-(3-dimethylaminopropyl)-N'-ethylcarbodiimide hydrochloride; Fmoc, 9*H*-fluoren-9-ylmethyloxycarbonyl; HATU, 2-(7-Aza-1*H*-benzotriazole-1-yl)-1,1,3,3-tetramethyluronium hexafluorophosphate; HOAt, 1-hydroxy-7-azabenzotriazole; HOBt, 1-hydroxybenzotriazole; MALDI-tof, Matrix Assisted Laser Desorption Ionization time-of-flight; Mtt, 4-methyltrityl; NMM, N-methyl morpholine; TFA, trifluoroacetic acid; TIS, triisopropylsilane.

Synthesis

Boc-(D)Ala-OAll. Boc-D-Ala-OH (1.89 g, 10 mmol) was solubilised in DCM (70 ml) and the solution was cooled at 0° C. 1.5 ml of DBU (1.2 equiv.) were added. A solution of allyl bromide (0.72 ml, 1 equiv.) in ACN (10 ml) was dropped along 15 minutes. The solution was

stirred at room temperature for 21 hours. After evaporation of the solvent, the crude product was dissolved in AcOEt and washed with 5% NaHCO₃, water, 1N KHSO₄ and water. The organic phase was dried over Na₂SO₄ and evaporated. The product was recovered as oil in 73% yield. ¹H NMR (200 MHz, CDCl₃): δ 5.89 (m, 1H), 5.22 (m, 3H), 4.99 (m, 1H), 4.57 (d, 2H), 4.24 (m, 1H), 1.38 (s, 9H), 1.34 (d, 3H). ¹³C NMR (50 MHz, CDCl₃): δ 173.04, 155.07, 131.68, 118.60, 79.86, 65.79, 49.30, 28.32, 18.69.

HCl×H-(D)Ala-OAll. Boc-D-Ala-OAll (1.67 g, 7.3 mmol) was solubilised in a 4N HCl in dioxane (5 ml) under argon. The solution was stirred for 30 minutes. After evaporation of the solvent, the product was obtained as a white solid in 90 % yield. ¹N NMR (200 MHz, CDCl₃) δ 5.89 (m, 1H), 5.26 (m, 2H), 4.68 (m, 2H), 4.26 (m, 1H), 1.70 (d, 3H). ¹³C NMR (50 MHz, CDCl₃) δ 169.87, 131.12, 119.24, 66.86, 49.361, 16.09.

Fmoc-Lys(Mtt)-OAll. Fmoc-Lys(Mtt)-OH (625 mg, 1 mmol) was solubilised in DCM (5 ml) in the presence of HOBt (153 mg, 1 equiv.) and EDC×HCl (211 mg, 1.1 equiv.). After 5 minutes, allyl alcohol (68 μl, 1 equiv.) and DMAP (12 mg, 0.1 equiv.) were added. After 27 hours HOBt (76 mg, 0.5 equiv.), EDC×HCl (105 mg, 0.55 equiv.), allyl alcohol (34 μl, 0.5 equiv.) and DMAP (12 mg, 0.1 equiv.) were added. The solution was stirred for 44 hours under the dark. The solvent was evaporated and the crude product was dissolved in AcOEt and washed with 5% NaHCO₃, water, 1N KHSO₄ and water. The organic phase was dried over Na₂SO₄ and evaporated. The product was recovered as oil in 94% yield. ¹N NMR (200 MHz, CDCl₃) δ 7.7((m, 2H), 7.62 (m, 2H), 7.47 (m, 4H), 7.25 (m, 14H), 5.87 (m, 1H), 5.26 (m, 3H), 4.63 (m, 2H), 4.39 (m, 3H), 4.17 (m, 1H), 2.30 (s, 3H), 2.14 (m, 2H), 1.51 (m, 6H). ¹³C NMR (50 MHz, CDCl₃) δ 172.18, 155.85, 146.27, 143.75, 141.29, 131.49, 128.57, 127.74, 127.66, 127.03, 126.17, 125.04, 119.92, 118.91, 66.98, 65.90, 53.84, 47.18, 43.34, 32.70, 23.02, 20.89.

H-Lys(Mtt)-OAll. Fmoc-Lys(Mtt)-OAll (240 mg, 0.36 mmol) was solubilised in a solution of 5:8 DEA/DCM (13 ml). The solution is stirred for 5 hours. After evaporation of the solvent, the product is dissolved in Et₂O and extracted with 1N KHSO₄. The acid solution was basified with solid NaHCO₃ and the desired product extracted with AcOEt. After washing with water and drying over Na₂SO₄, the solvent was evaporated affording an oily compound in quantitative yield. The product was used directly for the further reaction.

Reductive amination on the resin (5). 2-(3,5-Dimethoxy-4-formylphenoxy)ethyl polystyrene resin (100 mg, 62 μmol) was swollen in DMF (1.2 ml) in the presence of HCl×H-D-Ala-OAll (80 mg, 10 equiv.) and NaBH₃CN (38 mg, 10 equiv.) The reaction was followed

using FT-IR and after 26 hours the resin was washed with DMF, DCM, MeOH and dried with Et₂O. The presence of the secondary amine on the resin was verified using chloranil test.³

Synthesis of cyclo-(L-Lys-D-Ala)₃ (3). Fmoc-Lys(Mtt)-OH (194 mg, 5 equiv.) was solubilised in dry DCM (1 ml) in the presence of collidine (115 μ l, 14 equiv.) and activated with triphosgene (30 mg, 1.65 equiv.) for 1 minute. The solution is added to the resin **5** (62 μ mol) previously functionalised with H-D-Ala-OAll (see reductive amination). The resin was shaken for 30 minutes and extensively washed with DCM, DMF and Et₂O. Negative chloranil test confirmed the completeness of the coupling. The dipeptide-resin conjugate **6** (62 μ mol) was treated with Pd(Ph₃)₄ (143 mg, 2 equiv.) dissolved in 2 ml of DCM/AcOH/NMM 1850:100:50 for 6 hours under argon, affording **7**. H-Lys(Mtt)-OAll (159 mg, 5.8 equiv.) was solubilised in 1.5 ml of DMF and 600 μ l of DCM with HATU (94 mg 4 equiv.), HOAt (34 mg, 4 equiv.), CuCl₂ (4.2 mg, 0.5 equiv.) and collidine (74 μ l, 9 equiv.), and subsequently added to the resin **7** (62 μ mol). The resin was shaken for 2 hours and washed with DMF, DCM and Et₂O, affording **8**. Fmoc was removed with 25 % piperidine in DMF (2 \times 15 minutes) and Fmoc-D-Ala-OH (96 mg, 5 equiv.) activated with Bop (137 mg, 5 equiv.), HOBT (47 mg, 5 equiv.) and DIEA (162 μ l, 15 equiv.) in DMF was coupled for 1 hour. The coupling was repeated a second time using the same conditions. After Fmoc cleavage, the same procedure was applied for the coupling of the subsequent Fmoc-Lys(Mtt)-OH and Fmoc-D-Ala-OH, affording **10**. Allyl group was removed with Pd(Ph₃)₄ (143 mg, 2 equiv.) dissolved in 2 ml of DCM/AcOH/NMM 1850:100:50 for 6 hours under argon, affording **11**. Fmoc was removed with 25 % piperidine in DMF (2 \times 15 minutes), and the linear solid-supported peptide was cyclised head-to-tail in the presence of HOAt (34 mg, 4 equiv.), DIC (42 μ l, 4.4 equiv.) in a 5/2 solution of DMF/DCM (2.1 ml) for 3 hours, affording **13**. Mtt groups were finally removed using a solution of 85 % DCM, 10 % TIS and 5 % TFA (2 ml) (3 \times 2 minutes), affording **14**.

Part of the resin was cleaved with a solution of 90 % TFA, 5 % water and 5 % TIS (3 ml) for 3 hours. After precipitation in cold Et₂O the crude peptide **3** was lyophilised on a mixture of water/AcOH (9/1), characterised by analytical HPLC and mass spectrometry, and purified using semi-preparative HPLC. MALDI-Tof (*m/z*) [C₂₇H₅₁N₉O₆] calcd. 597.75; found 620.54 [M+Na]⁺.

Synthesis of ligand (1). Fmoc-Ahx-OH, Fmoc-Tyr(tBu)-OH, Fmoc-Tyr(tBu)-OH (\times 2), Fmoc-Gly-OH et Fmoc-Lys(Boc)-OH (15 equiv.) activated with Bop (15 equiv.), HOBT (15 equiv.) and DIEA (45 equiv.) in DMF were coupled to the resin bound cyclo-(L-Lys-D-Ala)₃

along 1 hour. Each coupling was repeated twice. After each coupling step, Fmoc was removed using 25 % piperidine in DMF (2×15 minutes). After the last Fmoc cleavage, the loading was recalculated affording a value of 28 μmol of final crude product on the resin. The final cyclic hexapeptide **1** was removed from the resin with a solution of 90 % TFA, 5 % water and 5 % TIS (3 ml) for 3 hours. After precipitation in cold Et_2O the crude peptide was lyophilised on a mixture of water/AcOH (9/1). The product was controlled by analytical HPLC, mass spectrometry and purified using semi-preparative HPLC. The purity of crude **1** was around 50%. After lyophilisation, 11.3 mg of pure **1** were obtained (Yield: 16% based on the loading after the last Fmoc cleavage). MALDI-Tof (m/z) [$\text{C}_{123}\text{H}_{183}\text{N}_{27}\text{O}_{27}$] calcd. 2471.93; found 2473.12 [$\text{M}+\text{H}$]⁺, 2495.35 [$\text{M}+\text{Na}$]⁺.

Synthesis of ligand (2). Ligand **2** was isolated during HPLC purification of ligand **1**. The product was characterised by mass spectrometry. MALDI-Tof (m/z) [$\text{C}_{91}\text{H}_{139}\text{N}_{21}\text{O}_{20}$] calcd. 1847.21; found 1848.20 [$\text{M}+\text{H}$]⁺, 1870.60 [$\text{M}+\text{Na}$]⁺.

Surface plasmon resonance analysis

BIACore™ 3000 (Biacore AB, Uppsala, Sweden) was used to evaluate the binding of CD40L mimetics to CD40. Flow cells of a Biacore AB CM5 Sensor Chip (Research Grade, Biacore AB) were pre-coated with a rabbit polyclonal antibody directed against murine Ig (RAM-Ig, Biacore AB, Uppsala, Sweden) using amine coupling at 30 $\mu\text{g}/\text{mL}$ in 10 mM acetate buffer, pH 5.5 according to the manufacturer's protocol. The chip was then flushed with 1 M ethanolamine hydrochloride pH 8.5 (Biacore AB) and 50 mM HCl to eliminate unbound antibody. Generally *ca* 10,000 RU of RAM-Ig was obtained after immobilisation. Biosensor assays were performed at 25°C with HBS-EP buffer (10 mM Hepes, pH 7.4, containing 0.15 M NaCl, 3.4 mM EDTA and 0.005% (v/v) P20 surfactant (Biacore AB)) as running buffer. Capture of soluble human CD40-mIg fusion protein (hCD40:mIg; Ancell corporation, Bayport, MN), of mouse anti-huCD40 antibody (Pharmingen, San Jose, CA) and of LG11-2, an IgG2a murine monoclonal antibody directed against H2B histone used as irrelevant control, was performed on individual flow cells at a flow rate of 5 $\mu\text{L}/\text{min}$ and at a concentration allowing to achieve equivalent protein mass binding.

Inhibition of human soluble CD40L binding to CD40: hCD40L:CD8 fusion protein (Ancell, Bayport, MN) was injected at 150 at a flow rate of 10 $\mu\text{L}/\text{min}$ in the presence of various concentrations of CD40L mimetics, over both the control channel and the CD40 channel for 5 minutes and allowed to dissociate for 5 additional minutes. The channels were regenerated for

10 s with 50 mN HCl. Sensorgrams of ligands in the absence of hCD40L:CD8 were subtracted from the sensorgrams of ligands co-injected with hCD40L:CD8, and then subtracted by the control sensorgrams. The inhibition capacity was estimated from the decrease in the initial linear association phase. Data were processed with the BIAevaluation v4.1 software (Biacore).

Measure of apoptosis

BL41 cells have been characterized as human Burkitt lymphomas. Cell death was evaluated either by measurement of a decrease in mitochondrial transmembrane potential ($\Delta\psi_m$) associated with a reduction of the cationic dye 3,3'-dihexyloxacarbocyanine iodide [DiOC₆(3)] (Interchim, Montluçon, France) uptake as demonstrated by flow cytometry, or by detection of phosphatidylserine externalisation by flow cytometry after co-labelling with annexin V-FITC and propidium iodide (PI). To analyse apoptosis by annexin V/PI labeling,⁴ cells were resuspended in 100 μ L of annexin V binding buffer (10 mM Hepes pH 7.4, 140 mM NaCl, 2.5 mM CaCl₂) containing 5 μ L of annexin V-FITC (Pharmingen, San Jose, CA) and 10 μ L of propidium iodide (PI) (Molecular Probes) at 10 μ g/mL and incubated at room temperature in the dark. After 20 min, 400 μ L of annexin V binding buffer were added and cells were analysed by flow cytometry. To analyse apoptosis by DiOC₆(3) uptake,⁵ approximately 1×10^6 cells washed in PBS were resuspended in 300 μ L of PBS containing 40 nM DiOC₆(3) and incubated at 37° C for 30 minutes. Cells were then directly analysed by flow cytometry (FACScalibur; CellQuest v3.3). Results are expressed as percentage of specific apoptosis according to the following formula: % specific apoptosis = [(% of apoptotic treated cells - % of apoptotic control cells) \times 100]/(100 - % of apoptotic control cells).

References

1. J. Neimark and J.-P. Briand, *Peptide Res.*, 1993, **6**, 219.
2. M. Goodman, A. Felix, L. Moroder and C. Toniolo, *Methods of Organic Chemistry (Houben-Weyl)*, Vol. E22a, Thieme, Stuttgart, 2002.
3. T. Vojkovsky, *Pept. Res.*, 1995, **8**, 236.
4. G. Koopman C. P. Reutelingsperger, G. A. Kuijten, R. M. Keehnen, S. T. Pals, M. H. van Oers, *Blood*, 1994, **84**, 1415.
5. A. Macho M. Castedo, P. Marchetti, J. J. Aguilar, D. Decaudin, N. Zamzami, P. M. Girard, J. Uriel, G. Kroemer, *Blood*, 1995, **86**, 2481.

CHAPTER 7

SMALL TRIVALENT ARCHITECTURES MIMICKING HOMOTRIMERS OF THE TNF SUPERFAMILY MEMBER CD40L: DELINEATING THE RELATIONSHIP BETWEEN STRUCTURE AND EFFECTOR FUNCTION

(submitted to JACS)

Sun, W., **Wieckowski, S.**, Trouche, N., Chaloin, O., Briand, J.-P.,
Hoebeke, J., Fournel, S., and Guichard, G.

CHAPTER 7

Validation of biochemical and biological screening assays has led to the initiation of a complete structure/activity study on mini-CD40Ls. We tried to optimize the core structure, the spacer arm and the CD40-binding motif. In parallel, we gained important informations on the mechanisms of action of mini-CD40Ls.

We have synthesized many mini-CD40L variants, and tested their binding capacity by surface plasmon resonance, their functional activity by apoptosis of lymphoma cells, their capacity to induce maturation of dendritic cells. We have first modified the core structure. Diverse chemical platforms with C_3 symmetry have been described in the literature, but only two structures from the seven tested have permitted to obtain functional CD40L mimetics. These data showed that the nature of the core structure is important for activity of mini-CD40Ls. We have then generated monomeric, dimeric and tetrameric forms of mini-CD40Ls. Although the dimeric form has some activity at higher concentrations on dendritic cells, trivalency was required for full functions. The spacer arm length was also submitted to modulation in order to optimized activity of mini-CD40L. Interestingly, we showed that the chemical nature of the linker arm is crucial for a proper function. Finally, we identified a second CD40-binding motif that has shown higher activity than the first generation of mini-CD40Ls.

This structure/activity study has led not only to the proposal of optimized mini-CD40Ls molecules, but has also provided some important informations on their mechanisms of action. These data would be of high importance for the design of optimized mini-CD40Ls, as well as for the design of mimetics of other members of the TNF family.

Small Trivalent Architectures Mimicking Homotrimers of the TNF Superfamily Member CD40L: Delineating the Relationship between Structure and Effector Function

*Weimin Sun,^{†,#} Sébastien Wieckowski,[†] Nathalie Trouche[†], Olivier Chaloin[†], Johan Hoebeke,[†] Sylvie
Fournel^{*†} and Gilles Guichard^{*†}*

CNRS, Institut de Biologie Moléculaire et Cellulaire, laboratoire d'Immunologie et Chimie
Thérapeutiques, 15 rue René Descartes, 67084 Strasbourg, France

**RECEIVED DATE (to be automatically inserted after your manuscript is accepted if required
according to the journal that you are submitting your paper to)**

TITLE RUNNING HEAD: Trivalent architectures mimicking CD40L homotrimers

*To whom correspondence should be addressed. E-mail: g.guichard@ibmc.u-strasbg.fr or
s.fournel@ibmc.u-strasbg.fr

[†]Immunologie et Chimie Thérapeutiques (ICT)

[#]Present Address: Institute of Biological Science and Technology, Beijing Jiaotong University, 3 Shang
Yuan Cun, Haidian District, 100044 Beijing, China.

Abstract. Synthetic multivalent ligands, owing to the presence of multiple copies of a recognition motif attached to a central scaffold, can mediate clustering of cell surface receptors and thereby function as effector molecules. This paper dissects the relationship between structure and effector function of synthetic multivalent ligands targeting CD40, a cell surface receptor of the tumor necrosis factor family receptor (TNF-R) superfamily. Triggering CD40 signaling in vivo can be used to enhance immunity against intracellular pathogens or tumors. A series of multimeric molecules have been prepared by systematically varying the shape and the valency of the *central scaffold*, the nature and the length of the *linker* as well as the sequence of the *receptor binding motif*. The data reported here *i)* suggest that radial distribution of CD40-binding units and C_3 -symmetry are preferred for optimal binding to CD40 and signaling; *ii)* underscores the importance of choosing an appropriate linker to connect the receptor binding motif to the central scaffold; and *iii)* show the versatility of planar cyclic peptides as templates for the design of CD40L mimetics. In particular, the (Ahx)₃-**B** trimeric scaffold-linker combination equally accommodated binding elements derived from distinct CD40L hot spot regions including AA"loop and β -strand E. The use of *miniCD40Ls* such as those reported here is complementary to other approaches (recombinant ligands, agonistic anti-receptor antibodies) and may find interesting therapeutic applications. Furthermore, the results disclosed in this paper provide the basis for future design of other TNF family member mimetics.

Introduction.

Protein-protein interactions are central to most biological processes from cellular communication to programmed cell-death and provide the basis for interesting therapeutic applications. Small molecules that can bind at protein-protein interfaces are thus of interest to inhibit undesired biological processes or to promote desired ones. The design of such molecules, however, is hampered by the large protein surfaces at interplay (1000-2000 Å²), as well as by the difficulty to identify defined “hot spot” residues, and to handle conformational, non sequential epitopes. Nevertheless, in the last decade the number of reports of synthetic molecules capable of blocking protein-protein interactions in a specific manner has grown steadily.¹ On the other hand, few protein mimetics with effector functions, that can both bind to a cell surface receptor and activate downstream signaling pathways have been described.

Ligand-induced oligomerization or aggregation of cell surface receptors (e.g. cytokine receptors, receptor tyrosine kinases, tumor necrosis factor (TNF) receptors, T-cell receptors (TCRs), Toll-like receptors (TLRs), and G-protein coupled receptors (GPCRs) for naming a few) is an important mechanism to initiate and control signaling in a number of biological processes.²⁻⁷ In this context, (small) synthetic molecules binding avidly to multiple copies of a receptor may be used to activate signaling pathways similar to the cognate ligand. Early studies on synthetic multivalent systems (mainly for antagonizing unwanted biological processes) have clearly demonstrated that it is possible through polyvalency to achieve tight binding with ligands of low or modest surface areas.⁸⁻¹¹ The possibility to create molecules with effector functions through multivalency has been recognized more recently.⁹⁻¹³ In the field of cytokine mimetics, dimeric peptides, C₂-symmetric organic molecules as well as dendrimers capable of dimerizing and activating erythropoietin receptor (EPO-R), thrompoietin receptor (TPO-R), or granulocyte–colony stimulating factor (G-CSF) receptor are worth mentioning.^{14,15}

While protein ligand induced dimerization is the mechanism of activation of receptors for cytokine and growth factors, signaling by members of the tumor necrosis factor receptor (TNF-R) family involves receptor trimerization. The geometry of the resulting ligand-receptor complex is favorable to the formation of an intracellular signaling complex.^{3a, 16} TNF-R family members can transduce a variety

of intracellular signals culminating in proliferation, differentiation, survival and death. Most of the 19 ligands and 29 receptors of the TNF/TNF-R superfamilies play an active role in the development, maintenance and function of the immune system.¹⁶ A few members are also implicated in other physiological processes such as bone remodeling or development of skin appendages. CD40 is expressed on antigen presenting cells (APCs) such as dendritic cells (DCs) and B-cells and by interacting with its ligand CD40L (CD154), leads to their activation and differentiation.¹⁷ Blockade of the CD40-CD40 ligand pathway is a potential immunomodulatory strategy for T-cell-mediated diseases. Administration of anti-CD40L antibodies has given encouraging results in the treatment of experimental autoimmune diseases as well as in the treatment of allograft rejection.^{18,19} Alternatively, triggering CD40 signaling *in vivo* can be used to enhance immunity against intracellular pathogens or tumor cells. The use of agonistic anti-CD40 antibodies for example has been shown to increase the efficacy of peptide-based anti-tumor vaccines.²⁰ These findings support a clinical use of CD40-stimulating agents as components of anti-cancer or anti-infectious vaccines and immunotherapies. Like other members of the TNF family, CD40L monomers self-assemble around a three-fold symmetry axis to form non-covalent homotrimers that can each bind three receptor molecules. The crystal structure of the extracellular domain of CD40L homotrimers²¹ and a homology model of the CD40L/CD40 complex²² have provided the ground for the rational design and synthesis of a first generation of CD40L mimetics.^{23,24} We have shown that rigid scaffolds with C_3 -symmetry combined with linkers of appropriate size and shape can serve to distribute a CD40-binding motif with a geometry and distances that could match that of the natural CD40L protein (Figure 1). A short loop sequence from the surface of CD40L encompassing three “hot-spot” residues (Lys143, Tyr145 and Tyr146 in the AA” loop) critical for binding to CD40, was initially chosen as a CD40 binding motif.

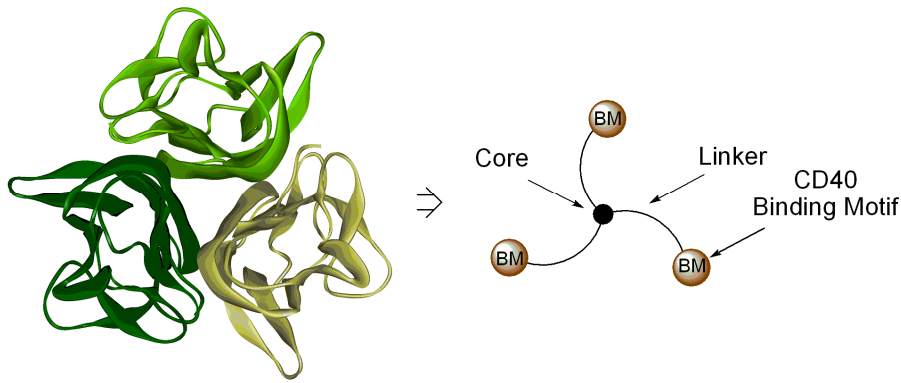
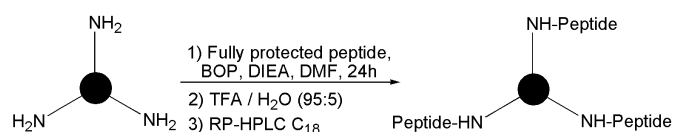


Figure 1. X-ray structure of CD40L homotrimer (PDB 1ALY) viewed down the C_3 axis and schematic representation of the structure-based approach to the design of CD40L homotrimers mimetics...

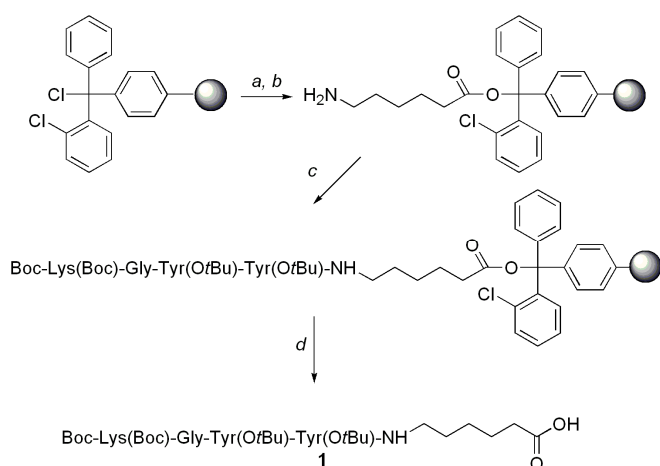
The gain in avidity that could result from a multivalent interaction with CD40 molecules was expected to overcome the relatively low binding energy of the short tetrapeptide sequence. Two trimeric molecules **A-1** and **B-1** built on the rigid cyclo(Lys-D-Ala)₃ and cyclo(β^3 -HLys) peptide rings **A** and **B** respectively (see chart 1) with amino hexanoic acid (Ahx) residues as additional spacer arms were found to bind in a specific manner to CD40 and to compete with the binding of CD40L homotrimers.²³ In various cell-based assays, **A-1** and **B-1** displayed effector functions that meet those of the much larger recombinant CD40L homotrimers, i.e. induction of apoptosis of Burkitt B-lymphomas and maturation of DCs. Both CD40L mimetics were shown recently to be effective *in vivo* and to promote the control of *T. cruzi* (i.e. the etiological agent of the *Chagas*' disease) infection in an experimental mouse model by overcoming the immunosuppression usually induced by the parasite.²⁵ However, the molecular determinants of the design of CD40L mimetics (hereby referred to as “*miniCD40Ls*”) with optimal CD40 binding properties and effector functions are not yet fully delineated. To assess the contribution of each individual components of the trivalent architecture, we have now undertaken a detailed study by systematically varying the shape and the valency of the core structure, the geometry and the length of the spacer arm as well as the nature of the CD40 binding motif.

Results and Discussion.

Ligand synthesis. All CD40L mimetics described in this study (except **E-1**, see supporting information) were synthesized according to Scheme 1 by fragment coupling in solution of a fully protected peptide fragment encompassing the receptor binding motif and a spacer arm, to the corresponding amino-functionalized core structure **A-0** to **L-0** (R = H). The protected CD40-binding peptides with their linker were prepared on solid support starting from a 2-chlorotrityl chloride resin as illustrated in Scheme 2 for the Lys-Gly-Tyr-Tyr-Ahx sequence. Peptide assembly on core structures was generally performed with BOP²⁶ as the coupling agent in DMF for 24 h, after which the crude fully protected multimeric construct was recovered by filtration after precipitation with a saturated NaHCO₃ solution, washed extensively with ethyl acetate and dried under high vacuum. All protecting groups were removed by treatment with trifluoroacetic acid (TFA) to afford crude ligands. Finally, ligands were purified by C₁₈ RP-HPLC and recovered in overall yields ranging from 6-37 %. It is noteworthy that the synthesis of **A-1** was routinely achieved on > 100 mg scale with an overall yield exceeding 25%. In an optimized process, the linear peptide precursor of scaffold **A**, H-(Lys(Boc)-D-Ala)₃-OH was assembled by solid-phase synthesis on a 2-chlorotrityl chloride resin. All ligands were identified by matrix-assisted laser desorption/ionization mass spectrometry (MALDI-MS) and their homogeneity was assessed by C₁₈ RP-HPLC with purity of all peptides determined to be > 99%, (see supporting information for detailed experimental procedures and characterization of all investigated ligands).



Scheme 1. General synthetic approach to trimeric CD40L ligands.



Scheme 2. Synthesis of the protected pentapeptide Boc-Lys(Boc)-Gly-Tyr(OtBu)-Tyr(OtBu)-Ahx-OH (**1**) (see Supporting Informations for details). Conditions: (a) Fmoc-6-Aminocaproic acid, DIEA, CH₂Cl₂; (b) 25% piperidine/DMF; (c) SPPS : Fmoc-Xaa-OH, BOP, HOBt, DIEA, DMF; (d) HFIP/CH₂Cl₂ (60:40 v/v).

Variations in shape and size of the central core. The nature of a scaffold for polyvalent display can significantly impact on the biological activity of synthetic multivalent ligands. Features such as geometry, valency, rigidity must be carefully tailored to ensure effective distribution of appended recognition patterns. This has been recognized in a number multivalent systems with a variety of poly-(oligo-)valent scaffolds (e.g. small synthetic scaffolds, dendrimers, polymers, liposomes, proteins and viral particles).^{10-12,27} Our previous finding that CD40L mimetics based on trimeric architectures **A** and **B** but not branched **E** exhibit effector functions in several cellular assays (maturation of D1 dendritic cell line²⁸, apoptosis of lymphoma B cells²⁹) and promote control of parasitemia during experimental *Trypanosoma cruzi* infections in mice tend to suggest that the rigidity of the central core is one determinant of the activity of CD40L mimetics.^{23a,25} This can be rationalized in term of the minimization of the conformational entropic cost.^{11a} It also suggests that effective trivalent display of a given CD40-binding motif with geometry and distances that match those in the cognate protein trimer imposes constraints on the overall geometry and dimensions of the (core+linker) element. To ascertain this trend, we have now considered an enlarged set of trimeric architectures falling into three categories

(chart 1) : macrocyclic (**A-D**), branched (**E,F**) and heterocyclic (**G-I**), varying in size (**A ~ C > B > I > G > E > H > F**, based on fully extended structures) and rigidity. Partially *N*-methylated *cyclo*-D,L- α -peptide **C** which displays a smaller number of H-bond donors than **A** was intended to modulate the possible self-assembling properties of the resulting ligands.³⁰ Macrocyclic ligand with receptor-binding motifs attached to the upper rim of a calix[6]triamine core structure (type **D**)³¹ were designed to investigate the effect of a more axial (assuming a cone conformation) distribution of the CD40 binding motif.^{32,33}

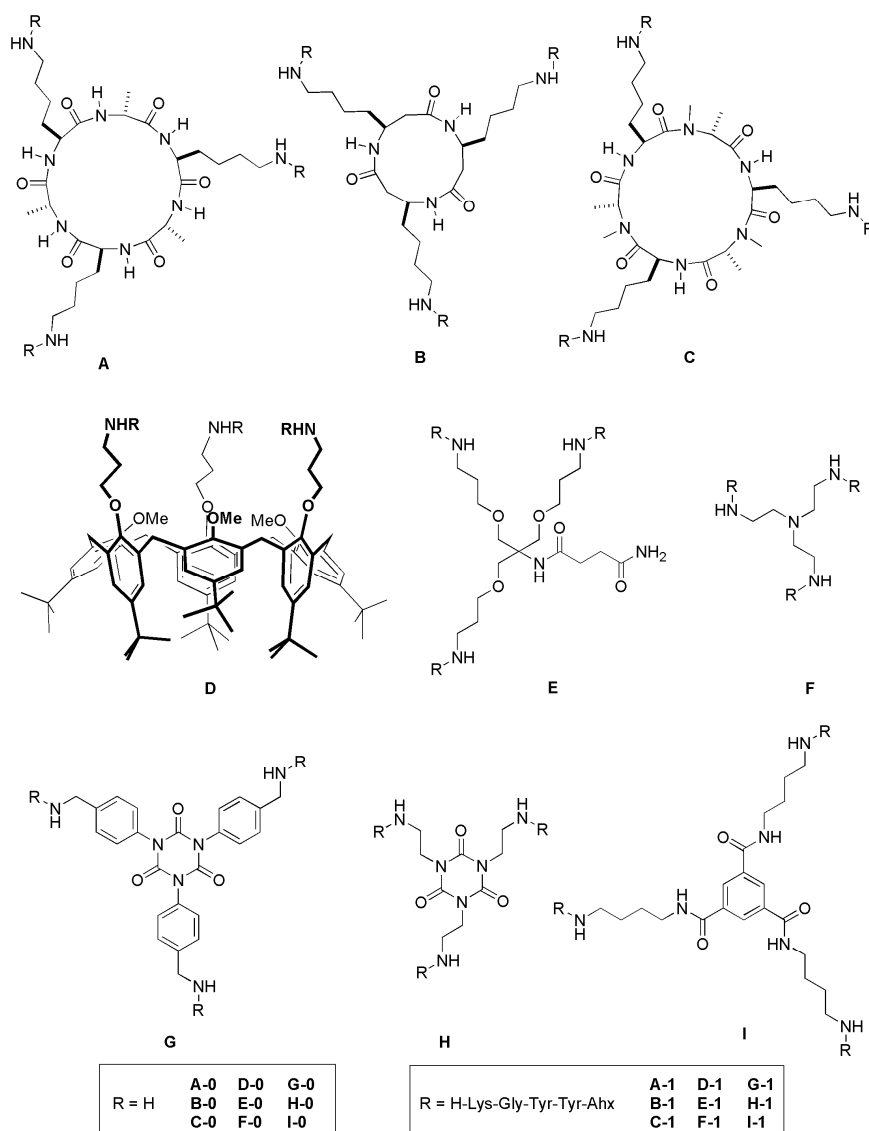


Chart 1. Trimeric architectures and ligands based on scaffolds **A-I**

The corresponding ligands **A-1** to **I-1** obtained by appending the pentapeptide sequence Lys-Gly-Tyr-Tyr-Ahx (**1**) have been evaluated for binding to recombinant human CD40 using surface plasmon resonance (SPR) and for their capacity to induce apoptosis of the BL41 human B-lymphoma cell line (Figures 1 and 2).

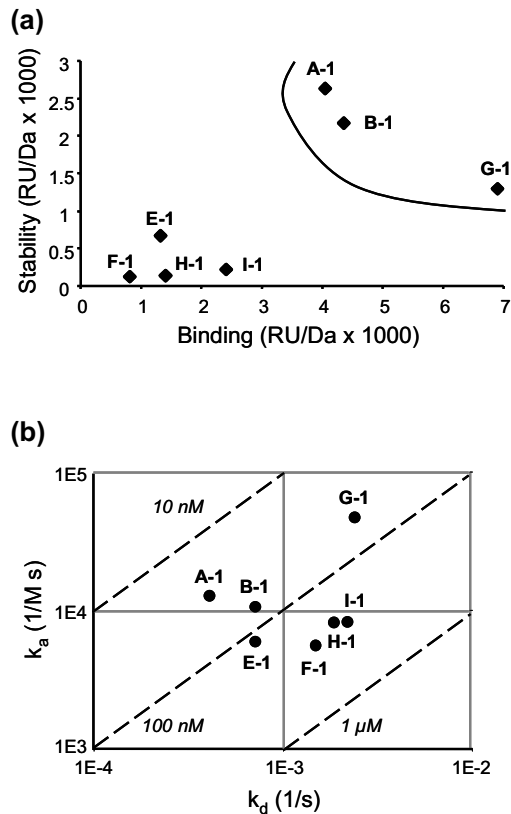


Figure 2. Comparison of *miniCD40Ls* **A-1** to **I-1** for binding to CD40 by surface plasmon resonance (SPR). (a) Screening of the molecules at 250 nM. Binding values correspond to response signal at the end of the association phase, and stability values correspond to response signal just after the beginning of the dissociation phase, all subtracted from the bulk refractive effect signal. Molecular weight (MW) differences between the molecules were taken into account by dividing values by MW/1000. The best ligands are encircled. (b) Graphical summary of the data generated from different concentrations of the mimetics. Kinetics values were all derived from the 1:1 Langmuir model. All results are representative of at least two independent experiments.

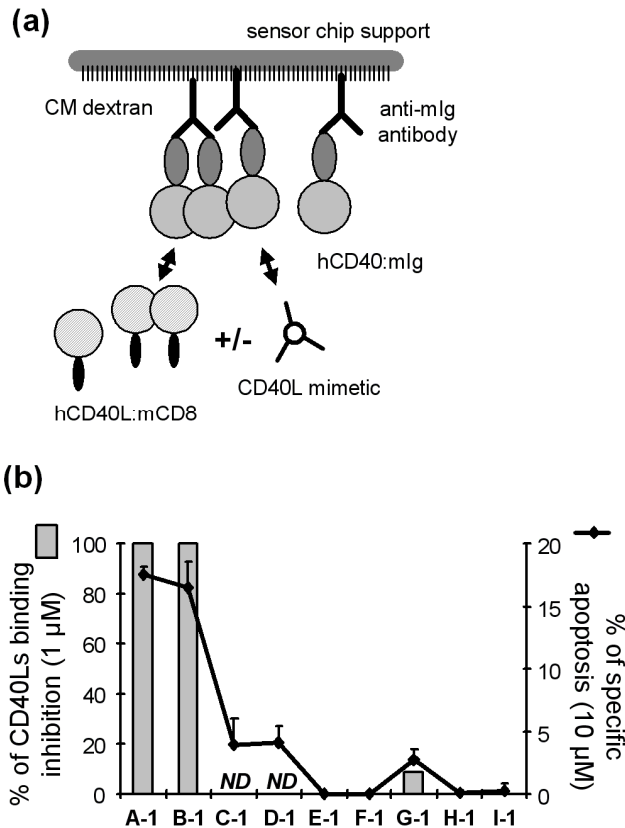


Figure 3. Comparison of *miniCD40Ls* A-1 to I-1 for their ability to inhibit binding of natural soluble human CD40L (CD40Ls) to CD40 and to induce apoptosis of the human lymphoma cell BL41. (a) Schematic representation of the SPR inhibition experiment. (b) Grey bars: values of the inhibition experiments. Percentage of inhibition at 1 μ M of mimetics is represented. They were derived from the slope of the CD40Ls mixed to the mimetics response signal subtracted from the response signal of the mimetics alone. Results are representative of two independent experiments. *ND*: not determinable because of aggregation; black line: induction of apoptosis of human lymphoma cell line BL41 after 16 h of treatment. Values compared are from percentage of specific apoptosis (see Material and Methods) obtained at 10 μ M of the different mimetics. Results are expressed as means \pm SEM of three independent experiments.

Screening of molecules **A-1** to **I-1** at 250 nM in a direct CD40 binding assay confirmed macrocyclic **A-1** and **B-1** and newly identified heterocyclic **G-1** as the best CD40 binders in the series in terms of binding capacity and interaction stability (Fig. 2a). A similar trend was observed when analysing kinetic binding parameters calculated from response sensorgrams acquired for various concentrations of *miniCD40Ls* (k_a versus k_d plots with isoaffinity lines are shown in Fig. 2b). Kinetic values were all derived from the 1:1 interaction Langmuir model (see experimental section for description of equations used).³³ Whereas the majority of ligand-CD40 interactions showed binding kinetics suitable for determination of the kinetic rate constants, SPR analysis was hampered for ligands **C-1** and **D-1** (partially *N*-methylated cycloD,L-hexapeptide and calix[6]arene cores respectively) because of the formation of aggregates in the conditions of the assay. Trimeric ligands were also compared in an inhibition SPR assay as shown in Figure 3a. At 1 μ M, only **A-1** and **B-1** were found to significantly inhibit the binding of soluble recombinant hCD40L:mCD8 to hCD40:mIg fusion protein (Fig. 3b). Molecule **G-1** was only a weak inhibitor. In parallel, all ligands were screened in a cell-based assay (Fig. 3b). Their capacity to induce apoptosis of CD40-positive human Burkitt B lymphoma cells was measured by the decrease of the mitochondrial membrane potential ($\Delta\Psi_m$).^{23a} **A-1** and **B-1** induced a high level of apoptosis at 10 μ M whereas all remaining ligands were only weakly active (**C-1**, **D-1**, **G-1**) or ineffective (**E-1**, **F-1**, **H-1**, **I-1**).

Ligands **A-1** and **B-1** differ from other tested ligands by the shape of their central core. The general structural features of $\text{cyclo}(\text{Xaa-D-Xbb})_n$ and $\text{cyclo}(\beta\text{-HXaa})_n$ peptides have been extensively investigated both in solution by NMR spectroscopy and in the solid state by XRD and PXR. ^{30, 34-37} In both series, the peptide backbone generally adopts a flat-ring conformation with side chain occupying equatorial positions along the ring's edge.³⁸ The results obtained by SPR and in cell-based assays with compounds **A-1** to **I-1** suggest in first approximation that a radial distribution of the CD40-binding motif is preferred. Among all ligands tested, **A-1** and **B-1** are those potentially providing the longest distance between the center of the trivalent system and the NH connecting the Ahx linker. Thus, our data also support the view that the distance between the center of the trivalent system and the NH of the

flexible linker connecting the CD40 binding motif should be above a minimum length (*vide infra*, section on modulation of the linker length).

Comparison to mono-, di- and tetravalent systems. In the next series of experiments, the importance of a C_3 -symmetric trivalent display was assessed by systematically varying the number of CD40 recognition elements appended to the cyclic D,L-peptide core (Chart 2).

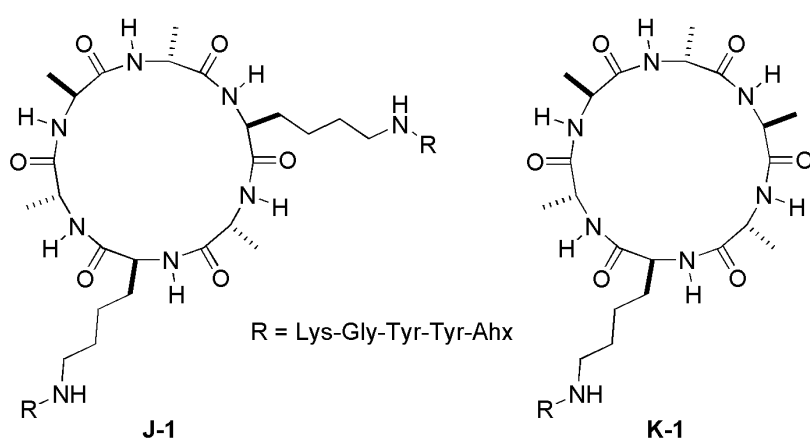


Chart 2.

We found that removing one CD40-binding motif while maintaining a radial distribution (**A-1**→ **J-1**) resulted in a strong decrease of the CD40 binding capacity (Fig. 4) and biological effects, i.e. apoptosis of human B-lymphoma cells (Fig. 5a) and maturation of mouse dendritic cells D1,²⁸ (Fig. 5b). Not surprisingly, ligand **K-1** with only one CD40-binding motif appended to a cyclic D,L-hexapeptide core was inactive.

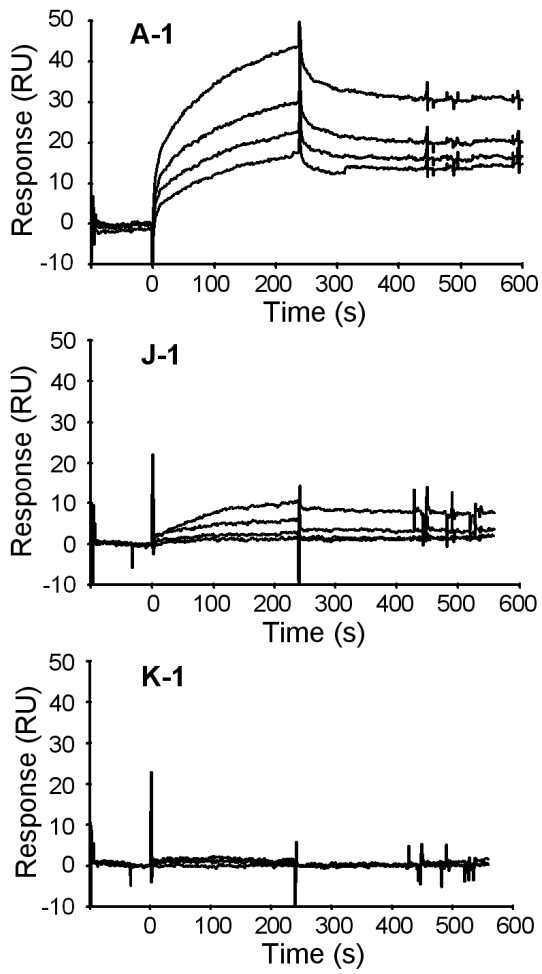


Figure 4. Influence of the valency of the ligands on their capacity to bind CD40. Direct binding of **A-1**, **J-1** and **K-1** to CD40 as shown by SPR. All data were obtained for mimetics concentration from 100 to 800 nM.

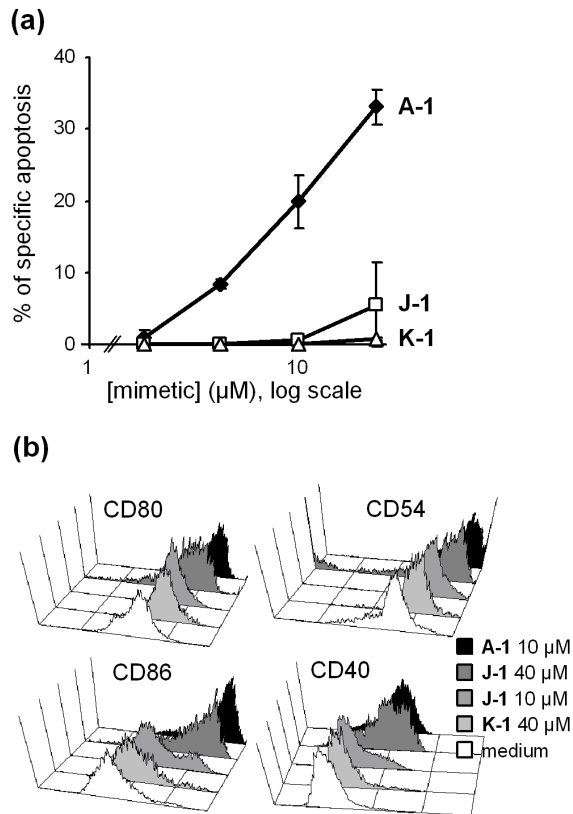


Figure 5. Influence of the valency of *miniCD40Ls* on effector functions (a) Induction of apoptosis of human lymphoma cell line BL41. Percentage of specific apoptosis (see experimental section) induced by the different mimetics at the indicated concentrations after 16 h of incubation. Results are expressed as means \pm SD of two independent experiments. (b) Expression of the maturation markers (CD80, CD54, CD86 and CD40) by the mouse dendritic cell line D1 as measured by flow cytometry after 24 h of incubation with the different mimetics at the indicated concentrations; white histogram: medium control.

We also investigated higher order multimeric structures. A C_4 -symmetrical tetrameric analogue of **A-1** based on cyclo(Lys-D-Ala)₄, **L-1** was synthesized³⁶ and tested for CD40 binding and B-lymphoma apoptosis (Fig. 6). However, **L-1** turned out to be less soluble than **A-1**. Although SPR binding data obtained at low concentration between 6 nM and 100 nM may be indicative of specific binding, the C_4 -symmetric ligand **L-1** was found to extensively aggregate above 200 nM under SPR conditions (see supporting information, Figure S1). Moreover, **L-1** was not able to induce significant apoptosis of B-

lymphomas at 10 μM . Overall these results together with those obtained with **J-1** and **K-1** support the view that C_3 -symmetry of the core structure and radial distribution of appended peptides are both determinants of the activity of CD40L mimetics.

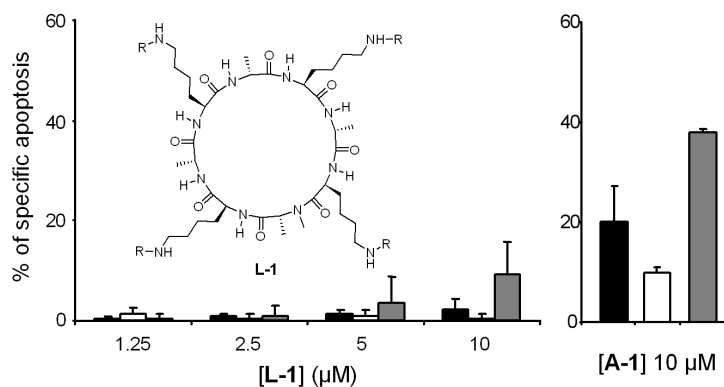
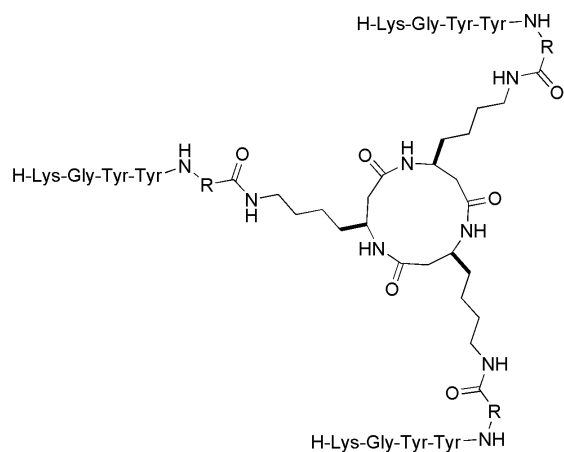


Figure 6. Tetrameric versus trimeric ligands. Percentage of specific apoptosis induced by **L-1** and **A-1** at the indicated concentrations after 16 h of incubation. Cells used in the assay are Human lymphoma cells BL41 (black) which express CD40, Jurkat cells (white) which do not express CD40 and Raji cells (grey bars) which express high level of CD40. Results are expressed as means \pm SEM of three independent experiments. Molecular structure of the tetravalent mimetic is shown in the inset.

Modulation of the linker portion. As discussed previously, the choice of an appropriate linker to connect the binding moieties in a multivalent system can be determinant. Rather than a rigid linker difficult to optimize, we opted for rather flexible oligomethylene or oligo(ethylene glycol) type spacers that we felt to be more appropriate to sample conformational space. In the crystal structure of the CD40L homotrimer, the distance between the alpha carbon ($^{\alpha}\text{C}$) of each hot-spot residues Lys¹⁴³ to Tyr¹⁴⁶ and the centroid of the equilateral triangle formed by the $^{\alpha}\text{C}$ of the three cognate residues in the trimer is comprised between 17 and 22 \AA . The α -amino group of the next residue in the sequence (Thr¹⁴⁷) is positioned ca 16 \AA apart from the centre of the trimer. When designing ligands based on scaffold **A**, the Ahx linker was originally selected to approach this distance. If one assumes that the

Lys(Ahx) side chain on the D,L-cyclohexapeptide core **A** adopts a fully extended conformation (~ 14.9 Å) as in the crystal structure of a related Ahx-Ahx peptide segment³⁹ and that the diameter of the core cyclohexapeptide is ~ 7.5 - 8 Å [based on the crystal structures^{34,35} of related cyclo(L-Val-D-Val)₃, cyclo(L-Phe-D-Phe)₃ and cyclo(*N*-MeLeu-D-Leu)₃], one can approximate the distance between the center of the core and the NH of the Ahx residue in **A-1** to a maximum value of ca 18-19 Å. The corresponding value in **B-1** should be smaller by ca 1.5 Å because of the smaller diameter of the 12-membered (β^3 -HLys)₃ core structure.^{37,40}

To investigate how the length and the nature of the linker can modulate the activity of CD40L mimetics, we have prepared a series of **B-1** variants (chart 3) with oligomethylene $[-(\text{CH}_2)_n-]$ tethers of length varying from $n = 3$ to $n = 7$ (Chart 3).



- | | |
|---|---|
| B-2 R = (CH ₂) ₃ (spacer Abu) | B-5 R = (CH ₂) ₇ (spacer Aoc) |
| B-3 R = (CH ₂) ₄ (spacer Apa) | B-6 R = (CH ₂) ₁₀ (spacer Aud) |
| B-1 R = (CH ₂) ₅ (spacer Ahx) | B-7 R = [(CH ₂ CH ₂ O)] ₂ -CH ₂ (spacer Ado) |
| B-4 R = (CH ₂) ₆ (spacer Ahp) | B-8 R = [(CH ₂ CH ₂ O)] ₄ -CH ₂ (spacer Ato) |

Chart 3.

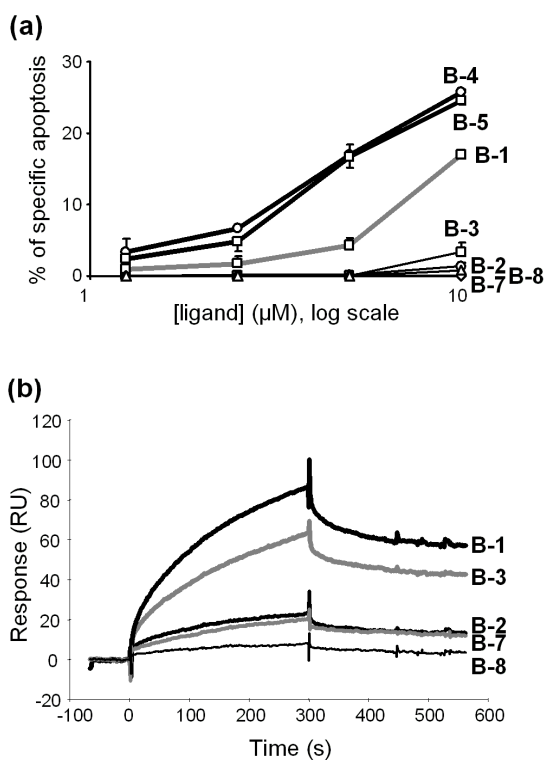


Figure 7. Influence of the length and nature of the linker. (a) Induction of apoptosis of human B-lymphoma BL41 cells. Percentage of specific apoptosis (see Experimental section) induced by the different mimetics at the indicated concentrations after 16 h of incubation. Results are expressed as means \pm SD of two independent experiments. (b) Direct binding to CD40 of **B-1** analogues at 200 nM as shown by SPR. Sensorgrams for **B-4** and **B-5** are not shown because of aggregation in the SPR conditions. All results are representative of at least two independent experiments.

Compound **B-2**, in which the oligomethylene chain is reduced by two carbons ($n = 3$), is no longer able to induce apoptosis of human B-lymphoma BL41 cells (Fig. 7a) and exhibits drastically reduced binding to CD40 (Fig. 7b). Significant binding to CD40 is retained when the length of the spacer is decreased by only one carbon (**B-3**), although its association rate is lower than for **B-1**, but the capacity to induce apoptosis is not restored. In contrast, analogues of **B-1** with one and two additional methylene groups (**B-4**, $n = 6$ and **B-5**, $n = 7$), respectively induced significantly higher levels of apoptosis compared to **B-1**. The finding that the level of apoptosis is considerably enhanced as the spacer length

increased from 3 to an optimal 6 carbon chain, and remains constant upon an additional increment in chain length from $n = 6$ to $n = 7$, is consistent with other studies.^{41,42} It has been shown previously, that in the case of flexible tethers, the effective molarity and potency are the highest for an optimal length and are only moderately affected by increments in chain length beyond this value.⁴² Unfortunately, aggregation of **B-4** and **B-5** under SPR conditions precluded their evaluation for binding to CD40. Further increments in chain length from the 7-carbon chain to the 10-carbon chain led to a compound (**B-6**) with even lower solubility that could not be evaluated in the two assays. To increase the water solubility of the ligands, we also explored modification of the spacer by substituting the saturated chain in **B-5** with a oligo(ethylene glycol) chain (EG_n) of similar length. This replacement resulted in a ligand (**B-7**) with dramatically reduced binding to CD40 and no apoptotic activity.. No improvement was observed upon increasing further the number of oligo(ethylene glycol) units (e.g. **B-8**).

Overall the data obtained with the β -peptide core structure **B** suggest that *n*-amino-alkanoic acids as tethers are superior to corresponding oligoethylene glycol amino acids to distribute the CD40-binding motif and that a minimum carbon chain length (e.g. $n = 5-7$) is required to ensure binding to CD40 and effector functions. This result may partially explained why ligands such as **F-1** and **H-1** based on TREN and isocyanurate failed to bind significantly to CD40 and to induce apoptosis of B-lymphoma cells. Even by assuming a fully extended conformation for the central core and the Ahx residue allowing a radial distribution of the CD40 binding motif, the distance between the center of the trimeric scaffold and the NH of the Ahx residue in **F-1** and **H-1** does not exceed 13 Å which is below the optimal 16 Å value.

The strong dichotomy observed between oligomethylene and oligo(ethylene glycol) tethers was not expected and its origin remains unclear. Such a differential behaviour has been documented previously in other systems including bivalent protein kinase C ligands⁴¹ and might result from significant conformational differences and/or from a different propensity to interact with the surface of proteins.

MiniCD40Ls based on conformationally restrained receptor binding motifs. To delineate the contribution to CD40 binding of each amino acid in the Lys-Gly-Tyr-Tyr sequence, we have previously prepared analogues of **B-1** singly substituted at each position by an alanyl (or glycyl) residue.²³ We found that Lys and both Tyr residues are critical to binding and effector functions, consistent with data obtained from site-directed mutagenesis studies using recombinant CD40L molecules.⁴³ However, the glycyl residue is quite permissive and can be substituted by Ala without major decrease in binding to CD40 and with no strong reduction in the apoptotic activity on lymphoma cells. Examination of the geometry of the AA'' loop in the crystal structure of CD40L reveals that the four residues of the Lys-Gly-Tyr-Tyr CD40 binding motif located at the top the loop adopt a β -turn type conformation centered on Gly¹⁴⁴ ($i+1$) and Tyr¹⁴⁵ ($i+2$) residues. The corresponding backbone torsion angle values ϕ_{i+1} , ψ_{i+1} and ϕ_{i+2} indicated on Figure 8 are close to values of an ideal reverse type II' β -turn [$\phi_{i+1} = +60^\circ (\pm 20^\circ)$, $\psi_{i+1} -120^\circ (\pm 20^\circ)$ and $\phi_{i+2} -80^\circ (\pm 20^\circ)$]. However, the precise conformation of the loop upon CD40 binding to CD40L remains to be elucidated.

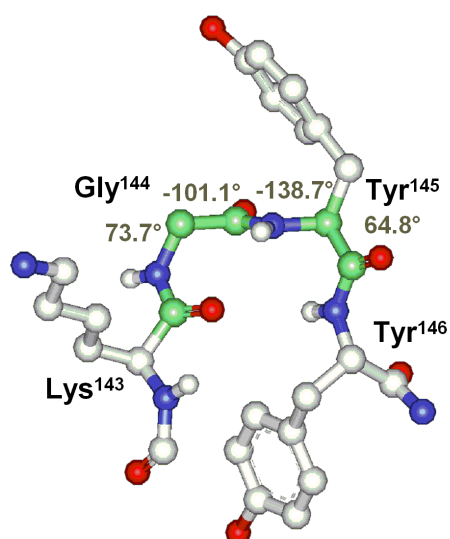


Figure 8. The reverse β -turn type conformation of the Lys¹⁴³-Gly-Tyr-Tyr¹⁴⁶ CD40-binding motif in the crystal structure of CD40L.²¹ The values of ϕ and ψ angles for residues $i+1$ (Gly¹⁴⁴) and $i+2$ (Tyr¹⁴⁵) are indicated.

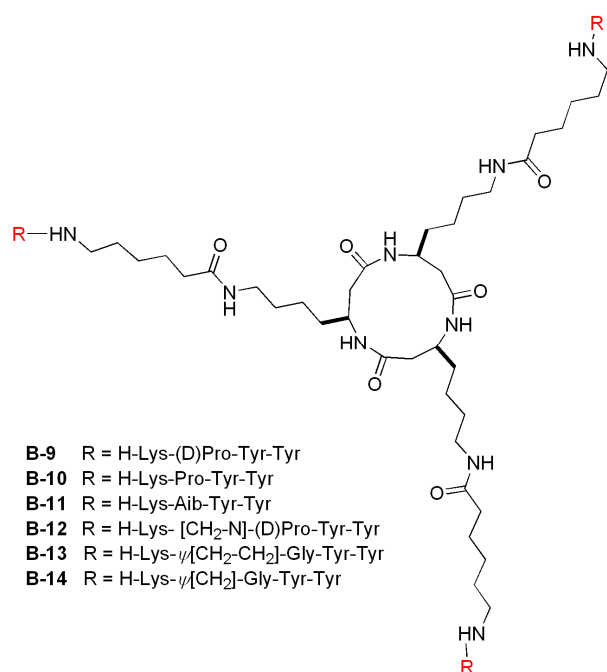


Chart 4.

To reduce the conformational space accessible to the glycyl residue and to approach the geometry of a reverse turn segment, we decided to introduce conformationally restricted amino acid residues such as D-Pro and Aib (α -amino isobutyric acid) which are known to facilitate β -turn conformations (chart 4).⁴⁴ Whereas favored (ϕ, ψ) angles for D-Pro ($+60^\circ, +30^\circ$ and $+60^\circ, -120^\circ$, respectively) are compatible with the requirements of the $i+1$ residue in both type I' and type II' β -turns, the (ϕ, ψ) space of Aib restricted to $(+60^\circ, +30^\circ)$ and $(-60^\circ, -30^\circ)$ values is compatible with type I and type I' β -turns. Interestingly, substituting D-Pro for Gly (**B-1** \rightarrow **B-9**) does not compromise binding to CD40 in SPR experiments. Analysis of kinetic data using the classical Langmuir monovalent model and local fittings revealed similar dissociation constants with K_D of 120 and 26 nM for **B-1** and **B-9**, respectively (see supporting information, Figure S2).⁴⁵ It is worth mentioning that the induction of apoptosis on human lymphoma cells was increased by this mutation, **B-9** being significantly more potent than **B-1** (Fig. 9).

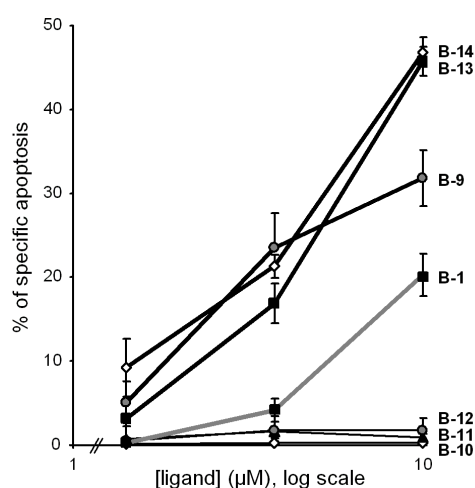
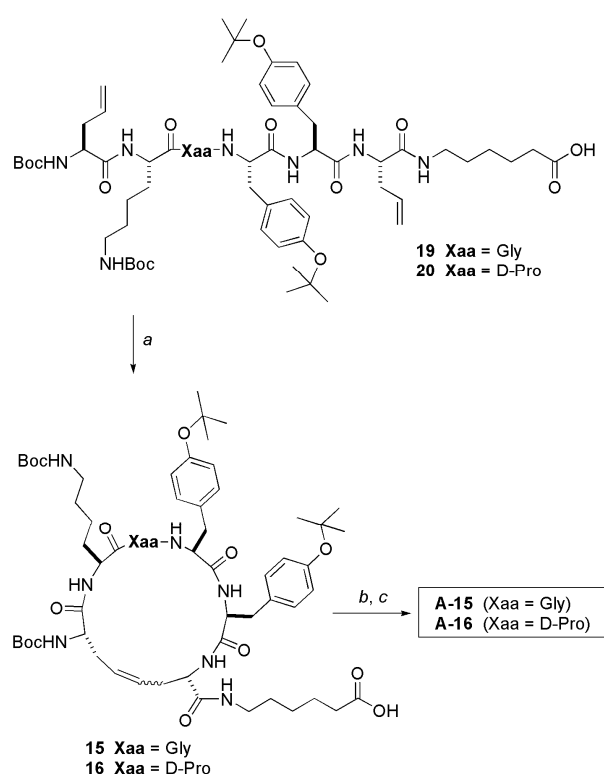


Figure 9. Induction of apoptosis of human B-lymphoma BL41 cells by analogues of **B-1** containing modifications in the CD40-binding motif. Percentage of specific apoptosis is shown at the indicated concentrations after 16 h of incubation. Results are expressed as means \pm SD of three independent experiments.

Preventing the possible formation of a reverse turn by substituting L-Pro for Gly (\rightarrow **B-10**) was detrimental for the apoptotic properties. Similarly, the insertion of an Aib residue at the $i+1$ position gave **B-11** which was not active on CD40 positive human lymphoma cells. Overall, these data give some hints about the bioactive conformation(s) of the Lys-Gly-Tyr-Tyr CD40-binding segment in *miniCD40Ls* and suggest possibilities to further modulate/optimize effector functions of *miniCD40Ls* using appropriate modifications centered on the Gly residue. The insertion of pseudopeptide bonds between i and $i+1$ residues to create local conformational perturbations that could eventually modulate the effector functions of *miniCD40Ls* **B-1** and **B-9** was also evaluated (chart 4). Whereas the introduction of a reduced peptide (methylene amino) bond $\psi(\text{CH}_2\text{N})$ was found to be detrimental for biological activity, analogues **B-13** and **B-14** with ethylene $\psi(\text{CH}_2\text{-CH}_2)$ and methylene $\psi(\text{CH}_2)$ bonds were significantly more potent than **B-1** in inducing apoptosis of CD40 positive B lymphoma cells. Noteworthy, in the Langmuir 1:1 model, **B-14** was found to bind CD40 with a K_D of 9 nM (see

supporting information, Figure S3). The introduction of a $\psi(\text{CH}_2)$ bond between Lys and Gly consists in the replacement of the Lys-Gly segment by a γ^{δ} -Lys residue. Similarly, substitution of γ -amino acid for α -amino acid residues in the central type-II' β -turn forming tetrapeptide fragment of octreotide, a potent analogue of somatostatin, led to the discovery of open-chain peptidomimetics with nanomolar affinities for certain human somatostatin receptor subtypes.⁴⁶



Scheme 3. *a* : Grubbs catalyst II; CH_2Cl_2 , 50°C , 7 days; *b* : **A-0** (0.3 equiv), BOP, DIEA, DMF, 24 h; *c* TFA/ H_2O (95:5)

Alternatively, the conformational space accessible to the linear receptor binding peptide can be dramatically reduced through cyclization. Ring-closing methathesis of fully protected linear hexapeptides **17** and **18** containing Lys-Gly-Tyr-Tyr and Lys-D-Pro-Tyr-Tyr epitopes and a free carboxylic acid tail, using Grubbs catalyst,⁴⁷ afforded cyclopeptides **15** and **16** ready for coupling onto triamine cores. The corresponding ligands **B-15** and **B-16** with cyclic CD40 binding segments were synthesized and

purified according to our general procedure and evaluated for binding to recombinant human CD40 by SPR and for effector functions. Although binding to CD40 was observed in direct SPR experiments (see supporting information, Figure S4),⁴⁸ **B-15** and **B-16** turned out to be inactive in the apoptotic assay (see supporting information, Figure S5). One can speculate that the loss of activity observed is associated with unwanted conformational changes and low population of a type II' β -turn conformation. Alternatively, the readily accessible and recently reinvestigated DL₄ cyclopentapeptide template could be used to enforce type II' β -turn conformation with the D-amino acid residue at the *i*+1 position.⁴⁹

Exploration of the CD40L surface: Mimetics based on a second CD40 binding motif. Molecular modeling experiments and X-ray crystal data, indicate that the surface area buried upon complexation of CD40L and CD40 is ca 850 Å² and is highly polar.²² Residues of CD40L in contact with CD40 are distributed over two CD40L molecules. Although the Lys-Gly-Tyr-Tyr loop motif from one subunit is critical for CD40L binding to CD40, site-directed mutagenesis studies have identified another hot spot region located on β -strand E and encompassing residues Arg²⁰³ and Arg²⁰⁷ (Figure 10).

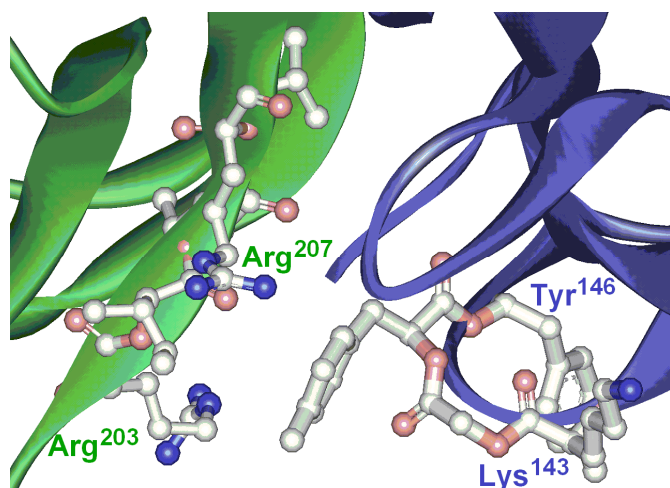


Figure 10. Part of the CD40 binding surface showing the relative positions of the putative CD40-binding sequences Lys¹⁴³-Gly-Tyr-Tyr¹⁴⁶ (AA" loop) and Arg²⁰³-Leu-Leu-Ile-Arg²⁰⁷ (β -strand E) selected for the construction of CD40L mimetics.

It has been suggested from site-directed mutagenesis and calculations that these positively charged side-chains (Lys¹⁴³, Arg²⁰³ and Arg²⁰⁷) can make contacts with oppositely charged residues on CD40, namely Glu⁶⁶, Glu⁷⁴, Asp⁸⁴, and Glu¹¹⁷ and that the resulting CD40-CD40L charged pairs Arg²⁰³-Glu⁷⁴, Arg²⁰⁷-Asp⁸⁴, Arg²⁰⁷-Glu¹¹⁷ have a net stabilizing effect on the complex. On the basis of distance considerations, calculation of desolvation energy and total electrostatic stabilization; the Arg²⁰³-Glu⁷⁴ pair (3.2 Å) was proposed to be the strongest salt bridge in the model. These data thus suggested to us that other sequences, derived from the second symmetry related subunit or combinations of sequences could in principle be used to design new CD40L mimetics. Two linear pentapeptide sequences mapping residues Gly¹⁹⁹ to Arg²⁰⁷ on loop DE and β -strand E and containing Arg²⁰³ (N- or C-terminal) were considered as possible CD40 binding units. The corresponding trimeric architectures were assembled on β -tripeptide core **B** with an Ahx linker and compared directly to *miniCD40L B-1* in SPR and cellular assays. The results are reported in Figure 11.

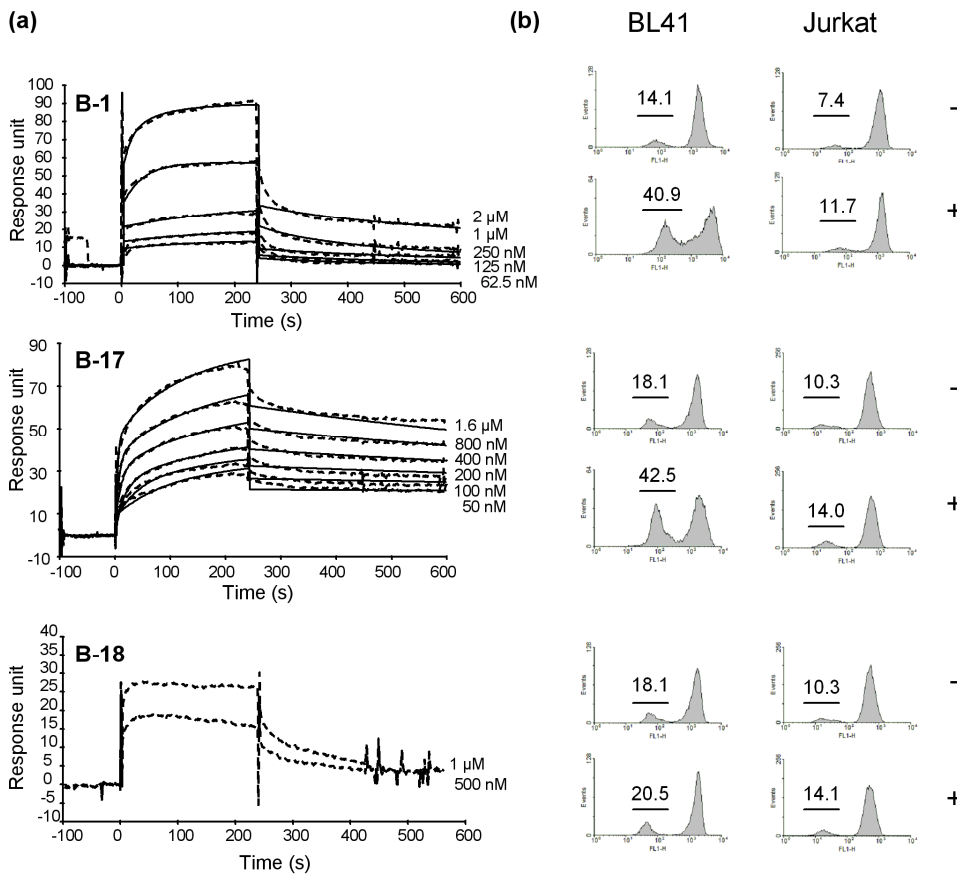


Figure 11. Comparison of miniCD40Ls with binding motifs derived from distinct CD40L hot spot regions (e.g. Lys¹⁴³-Gly-Tyr-Tyr¹⁴⁶ from the AA''loop (**B-1**), Arg²⁰³-Leu-Leu-Ile-Arg²⁰⁷ from β -strand E (**B-17**) and Gly¹⁹⁹-Arg-Phe-Ile-Arg²⁰³ from DE loop (**B-18**)). (a) Direct binding to CD40 at different concentrations of mimetics as shown by SPR. All results are representative of at least two independent experiments. Dashed lines represent experimental curves, straight lines fitting curves. (b) Induction of apoptosis of human B-lymphoma BL41 cells and human Jurkat CD40-negative cells after 16 h of incubation with 10 μ M of the different mimetics (+), or in culture medium alone (-). Results are representative of three independent experiments. Percentage of apoptotic cells is shown above the apoptotic left-peak on each histogram.

SPR measurements at different concentration (Fig. 11a) showed that compound **B-17** (R = H-Arg-Leu-Leu-Ile-Arg), but not **B-18** (R = H-Gly-Arg-Phe-Ile-Arg), binds significantly to CD40. Analysis of

kinetic data using the Langmuir 1:1 model and local fittings gave an mean K_D of 4.4 nM for **B-17** (vs 120 nM for **B-1**). Like for **B-1**, local fitting using a trivalent model gave lower χ^2 values (0.54 versus 7.5 for the langmuir 1:1 model and 2:1 for a divalent model), supporting binding in a trivalent manner. Interestingly, **B-17** was also found to be as potent as **B-1** in inducing apoptosis of human lymphoma B-cells (42.5 % apoptosis versus 40.9 % at 10 μ M after 16h of treatment, Fig 11b). Preliminary data also indicate that **B-17** like **B-1** is effective in inducing the maturation of the D1 dendritic cell line (data not shown). Overall, these biochemical and biological data underscore further the versatility of rigid and planar α - and β -cyclopeptide based scaffolds **A** and **B** for the design of *miniCD40Ls*.

Conclusion.

Molecules with multiple copies of a recognition motif appended to a central scaffold have unique properties that differ from that of monovalent compounds. In particular, designed multivalent systems can mediate cell-surface receptor oligomerization and display effector functions.¹² *MiniCD40Ls* are relatively small (< 3 kDa) rationally designed synthetic multimeric architectures that mimic, both *in vitro*²³ and *in vivo*²⁵, the effects of CD40L, a non covalent homotrimeric protein belonging to the TNF superfamily. Because they are chemically defined and tunable, synthetic multivalent ligands are very attractive molecules to delineate molecular determinants of effector functions and to control receptor assembly in signal transduction.¹² Our data are consistent with C_3 -symmetry and radial distribution of the CD40-binding motif being two essential features leading to mimetics with effector functions. The distance between the center of the scaffold and the binding moiety is also a critical element of the design. Flat cyclic peptides of 5-8 Å diameter (e.g. **A** and **B**) with side arms linked to flexible oligomethylene spacers are very versatile systems for trivalent display of CD40-binding motifs.⁵⁰ For example, *miniCD40Ls* **B-1** and **B-17** which utilize distinct CD40-binding elements, namely Lys¹⁴³-Tyr¹⁴⁶ on loop AA' and Arg²⁰³-Arg²⁰⁷ on β -strand E have the same trimeric scaffold-linker combination (Ahx)₃-**B**. Examination of the crystal structure of homotrimeric CD40L²¹ shows however that the two equilateral triangles whose vertices are formed by the three α -amino groups of the residue immediately

following Tyr¹⁴⁶ and Arg²⁰⁷ (Thr¹⁴⁷ and Ala²⁰⁸ respectively) largely differ in size, with centroid to vertex distances of ca 16 Å and 10 Å, respectively (Figure 12).

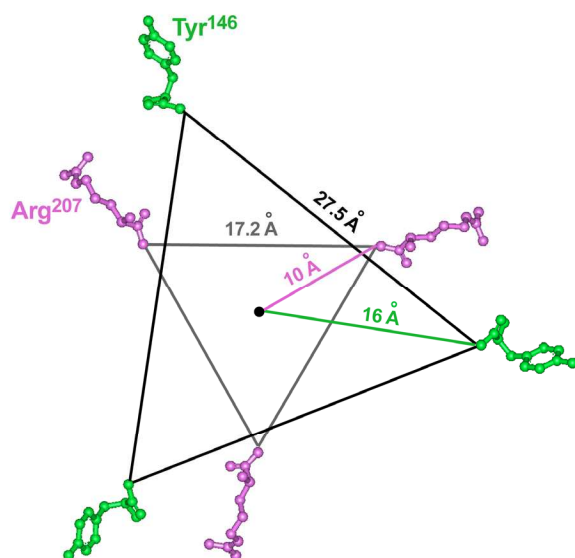


Figure 12. Schematic representation of the two equilateral triangles whose vertices are formed by α -amino groups of residues immediately following Tyr¹⁴⁶ (green) and Arg²⁰⁷ (pink) according to the X-ray crystal coordinates of homotrimeric CD40L.²¹ Distances from centroid to vertex are indicated.

Although this observation underscores the versatility of the (Ahx)₃-**B** system, it also suggests that, a scaffold-linker combination consisting of a shorter linker or a smaller scaffold (e.g. heterocyclic) could be considered in principle to tether the Arg²⁰³-Arg²⁰⁷ binding moiety.

All TNF superfamily members share the same overall topology and are active as homotrimers. Thus, one can conceive that a general approach based on the use of peptide templates **A** and **B** could be transposable to other TNF family members. While this work was in progress, researchers at Genentech reported peptide sequences that specifically bind to the human DR5 (hDR5), one of the signaling receptors for TNF related apoptosis-inducing ligand (TRAIL).⁵¹ Interestingly, oligomeric forms were generated by fusion of these peptides to leucine zipper variants that form either dimers, trimers or tetramers.⁵² Avidity to hDR5 was significantly improved through trimerization or tetramerization of

the DR5-binding peptide. However, only the tetrameric form was found to display a significant cytotoxic activity. These results which confirm that peptide scaffolding on multivalent core structures is a viable approach to generate *miniTNFs*, also expand the set of eligible multimeric architectures. It is worth mentioning that self-organization into non covalent homotrimers with C_3 -symmetry axis is not limited to TNF family members and is also a structural feature of unrelated proteins such as TNF receptor-associated factor (TRAF),⁵³ collectins (e.g. mannan binding lectins (MBLs), surfactant proteins SP-A and SP-D),⁵⁴ members of the C1q family⁵⁵ or adenovirus fiber head, (knob domain), emanating from the vertices of the icosahedral capsid.⁵⁶ It remains to be seen whether these protein trimers could also be mimicked with trimeric architectures such as those reported here.

By signaling through CD40, CD40L plays an active role in a variety of immune responses, allowing B-cell to differentiate, proliferate and isotype class switch, activating antigen presenting cells (e.g. dendritic cells) and mediating T-cell help for cytotoxic T lymphocytes.. Therefore, small molecule CD40L mimetics could be potentially useful as immunopotentiators. TNF family ligands are type II transmembrane proteins with an extracellular, homotrimeric C-terminal TNF homology domain that is frequently released as a soluble cytokine upon proteolytic processing. However, receptor trimerization of TNFR superfamily members by their soluble ligands is not always sufficient to reach the activation threshold. In particular, full activation of CD40 which leads to B-cell proliferation and isotype switching requires higher order receptor oligomerization. This is typically achieved by membrane-bound CD40L, but also by cross-linking with antibodies or by using artificial fusion proteins consisting of multiple copies (two or four) of CD40L trimers.⁵⁷ By analogy, it is tempting to speculate that similar synergistic effects could be generated through multivalent display of *miniCD40Ls*. CD40L mimetics disclosed in this work together with their higher order multimeric versions would certainly constitute a unique set of probes to investigate the relationship between receptor oligomerization and cell signal transduction. This possibility will be addressed in future extension of this work.

Experimental Section.

Synthesis of ligands. See Supporting Information.

Biological Reagents. Recombinant soluble human CD40-mouse Ig fusion protein (rshCD40:mIg) and recombinant soluble human CD40L coupled to the mouse CD8- α extracellular domain (rshCD40L:mCD8) were purchased from Ancell corporation (Bayport, MN). Surfactant P20 was purchased from Biacore AB (Uppsala, Sweden). The 3,3'-dihexyloxycarbocyanine iodide DiOC₆(3) dye was purchased from Interchim (Montluçon, France). Fluorescein isothiocyanate (FITC)-conjugated anti-mouse CD40 (3/23 clone), FITC anti-human CD40 (5C3 clone), phycoerythrin (PE) anti-mouse CD54 (3E2 clone), PE anti-mouse CD80 (16-10A1 clone) and PE anti-mouse CD86 (GL1 clone) mAbs were purchased from Pharmingen (San Jose, CA). Low endotoxin recombinant mouse granulocyte/macrophage colony-stimulating factor (rmGM-CSF) was purchased from USBiological (Swampscott, MA).

Surface plasmon resonance (SPR) analysis. BIAcore™ 3000 (Biacore AB) was used to evaluate the binding of CD40L mimetics to CD40. Flow cells of a CM5 sensor chip (Research Grade, Biacore AB) were precoated with rabbit polyclonal antibodies directed against mouse immunoglobulin (Ig) domain (RAM-Ig, Biacore AB) using amine coupling at 30 μ g/mL in 10 mM acetate buffer, pH 5.5 according to the manufacturer's instructions. The chip was then flushed with 1 M ethanolamine hydrochloride pH 8.5 (Biacore AB) and 50 mM HCl to eliminate unbound antibody. Generally *ca* 10,000 RU, corresponding to 10 ng/mm², of RAM-Ig were immobilized. Biosensor assays were performed at 25 °C with HBS-EP buffer [10 mM HEPES (pH 7.4), containing 0.15 M NaCl, 3.4 mM EDTA and 0.005% v/v surfactant P20] as running buffer. Capture of rshCD40:mIg and of LG11-2, a mouse IgG2a mAb directed against H2B histone used as irrelevant control (purified by protein G affinity chromatography from hybridoma supernatant), was performed on individual flow cells at a flow rate of 5 μ L/min and at a concentration allowing to achieve equivalent protein mass binding. A small amount of protein was captured, *ca* 450 response units (RU), sufficient for the detection of the binding of the CD40 ligands, and limiting the mass transport and rebinding artefacts.

CD40L mimetics and rshCD40L:mCD8 were then injected (kinetic mode) at a flow rate of 30 μ L/min over the control and CD40 channels for 4 min and allowed to dissociate for an additional 3 min. The flow cells were regenerated for 30 s with 50 mM HCl. A 1 Hz acquisition mode was sufficient for subsequent good assessment of kinetic constants. Control sensorgrams were subtracted from the CD40 ones and analyzed by BIAevaluation 4.1 with various models.

The simplest "Langmuir 1:1" model was first used to assess the binding kinetics of the interaction. A complete description of equations used for kinetics data determination can be found in the Biacore AB

Handbook and is summarized in supplementary materials. The trivalent analyte model (37, 38) was also used to evaluate the stoichiometry and to get some details on the mechanism of the binding, in particular the distinct rates for all binding and conformational change events, but due to complexity of the equations and the limited integrative possibilities offered by the BIAevaluation software, cooperativity was assessed with the R_{eq} values from a trivalent model with freedom in the determination of the association and dissociation rate constants of the first interaction, and the R_{max} value as well as all other rate constants globally processed for the sets of concentrations of the CD40-ligands.

Accuracy of the fits was measured by the *Chi square* (χ^2) value, which evaluates the deviation of the fitted model from the experimental points. Residuals were also shown to give better insight whether a model is accurate as the bandwidth and its shape reveal the differences between the fitted curve and the experimental data.

Surface plasmon resonance (SPR) analysis; summary of the equations used for the determination of the kinetics data. The simplest model, the Langmuir 1:1 one, was first used to assess the binding kinetics of the interaction. In the further equations, L denotes the ligand captured on the immobilized rabbit anti-mouse Ig, in our case the receptor CD40, and A denotes the analyte injected on the chip, that is either of the CD40L or *miniCD40Ls*. When A interacts with L forming the LA complex due to diffusion, collision and binding, in function of time with the association rate constant k_a ($M^{-1} s^{-1}$), but can also disappear with dissociation rate constant k_d (1/s) to release A from L (Eq. 1).



Equilibrium is reached when the rate of association (Eq. 2) equals the rate of dissociation, that is when the number of dissociation events compensates the number of association events.

$$\frac{d[LA]}{dt} = k_a[L][A] - k_d[LA] \quad (2)$$

In our conditions, equilibrium can not be reached at the end of the injection phase, but values at equilibrium could be extrapolated, especially the dissociation constant K_D (M), using the kinetic values obtained from the individual experimental curves of the association and dissociation phases (Eq. 3).

$$\frac{[L][A]}{[LA]} = \frac{k_d}{k_a} = K_D \quad (3)$$

Rewriting Eq. 2 in terms of concentration and responses, we obtain Eq. 4.

$$\frac{dR}{dt} = k_a C(R_{\max} - R_t) - k_d R_t \quad (4)$$

In Eq. 4, R_t corresponds to the response signal of the formed complex at t time, C represents the concentration of CD40-ligands and R_{\max} the maximal feasible response signal, depending on the total CD40 binding capacity (or activity) on the sensor chip. In this case we assume that free ligand equals maximal capacity minus bound receptor.

The data extracted from the experimental curves as well as the known input parameters are used by the algorithm and assessed by numerical integration to calculate the different parameters needed. One can then determine the values for signal response at equilibrium (R_{eq}), that is for t value tending to infinite, from the kinetic constants and the R_{\max} calculated parameter (Eq. 5).

$$R_{\text{eq}} = \frac{k_a \text{Conc} \times R_{\max}}{k_a \text{Conc} + k_d} \quad (5).$$

Culture of lymphoma cells and measurement of apoptosis. BL41 Burkitt lymphoma and Jurkat human T leukemia cells were cultured in RPMI 1640 (Cambrex Bioscience, Verviers, Belgium) supplemented with 10% of heat-decomplemented fetal bovine serum (FBS; Dominique Dutscher, Brumath, France) and gentamicin (10 $\mu\text{g}/\text{mL}$, Cambrex). For apoptosis assays, cells (5×10^5 cells/mL) were incubated at 37 °C in flat-bottom 96-well plates at the indicated times and concentrations in the presence of various *miniCD40Ls* in 200 μL of complete medium. After incubation, cells were washed with phosphate-buffered saline (PBS) and apoptosis was evaluated by measurement of a decrease in mitochondrial transmembrane potential ($\Delta\psi_m$) associated with a reduction of the cationic dye DiOC₆(3) uptake, as detected by flow cytometry. Cells were resuspended in 300 μL of PBS containing 20 nM of DiOC₆(3) and incubated at 37 °C for 20 min ant then directly analyzed by flow cytometry.

Results are expressed as the percentage of specific apoptosis according to the following formula: % of specific apoptosis = 100(% apoptotic treated cells - % spontaneous apoptotic control cells)/(100 - % spontaneous apoptotic control cells).

Culture and maturation of D1 mouse dendritic cells. D1 cells have been described as a MHC class II-positive growth factor-dependent immature dendritic cells, derived from adult mouse spleen maintained in lineage without being transformed. Cells were cultured in non-treated plastic dishes IMDM with HEPES and L-glutamine (Cambrex), supplemented with 10% of heat-decomplemented FBS, gentamicin (10 $\mu\text{g}/\text{mL}$), 10 μM β -mercaptoethanol, and 10 ng/mL of rmGM-CSF. For cellular

assays, 2×10^5 cells/mL were cultured for 24 h in 24-well untreated polystyrene microplates (Evergreen Scientific, Los Angeles, CA). Then, fresh medium containing the various *miniCD40Ls* was added. After an additional 24 h of incubation, cells were washed with cold PBS and harvested with 2 mL of PBS containing 2 mM EDTA. After centrifugation, cells were resuspended in cold PBS and analyzed for cell surface phenotyping by flow cytometry.

Flow cytometry analysis. For measurement of apoptosis, lymphoma cells were analyzed directly after the staining procedure. For phenotyping, D1 cells were stained in PBS containing 2% FBS at 4 °C for 20 min with the various antibodies used at concentration recommended by the manufacturer. After two washes in PBS, cells were analyzed by flow cytometry with a FACSCalibur[®]. At least 1×10^5 events were acquired for each experiment using CellQuest version 3.3 (Becton Dickinson, Pont de Claix, France) and the data were processed with WinMDI version 2.8 freeware (Joseph Trotter, Scripps Research Institute, <http://facs.scripps.edu/software.html>).

Acknowledgment. This work was supported by the CNRS, the Ministère de la Recherche (ACI « Jeunes Chercheurs »), « La Ligue contre le Cancer » and INCA. WS was supported by the Ministère de la Recherche and the Fondation pour la Recherche Médicale (FRM). NT was supported by « La Ligue contre le Cancer ». SW was supported by grants from the Ministère de la Recherche and from the Fondation pour la Recherche Médicale. We thank N. Bonnefoy-Berard and M. Flacher for providing the lymphoma cells, C.J.M. Melief for providing the dendritic cell line D1, M. Monestier for providing the LG11-2 hybridoma. The authors acknowledge O. Reinaud for a generous gift of calix[6]triamine **D-0**.

Supporting Information Available. Detailed procedures and characterization data of all ligands additional surface plasmon resonance (SPR) sensorgrams. This material is available free of charge via internet at <http://pubs.acs.org>.

References

- (1) For review, see : (a) Davis, J. M.; Tsou, L. K.; Hamilton, A. D. *Chem Soc Rev.* **2007**, *36*, 326-334; (b) Zhao, L; Chmielewski, J. *Curr. Opin. Struct. Biol.* **2005**, *15*, 31-34; (c) Arkin, M. R.; Wells, J. A. *Nature Rev. Drug Discov.* **2004**, *3*, 301-317. (d) Pagliaro, P.; Felding, J.; Audouze, K.; Nielsen, S. J., Terry, R. B.; Krog-Jensen, C.; Butcher, S. *Curr. Opin. Chem. Biol.* **2004**, *8*, 442-449. (e) Berg, T. *Angew. Chem. Int. Ed.* **2003**, *42*, 2462-2481; *Angew. Chem.* **2003**, *115*, 2566-2586. (f) Toogood, P. L. *J. Med. Chem.* **2002**, *45*, 1543-1558. (g) Peczuh, M. W.; Hamilton, A. D. *Chem. Rev.* **2000**, *100*, 2749-2494. (h) Cochran, A. G. *Chem. Biol.* **2000**, *7*, R85-R94.

- (2) (a) Austin, D. J.; Crabtree, G. R.; Schreiber, S. L. *Chem Biol.* **1994**, *1*, 131-6; (b) Klemm, J. D.; Crabtree, G. R.; Schreiber, S. L. *Annu. Rev. Immunol.* **1998**, *16*, 569-592.
- (3) (a) Heldin, K. -H. *Cell* **1995**, *80*, 214-223; (b) Heldin, C. H.; Ostman, A. *Growth Factor Rev.* **1996**, *7*, 3-10.
- (4) (a) Schlessinger, J. *Cell* **2000**, *103*, 211-225; (b) Lemmon, M. A.; Schlessinger, J. *Methods Mol. Biol.* **1998**, *84*, 49-71.
- (5) (a) Germain, R. N. *Curr. Biol.* **1997**, *7*, R640-644; (b) Alarcón, B.; Swamy, M.; van Santen, H. M.; Schamel, W. W. A. *Embo reports* **2006**, *7*, 490-495.
- (6) (a) Ozinsky, A.; Underhill, D. M.; Fontenot, J. D.; Hajjar, A. M.; Smith, K. D.; Wilson, C. B.; Schroeder, L.; Aderem, A. *Proc. Natl. Acad. Sci. USA* **2000**, *97*, 13766-13771; (b) Choe, J.; Kelker M. S.; Wilson, I. A. *Science* **2005**, *309*, 581-585; (c) Kirk, P.; Bazan, J. *Immunity*, **2005**, *23*, 347-350.
- (7) (a) Bouvier, M.; *Nature Rev. Neurosci.* **2001**, *2*, 274-286 ; (b) George, S. R.; O'Dowd, B. F.; Lee, S. P.; *Nature Rev. Drug Discov.* **2002**, *1*, 808-820; (c) Park, P. S.; Filipek, S.; Wells, J. W.; Palczewski, K.; *Biochemistry* **2004**, *43*, 15643-15656; (d) Prinster, S. C.; Hague, C.; Hall, R. A. *Pharmacol. Rev.* **2005**, *57*, 289-298; (e) Bulenger, S.; Marullo, S.; Bouvier, M.; *Trends Pharmacol Sci.* **2005** *26*, 131-137.
- (8) For early examples of carbohydrate-based multivalent inhibitors (glycopolymers and glycodendrimers) of influenza virus hemagglutinin binding to host cells, see: (a) Spaltenstein, A.; Whitesides, G. M. *J. Am. Chem. Soc.* **1991**, *113*, 686-687. (b) Sabesan, S.; Duus, J. O.; Domaille, P. Kelm, S. Paulson, J. C. *J. Am. Chem. Soc.* **1991**, *113*, 5865-5866. (c) Gamian, A.; Chomik, M.; Laferriere, C. A.; Roy, R. *Can. J. Microbiol.* **1991**, *37*, 233-237. (d) Kingery-Wood, J. E.; Williams, K. W.; Sigal, G. B.; Whitesides G. M. *J. Am. Chem. Soc.* **1992**, *114*, 7303-7305; (e) Sparks, M. A.; Williams, K. W.; Whitesides, G. M. *J. Med. Chem.*; **1993**; *36*, 778-783; (f) Roy, R.; Pon, R. A.; Tropper, F. D.; Andersson, F. O.; *J. Chem. Soc., Chem. Commun.* **1993**, 264-265; (g) Roy, R.; Zanini, D.; Meunier, S. J.; Romanowska, A. *J. Chem. Soc., Chem. Commun.* **1993**, 1869-1872.
- (9) For early examples of bivalent opioid ligands, see (a) Portoghese, P. S. *J. Med. Chem.* **2001**; *44*, 2259-2269; (b) Erez; M.; Takemori, A. E. ; Portoghese, P. S. *J. Med. Chem.* **1982**, *25*, 847-849. Portoghese, P. S.; Larson, D. L.; Sayre, L. M.; Yim, C. B.; (c) Ronsisvalle, G.; Tam, S. W.; Takemori, A. E. *J. Med. Chem.* **1986**, *29*, 1855-1861.
- (10) Choi, S. K. *Synthetic Multivalent Molecules: Concepts and Biochemical Applications*, Wiley-Interscience, Hoboken, NJ. 2004
- (11) For reviews see : (a) Mammen, M.; Choi, S.-K.; Whitesides, G. M. *Angew. Chem. Int. Ed.* **1998**, *37*, 2755-2794. (b) Kiessling, L. L.; Gestwicki, J. E.; Strong, L. E. *Curr. Opin. Chem. Biol.* **2000** *4*, 696-703. (c) Kiessling, L. L.; Pohl, N. L. *Chem. Biol.* **1996**, *3*, 71-77.
- (12) For review, see: Kiessling, L. L.; Gestwicki, J. E.; Strong, L. E.; *Angew. Chem. Int. Ed. Engl.* **2006**, *45*, 2348-68.
- (13) Selected examples : (a) Gestwicki, J. E.; Strong, L. E.; Kiessling, L. L. *Chem. Biol.* **2000**, *7*, 583-91. (b) Gestwicki J. E.; Kiessling, L. L. *Nature* **2002**, *415*, 81-84; (c) Kramer, R. H.; Karpen, J. W. *Nature* **1998**, *395*, 710-713. (d) Pattarawarapan, M.; Reyes, S.; Xia, Z.; Zaccaro, M.C.; Saragovi, H.U.; Burgess, K. *J. Med. Chem.* **2003**, *46*, 3565-3567.
- (14) Reviews on small molecule cytokine mimetics : (a) Whitty, A.; Borysenko, C. W. *Chem. Biol.* **1999**, *6*, R107-R118; (b)
- (15) (a) Wrighton, N.C.; Farrell, F.X.; Chang, R.; Kashyap, A.K.; Barbone, F.P.; Mulcahy, L.S.; Johnson, D.L.; Barrett, R.W.; Jolliffe, L.K.; Dower, W.J. *Science* **1996**, *273*, 458-463; (b) Livnah, O.; Stura, E.A.; Johnson, D.L.; Middleton, S.A.; Mulcahy, L.S.; Wrighton, N.C.; Dower, W.J.; Jolliffe, L.S.. Wilson, I.A. *Science* **1996**, *273*, 464-471; (c) Johnson, D.L.; Farrell, F.X.; Barbone, F.P.; McMahon, F.J.; Tullai, J.; Kroon, D.; Freedy, J.; Zivin, R.A.; Mulcahy, L.S.; Jolliffe, L.K. *Chem. Biol.* **1997**, *4*, 939-950. (d)

- Cwirla, S.E.; Balasubramanian, P.; Duffin, D.J.; Wagstrom, C.R.; Gates, C.M.; Singer, S.C.; Davis, A.M.; Tansik, R.L.; Mattheakis, L.C.; Boytos, C.M.; Schatz, P.J.; Baccanari, D.P.; Wrighton, N.C.; Barrett, R.W.; Dower, W.J. *Science* **1997**, *276*, 1696-1699. (e) Qureshi, S.A.; Kim, A.M.; Konteatis, Z.; Biazzo, D.E.; Motamedi, H.; Rodrigues, R.; Boice, J.A.; Calaycay, J.R.; Bednarek, M.A.; Griffin, P.; Gao, Y.-D.; Chapman, K.; Mark, D.F. *Proc. Natl. Acad. Sci. USA* **1999**, *12*, 12156-12161; (f) Goldberg, J.; Jin, Q.; Ambroise, Y.; Satoh, S.; Desharnais, J.; Capps, K.; Boger, D.L. *J. Am. Chem. Soc.* **2002**, *124*, 544-555; (g) Tian, S.-S.; Lamb, P.; King, A.G.; Miller, S.G.; Kessler, L.; Luengo, J.I.; Averill, L.; Johnson, R.K.; Gleason, J.G.; Pelus, L.M.; Dillon, S.B.; Rosen, J. *Science* **1998**, *281*, 257-259.
- (16) (a) Bodmer, J.L.; Schneider, P.; Tschopp, J. *Trends Biochem. Sci.* **2002**, *27*, 19-26; (b) Locksley, R.M.; Killen, N.; Lenardo, M.J. *Cell* **2001**, *104*, 487-501.
- (17) For reviews, see: (a) van Kooten C., Banchereau, J. CD40-CD40 ligand. *J. Leuk. Biol.*, **2000**, *67*, 1-17; (b) Diehl, L.; Den Boer, A. T.; van der Voort, E. I.; Melief, C. J.; Offringa, R.; Toes, R. E. *J. Mol. Med.* **2000**, *78*, 363-371; (c) Grewal, I.S.; Flavell, R.A. *Annu. Rev. Immunol.* **1998**, *16*, 111-135. (d) Van Kooten, C.; Banchereau, J. *Adv. Immunol.* **1996**, *61*, 1-77; (e) Grewal, I. S.; Flavell, R.A. *Immunol. Today* **1996**, *17*, 410-414; (f) Noelle, R.J. *Immunity* **1996**, *4*, 415-419.
- (18) (a) Howard, L. M.; Miga, A. J.; Vanderlugt, C. L.; Dal Canto, M. C.; Laman, J. D.; Noelle, R. J.; Miller, S. D. *J Clin Invest.* **1999**, *103*, 281-290; (b) Kirk, A. D. et al. *Nat. Med.* **1999**, *5*, 686-693.
- (19) Phase I/II studies in humans with lupus nephritis or multiple sclerosis revealed significant immunomodulatory effects of anti-CD40L monoclonal antibody treatment. However, because of some thromboembolic complications in early clinical trials, further human studies with anti-CD40L antibody have been temporary halted and future clinical use is uncertain. See comment in : Couzin J. *Science* **2005**, *307*, 1712-1715
- (20) Peptide antitumour vaccine
- (21) Karpusas, M.; Lucci, J.; Ferrant, J.; Benjamin, C.; Taylor, F.R.; Strauch, K.; Garber, E.; Hsu, Y.M. *Structure* **2001**, *9*, 421-429.
- (22) Singh, J.; Garber, E.; Van Vlijmen, H.; Karpusas, M.; Hsu, Y.M.; Zheng, Z.; Naismith, J.; Thomas, D. *Protein Science* **1998**, *7*, 1124-1135.
- (23) (a) Fournel, S.; Wieckowski, S.; Sun, W.; Trouche, N.; Dumortier, H.; Bianco, A.; Chaloin, O.; Habib, M.; Peter, J.-C.; Schneider, P.; Vray, B.; Toes, R. E.; Offringa, R.; Melief, C. J. M. ; Hoebeke, J.; Guichard, G.. *Nature Chem. Biol.* **2005** *1*, 377-382; (b) Bianco, A.; Fournel, S.; Wieckowski, S.; Hoebeke, J.; Guichard, G. *Org. Biomol. Chem.* **2006**, *4*, 1461-1463.
- (24) S. G Hymowitz, S. G.; Ashkenazi, A. *Nature Chem. Biol.* **2005** *1*, 353 – 354; (b) Gibson S. E.; Castaldi, M. P. *Angew Chem Int Ed Engl.* **2006**, *45*, 4718-4720.
- (25) Habib, M.; Chamekh, M.; Noval Rivas, M.; Wieckowski, S; Sun, W.; Bianco, A.; Trouche, N.; Chaloin, O.; Dumortier, H.; Goldman, M.; Guichard, G.; Fournel, S.; Vray, B. *J. Immunol.* **2007**, in press.
- (26) Castro, B.; Dormoy, J. R.; Evin, G.; Selve, C. *Tetrahedron Lett.* **1975**, 1219-1222.
- (27) Gestwicki, J. E.; Cairo, C. W.; Strong, L. E.; Oetjen, K. A.; Kiessling, L. L. *J. Am. Chem. Soc.* **2002**, *124*, 14922-14933. ...
- (28) Schuurhuis, D. H.; Laban, S.; Toes, R. E. M.; Ricciardi-Castagnoli, P.; Kleijmeer, M. J.; van der Voort, E. I. H. Rea, D.; Offringa, O.; Geuze, H. J.; Melief, C. J. M.; Ossendorp, F.. *J. Exp. Med.* **2000**, *192*, 145-150.
- (29) B-lymphoma cells undergo apoptosis upon engagement of CD40 by recombinant CD40L. See: Frisan, T.; Donati, D.; Cervenak, L.; Wilson, J.; Masucci, M. G.; Bejarano, M. T. *Int. J. Cancer*, **1999**, *83*, 772-779.

- (30) Bong, D. T.; Clark, T. D.; Granja, J. R.; Ghadiri, M. R. *Angew. Chem. Int. Ed.* **2001**, *40*, 988-1011 and references therein.
- (31) Gac, S.; Zeng, X.; Reinaud, O.; Jabin, I. *J. Org. Chem.* **2005**, *70*, 1204-1210.
- (32) For use of calixarenes as templates for the recognition of protein surfaces, see : a) Baldini, L.; Casnati, A.; Sansone, F.; Ungaro, R. *Chem Soc Rev.* **2007**, *36*, 254-266. Park, H. S.; Lin Q.; Hamilton, A. D. *Proc Natl Acad Sci U S A.* **2002**, *99*, 5105-5109; b) Blaskovich, M. A.; Lin, Q.; Delarue, F. L.; Sun, J.; Park, H. S.; Coppola, D.; Hamilton, A. D.; Sebt, S. M. *Nat Biotechnol.* **2000**, *18*, 1065-1070; c) Park, H. S.; Lin, Q.; Hamilton, A. D. *J. Am. Chem. Soc.* **1999**; *121*, 8-13.
- (33) In the case of **A-1**, SPR data fit better with a trivalent model than with the classical "Langmuir 1:1" monovalent one [χ^2 values which indicate the accuracy of the fits are 0.43 and 0.85, respectively] suggesting that this interaction is of one *miniCD40L* for three CD40 receptors stoichiometry. Wieckowski, S.; Trouche, N.; Chaloin, O.; Guichard, G.; Fournel, S.; Hoebeke, J. *Biochemistry*, **2007**, *46*, 3482-3493.
- (34) For studies on partially *N*-alkylated C_3 -symmetric cyclic D,L-hexapeptides structures, see (a) Tomasi, L.; Lorenzi, G. P. *Helv. Chim. Acta* **1987**, *70*, 1012-1016. (b) Saviano, M.; Lombardi, A.; Pedone, C.; Di Blasio, B.; Sun, X. C.; Lorenzi, G. P. *J. Incl. Phenom.* **1994**, *18*, 27-36. (d) Sun, X. C.; Lorenzi, G. P. *Helv. Chim. Acta* **1994**, *77*, 1520-1526.
- (35) For crystal structures of cyclo(L-Val-D-Val)₃ and cyclo(L-Phe-D-Phe)₃, hexapeptides see: Pavone, V.; Benedetti, E.; Di Blasio, B.; Lombardi, A.; Pedone, C.; Tomasich, L.; Lorenzi, G. *Biopolymers*, **1989**, *28*, 215-223.
- (36) For studies on cyclic D,L-octapeptides, see: (a) Ghadiri, M. R.; Granja, J. R.; Milligan, R. A.; McRee, D. E.; Khazanovich, N. *Nature* **1993**, *366*, 324-327. (b) Khazanovich, N.; Granja, J. R.; McRee, D. E.; Milligan, R. A.; Ghadiri, M. R. *J. Am. Chem. Soc.* **1994**, *116*, 6011-6012. (c) Hartgerink, J. D.; Granja, J. R.; Milligan, R. A. Ghadiri, M. R. *J. Am. Chem. Soc.* **1996**, *118*, 43-50.
- (37) (a) For the NMR structure determination of cyclo(β^3 -HGlu)₃ in D₂O, see: Gademann, K.; Seebach, D. *Helv. Chim. Acta* **1999**, *82*, 957-962; (b) For XRD studies of three stereoisomers of cyclo(β^3 -HAla)₄, see: Seebach, D.; Matthews, J. L.; Meden, A.; Wessels, T.; Baerlocher, C.; McCusker, L. B. *Helv. Chim. Acta* **1997**, *80*, 173-182.
- (38) Although cyclo L,D-peptides show propensity to self-assemble into H-bonded tubular stacks in the solid state and in non polar solvents, there is no indication that **A-1** aggregates in aqueous solution.
- (39) Kasai, N.; Yamanaka, T.; Miki, K.; Tanaka, N.; Post, B.; Morawetz, H. *Acta Crystallogr., Sect. B*, **1981**, *37*, 1628-1630.
- (40) The crystal structures of a number of isosteric cyclic tri(β -hydroxy alkanooates) have been solved. In crystal, these compounds generally adopt a flat nearly equilateral triangular shape with all carbonyl groups pointing in one direction, very similar to the model calculated for cyclo(β^3 -HGlu)₃ (ref 36a) with a distance between the center of gravity of the triangle and the β^3 C ranging from 2.62 to 2.75 Å. See: (a) Seebach, D.; Muller, H.-M.; Burger, H. M.; Plattner, D. A. *Angew. Chem. Int. Ed.* **1992**, *31*, 434; (b) Seebach, D.; Hoffmann, T.; Kuhnle, F. N. M.; Lengweiler, U. D. *Helv. Chim. Acta* **1994**, *77*, 2007-2034.
- (41) Sridhar, J.; Wei, Z.-L.; Nowak, I.; Lewin, N. E.; Ayres, J. A.; Pearce, L. V.; Blumberg, P. M.; Kozikowski, A. P. *J. Med. Chem.*, **2003**; *46*, 4196-4204.
- (42) Krishnamurthy, V. M.; Semetey, V.; Bracher, P. J.; Shen, N.; Whitesides, G. M. *J. Am. Chem. Soc.* **2007**, ASAP Article; DOI: 10.1021/ja066780e.
- (43) (a) Bajorath, J.; Chalupny, N. J.; Marken, J. S.; Siadak, A. W.; Skonier, J.; Gordon, M.; Hollenbaugh, D.; Noelle, R. J.; Ochs, H. D.; Aruffo, A. *Biochemistry* **1995**, *34*, 1833-1844; (b) Bajorath, J.; Marken, J. S.;

Chalupny, N. J.; Spoon, T. L.; Siadak, A. W.; Gordon, M.; Noelle, R. J.; Hollenbaugh, D.; Aruffo, A. *Biochemistry* **1995**, *34*, 9884-9892.

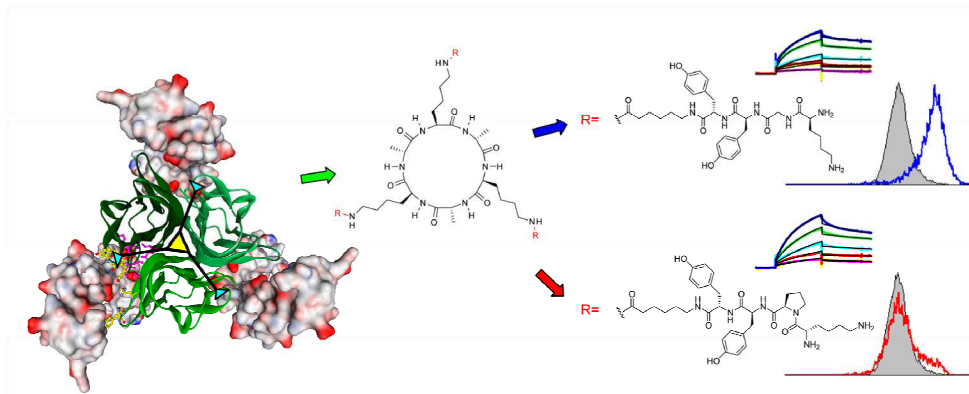
- (44) For reviews, see: (a) Venkatraman, J.; Shankaramma, S. C.; Balaram, P. *Chem. Rev.* **2001**, *101*, 3131-3152; (b) Rose, G. D.; Gierasch, L. M.; Smith, J. A. *Adv. Prot. Chem.* **1985**, *37*, 1-110.
- (45) It is noteworthy that similar results were obtained for analogous ligands **A-1** and **A-9** (ref 32). In this case, K_D calculated using the Langmuir 1:1 model and local fitting models were 121 and 183 nM, respectively. Analysis of cooperativity using Hill plots suggested that the interaction with **A-1**/CD40 interaction is cooperative (Hill coefficient $h = 2.9$) and that this cooperativity is lost upon replacing Gly by D-Pro ($h = 1.0$).
- (46) Seebach, D; Schaeffer, L.; Brenner, M.; Hoyer, D., *Angew. Chem. Int. Ed.* **2003**, *42*, 776-778.
- (47) Scholl, M.; Ding, S.; Lee, C. W.; Grubbs, R. H. *Org. Lett.* **1999**; *1*, 953-956.
- (48) In the case of **B-15**, fitting of SPR data was better achieved with divalent and trivalent models ($\chi^2 = 0.271$ and 0.269, respectively) than with the "Langmuir 1:1" monovalent model ($\chi^2 = 0.843$).
- (49) (a) Mierke, D.F.; Kurz, M.; Kessler, H. *J. Am. Chem. Soc.* **1994**, *116*, 1042-1049; (b) Heller, M.; Sukopp, M. *J. Am. Chem. Soc.* **2006**, *128*, 13806-1381.
- (50) For selected examples of polyvalent systems based on cyclic peptide templates of different topology, see: a) Singh, Y.; Dolphin, G. T.; Razkin, J.; Dumy, P. *ChemBiochem* **2006**, *7*, 1298-1314. b) Boturyn, D.; Coll, J.-L.; Garanger, E.; Favrot, M.-C.; Dumy, P. *J. Am. Chem. Soc.* **2004**, *126*, 5730-5739; c) Zhang, Z.; Liu, J.; Verlinde, C. L. M. J.; Hol, W. G. J.; Fan, E. *J. Org. Chem.* **2004**, *69*, 7737-7740
- (51) Li, B.; Russell, S. J.; Compaan, D. M.; Totpal, K.; Marsters, S. A.; Ashkenazi, A.; Cochran, A. G.; Hymowitz, S. G.; Sidhu, S. S. *J. Mol. Biol.* **2006**, *361*, 522-36.
- (52) Hakansson, K.; Reid, K. B. *Protein Sci.* **2000**, *9*, 1607-1617.
- (53) McWhirter, S. M. , Pullen, S. S.; Holton, J. M.; Crute, J. J.; Kehry, M. R., Alber, T. *Proc Natl Acad Sci USA.* **1999**, *96*, 8408-8413.
- (54) Kishore, U.; Gaboriaud, C.; Waters, P.; Shrive, A. K.; Greenhough, T. J.; Reid, K. B.; Sim, R. B.; Arlaud, G. J. *Trends Immunol.* **2004**, *25*, 551-561.
- (55) Harbury, P. B.; Zhang, T.; Kim, P. S.; Alber, T. 1993, *Science*, **262**, 1401-1407.
- (56) Bewley, M. C.; Springer, K.; Zhang, Y. B., Freimuth, P.; Flanagan, J. M. *Science* **1999**, *286*, 1579-1583.
- (57) Holler, N.; Tardivel, A.; Kovacsovic-Bankowski, M.; Hertig, S.; Gaide, O.; Martinon, F.; Tinel, A.; Deperthes, D.; Calderara, S.; Schulthess, T.; Engel, J.; Schneider, P.; Tschopp, J. *Mol. Cell. Biol.* **2003**, *23*, 1428-1440.

CHAPTER 8

COOPERATIVITY IN THE INTERACTION OF SYNTHETIC CD40L MIMETICS WITH CD40 AND ITS IMPLICATION IN CELL SIGNALING

Biochemistry 46, 3482-3493 (2007)

Wieckowski, S., Trouche, N., Chaloin, O., Guichard, G., Fournel, S., and Hoebeke, J.



CHAPTER 8

As shown in chapter 7, modulation of the mini-CD40Ls has permitted to study their mechanisms of action. We have generated mini-CD40L variants with point mutations in the CD40-binding motif, and biotinylated mini-CD40Ls, which have provided interesting tools for the study of CD40 biology. We have attempted to stabilize the CD40-binding peptide in a conformation close to the loop adopted by this sequence during the interaction of natural CD40L with its cognate receptor.

We have thus generated a molecule that includes the non-natural amino acid D-proline, and compared it to the normal mini-CD40L in binding assay, apoptosis of lymphoma, maturation of dendritic cells and induction of key signaling pathways.

We demonstrated by surface plasmon resonance experiments that the mutated mini-CD40L did not bind to CD40 in a cooperative manner, in contrast to the non-mutated mini-CD40L. Both molecules induced apoptosis of lymphoma cells with the same efficiency, but the mutated form did not induce maturation of dendritic cells. Moreover, it did not activate the NF- κ B pathway, albeit it induced expression of *IL12 p40* mRNA. We thus provided a correlation between the binding property to the receptor and the intracellular signaling.

Mini-CD40Ls provide a tool of great importance for the study of cellular biology. One could now easily reach the physico-chemical properties of a receptor-ligand interaction, and study the cellular effects they imply. Moreover, the mutated mini-CD40L could be used to target cell-specific CD40-induced signaling pathways, and might find therapeutical applications.

Cooperativity in the interaction of synthetic CD40L mimetics with CD40 and its implication in cell signaling

Sébastien WIECKOWSKI, Nathalie TROUCHE, Olivier CHALOIN, Gilles GUICHARD, Sylvie FOURNEL, and Johan HOEBEKE

Biochemistry, 2007, Vol. 46, Pages 3482-3493

Pages 157-168 :

La publication présentée ici dans la thèse est soumise à des droits détenus par un éditeur commercial.

Pour les utilisateurs ULP, il est possible de consulter cette publication sur le site de l'éditeur :

<http://dx.doi.org/10.1021/bi602434a>

La version imprimée de cette thèse peut être consultée à la bibliothèque ou dans un autre établissement via une demande de prêt entre bibliothèques (PEB) auprès de nos services :

<http://www-sicd.u-strasbg.fr/services/peb/>

Supporting Information

Cooperativity in the interaction of synthetic CD40L mimetics with CD40 and its implication in cell signaling[†]

Sébastien Wieckowski, Nathalie Trouche, Olivier Chaloin, Gilles Guichard,

Sylvie Fournel^{}, and Johan Hoebeke^{*}*

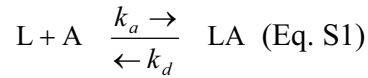
CNRS UPR 9021, Immunologie et Chimie Thérapeutiques, Institut de Biologie
Moléculaire et Cellulaire, 15 rue René Descartes, 67084 Strasbourg, France

TITLE RUNNING HEAD: Synthetic CD40L mimetic, cooperativity and cell signaling

^{*}To whom correspondence should be addressed. S.F.: Tel. (33)3 88 41 70 24; Fax (33)3
88 61 06 80; e-mail s.fournel@ibmc.u-strasbg.fr. J.H.: Tel. (33)3 88 41 70 24; e-mail
j.hoebeke@ibmc.u-strasbg.fr.

Surface plasmon resonance (SPR) analysis; summary of the equations used for the determination of the kinetics data

The simplest model, the Langmuir 1:1 one, was first used to assess the binding kinetics of the interaction. In the further equations, L denotes the ligand captured on the immobilized rabbit anti-mouse Ig, in our case the receptor CD40, and A denotes the analyte injected on the chip, that is either of the CD40L or *mini-CD40Ls*. When A interacts with L forming the LA complex due to diffusion, collision and binding, in function of time with the association rate constant k_a (1/M.s), but can also disappear with dissociation rate constant k_d (1/s) to release A from L (Eq. S1).



Equilibrium is reached when the rate of association (Eq. S2) equals the rate of dissociation, that is when the number of dissociation events compensates the number of association events.

$$\frac{d[LA]}{dt} = k_a \cdot [L] \cdot [A] - k_d \cdot [LA] \quad (\text{Eq. S2})$$

In our conditions, equilibrium can not be reached at the end of the injection phase, but values at equilibrium could be extrapolated, especially the dissociation constant K_D (M), using the kinetic values obtained from the individual experimental curves of the association and dissociation phases (Eq. S3).

$$\frac{[L] \cdot [A]}{[LA]} = \frac{k_d}{k_a} = K_D \quad (\text{Eq. S3})$$

Rewriting Eq. S2 in terms of concentration and responses, we obtain Eq. S4.

$$\frac{dR}{dt} = k_a \cdot C \cdot (R_{max} - R_t) - k_d \cdot R_t \quad (\text{Eq. S4})$$

In Eq. S4, R_t corresponds to the response signal of the formed complex at t time, C represents the concentration of CD40-ligands and R_{max} the maximal feasible response signal, depending on the total CD40 binding capacity (or activity) on the sensor chip. In this case we assume that free ligand equals maximal capacity minus bound receptor.

The data extracted from the experimental curves as well as the known input parameters are used by the algorithm and assessed by numerical integration to calculate the different parameters needed. One can then determine the values for signal response at equilibrium (R_{eq}), that is for t value tending to infinite, from the kinetic constants and the R_{max} calculated parameter (Eq. S5).

$$R_{eq} = \frac{k_a \cdot Conc \cdot R_{max}}{k_a \cdot Conc + k_d} \quad (\text{Eq. S5}).$$

Figure S1

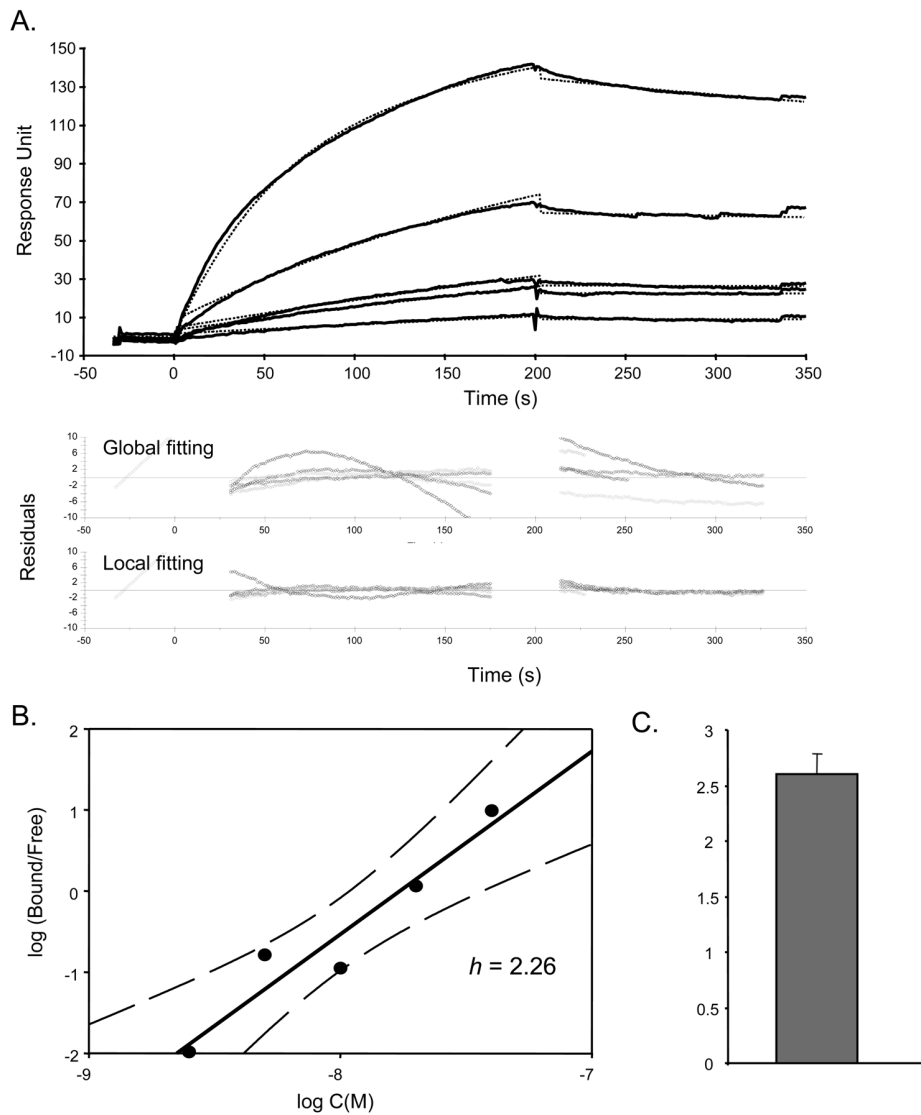


Figure S1. SPR experiments and analysis of cooperativity for the rshCD40L:mCD8 protein. (A) Study of the direct binding of rshCD40L:mCD8 on rshCD40:mIg as shown by SPR. The graph represents the binding data for each ligand (black lines) and the fitting curves (dashed lines) using the trivalent model with rate constants for the first binding event determined by local fitting. One experiment representative of three is shown. (B) Hill representation for rshCD40L:mCD8 using data extracted from sensorgrams of experiment shown in (A). The Bound and Free denotes the R_{eq} and R_{max} minus R_{eq} respectively. C denotes the concentration of CD40L injected. Hill number h , assessed by linear regression, is indicated. 95% confidence intervals are indicated (dash lines). (C) Means \pm SE of the h value from three independent experiments.

Appendix (for response to reviewers use only)

Cooperativity in the interaction of synthetic CD40L
mimetics with CD40 and its implication in cell
signaling[†]

Sébastien Wieckowski, Nathalie Trouche, Olivier Chaloin, Gilles Guichard,

Sylvie Fournel^{}, and Johan Hoebeke^{*}*

CNRS UPR 9021, Immunologie et Chimie Thérapeutiques, Institut de Biologie Moléculaire et
Cellulaire, 15 rue René Descartes, 67084 Strasbourg, France

TITLE RUNNING HEAD: Synthetic CD40L mimetic, cooperativity and cell signaling

^{*}To whom correspondence should be addressed. S.F.: Tel. (33)3 88 41 70 24; Fax (33)3 88 61 06 80; e-mail s.fournel@ibmc.u-strasbg.fr. J.H.: Tel. (33)3 88 41 70 24; e-mail j.hoebeke@ibmc.u-strasbg.fr.

Binding of A-1 to rshCD40:mIg never reached equilibrium

An independent SPR experiment using **A-1** and rshCD40:mIg was performed strictly in the conditions described in the text, excepted the injection length was 8 minutes, the maximum permitted by the Biacore 3000 system in our conditions. Sensorgrams for **A-1** at 125, 500 and 1,000 nM are represented on figure A1.

The rshCD40:mIg construct oligomerizes in solution

The recombinant soluble human CD40-mouse Ig fusion protein (rshCD40:mIg) used in this work (Ansell corporation, Bayport, MN) was diluted at 25 ng/ μ L in HBS-EP containing the reducing agent β -mercaptoethanol (β ME) at 100 mM (lanes 1, 2 and 3, 4) or not (lanes 5, 6), and boiled (Δ) for 5 minutes (lanes 1, 2 and 5, 6) or not, before loading of 0.25 μ g of protein (10 μ L) on a 10% SDS polyacrylamide gel. All these preparations were loaded in duplicate on the gel. After electrophoresis and transfer, the nitrocellulose membrane was saturated with Tris-buffered saline (TBS) containing 0.5% (w/v) Tween 20 (TBS-T) and 5% (w/v) non-fat milk (TBS-T/milk) overnight at 4°C. The membrane was then incubated at room temperature for 1 h with the GAM antibody diluted 1/2,000 in TBS-T/milk. After 3 washes with TBS-T, the membrane was incubated with ECL reagent (Amersham). The radiography is shown on figure A2.

When comparing the reduced (lanes 1, 2) and non-reduced protein preparations (lanes 5, 6), the proportion of monovalent CD40 was significantly decreased from 71% to 21%. More than 75% of the CD40 is at least divalent in non-reducing conditions (lanes 5, 6). Furthermore, we found less than 15% of free IgG, which does not appear in non-reducing conditions (lanes 1, 2), and less than 5% (lanes 1, 2) and 3% (lanes 5, 6) of degraded IgG in reducing and non-reducing conditions respectively.

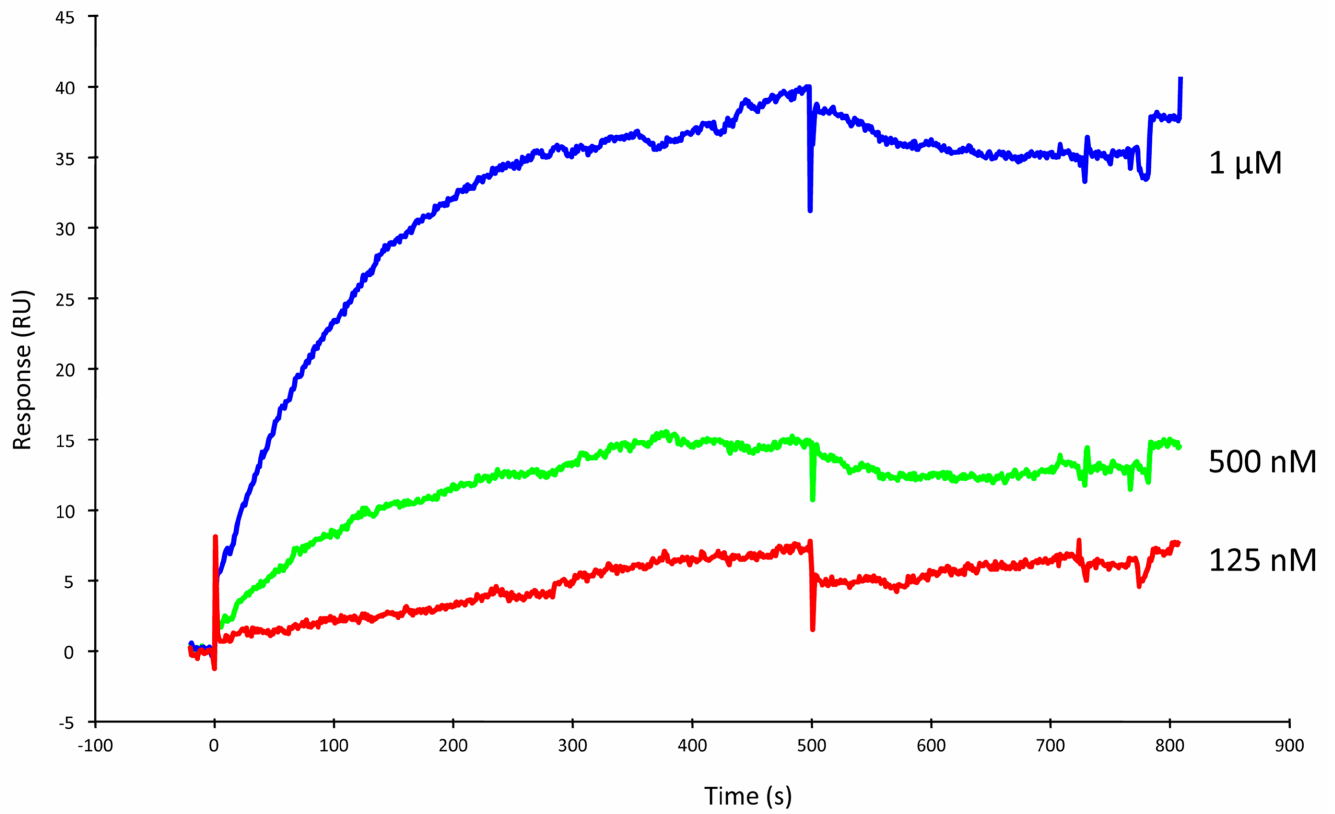


Figure A1. *Binding of A-1 to rshCD40:mIg never reached equilibrium.* SPR experiment using **A-1** and rshCD40:mIg as described in the text, but with extended association phase.

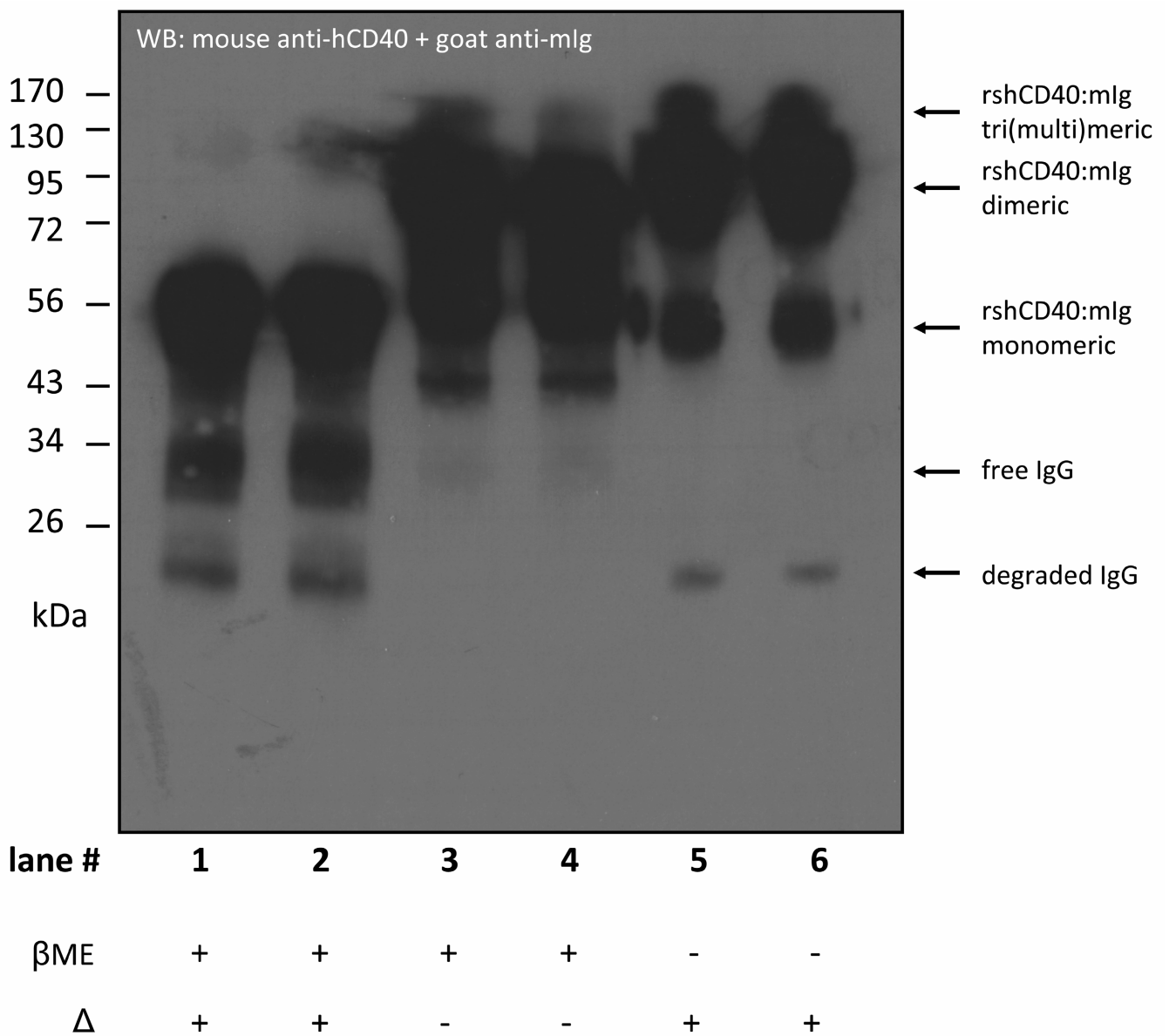


Figure A2. *The rshCD40:mIg construct oligomerizes in solution.* SDS-PAGE of the rshCD40:mIg construct in reducing and non-reducing conditions.

CHAPTER 9

CELL-SPECIFIC SIGNALING INDUCED BY SYNTHETIC CD40L MIMETICS IN MALIGNANT AND NORMAL CELLS

(in preparation)

Wieckowski, S., Trouche, N., Guichard, G., and Fournel, S.

CHAPTER 9

CD40-based immunotherapy has provided important pre-clinical clues in treatment of various cancers. Nevertheless, implication of CD40-signaling in the complex network of cells implied in tumorigenesis is not completely understood. We provided informations on the cell signaling pathways induced by CD40 triggering with mini-CD40L on different cell types. As this work is currently under investigation, we could only give in this chapter a partial view of the implicated pathways.

Mini-CD40L was used to depict cell signaling pathways activated downstream CD40 in human and mouse lymphoma, in mouse carcinoma, and in mouse dendritic cells and B lymphocytes. Many authors have described pathways engaged by CD40, and showed that both the cell-type and the nature of the stimulus (anti-CD40 mAb, scFv, soluble or membranous CD40L) are important parameters, depicting the existence of cell-specific and stimulus-dependent signaling pathways engaged by CD40. Here we showed that mini-CD40L induces apoptosis of many CD40-positive human and mouse malignancies, independently of CD95. This suggests that mini-CD40Ls might be used as direct inducers of apoptosis on many malignant cells. Furthermore, it induced maturation of bone-marrow dendritic cells. In addition to expressing IL-12, mini-CD40L-activated dendritic cells also secrete IL-23, a cytokine related to IL-12 but that has specific functions. Interestingly, mini-CD40L induced proliferation of B lymphocytes synergistically with IL-4. Mechanisms of CD40-mediated apoptosis in lymphoma cells are not yet fully understood. We showed here that the mini-CD40L-induced apoptosis in lymphoma cells is in part independent on caspases, but involve protein tyrosine-phosphatases and protein tyrosine-kinases. We have also enhance the mini-CD40L apoptotic effect in the presence of inhibitor of the survival pathway protein Akt. In dendritic cells, the p38 and MEK1/2 MAPK pathways were activated by mini-CD40Ls in dendritic cells, and we showed implication of PI3K. Although the NF- κ B pathway is activated by mini-CD40L in dendritic cells and carcinoma, we did not detect it in lymphoma cells, suggesting that different pathways are activated although they all induce the same biological effects. Finally, we observed some reorganization of lipid rafts on lymphoma and carcinoma cells, subsequently to activation with mini-CD40L, suggesting that their effects involve these microdomains.

Although our results are preliminary, they provide essential data on cell signaling induced by mini-CD40Ls in various cell types, and confirm the cell specificity of CD40-engaged signaling pathways.

Cell-Specific Signaling Induced by Synthetic CD40L Mimetics in Malignant and Normal Cells[†]

[†]This work was supported by the Centre National de la Recherche Scientifique, the Institut National du Cancer and the Agence Nationale de Recherches contre le SIDA. S.W. was supported by grants from the Ministère de la Recherche and from the Fondation pour la Recherche Médicale. N.T. was supported by La Ligue contre le Cancer.

*Sébastien Wieckowski, Nathalie Trouche, Gilles Guichard, and Sylvie Fournel**

CNRS, Immunologie et Chimie Thérapeutiques, Institut de Biologie Moléculaire et Cellulaire, 15 rue René Descartes, 67084 Strasbourg, France

TITLE RUNNING HEAD: Mini-CD40L, Cell-Specific Signaling and Applications to Biology of Cancer

*To whom correspondence should be addressed. S.F.: Tel. (33)3 88 41 70 24; Fax (33)3 88 61 06 80; e-mail s.fournel@ibmc.u-strasbg.fr.

¹Abbreviations: CD40L, CD40 ligand (CD154); TNF, tumor necrosis factor; TNF-R, TNF receptor; TRAF, TNF-R-associated factor; APC, antigen-presenting cells; DC, dendritic cell; MHC, major histocompatibility complex; mAb, monoclonal antibody;

GM-CSF, granulocyte-macrophage colony-stimulating factor; LPS, lipopolysaccharide; RT-PCR, reverse transcription-polymerase chain reaction; GAPDH, glyceraldehyde-3-phosphate dehydrogenase; $\Delta\psi_m$, mitochondrial transmembrane potential; DiOC₆(3), 3,3'-dihexyloxacarbocyanine iodide; PTP, protein tyrosine-phosphatase; PTK, protein tyrosine-kinase; Na₃VO₄, orthovanadate; Wrt, wortmannin.

ABSTRACT: Engagement of CD40 induces various cellular responses including proliferation, differentiation and apoptosis. Due to the particular geometry of the CD40 and CD40L proteins, which belong to the tumor necrosis factor (TNF) receptor and TNF family respectively, signaling pathways associated with them greatly differ not only according to cellular context, but also to nature of the stimulus. To better understand cell signaling induced by CD40, we have developed a small synthetic molecule that mimics the natural soluble CD40L. Using this synthetic tool, we dissected cellular events engaged from interaction with its cognate receptor at the plasma membrane, to translocation of common transcription factors to the nucleus. This study provided useful informations regarding the CD40-activated pathways leading to apoptosis in malignant cells and leading to activation of normal cells including dendritic cells and B lymphocytes.

CD40 ligand (CD40L)¹ is a 33–39 kDa type II transmembrane glycoprotein (1-3), which belongs to the TNF family (4, 5). It is not only transiently expressed at the surface of activated T lymphocytes (6, 7), but also on many other cell-types including activated B lymphocytes, dendritic cells (DC), natural killer cells and platelets (8). CD40L also exists as a soluble homotrimeric form which is fully biologically active (9, 10). It was detected in the serum of patients with chronic lymphocytic leukemia in elevated levels compared to healthy donors (11), as well as in many pathological contexts (12-17), suggesting its implication in various diseases. Its receptor CD40, a member of the TNF receptor (TNF-R) family, is a type I glycoprotein with a molecular weight of 43–48 kDa (18). Although CD40 was first described on neoplastic urethelium (19, 20) and many malignant B cells (21, 22), it is constitutively expressed on normal antigen-presenting cells (APC) including B cells, DCs and macrophages/monocytes, and is present on non-hematopoietic cells including vascular endothelial cells and fibroblasts. It is also upregulated in non-healthy conditions as reviewed by Schonbeck *et al.* (8).

CD40L promotes B cell rescue from apoptosis, proliferation, differentiation into germinal center cells, up-regulation of costimulatory and activation molecules, immunoglobulin isotype switching, selection and maturation into memory cells (23, 24). Moreover, CD40 triggering at the surface of DCs enhances survival, as well as antigen presenting functions by increase of major histocompatibility class II and accessory molecules expression, and secretion of key cytokines including interleukin (IL)-12. Finally, the CD40–CD40L interaction promotes antimicrobial and cytotoxic activities to macrophages by up regulating expression of pro-inflammatory molecules, cytokines and chemokines (24). Activation of DCs has been shown to be essential in the priming of CD8⁺ T lymphocytes by CD4⁺ helper T cells (25, 26).

Interestingly, CD40 was shown to be overexpressed in a broad range of tumor cells such as carcinoma, leukemia, lymphoma and multiple myeloma, in which ligation of CD40 with a soluble recombinant or membrane-bound CD40L, or with agonistic monoclonal antibodies (mAb) leads to apoptosis (27-31).

Active forms of soluble and membrane CD40L are non-covalently bound homotrimers (32), which interact with three CD40 monomers forming, similarly to the TNF/TNFR interaction (33), a well-ordered stoichiometrically defined 3:3 hexameric complex (34).

The cytoplasmic tail of CD40 lacks intrinsic enzymatic activity (35), but interaction of CD40 with its cognate ligand allows the translocation of the receptor to lipid rafts (36, 37) and the formation of a properly organized signalosome under the plasma membrane. Recruitment of certain TNF-R-associated factors (TRAFs) adaptor proteins might participate in initiation of downstream pathways (38). Degree of CD40 crosslinking is an important factor for initiation of specific intracellular signals (39). Thus, CD40L, either soluble or membrane-bound, anti-CD40 mAbs or single-chain fragment variable might have different behaviors (40-43). Signal transduction may also require some allosteric movements through the entire receptor molecule to be processed correctly into the cytoplasm. Finally, signal depends on numerous parameters, including the nature of the stimulus, in particular the geometry and oligomerization state of the receptor recognition element, as well as the cellular context of the target which provides the specific set of intermediary molecules implicated in particular pathways.

We have reported on the structure based design of small peptide-based molecules with C_3 symmetry, named mini-CD40Ls, that can mimic CD40L homotrimers (44, 45). These synthetic molecules, in particular mini-CD40L **1**, interact with CD40 and reproduce the functional cellular effects of soluble CD40L as B lymphoma cell apoptosis, B lymphocyte activation and dendritic cell maturation. Recently, we accounted for the *in vivo* application of mini-CD40Ls in the control of experimental *Trypanozoma cruzi* infection in mice by activation of a CTL response (Habib et al., *J Immunol*, in press). In parallel, we have demonstrated that a mini-CD40L mutated in the CD40-binding motif, which bound to CD40 in a non-cooperative manner, did not engage the same signaling pathways than the non-mutated mini-CD40L (46). These data suggest that one might direct the nature of a signal in certain cell types by modifying the manner by which a ligand interacts with its receptor.

Here we depict signals engaged by mini-CD40Ls **1** in lymphoma and carcinoma cell lines, from the rearrangement of lipid rafts, to the induction of the classical pathway mitogen-activated protein kinase (MAPK), induction of apoptosis independently of caspases, and translocation of the transcription factor NF- κ B p50. In the same manner, we provide more data on the mini-CD40L-induced maturation of dendritic cells and show that it upregulates expression of IL-23 via the p38 and MEK1/2 MAPK pathways.

Finally, IL-4 and mini-CD40L **1** induced synergistic pathways leading to the proliferation of normal B cells, as described with the natural CD40L. This report and our previous works lead to the proposal of an interesting new tool for the study of biology of cancer, but also of a potential molecule for future cancer immunotherapy.

MATERIALS AND METHODS

CD40L Mimetic Synthesis. Detailed synthesis of mini-CD40L **A-1** was described previously (44, 45). For sample preparation, ligands was dissolved in Milli-Q deionized water at a concentration of 1 mM before further dilution to the indicated concentrations in appropriate buffer or medium.

Reagents. The 3,3'-dihexyloxacarbocyanine iodide DiOC₆(3) dye was purchased from Interchim (Montluçon, France). Lipopolysaccharide (LPS) from *Escherichia coli* (strain 0111.B4), Wortmannin from *Penicillium funiculosum*, recombinant murine IL-4 and cholera toxin subunit B (CTB)-FITC were obtained from Sigma-Aldrich (St. Louis, MO). Low-endotoxin recombinant mouse granulocyte/macrophage colony-stimulating factor (rmGM-CSF), anti-p38 and anti-MEK1/2 both total and phosphorylated were purchased from USBiological (Swampscott, MA). Anti-caspase 3, mouse anti-human Fas-neutralizing Ab (clone ZB4), anti-phosphotyrosine mAb 4G10, fluorescein isothiocyanate (FITC)-conjugated anti-mouse CD40 (3/23 clone), FITC anti-human CD40 (5C3 clone), phycoerythrin (PE) anti-mouse CD54 (3E2 clone), PE anti-mouse CD80 (16-10A1 clone), PE anti-mouse CD86 (GL1 clone), PE anti-human CD95, FITC anti-human CD40L, purified anti-CD40L mAb (TRAP1 clone), and FITC anti-human CD19 mAbs were purchased from Pharmingen (San Jose, CA), anti-I κ B- α rabbit antiserum and anti-actin mouse monoclonal antibody (C4 clone) from Pharmingen, anti-NF- κ B p50 from Abcam, and the agonistic anti-CD95 mAb 7C11 from Immunotech. Caspases inhibitors Z-DEVD-fmk, Z-YVAD-fmk, Z-IETD-fmk, Z-VEID-fmk, and Z-VAD-fmk were purchased from Upstate. Peroxidase-labeled goat anti-mouse (GAM) and goat anti-rabbit (GAR) antibodies, as well as the enhanced chemiluminescence (ECL) reagent detection kit for Western immunoblotting were purchased from Amersham (Little Chalfont, Buckinghamshire, U.K.). Akt inhibitor and Pifithrin- α were obtained from Calbiochem.

Culture of Lymphoma Cells and Measurement of Apoptosis. BL41, Raji, BL60, BJAB, Ramos and BP3 Burkitt lymphoma, Jurkat human T leukemia cells, as well as 3T6 fibroblasts and CD40L transfected 3T6 cell lines were cultured in RPMI 1640 with ultra-

glutamine (Cambrex Bioscience, Verviers, Belgium) supplemented with 10% of heat-decomplemented fetal bovine serum (FBS; Dominique Dutscher, Brumath, France) and gentamicin (10 µg/mL, Cambrex). The A20 and WEHI mouse lymphoma and Renca mouse renal carcinoma cells were cultured in RPMI supplemented with 10% of heat-decomplemented FBS, gentamicin (10 µg/mL), 2 mM HEPES, and 10 µM β-mercaptoethanol.

For apoptosis assays, cells (5×10^5 cells/mL) were incubated at 37 °C in flat-bottom 96-well plates at the indicated times in the presence of mini-CD40L in 200 µL of the respective complete medium. For solid tumor transfer, Renca cells were harvested in BSS with 2% FBS, and 2×10^5 cells injected sub-cutaneously in the flanks of 8-week old female BALB/c mice. Approximately twenty days post-transplantation, tumors were harvested and cells recovered with Trypsin-free cell dissociation buffer (Sigma). After incubation, cells were harvested, Renca cells were detached with citric saline buffer, and washed with phosphate-buffered saline (PBS). Apoptosis was then evaluated by measurement of the decrease in mitochondrial transmembrane potential ($\Delta\psi_m$) associated with a reduction of the level of cationic dye DiOC₆(3) uptake, as detected by flow cytometry; cells were resuspended in 300 µL of PBS containing 20 nM DiOC₆(3), and incubated at 37 °C for 20 min, and then directly analyzed by flow cytometry.

Results are expressed as the percentage of specific apoptosis according to the following formula: % of specific apoptosis = $100(\% \text{ apoptotic treated cells} - \% \text{ spontaneous apoptotic control cells}) / (100 - \% \text{ spontaneous apoptotic control cells})$.

Purification and culture of splenic B cells. Spleens were removed from 5-12 week-old BALB/c mice. Splenic B cells were prepared by positive selection using magnetic beads coated with anti-CD19 mAb (MACS, Milteny biotech, Germany). This fraction contained more than 95% of B220⁺ cells. B cells (3×10^6 /mL) were then cultured in RPMI 1640 medium supplemented with 10% of heat-decomplemented FBS, gentamicin (10 µg/mL), 2 mM HEPES and 10 µM β-mercaptoethanol in the presence indicated inducers. Cells were pulsed with 1 µCi/well of tritiated thymidine (ICN, Irvine, CA) during the last 20 h of culture and [³H]-thymidine uptake was measured after 72 h using a Matrix 9600 direct beta counter (Packard, Meriden, CT). The results are expressed in cpm.

Culture and Maturation of D1 Mouse Dendritic Cells. D1 cells have been described as a MHC class II–positive growth factor–dependent immature dendritic cells, derived from adult mouse spleen, and maintained in lineage with no transformation (47). Cells were cultured in non-treated plastic dishes, in IMDM with HEPES and L-glutamine (Cambrex) supplemented with 10% of heat-decomplemented FBS, gentamicin (10 µg/mL), 10 µM β-mercaptoethanol, and 10 ng/mL of rmGM-CSF. For cellular assays, 2×10^5 cells/mL were cultured for 24 h in 24-well untreated polystyrene microplates (Evergreen Scientific, Los Angeles, CA). Then, fresh medium containing the various inducers was added. After a further 24 h incubation, supernatants were recovered and stored for ELISA, and cells were washed with cold PBS and harvested with 2 mL of PBS containing 2 mM EDTA. After centrifugation, cells were resuspended in cold PBS and analyzed for cell surface phenotyping by flow cytometry, or used for immunoblotting and RT-PCR.

Generation of BMDC. Method was described elsewhere (48). Briefly, femurs and tibiae of female 8-12 week-old BALB/c mice were removed and purified from the surrounding muscle tissue. Then, both ends were cut with scissors and the marrow flushed with Hank's balanced salt solution (HBSS; Cambrex Bioscience, Verviers, Belgium). Clusters were disintegrated by vigorous pipetting. Ten centimeters diameter bacteriological Petri dishes (Dominique Dutscher, Brumath, France) were used for bone marrow cell culture, and 24-well untreated polystyrene microplates (Evergreen Scientific) for DCs maturation assays. Cells were cultured in RPMI 1640 with Ultraglutamine (Cambrex) supplemented with Gentamicin (10 µg/mL), 50 µM β-mercaptoethanol and 10% heat-inactivated FBS. At day 0, bone marrow cells were seeded at 2×10^6 per 10 cm–dish in 10 mL of complete medium containing 20 ng/mL rmGM-CSF (USBiological). At day 3 another 10 mL of complete medium containing 20 ng/mL rmGM-CSF were added to the plates. At day 6 and 8 half of the culture supernatant was collected, centrifuged, the cell pellet was resuspended in 10 mL fresh complete medium containing 20 ng/mL rmGM-CSF, and given back to the original plates. At day 10, DCs were gently harvested with HBSS containing 2% FBS and 2 mM

EDTA, washed twice in HBSS and resuspended in complete medium containing 10 ng/mL rmGM-CSF and seeded in 24-well plate for further 24h of maturation in the presence of the various inducers.

Flow Cytometry Analysis. For measurement of apoptosis, lymphoma cells were analyzed directly after the staining procedure. For phenotyping, BL41, D1 and BMDC cells were stained in PBS containing 2% FBS at 4 °C for 20 min with the various antibodies used at a concentration recommended by the manufacturer. For staining of lipid raft, cells were first fixed in 1% paraformaldehyde in PBS for 30 min at room temperature, and then incubated in PBS containing 10 µg/mL of CTB-FITC. After 1 hour of incubation, cells were washed twice in PBS, and analyzed by flow cytometry with a FACSCalibur[®]. At least 1×10^4 events were acquired for each experiment using CellQuest version 3.3 (Becton Dickinson, Pont de Claix, France), and data were processed with WinMDI version 2.8 (Jo. Trotter, Scripps Research Institute, La Jolla, CA; <http://facs.scripps.edu/software.html>).

Epifluorescence and confocal microscopy. Cells were treated as described in figure legends. After two washes in PBS, cells were resuspended in ready to use Fluorescent Mounting Medium (DakoCytomation) and mounted between glass slide and coverslip. The distribution of fluorescence was analyzed with an Olympus BX51 microscope with a FITC wide-band cube (460-490 nm excitation filter; 515-550 nm emission transmission range) using the AnalySIS 3.0 software.

Imaging data were also collected using an inverted Zeiss LSM 510 Meta confocal laser scanning microscope (Zeiss, Jena, Germany). A track allowing excitation at 488 nm (Ar-ion laser) and detection of emission wavelengths within 505-550 nm after total reflection by a mirror was set up. Data were processed with the ImageJ 1.37v freeware (Wayne Rasband, National Institutes of Health, <http://rsb.info.nih.gov/ij>), and the LSM Reader 4.0 plugin (Patrick Pirrotte, Yannick Krempf and Jérôme Mutterer, Institute for Molecular Biology of Plants, Strasbourg, France).

Western Blotting. Total cellular extracts were prepared by treatment in lysis buffer [50 mM Tris-HCl (pH 7.4), 300 mM NaCl, 10% glycerol, 0.5% Triton X-100, 2 mM EDTA, 2 mM activated-sodium orthovanadate, and protease inhibitor cocktail (Sigma Aldrich)] for 20 min on ice. Lysates were clarified by centrifugation at 10,000g for 20 min at 4 °C and quantified for total protein concentration with the bicinchoninic acid assay (BCA, Pierce, Rockford, IL). Ten micrograms of total cellular proteins was separated by 10% SDS-polyacrylamide gel electrophoresis and transferred to a nitrocellulose membrane. The membrane was saturated with Tris-buffered saline (TBS) containing 0.5% (w/v) Tween 20 (TBS-T) and 5% (w/v) non-fat milk (TBS-T/milk) for 1 h at room temperature and then incubated overnight at 4 °C with the anti-IκB-α or anti-actin antibody diluted 1:2000 in TBS-T/milk. After three washes with TBS-T at room temperature, the membrane was incubated at room temperature for 1 h with respectively the GAR or GAM antibody diluted 1:5000 in TBS-T/milk. After three washes with TBS-T, the membrane was incubated with ECL reagent (Amersham), and the relative signal intensity of each band was quantified by densitometry with the gel analyzer tool integrated in the ImageJ 1.37v freeware (<http://rsb.info.nih.gov/ij/>) after scanning of the radiography.

Comparative reverse transcription (RT)-polymerase chain reaction (PCR). Expression of the *IL23 p19* messenger RNA (mRNA) was evaluated by comparative RT-PCR as described previously. Total RNA was isolated from D1 cells with TriReagent-LS (Molecular Research Center, Inc., Cincinnati, OH) and converted to complementary DNA (cDNA) with Moloney-Murine leukemia virus reverse transcriptase (Sigma Aldrich) according to the manufacturer's instructions. The primers used to amplify *IL23 p19* cDNA were as follow: forward, 5' AAT GTG CCC CGT ATC C 3'; reverse, 5' GGA GGT GTG AAG TTG CT 3'.

As a constant probe, the cDNA sequence of the housekeeping gene glyceraldehyde phosphate dehydrogenase (*GAPDH*) was also amplified using the following primers: forward, 5' CGT CCC GTA GAC AAA ATG GTG 3'; reverse, 5' GTG GAT GCA GGG ATG ATG TTC 3'.

The sizes of the amplified products were 180 bp for *IL23 p19* and 642 bp for *GAPDH*. A thermal cycle of 30 s at 94 °C, 45 s at 56 °C, and 45 s at 74 °C was used 32 times for

IL23 p19 and 22 times for *GAPDH* using the Taq DNA polymerase (Promega, Madison, WI) according to the manufacturer's instructions. Five microliters of each amplicon was taken from the exponential phase of the PCR (set up before each test) and analyzed by electrophoresis on a 1% agarose gel in a 10 mM sodium borate, 2 mM EDTA and 2 µg/mL ethidium bromide buffer. Imaging data of the ethidium bromide-stained amplified products were obtained with the ChemiDoc XRS system (Bio-Rad, Hercules, CA) using Quantity One.

IL-23 ELISA (p19/p40). The mouse IL-23 (p19/p40, IL-23) ELISA Ready-SET-Go! kit was purchased from eBioscience and was used according to the manufacturer instructions.

RESULTS

Mini-CD40L 1 induces apoptosis of various malignant cells. We have demonstrated that mini-CD40L 1 induced apoptosis of human Burkitt's lymphoma cells BL41 and Raji, and of mouse B lymphoma A20 but not the T leukemia cell line Jurkat (44). Here, we examined the pro-apoptotic effect of this CD40L mimetic on a larger spectrum of CD40-positive malignant cells. Mini-CD40L 1 was tested on other human B lymphoma cell lines including BL60, BJAB, Ramos and BP3, and another mouse B lymphoma, the WEHI 231 cell line (Figure 1A). All of these cells were sensitive to apoptosis induced by mini-CD40L 1 in a dose-response manner, with a concentration corresponding to 50% of specific apoptosis (C_{50}) varying from 10 µM (BP3) to more than 50 µM (BL41) after 16 h of incubation, depending on the cell line. We also tested mini-CD40L 1 on the mouse renal carcinoma cell line Renca. These cells were highly responsive as we could measure an C_{50} of approximately 5 µM (Figure 1B). Interestingly, cells recovered from a Renca solid tumor grown for 2 weeks in BALB/c mouse have not lost their sensibility to mini-CD40L 1-induced apoptosis (Figure 1B). This suggests a potential application in treating CD40-positive solid tumors. Nevertheless, we could not make a direct association between the expression level of CD40 and the level of apoptosis induced by mini-CD40L 1 (Figure 1A,B). Thus, differential responsiveness to apoptosis induced by mini-CD40L,

and certainly apoptosis induced by soluble CD40L, could not be simply explained by differences in density of CD40 at the plasma membrane on the different cells.

Mini-CD40L 1 induces maturation of dendritic cells and synergizes with IL-4 for B lymphocytes proliferation. We have demonstrated that, although mini-CD40L **1** was cytotoxic for malignant cells, it induced maturation of the dendritic cell line D1, and induced proliferation of normal mouse B lymphocytes purified from BALB/c mouse spleen in the presence of an anti-CD40 mAb (44). Furthermore, we have recently shown that mini-CD40Ls control experimental *Trypanozoma cruzi* infection in mice by activation of a CTL response (Habib *et al.*, J. Immunol, in press). Our results are in accordance to data from experiments that have used agonistic anti-CD40 mAbs or CD40L derivatives to activate immune response and to induce direct cytotoxicity of malignant cells. Here, we looked for mini-CD40L **1** activity on bone marrow-derived dendritic cells (BMDC) from BALB/c mice. BMDC were cultured for 24 h in the presence of mini-CD40L **1**, of the positive control LPS, or of a mini-CD40L control consisting of the CD40-binding peptide, and assessed for expression of the maturation markers CD40, CD54 (ICAM-1), CD80 (B7-1) and CD86 (B7-2). Mini-CD40L **1** efficiently induced maturation of BMDC CD11c⁺ cells, although the level of maturation was not as high as the level of maturation induced by LPS (Figure 2A). To better understand mechanisms of activation of soluble CD40L on DCs, we identified the cytokines produced by them. D1 cells were incubated in the presence of mini-CD40L **1** for 16 h and assessed by RT-PCR for the production of *IL23 p19* mRNA. IL-23 shares the p40 subunit with IL-12 and was shown to have similar functions to IL-12 (49). Nevertheless, it promotes different immunological pathways and act in cooperation with IL-12 to modulate cellular immune responses (50). We have demonstrated that mini-CD40L **1** induced production of *IL12/IL23 p40* mRNA (44), but we have never detected any enhanced production of *IL12 p19* mRNA in these conditions (data not shown). Here we showed that mini-CD40L **1** induced elevated transcription of *IL23 p19* (Figure 2B). This was correlated with the production of IL-23 p19/p40 protein in supernatants of D1 cells cultured with mini-CD40L **1** at different concentrations after 16 h, as detected by ELISA (Figure 2C). Thus, mini-CD40Ls could induce CD8⁺ response since they activate

DCs and induce their production of IL-12 and IL-23. Finally, we evaluated the efficiency of mini-CD40L **1** in induction of normal B cell proliferation. We have demonstrated that mini-CD40L **1** could not induce proliferation of mouse splenic B cell purified from BALB/c mouse. As anti-CD40 mAb was efficient to some extent, combination of the two molecules led to a synergistic induction of B cell proliferation, suggesting that B cell activation need a higher level of CD40 cross-linking (44). Since recent finding that cooperativity in the interaction of mini-CD40Ls with CD40 is implicated in the cellular pathways they activate (46), one could not reject that certain signaling pathways necessitate some allosteric change in the receptor structure. Here we demonstrated that mini-CD40L **1** synergizes with sub-mitogenic concentrations of IL-4 in induction of B cell proliferation (Figure 2D). This result is consistent with data obtained on human B cells cultured in the presence of both soluble CD40L and IL-4 (10).

Mini-CD40L 1-induced apoptosis in lymphoma is CD95-independent. Membrane-bound CD40L (mCD40L) was described to induce expression of CD95 (Fas) on B lymphoma cell, sensitizing them to Fas-mediated apoptosis (51). We tested the capacity of mini-CD40L **1** to inhibit expression of CD95 induced by a membrane form of CD40L, stably expressed by 3T6 fibroblasts (3T6-CD40L) cells, on B lymphoma cells. As shown in Figure 3A, 3T6-CD40L induced expression of CD95 on B lymphoma BL41 cells, and an anti-CD40L mAb completely inhibited this effect. Mini-CD40L **1** showed inhibition of CD95 expression induced by mCD40L in a dose-dependent manner, with approximately 35% efficiency at 25 μ M. Although the mini-CD40L could not compete completely with mCD40L, it did not induce by itself expression of CD95, similarly to soluble CD40L (sCD40L) (Figure 3B). Interestingly, the anti-CD40 mAb was able to induce to some extent expression of CD95. Furthermore, we did not detect apoptosis of B lymphoma cells incubated with either the anti-CD40 mAb or mCD40L (data not shown). These results demonstrate that the nature of CD40 triggering at the surface of lymphoma cells greatly determine the signaling transduced, and the overall cellular effect. Finally, we showed that mini-CD40L **1**-induced apoptosis of lymphoma cells is independent of CD95. We used the antagonist anti-CD95 mAb ZB4 that efficiently inhibited apoptosis

induced by an agonistic anti-CD95 mAb 7C11 on Jurkat T cells (Figure 3C). The ZB4 mAb had not influence on mini-CD40L **1**-induced apoptosis (Figure 3C).

*Cell signaling induced by mini-CD40L **1** in lymphoma cells.* We could use mini-CD40L **1** as a tool to characterize cellular mechanisms underlying the apoptotic effect of soluble CD40L. CD40L was shown to activate caspase 3 in carcinoma cells (52). We first studied by immunoblotting caspase 3 activation in B lymphoma Raji cells incubated with sCD40L or mini-CD40L **1** for 16 h. Although the processed active form of caspase 3 has accumulated in Jurkat cell treated with the agonistic anti-CD95 mAb 7C11, neither sCD40L nor mini-CD40L **1** could enhance the level of active caspases 3 (Figure 4A). This result was confirmed in an apoptosis assay in the presence of caspase inhibitors (Figure 4B). The inhibitor of caspase 3 and 7 Z-DEVD-fmk only slightly decreased the level of apoptosis induced by mini-CD40L **1**. Comparable results were obtained with Z-YVAD-fmk and Z-IETD-fmk, that inhibit caspases 1 and 4, and caspase 8 respectively. The Z-VEID-fmk inhibitor of caspase 6 was not active at all. Interestingly, the pan-caspase inhibitor Z-VAD-fmk was efficient up to 27%. Various conditions of inhibition were tried, with either longer preincubation time with caspase inhibitors before adding mini-CD40L and higher concentrations of inhibitors, but we never observed inhibition of apoptosis (data not shown), suggesting that apoptosis induced by mini-CD40L **1** is only partly mediated by caspase-dependent signaling. We are currently investigating the implication of serine proteases in the pro-apoptotic effect of mini-CD40L **1** on lymphoma. Serine proteases have been shown for example to contribute to CD44-mediated apoptosis in leukemia cells (53). Nevertheless, we have already observed some interesting intracellular effects mediated by mini-CD40L **1** as the implication of tyrosine-kinases and/or tyrosine-phosphatase. As shown by immunoblotting, mini-CD40L **1** induced tyrosine-phosphorylation on two groups of proteins in mouse A20 cells after 45 min of incubation, (Figure 4C). Interestingly, tyrosine-dephosphorylation was detected after 16 h of incubation, as shown by immunoblotting on Raji cell extracts after (Figure 4D). Earlier studies on lymphoma cells have indicated that the early events in CD40 signaling involved the complex interaction between protein tyrosine-phosphatases (PTP) and protein tyrosine kinases (PTK) (54).

We used the pan-phosphatase inhibitor sodium orthovanadate (Na_3VO_4) in apoptosis assays and observed a synergy between Na_3VO_4 and mini-CD40L **1** (Figure 4E). This suggests that mini-CD40L **1**-activated signaling pathways implicate PTP. In contrast, the PI3K inhibitor wortmannin (Wrt) only slightly influenced mini-CD40L **1**-induced apoptosis (Figure 4F). This observation contrasts with detection of PI3K activation in lymphoma cells treated with an anti-CD40 mAb (55). Nevertheless, inhibitor of Akt could synergize with mini-CD40L **1** (Figure 4G). Although we have shown that pathways engaged by different types of CD40 inducers could completely differ, we can not exclude a timing artifact, what we are currently checking. Moreover, the p53 inhibitor pifithrin- α (PFT- α) also synergized with mini-CD40L **1** (Figure 4H). For the moment, we can not give a complete view of signaling induced by mini-CD40L in lymphoma cells. Other pathways are currently under investigation. We have summarized results described here and in our previous works at the end of this paper (Figure 8).

*Cell signaling induced by mini-CD40L **1** in DCs.* Both the p38 and MEK1/2 MAPK pathways were shown to be induced by anti-CD40 mAb in human DCs (56). Here we showed that mini-CD40L **1** activated p38 and MEK1,2 in a dose-dependent manner (Figure 5A). Interestingly, although LPS activated the p38 pathway, it failed to induce the MEK1/2 pathways (Figure 5A). We are currently looking for activated downstream proteins, in particular the ERK1/2 and MK2 kinases are of particular interest (Figure 8). Furthermore, we showed that mini-CD40L **1** requires the PI3K pathway for maturation of DCs. D1 cell maturation induced by mini-CD40L **1** was greatly impaired in the presence of Wrt, as seen by the expression of maturation markers CD54 and CD86 after 24 h of incubation (Figure 5B). This is consistent with a paper that has described activation of the PI3K/Akt pathway in mouse DCs induced by soluble CD40L (57). Thus, our synthetic molecule is likely to mimic the soluble CD40L, even at the level of cell signaling.

*NF- κ B activation induced by mini-CD40L **1** in lymphoma and carcinoma cells.* Translocation of the NF- κ B transcription factor to the nucleus subsequent to its activation induced by CD40 was described in lymphoma (58) as well as in carcinoma cells (52). Therefore, we studied activation of NF- κ B in these cells. Mouse B lymphoma cells were

incubated with mini-CD40L **1** for 45 min and assessed by immunoblotting for I κ B- α degradation that precedes NF- κ B activation. Although LPS induced a net degradation of I κ B- α , mini-CD40L **1** could not activate this NF- κ B pathway. (Figure 6A). In the same manner, the carcinoma cells Renca were treated with mini-CD40L **1** at different times and concentrations. In these cells, mini-CD40L **1** efficiently induced degradation of I κ B- α (Figure 6B). Moreover, the functional translocation of NF- κ B to the nucleus was demonstrated by immunofluorescence and confocal microscopy on Renca cell treated for 45 min, fixed and permeabilized (Figure 6C). Thus, mini-CD40L **1** was shown to induce apoptosis on both the lymphoma and carcinoma cells. Nevertheless, signaling pathways engaged in this effect differ according to the cell type. Other MAPK pathways are currently investigated in carcinoma cells to better understand the differences in signaling pathways engaged by mini-CD40Ls. Noteworthy, activation of the alternative NF- κ B pathway has been described in CD40-activated DCs (59), B lymphocytes and transfected endothelial cells (60), but never in carcinoma nor in lymphoma cells. We are currently exploring this possibility with mini-CD40L **1**.

*Reorganization of lipid rafts induced by mini-CD40L **1** in lymphoma and carcinoma cell.* Rafts have been shown to play an important role in CD40-induced signaling, in particular in DCs (37) and B cell lymphoma (61). We first observed organization of these lipid microdomains at the surface of mouse B lymphoma cells incubated with mini-CD40L **1** for 1 h. Lipid rafts were stained with fluorescent-labeled subunit B of cholera toxin (CTB) on fixed cells. As shown in Figure 7A, unstimulated cells present punctuated fluorescence of very low intensity at the cell surface. Incubation of cells with mini-CD40L **1** led to an increase of the overall fluorescence, and most notably, a complete reorganization of lipid microdomains as filaments (Figure 7A, right). Such a filamentous staining was described for TRADD during TNF signaling (62). We hypothesize that CD40 triggering initiates a complete reorganization of the signalosome at the membrane. Implication of the cytoskeletal network is under investigation. Increase of fluorescence intensity of raft staining was confirmed by flow cytometry on the human B lymphoma BL41 cells (Figure 7B). Our results suggest that mini-CD40L **1** induce expression and/or translocation of raft components, as the ganglioside GM1 which is recognized by CTB, to

the extracellular side of the plasma membrane. Finally, mini-CD40L 1 induced similar effect on carcinoma (Figure 7C). On this epifluorescence image, staining appears like pili protuberating from the cell surface.

DISCUSSION

Like cells expressing other members of the TNF-R family (63), CD40-expressing cells are interesting targets for cancer immunotherapy. However, CD40-based therapies increase cytotoxic responses and could also treated CD40-negative malignancies (64, 65). This could be achieved by activating DCs and/or inducing differentiation of CD8⁺ T lymphocytes, or sensitizing tumor cells to other anti-cancer agents (66). Recently, a combination antibody-based therapy was proposed that conjugates the induction of tumor cell apoptosis by agonistic anti-TRAIL DR5, and the triggering of CD8⁺ cells by activation through CD40 and CD137 with the respective agonist antibodies (67). Furthermore, various phase 1 studies of CD40-targeted therapy in cancer patients have demonstrated relative good responses against some malignancies (68). These data reinforce the importance for developing new CD40 agonist molecules with less side effects and high chemical and biological stability, and that are amenable to large scale production.

However, the complex roles of the CD40 and CD40L proteins in different cells during tumorigenesis are not yet fully understood, but their comprehensive knowledge would be a prerequisite to the continuation and improvement of current strategies based on CD40 for treating cancer. For evidence, the recent finding that CD40 promotes neovascularization in a tumor-prone transgenic mouse model should alerts clinical investigators (69).

CD40-dependent signaling pathways have been depicted in many cell types (70). For example, activation of p38 and JNK have been described in B lymphocytes (71). Activation of the NF- κ B alternative pathway in DC (59). Ras, Raf, Rho and phosphatidylinositol 3-kinase (PI3K) activation was shown in endothelial cells (72). Caspases 3 and 8 (73) and caspase 9 activation was detected in carcinoma (74), and PI3K,

phospholipase C γ 2 (PLC γ 2) and Lyn in Burkitt lymphoma (55). Nevertheless, these data are lacking reliability, since they have been obtained using different types of stimuli, including anti-CD40 mAb, soluble or membrane-bound CD40L. The most striking example is the non-activity of mini-CD40L **1** on the degradation of I κ B- α in lymphoma cells (Figure 6A), what contrasts with data from the literature obtained on the same cell-type (75).

Here, we depicted some signaling pathways activated by mini-CD40L **1** in different cell types. We noticed that mini-CD40L **1**-induced signaling differs among cell type, even if it leads to the same biological outcome, as seen for apoptosis in lymphoma and carcinoma cells. In addition, mini-CD40L **1** activated DCs and B lymphocytes, suggesting that it could be used in anti-cancer treatment by both inducing an efficient immune response and directing cytotoxicity to malignant cells.

Because this work is still under investigation, we will not discuss further on these pathways, but better summarize on Figure 8 all the known pathways induced by mini-CD40L **1**, including results from our earlier studies.

ACKNOWLEDGMENTS

We thank our colleagues at the “laboratoire d’Immunologie et Chimie Thérapeutiques” for continuous interest and insightful discussions, in particular J.-P. Briand and S. Muller for continuous support; N. Bonnefoy-Berard and M. Flacher for providing the lymphoma cells, C.J.M. Melief for providing the dendritic cell line D1.

REFERENCES

1. Graf, D., Korthauer, U., Mages, H. W., Senger, G., and Kroczeck, R. A. (1992) Cloning of TRAP, a ligand for CD40 on human T cells, *Eur J Immunol* 22, 3191-3194.
2. Hollenbaugh, D., Grosmaire, L. S., Kullas, C. D., Chalupny, N. J., Braesch-Andersen, S., Noelle, R. J., Stamenkovic, I., Ledbetter, J. A., and Aruffo, A. (1992) The human T cell antigen gp39, a member of the TNF gene family, is a ligand for the CD40 receptor: expression of a soluble form of gp39 with B cell co-stimulatory activity, *Embo J* 11, 4313-4321.
3. Gauchat, J. F., Aubry, J. P., Mazzei, G., Life, P., Jomotte, T., Elson, G., and Bonnefoy, J. Y. (1993) Human CD40-ligand: molecular cloning, cellular distribution and regulation of expression by factors controlling IgE production, *FEBS Lett* 315, 259-266.
4. Locksley, R. M., Killeen, N., and Lenardo, M. J. (2001) The TNF and TNF receptor superfamilies: integrating mammalian biology, *Cell* 104, 487-501.
5. Bodmer, J. L., Schneider, P., and Tschopp, J. (2002) The molecular architecture of the TNF superfamily, *Trends Biochem Sci* 27, 19-26.
6. Armitage, R. J., Fanslow, W. C., Strockbine, L., Sato, T. A., Clifford, K. N., Macduff, B. M., Anderson, D. M., Gimpel, S. D., Davis-Smith, T., Maliszewski, C. R., and et al. (1992) Molecular and biological characterization of a murine ligand for CD40, *Nature* 357, 80-82.
7. Noelle, R. J., Roy, M., Shepherd, D. M., Stamenkovic, I., Ledbetter, J. A., and Aruffo, A. (1992) A 39-kDa protein on activated helper T cells binds CD40 and transduces the signal for cognate activation of B cells, *Proc Natl Acad Sci U S A* 89, 6550-6554.
8. Schonbeck, U., and Libby, P. (2001) The CD40/CD154 receptor/ligand dyad, *Cell Mol Life Sci* 58, 4-43.
9. Lane, P., Brocker, T., Hubele, S., Padovan, E., Lanzavecchia, A., and McConnell, F. (1993) Soluble CD40 ligand can replace the normal T cell-derived CD40 ligand signal to B cells in T cell-dependent activation, *J Exp Med* 177, 1209-1213.
10. Mazzei, G. J., Edgerton, M. D., Losberger, C., Lecoanet-Henchoz, S., Graber, P., Durandy, A., Gauchat, J. F., Bernard, A., Allet, B., and Bonnefoy, J. Y. (1995) Recombinant soluble trimeric CD40 ligand is biologically active, *J Biol Chem* 270, 7025-7028.
11. Younes, A., Snell, V., Consoli, U., Clodi, K., Zhao, S., Palmer, J. L., Thomas, E. K., Armitage, R. J., and Andreeff, M. (1998) Elevated levels of biologically active soluble CD40 ligand in the serum of patients with chronic lymphocytic leukaemia, *Br J Haematol* 100, 135-141.
12. Kato, K., Santana-Sahagun, E., Rassenti, L. Z., Weisman, M. H., Tamura, N., Kobayashi, S., Hashimoto, H., and Kipps, T. J. (1999) The soluble CD40 ligand sCD154 in systemic lupus erythematosus, *J Clin Invest* 104, 947-955.
13. Aukrust, P., Muller, F., Ueland, T., Berget, T., Aaser, E., Brunsvig, A., Solum, N. O., Forfang, K., Froland, S. S., and Gullestad, L. (1999) Enhanced levels of soluble and membrane-bound CD40 ligand in patients with unstable angina. Possible reflection of T lymphocyte and platelet involvement in the pathogenesis of acute coronary syndromes, *Circulation* 100, 614-620.
14. Cipollone, F., Mezzetti, A., Porreca, E., Di Febbo, C., Nutini, M., Fazio, M., Falco, A., Cuccurullo, F., and Davi, G. (2002) Association between enhanced soluble CD40L and prothrombotic state in hypercholesterolemia: effects of statin therapy, *Circulation* 106, 399-402.

15. Danese, S., Katz, J. A., Saibeni, S., Papa, A., Gasbarrini, A., Vecchi, M., and Fiocchi, C. (2003) Activated platelets are the source of elevated levels of soluble CD40 ligand in the circulation of inflammatory bowel disease patients, *Gut* 52, 1435-1441.
16. Vishnevetsky, D., Kiyani, V. A., and Gandhi, P. J. (2004) CD40 ligand: a novel target in the fight against cardiovascular disease, *Ann Pharmacother* 38, 1500-1508.
17. Sui, Z., Sniderhan, L. F., Schifitto, G., Phipps, R. P., Gelbard, H. A., Dewhurst, S., and Maggirwar, S. B. (2007) Functional Synergy between CD40 Ligand and HIV-1 Tat Contributes to Inflammation: Implications in HIV Type 1 Dementia, *J Immunol* 178, 3226-3236.
18. Stamenkovic, I., Clark, E. A., and Seed, B. (1989) A B-lymphocyte activation molecule related to the nerve growth factor receptor and induced by cytokines in carcinomas, *Embo J* 8, 1403-1410.
19. Koho, H., Paulie, S., Ben-Aissa, H., Jonsdottir, I., Hansson, Y., Lundblad, M. L., and Perlmann, P. (1984) Monoclonal antibodies to antigens associated with transitional cell carcinoma of the human urinary bladder. I. Determination of the selectivity of six antibodies by cell ELISA and immunofluorescence, *Cancer Immunol Immunother* 17, 165-172.
20. Paulie, S., Koho, H., Ben-Aissa, H., Hansson, Y., Lundblad, M. L., and Perlmann, P. (1984) Monoclonal antibodies to antigens associated with transitional cell carcinoma of the human urinary bladder. II. Identification of the cellular target structures by immunoprecipitation and SDS-PAGE analysis, *Cancer Immunol Immunother* 17, 173-179.
21. Paulie, S., Ehlin-Henriksson, B., Mellstedt, H., Koho, H., Ben-Aissa, H., and Perlmann, P. (1985) A p50 surface antigen restricted to human urinary bladder carcinomas and B lymphocytes, *Cancer Immunol Immunother* 20, 23-28.
22. Uckun, F. M., Gajl-Peczalska, K., Myers, D. E., Jaszcz, W., Haissig, S., and Ledbetter, J. A. (1990) Temporal association of CD40 antigen expression with discrete stages of human B-cell ontogeny and the efficacy of anti-CD40 immunotoxins against clonogenic B-lineage acute lymphoblastic leukemia as well as B-lineage non-Hodgkin's lymphoma cells, *Blood* 76, 2449-2456.
23. Banchereau, J., Bazan, F., Blanchard, D., Briere, F., Galizzi, J. P., van Kooten, C., Liu, Y. J., Rousset, F., and Saeland, S. (1994) The CD40 antigen and its ligand, *Annu Rev Immunol* 12, 881-922.
24. van Kooten, C., and Banchereau, J. (2000) CD40-CD40 ligand, *J Leukoc Biol* 67, 2-17.
25. Bennett, S. R., Carbone, F. R., Karamalis, F., Flavell, R. A., Miller, J. F., and Heath, W. R. (1998) Help for cytotoxic-T-cell responses is mediated by CD40 signalling, *Nature* 393, 478-480.
26. Schoenberger, S. P., Toes, R. E., van der Voort, E. I., Offringa, R., and Melief, C. J. (1998) T-cell help for cytotoxic T lymphocytes is mediated by CD40-CD40L interactions, *Nature* 393, 480-483.
27. Funakoshi, S., Longo, D. L., Beckwith, M., Conley, D. K., Tsarfaty, G., Tsarfaty, I., Armitage, R. J., Fanslow, W. C., Spriggs, M. K., and Murphy, W. J. (1994) Inhibition of human B-cell lymphoma growth by CD40 stimulation, *Blood* 83, 2787-2794.
28. Hirano, A., Longo, D. L., Taub, D. D., Ferris, D. K., Young, L. S., Eliopoulos, A. G., Agathangelou, A., Cullen, N., Macartney, J., Fanslow, W. C., and Murphy, W. J. (1999) Inhibition of human breast carcinoma growth by a soluble recombinant human CD40 ligand, *Blood* 93, 2999-3007.
29. French, R. R., Chan, H. T., Tutt, A. L., and Glennie, M. J. (1999) CD40 antibody evokes a cytotoxic T-cell response that eradicates lymphoma and bypasses T-cell help, *Nat Med* 5, 548-553.

30. Tong, A. W., Seamour, B., Chen, J., Su, D., Ordonez, G., Frase, L., Netto, G., and Stone, M. J. (2000) CD40 ligand-induced apoptosis is Fas-independent in human multiple myeloma cells, *Leuk Lymphoma* 36, 543-558.
31. Fujita, N., Kagamu, H., Yoshizawa, H., Itoh, K., Kuriyama, H., Matsumoto, N., Ishiguro, T., Tanaka, J., Suzuki, E., Hamada, H., and Gejyo, F. (2001) CD40 ligand promotes priming of fully potent antitumor CD4(+) T cells in draining lymph nodes in the presence of apoptotic tumor cells, *J Immunol* 167, 5678-5688.
32. Karpusas, M., Hsu, Y. M., Wang, J. H., Thompson, J., Lederman, S., Chess, L., and Thomas, D. (1995) 2 A crystal structure of an extracellular fragment of human CD40 ligand, *Structure* 3, 1031-1039.
33. Banner, D. W., D'Arcy, A., Janes, W., Gentz, R., Schoenfeld, H. J., Broger, C., Loetscher, H., and Lesslauer, W. (1993) Crystal structure of the soluble human 55 kd TNF receptor-human TNF beta complex: implications for TNF receptor activation, *Cell* 73, 431-445.
34. Singh, J., Garber, E., Van Vlijmen, H., Karpusas, M., Hsu, Y. M., Zheng, Z., Naismith, J. H., and Thomas, D. (1998) The role of polar interactions in the molecular recognition of CD40L with its receptor CD40, *Protein Sci* 7, 1124-1135.
35. Inui, S., Kaisho, T., Kikutani, H., Stamenkovic, I., Seed, B., Clark, E. A., and Kishimoto, T. (1990) Identification of the intracytoplasmic region essential for signal transduction through a B cell activation molecule, CD40, *Eur J Immunol* 20, 1747-1753.
36. Hostager, B. S., Catlett, I. M., and Bishop, G. A. (2000) Recruitment of CD40 and tumor necrosis factor receptor-associated factors 2 and 3 to membrane microdomains during CD40 signaling, *J Biol Chem* 275, 15392-15398.
37. Vidalain, P. O., Azocar, O., Servet-Delprat, C., Rabourdin-Combe, C., Gerlier, D., and Manie, S. (2000) CD40 signaling in human dendritic cells is initiated within membrane rafts, *Embo J* 19, 3304-3313.
38. Wajant, H., Henkler, F., and Scheurich, P. (2001) The TNF-receptor-associated factor family: scaffold molecules for cytokine receptors, kinases and their regulators, *Cell Signal* 13, 389-400.
39. Paulie, S., Rosen, A., Ehlin-Henriksson, B., Braesch-Andersen, S., Jakobson, E., Koho, H., and Perlmann, P. (1989) The human B lymphocyte and carcinoma antigen, CDw40, is a phosphoprotein involved in growth signal transduction, *J Immunol* 142, 590-595.
40. Bjorck, P., Braesch-Andersen, S., and Paulie, S. (1994) Antibodies to distinct epitopes on the CD40 molecule co-operate in stimulation and can be used for the detection of soluble CD40, *Immunology* 83, 430-437.
41. Fanslow, W. C., Srinivasan, S., Paxton, R., Gibson, M. G., Spriggs, M. K., and Armitage, R. J. (1994) Structural characteristics of CD40 ligand that determine biological function, *Semin Immunol* 6, 267-278.
42. Ledbetter, J. A., Francisco, J. A., Siegall, C. B., Gilliland, L. K., Hollenbaugh, D., Aruffo, A., Siadak, A. W., Mischel-Petty, N., Grosmaire, L. S., Gordon, M. L., Brown, T. J., Moran-Davis, P., Mittler, R. S., Kiener, P. A., and Nadler, S. G. (1997) Agonistic activity of a CD40-specific single-chain Fv constructed from the variable regions of mAb G28-5, *Crit Rev Immunol* 17, 427-435.
43. Pound, J. D., Challa, A., Holder, M. J., Armitage, R. J., Dower, S. K., Fanslow, W. C., Kikutani, H., Paulie, S., Gregory, C. D., and Gordon, J. (1999) Minimal cross-linking and epitope requirements for CD40-dependent suppression of apoptosis contrast with those for promotion of the cell cycle and homotypic adhesions in human B cells, *Int Immunol* 11, 11-20.
44. Fournel, S., Wieckowski, S., Sun, W., Trouche, N., Dumortier, H., Bianco, A., Chaloin, O., Habib, M., Peter, J. C., Schneider, P., Vray, B., Toes, R. E., Offringa, R., Melief, C.

- J., Hoebeke, J., and Guichard, G. (2005) C3-symmetric peptide scaffolds are functional mimetics of trimeric CD40L, *Nat Chem Biol* 1, 377-382.
45. Bianco, A., Fournel, S., Wieckowski, S., Hoebeke, J., and Guichard, G. (2006) Solid-phase synthesis of CD40L mimetics, *Org Biomol Chem* 4, 1461-1463.
 46. Wieckowski, S., Trouche, N., Chaloin, O., Guichard, G., Fournel, S., and Hoebeke, J. (2007) Cooperativity in the Interaction of Synthetic CD40L Mimetics with CD40 and Its Implication in Cell Signaling, *Biochemistry* 46, 3482-3493.
 47. Winzler, C., Rovere, P., Rescigno, M., Granucci, F., Penna, G., Adorini, L., Zimmermann, V. S., Davoust, J., and Ricciardi-Castagnoli, P. (1997) Maturation stages of mouse dendritic cells in growth factor-dependent long-term cultures, *J Exp Med* 185, 317-328.
 48. Lutz, M. B., Kukutsch, N., Ogilvie, A. L., Rossner, S., Koch, F., Romani, N., and Schuler, G. (1999) An advanced culture method for generating large quantities of highly pure dendritic cells from mouse bone marrow, *J Immunol Methods* 223, 77-92.
 49. Watford, W. T., Moriguchi, M., Morinobu, A., and O'Shea, J. J. (2003) The biology of IL-12: coordinating innate and adaptive immune responses, *Cytokine Growth Factor Rev* 14, 361-368.
 50. Langrish, C. L., McKenzie, B. S., Wilson, N. J., de Waal Malefyt, R., Kastelein, R. A., and Cua, D. J. (2004) IL-12 and IL-23: master regulators of innate and adaptive immunity, *Immunol Rev* 202, 96-105.
 51. Schattner, E. J., Mascarenhas, J., Bishop, J., Yoo, D. H., Chadburn, A., Crow, M. K., and Friedman, S. M. (1996) CD4+ T-cell induction of Fas-mediated apoptosis in Burkitt's lymphoma B cells, *Blood* 88, 1375-1382.
 52. Davies, C. C., Bem, D., Young, L. S., and Eliopoulos, A. G. (2005) NF-kappaB overrides the apoptotic program of TNF receptor 1 but not CD40 in carcinoma cells, *Cell Signal* 17, 729-738.
 53. Maquarre, E., Artus, C., Gadhoun, Z., Jasmin, C., Smadja-Joffe, F., and Robert-Lezenes, J. (2005) CD44 ligation induces apoptosis via caspase- and serine protease-dependent pathways in acute promyelocytic leukemia cells, *Leukemia* 19, 2296-2303.
 54. Faris, M., Gaskin, F., Parsons, J. T., and Fu, S. M. (1994) CD40 signaling pathway: anti-CD40 monoclonal antibody induces rapid dephosphorylation and phosphorylation of tyrosine-phosphorylated proteins including protein tyrosine kinase Lyn, Fyn, and Syk and the appearance of a 28-kD tyrosine phosphorylated protein, *J Exp Med* 179, 1923-1931.
 55. Ren, C. L., Morio, T., Fu, S. M., and Geha, R. S. (1994) Signal transduction via CD40 involves activation of lyn kinase and phosphatidylinositol-3-kinase, and phosphorylation of phospholipase C gamma 2, *J Exp Med* 179, 673-680.
 56. Aicher, A., Shu, G. L., Magaletti, D., Mulvanian, T., Pezzutto, A., Craxton, A., and Clark, E. A. (1999) Differential role for p38 mitogen-activated protein kinase in regulating CD40-induced gene expression in dendritic cells and B cells, *J Immunol* 163, 5786-5795.
 57. Arron, J. R., Vologodskaya, M., Wong, B. R., Naramura, M., Kim, N., Gu, H., and Choi, Y. (2001) A positive regulatory role for Cbl family proteins in tumor necrosis factor-related activation-induced cytokine (trance) and CD40L-mediated Akt activation, *J Biol Chem* 276, 30011-30017.
 58. Berberich, I., Shu, G. L., and Clark, E. A. (1994) Cross-linking CD40 on B cells rapidly activates nuclear factor-kappa B, *J Immunol* 153, 4357-4366.
 59. Yanagawa, Y., and Onoe, K. (2006) Distinct regulation of CD40-mediated interleukin-6 and interleukin-12 productions via mitogen-activated protein kinase and nuclear factor kappaB-inducing kinase in mature dendritic cells, *Immunology* 117, 526-535.
 60. Coope, H. J., Atkinson, P. G., Huhse, B., Belich, M., Janzen, J., Holman, M. J., Klaus, G. G., Johnston, L. H., and Ley, S. C. (2002) CD40 regulates the processing of NF-kappaB2 p100 to p52, *Embo J* 21, 5375-5385.

61. Pham, L. V., Tamayo, A. T., Yoshimura, L. C., Lo, P., Terry, N., Reid, P. S., and Ford, R. J. (2002) A CD40 Signalosome anchored in lipid rafts leads to constitutive activation of NF-kappaB and autonomous cell growth in B cell lymphomas, *Immunity* 16, 37-50.
62. Fotin-Mleczek, M., Henkler, F., Samel, D., Reichwein, M., Hausser, A., Parmryd, I., Scheurich, P., Schmid, J. A., and Wajant, H. (2002) Apoptotic crosstalk of TNF receptors: TNF-R2-induces depletion of TRAF2 and IAP proteins and accelerates TNF-R1-dependent activation of caspase-8, *J Cell Sci* 115, 2757-2770.
63. Tamada, K., and Chen, L. (2005) Renewed interest in cancer immunotherapy with the tumor necrosis factor superfamily molecules, *Cancer Immunol Immunother*, 1-8.
64. Tutt, A. L., O'Brien, L., Hussain, A., Crowther, G. R., French, R. R., and Glennie, M. J. (2002) T cell immunity to lymphoma following treatment with anti-CD40 monoclonal antibody, *J Immunol* 168, 2720-2728.
65. van Mierlo, G. J., den Boer, A. T., Medema, J. P., van der Voort, E. I., Franssen, M. F., Offringa, R., Melief, C. J., and Toes, R. E. (2002) CD40 stimulation leads to effective therapy of CD40(-) tumors through induction of strong systemic cytotoxic T lymphocyte immunity, *Proc Natl Acad Sci U S A* 99, 5561-5566.
66. Eliopoulos, A. G., and Young, L. S. (2004) The role of the CD40 pathway in the pathogenesis and treatment of cancer, *Curr Opin Pharmacol* 4, 360-367.
67. Uno, T., Takeda, K., Kojima, Y., Yoshizawa, H., Akiba, H., Mittler, R. S., Gejyo, F., Okumura, K., Yagita, H., and Smyth, M. J. (2006) Eradication of established tumors in mice by a combination antibody-based therapy, *Nat Med* 12, 693.
68. Vonderheide, R. H. (2007) Prospect of targeting the CD40 pathway for cancer therapy, *Clin Cancer Res* 13, 1083-1088.
69. Chiodoni, C., Iezzi, M., Guiducci, C., Sangaletti, S., Alessandrini, I., Ratti, C., Tiboni, F., Musiani, P., Granger, D. N., and Colombo, M. P. (2006) Triggering CD40 on endothelial cells contributes to tumor growth, *J Exp Med* 203, 2441-2450.
70. Grammer, A. C., and Lipsky, P. E. (2000) CD40-mediated regulation of immune responses by TRAF-dependent and TRAF-independent signaling mechanisms, *Adv Immunol* 76, 61-178.
71. Gallagher, E., Enzler, T., Matsuzawa, A., Anzelon-Mills, A., Otero, D., Holzer, R., Janssen, E., Gao, M., and Karin, M. (2007) Kinase MEKK1 is required for CD40-dependent activation of the kinases Jnk and p38, germinal center formation, B cell proliferation and antibody production, *Nat Immunol* 8, 57-63.
72. Flaxenburg, J. A., Melter, M., Lapchak, P. H., Briscoe, D. M., and Pal, S. (2004) The CD40-induced signaling pathway in endothelial cells resulting in the overexpression of vascular endothelial growth factor involves Ras and phosphatidylinositol 3-kinase, *J Immunol* 172, 7503-7509.
73. Eliopoulos, A. G., Davies, C., Knox, P. G., Gallagher, N. J., Afford, S. C., Adams, D. H., and Young, L. S. (2000) CD40 induces apoptosis in carcinoma cells through activation of cytotoxic ligands of the tumor necrosis factor superfamily, *Mol Cell Biol* 20, 5503-5515.
74. Georgopoulos, N. T., Steele, L. P., Thomson, M. J., Selby, P. J., Southgate, J., and Trejdosiewicz, L. K. (2006) A novel mechanism of CD40-induced apoptosis of carcinoma cells involving TRAF3 and JNK/AP-1 activation, *Cell Death Differ* 13, 1789-1801.
75. Hollmann, A. C., Q. Gong, and T. Owens. (2002) CD40-mediated apoptosis in murine B-lymphoma lines containing mutated p53. *Exp Cell Res* 280, 201-211.

FIGURE LEGENDS

Figure 1. Induction of apoptosis with mini-CD40L **1** (46) on various human and mouse lymphoma cells, as detected by a reduction in the $\Delta\psi_m$. (A) Effect of mini-CD40L **1** on human B lymphoma cell lines BL41, Raji, BL60, BJAB, Ramos and BP3, and on mouse B lymphoma cell lines A20 and WEHI 231, after incubation for 16 h. (B) Mini-CD40L **1** induced apoptosis of Renca cells, both from maintenance (Renca cell line) or freshly recovered from solid tumors transplanted in BALB/c mice (BALB/c Renca). Membrane expression of the human or mouse CD40 protein as measured by flow cytometry are shown in the inset for each cell line. Results are representative of at least two independent experiments.

Figure 2. Mini-CD40L **1** induces maturation of BMDC, up-regulates IL-23 production in D1 cells, and synergizes with IL-4 in the proliferation of B lymphocytes. (A) BMDC were treated with LPS (10 $\mu\text{g/mL}$), mini-CD40L **1** (10 μM) or a control mini-CD40L consisting of the CD40-binding peptide with spacer and lacking the core platform (40 μM), or left in medium alone for 24 h. Cells were then stained for the maturation markers CD40, CD54, CD80 and CD86. (B) Mini-CD40L **1** induced expression of *IL23 p19* mRNA as measured by comparative RT-PCR after treatment for 16 h. *GAPDH* was used as a housekeeping gene control. (C) The IL-23 p19/p40 cytokine was measured in the supernatant of D1 cells treated with mini-CD40L **1** at the indicated concentration for 16 h by ELISA. (D) Normal CD19-positive lymphocytes were purified from spleen of BALB/c mice and incubated with mini-CD40L **1** in the presence or not of IL-4 at the

indicated concentration for 72 h, including a pulse of ^3H -thymidine of 16 h. Results are expressed in cpm. Data are representative of two independent experiments.

Figure 3. CD95 is not implicated in the pro-apoptotic effects of mini-CD40L of human B lymphoma. (A) Inhibition of the membrane CD40L-induced expression of CD95 (Fas) by mini-CD40L as detected by flow cytometry after incubation of BL41 (CD19-positive) with 3T6 or 3T6-CD40L cells in the presence or not of mini-CD40L **1** or an anti-CD40L mAb (6 $\mu\text{g}/\text{mL}$) for 24 h. Percentage of $\text{CD19}^+\text{CD95}^+$ cells is indicated for each dot plot. (B) Induction of the expression of Fas by soluble recombinant CD40L, mini-CD40L or an anti-CD40 mAb, as detected by flow cytometry after a 24 h. Treatment Percentage of CD95^+ cells is given for each dot plot. (C) Effect of the antagonistic anti-CD95 mAb ZB4 on the apoptotic effect of mini-CD40L on BL41 cells as detected by a reduction in the in $\Delta\psi_m$. Efficiency of ZB4 was tested on the apoptotic effect of the agonistic anti-CD95 mAb 7C11 on Jurkat cells. Percentage of apoptotic cells are indicated for each panel. All the data are representative of two independent experiments.

Figure 4. Signaling implicated in the pro-apoptotic effect of mini-CD40L **1** in lymphoma cells. (A) Activation of caspase 3 was assessed by degradation of the pro- to the active-form as detected by immunoblotting on cell extracts after 16 h of incubation with the indicated stimulus. Positive control was provided by incubation of Jurkat T cells with agonistic anti-CD95 mAb. (B) Inhibition of apoptosis in BL41 cells by various caspase inhibitors as detected by a reduction in the $\Delta\psi_m$ after 4 h of pre-treatment with or without

the indicated caspase inhibitor at 40 μM for 1×10^6 cells/mL, and an additional 16 h of treatment with mini-CD40L **1**. Final concentrations of caspase inhibitors and mini-CD40L were 20 μM each, for 5×10^6 cells/mL. Data are representative of three independent experiments with various times of pre-treatment with the caspase inhibitors. (C) The mouse B lymphoma A20 cells were incubated with mini-CD40L **1** at the indicated concentrations. After 45 min, cell extracts were blotted against anti-phosphotyrosine. (D) Human B lymphoma Raji cells were incubated with mini-CD40L **1** at the indicated concentration. After 16 h of incubation, cells extracts were blotted against anti-phosphotyrosine. (E) Orthovanadate (Na_3VO_4), a pan phosphatase inhibitor, was added to Raji cell culture in the presence of the indicated concentration of mini-CD40L **1**. After 16 h of incubation, apoptosis was assessed by decrease of $\Delta\psi_m$. (F) Induction of apoptosis in BL41 cells by mini-CD40L **1** in the presence of Wortmannin, an inhibitor of PI3-K (F), pifithrin- α , an inhibitor of p53 (G), or inhibitor of Akt (H) was also detected. Data are representative of two independent experiments.

Figure 5. Signaling induced in D1 dendritic cells. (A) Induction of the p38 and MEK1/2 MAPK pathways by mini-CD40L. Cells were treated with mini-CD40L **1** at the indicated concentration for 45 min and cell extracts assessed by immunoblotting with anti-phospho-p38 and anti-p38 as an internal loading control. Ratio of the intensity of the band of the phosphorylated form on the intensity of the band of total, form were calculated and reported to the ratio calculated for the medium. An independent similar experiment was achieved for detection of the MEK1/2 pathway activation. Data are representative of two independent experiments. (B) Implication of PI3-K in the

maturation effect of mini-CD40L **1**. D1 cells were treated with mini-CD40L **1** at 5 μM for 24 h in the presence or not of Wortmannin at 80 nM and stained for the maturation markers CD54 and CD86. Filled histograms represent cells treated in medium, and open histograms represent cells treated with mini-CD40L **1**.

Figure 6. Activation of the NF- κ B pathway in lymphoma and carcinoma cells. (A) Mouse B lymphoma cells A20 were treated for 45 min with mini-CD40L **1** at the indicated concentration, or LPS at 10 $\mu\text{g}/\text{mL}$. Cell extracts were then blotted for determination of I κ B- α degradation. (B) Activation of the NF- κ B pathway in Renca carcinoma cells treated with mini-CD40L **1** at the indicated time and concentration, as assessed by detection of I κ B- α degradation. (C) Translocation of NF- κ B p50 to the nucleus of Renca cells incubated with CD40L. Renca cells were treated for 1 h, washed, fixed in 2% paraformaldehyde, permeabilized in Triton X-100 for 5 min, and incubated with rabbit anti-NF- κ B for 2 h. Thus, cells were incubated with goat anti-rabbit immunoglobulin conjugated to Alexa Fluor 488 for 1 h. After two washes in PBS, cells were resuspended in Fluorescent Mounting Medium and analyzed by confocal microscopy. Bright field and fluorescence channels are shown merged. Yellow bar represents 5 μm . All these data are representative of two independent experiments.

Figure 7. Reorganization of the lipid rafts subsequent to treatment with mini-CD40L **1**. (A) Mini-CD40L **1** induced rearrangement of lipid rafts at the plasma membrane of A20 as observed by epifluorescence microscopy. Cells were incubated in medium alone or with 10 μM mini-CD40L **1** at 37 $^{\circ}\text{C}$ for 1 h, washed, fixed in 1% paraformaldehyde for

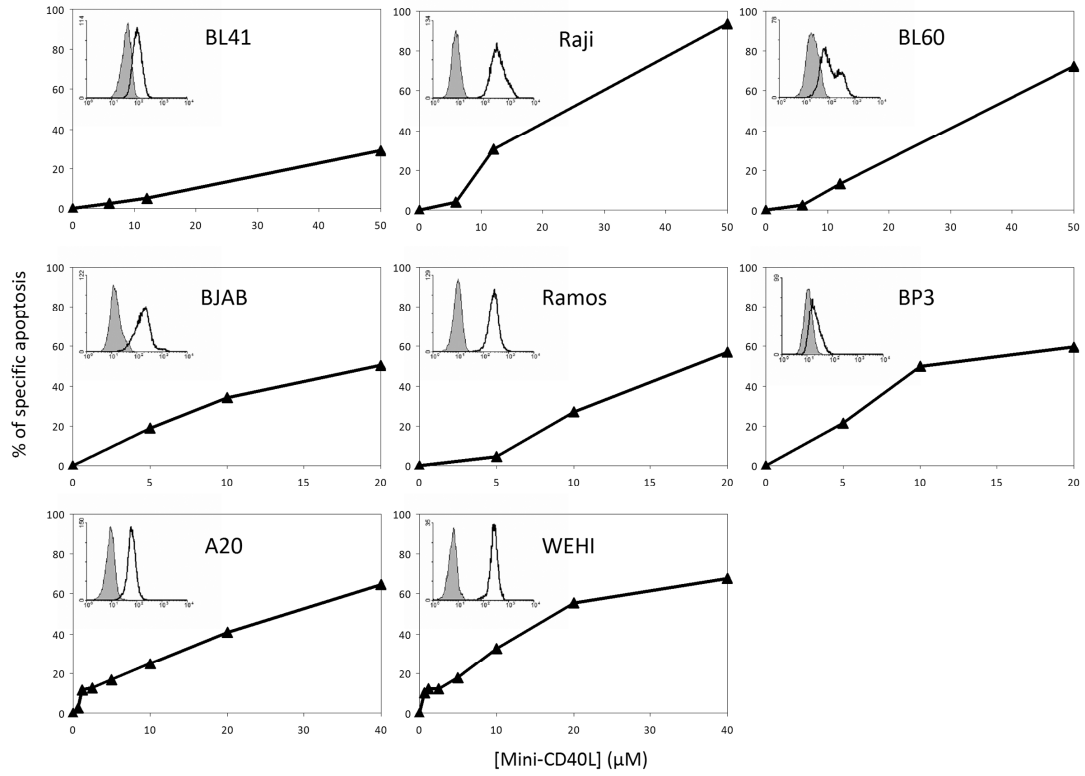
10 min and thus stained with CTB-FITC at 10 $\mu\text{g}/\text{mL}$ for 30 min in PBS. Yellow bar represents 5 μm (B) In the same manner, CTB-FITC and autofluorescence staining intensities were measured by flow cytometry after treatment with the indicated concentration of mini-CD40L **1**. (C) CTB-FITC staining of Renca carcinoma cells treated with 10 μM of mini-CD40L **1** for 30 min. Data are representative of two independent experiments.

Figure 8. Summary of the signaling pathways induced by mini-CD40L **1** in various cell types. Pathways that have been directly shown to be activated by mini-CD40L **1** are represented by red arrow (activation) or red line (inhibition). Biological effects are denoted in red. Pathways that have been shown not to be implicated in mini-CD40L **1** signaling are represented as crossed arrows. Pathways that may be implicated and that are currently under investigation are indicated by the “?” symbol.

FIGURES

Figure 1

A.



B.

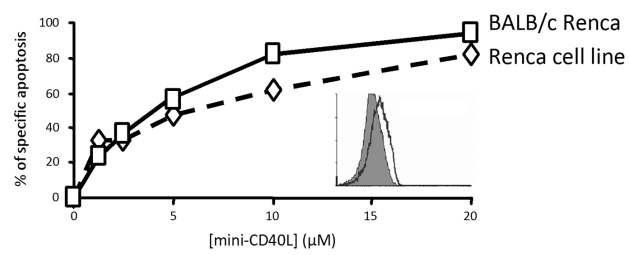


Figure 2

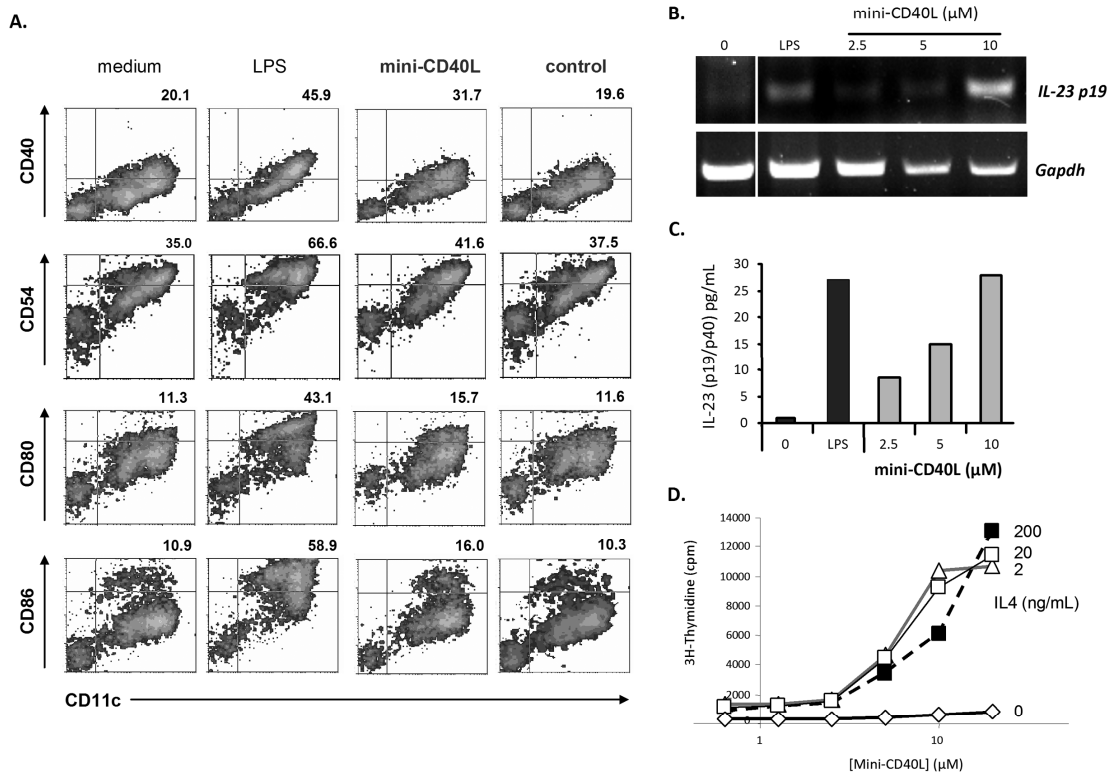


Figure 3

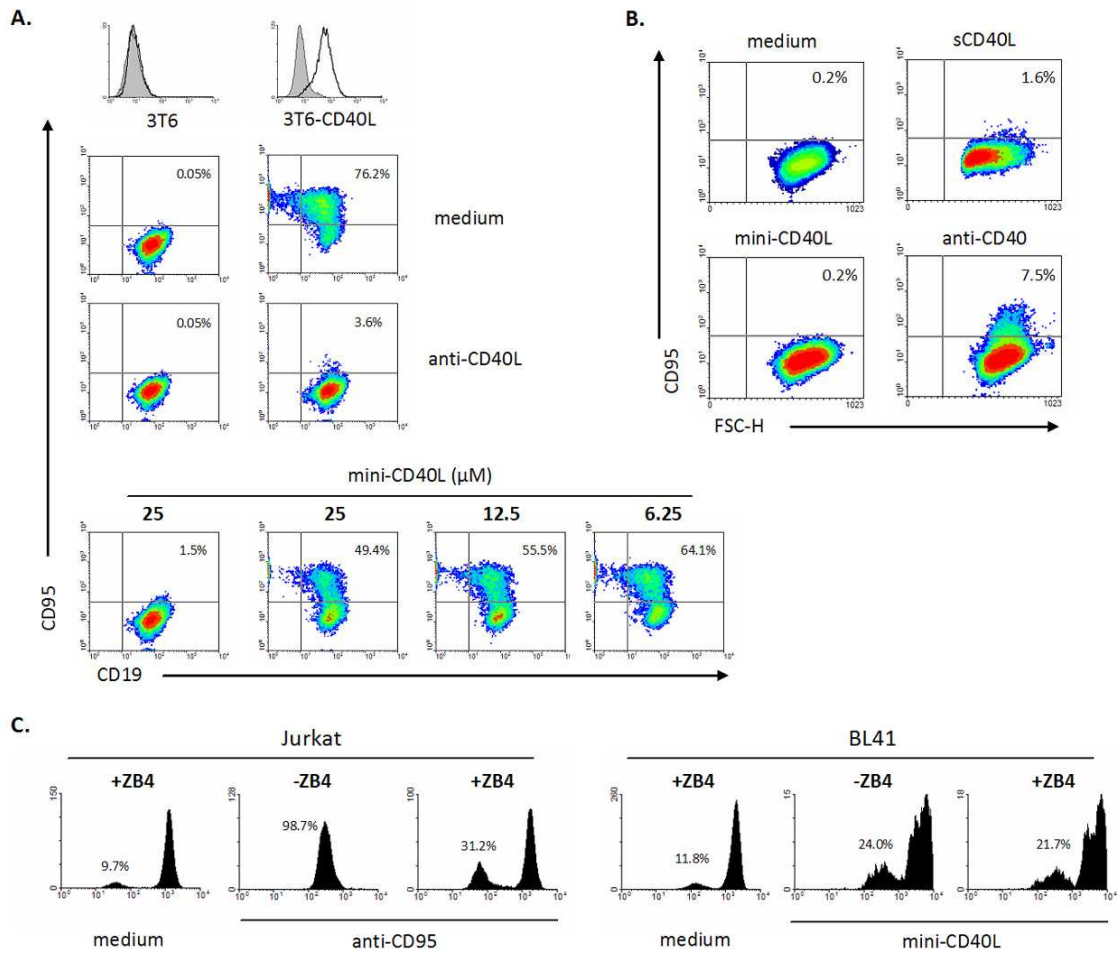


Figure 4

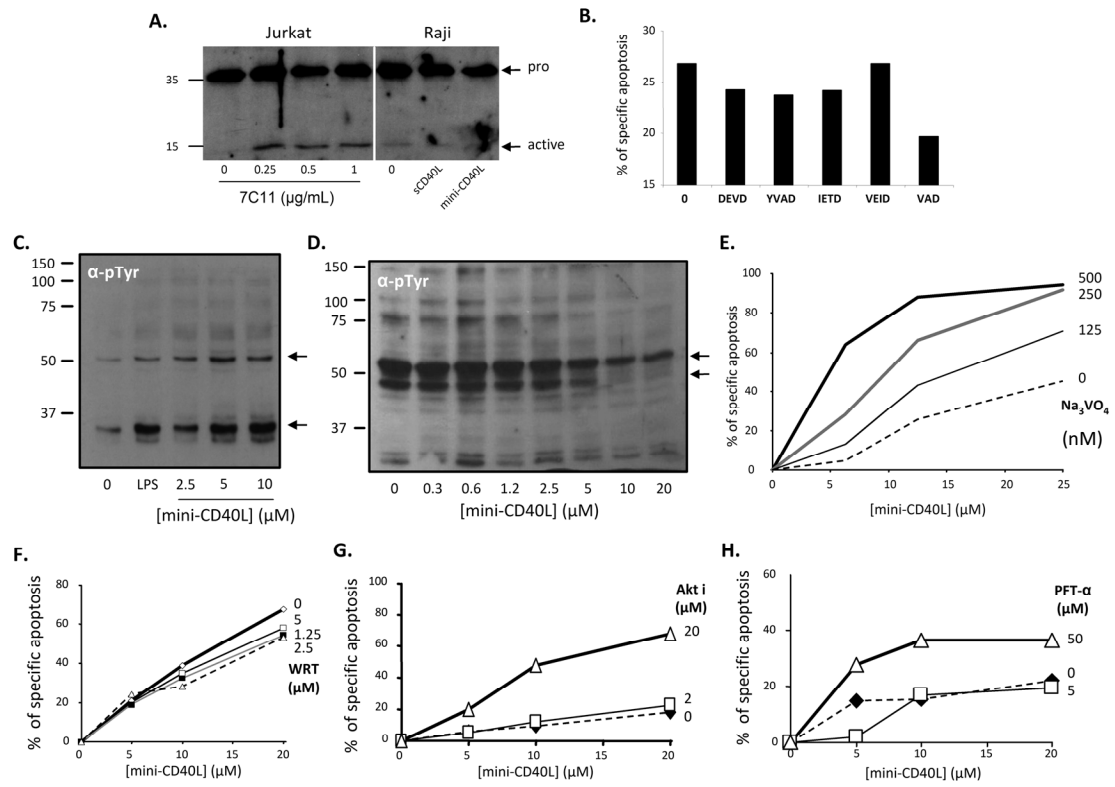


Figure 5

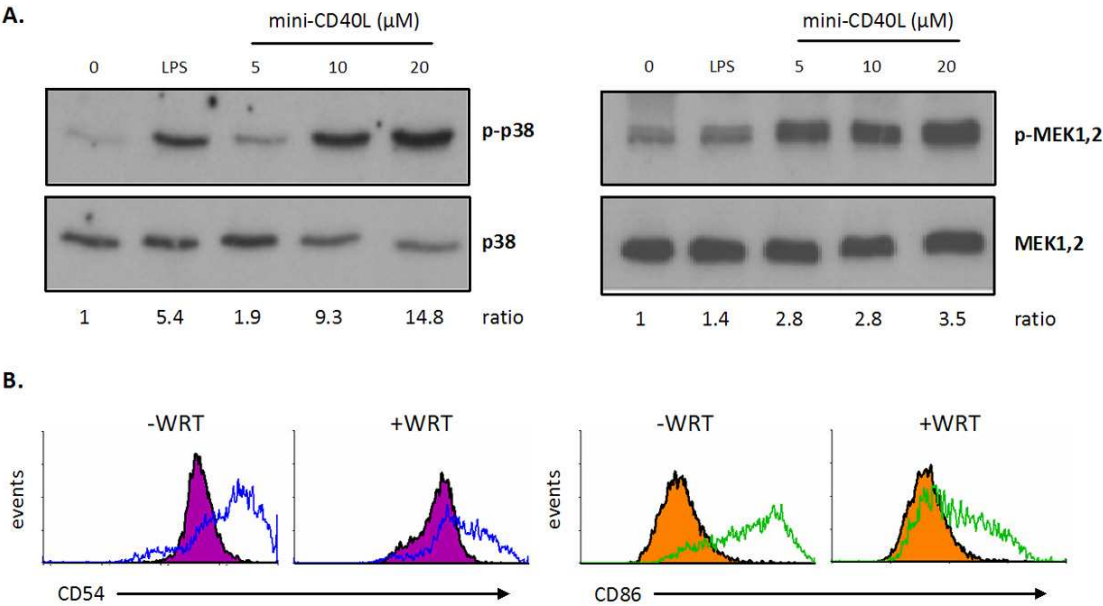


Figure 6

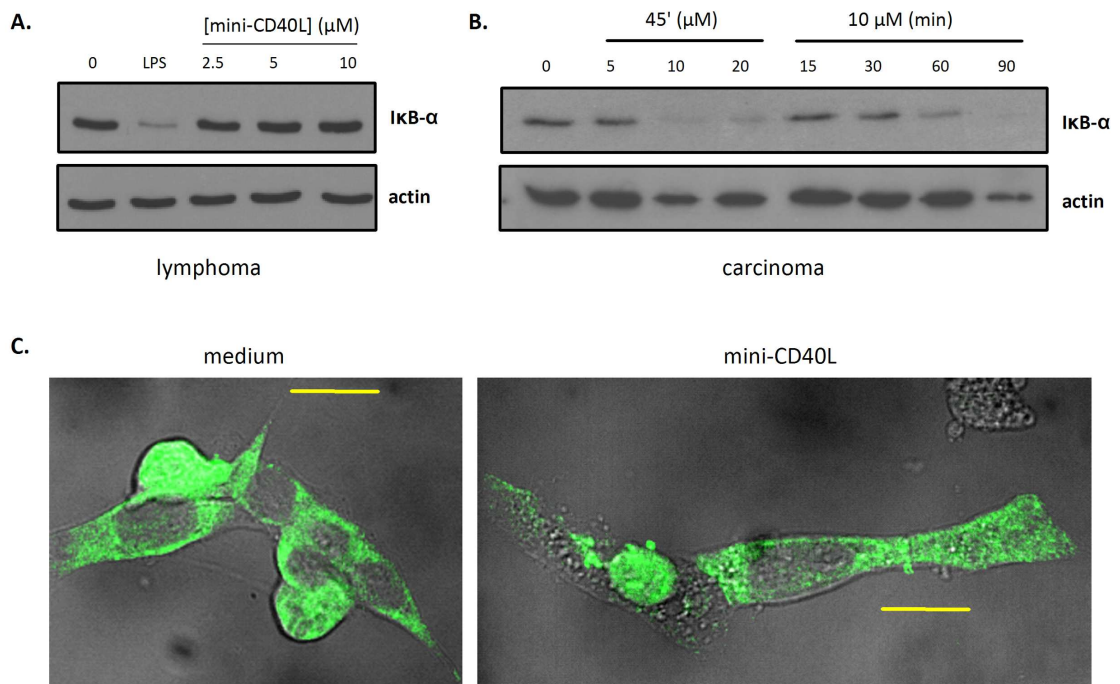
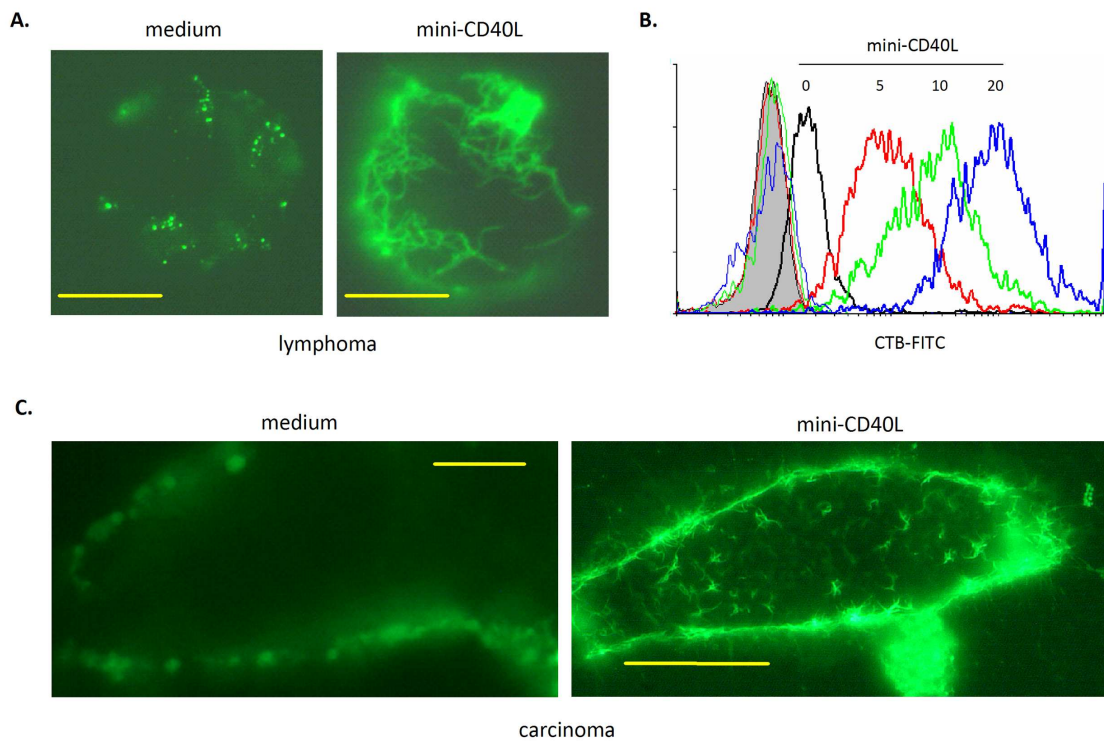


Figure 7



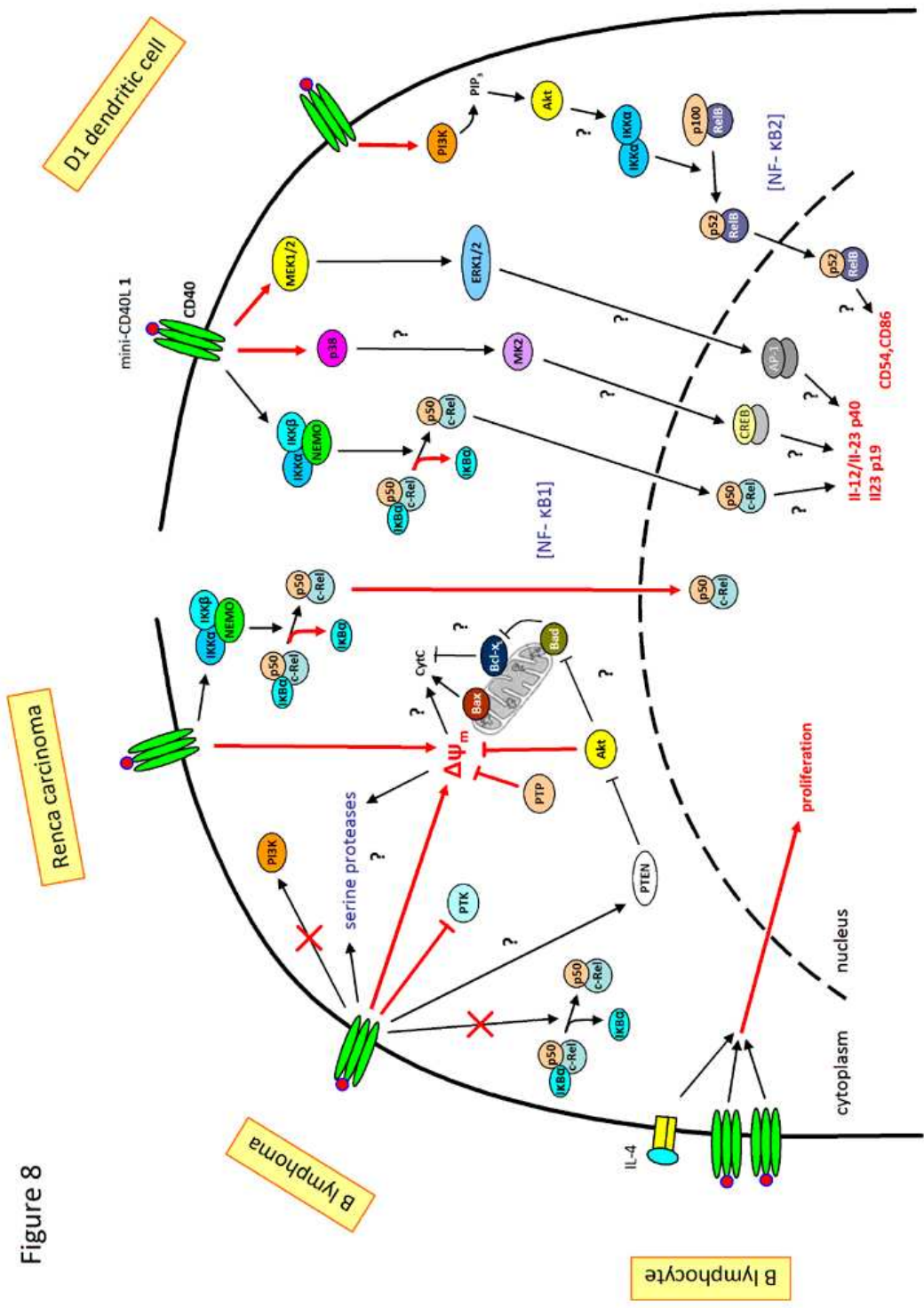


Figure 8

CHAPTER 10

SMALL MOLECULE CD40L MIMETICS PROMOTE CONTROL OF PARASITEMIA AND ENHANCE T CELLS PRODUCING INTERFERON- γ DURING EXPERIMENTAL TRYPANOSOMA CRUZI INFECTION[†]

J Immunol 178, 6700-6704 (2007)

Habib, M., Rivas, M. N., Chamekh, M., **Wieckowski, S.**, Sun, W.,
Bianco, A., Trouche, N., Chaloin, O., Dumortier, H., Goldman, M.,
Guichard, G., Fournel, S., and Vray, B. [[†] collaboration]

CHAPTER 10

From the start of the study, we have provided numerous informations on the efficiency of mini-CD40L in various biochemical and biological systems. We have demonstrated that mini-CD40Ls i) induce a clear pro-apoptotic effect on malignant cells, and ii) initiate both dendritic cells and B lymphocyte activation. The last chapter describes the *in vivo* application of mini-CD40Ls.

Here we gave evidences for the efficiency of mini-CD40Ls in controlling parasitemia during experimental *Trypanosoma cruzi* infection in mice. CD40L mimetics decreased infection and enhanced survival of infected mice. This was explained by the impairment of immunosuppression induced by the pathogen. In particular, number of CD8⁺ T cells that express IFN γ was increased in infected mice treated with mini-CD40Ls. We suggested that this effect implies activation of dendritic cells. Moreover, a memory response was detected as a challenge infection with a different strain of parasite was totally abolished. Thus, mini-CD40Ls could sustain the T_H1 immune response that is normally inhibited by the parasite, and induce vaccination.

Our results, shared with collaborators from the Laboratoire d'Immunologie Expérimentale in Brussels, prove that mini-CD40Ls are applicable *in vivo*. They were effective in experimental infection with *Trypanosoma cruzi* and elicited an efficient immune response. We are currently investigating their efficiency in various mouse models of cancer immunotherapy.

Cutting edge: small molecule CD40 ligand mimetics promote control of parasitemia and enhance T cells producing IFN- γ during experimental *Trypanosoma cruzi* infection

Mohammed HABIB, Magali NOVAL RIVAS, Mustapha CHAMEKH, Sébastien WIECKOWSKI, Weimin SUN, Alberto BIANCO, Nathalie TROUCHE, Olivier CHALOIN, Hélène DUMORTIER, Michel GOLDMAN, Gilles GUICHARD, Sylvie FOURNEL, and Bernard VRAY

Journal of immunology, 2007, Vol. 178, Pages 6700 - 6704

Pages 215-219 :

La publication présentée ici dans la thèse est soumise à des droits détenus par un éditeur commercial.

Pour les utilisateurs ULP, il est possible de consulter cette publication sur le site de l'éditeur :

<http://www.jimmunol.org/cgi/content/full/178/11/6700?>

La version imprimée de cette thèse peut être consultée à la bibliothèque ou dans un autre établissement via une demande de prêt entre bibliothèques (PEB) auprès de nos services :

<http://www-sicd.u-strasbg.fr/services/peb/>

CONCLUSION AND PERSPECTIVES

CONCLUSION AND PERSPECTIVES

The CD40–CD40L interaction plays an essential role in development of both humoral and cellular immune responses. Importance of the CD40–CD40L duet has led many groups to use CD40–based therapeutics, to either inhibit or activate immune responses. Moreover, an interesting direct cytotoxic effect has been documented on CD40–positive malignant cells. We have proposed an original synthetic multivalent molecule that can act as functional ligand of CD40. CD40 and CD40L belong to the TNF-R and TNF superfamilies respectively. TNF family proteins self assemble in a C_3 symmetry, and form with their cognate receptors hexavalent complexes important for activation of intracellular signaling pathways.

On the basis of available three-dimensional data on the CD40–CD40L interaction, we have generated functional CD40L mimetics, named mini-CD40Ls, which respect the trimeric geometry of CD40L and present hot-spot residues important for the interaction with CD40.

We first described the design and synthesis of mini-CD40Ls, and established their function as mimetics of the natural soluble CD40L. We chose surface plasmon resonance (SPR) as the main method for analysis of mini-CD40Ls binding to recombinant CD40. This assay gave us precise informations on the kinetics rates for the mini-CD40L–CD40 interaction without the need to label our molecules. Using SPR, we proved that mini-CD40Ls inhibit the binding of recombinant soluble CD40L to CD40.

To easily assess biological activity of mini-CD40Ls, we used the natural property of B lymphoma to enter apoptosis after CD40 activation. We also tested mini-CD40Ls on the immature dendritic cell line D1 and could show that, whereas mini-CD40Ls were cytotoxic for CD40–positive B lymphoma and carcinoma cells, they induced maturation of dendritic cells. Moreover, mini-CD40Ls clearly activate the NF- κ B pathway and induce expression of *IL12 p40* mRNA in D1 cells.

The important question of the specificity of mini-CD40Ls toward CD40 has come early. We have now accumulated a large body of evidence supporting specificity of binding. First, we did not detect binding of mini-CD40Ls to various other members of the TNF-R family. Second, we showed that mini-CD40Ls bind to an epitope different than the anti-CD40 epitope on CD40, just as did recombinant soluble CD40L. Third, a biotin-labelled version of mini-CD40L was generated to show colocalization with CD40 at the cell surface. Importantly, the biotinylated mini-CD40L did not bind to CD40–negative cells. This was consistent with the inefficiency of mini-CD40Ls on CD40–negative leukemia T cells. Fourth, mini-CD40Ls that

CONCLUSION AND PERSPECTIVES

had residues mutated in the CD40-binding motif, known as hot-spot residues in the CD40-CD40L interaction, have completely lost their capacity to bind to CD40 and to induce biological effects. Fifth, mini-CD40Ls could act as inhibitors of the membrane-bound CD40L as demonstrated in the assay of expression of CD95 on lymphoma cells. And sixth, we have recently showed that mini-CD40Ls were not active in CD40-deficient mice in a model of parasite infection in mice.

Although these results highly suggest that effects of mini-CD40L are mediated by CD40, recent studies have demonstrated that CD40L binds to other molecules, as for example integrins. Moreover, there is no back knowledge on the physicochemical properties of molecules such as mini-CD40Ls.

We were not able to completely inhibit biotinylated-mini-CD40L staining with a recombinant soluble CD40 protein. But, as discussed later, interaction of mini-CD40Ls with soluble constructs of CD40 is not as efficient as with CD40 presented in a two dimensional lattice. Furthermore, many attempts to block expression of CD40 by small interfering RNAs were unsuccessful due to inefficiency of many conventional methods of transfection to lymphoma cells. To complete this study, future attempts will be performed using stringenter methods as i) nucleofection or infection, ii) cell penetrating peptides coupled to siRNA or to peptide nucleic acid antisense inhibitor, iii) penetration with carbon nanotubes, that have been developed by another team in our lab.

We also plan to test mini-CD40Ls on bone marrow-derived dendritic cells and on B lymphocytes produced from CD40-deficient mice. Antagonist anti-CD40 mAbs would be another solution, but its action on the CD40 structure should be first precisely defined to avoid any synergistic effect due to allosteric modifications. One could also imagine antagonism with a pre-ligand binding assembly domain-like molecule of CD40 that remains to be designed. Activity of mini-CD40Ls will be evaluated on cells transfected with CD40 and, for example on macrophages that were shown to up-regulate CD40 when exposed to inflammatory context. Finally, we envision to fish interaction partners of mini-CD40Ls by co-immunoprecipitation of the biotinylated mini-CD40L with streptavidin.

Another experiment gave us some insights into the mechanisms of activation of CD40 at the membrane. Staining of CD40-positive cells with biotinylated mini-CD40L was significantly reduced at 4 °C, suggesting that movements at the membrane may be essential

CONCLUSION AND PERSPECTIVES

for mini-CD40Ls interaction with its receptor. One could think that Brownian agitation within mini-CD40Ls or within the receptor protein, or cytoskeleton activity have an important role in the biological effects induced by mini-CD40Ls. But since lipid rafts have been demonstrated to clearly participate in the CD40-mediated cell signaling, it would be worth studying their implication in the mechanism of action of our CD40L mimetics. In particular, we could purify raft microdomains after incubation of cells in the presence of mini-CD40L and determine all the components of the signalosome. Molecules that disrupt membrane rafts should also be used. Colocalization experiments with rafts markers and biotinylated mini-CD40Ls are currently under investigation. Our molecules may thus represent interesting tools for studying at the membrane the complex mechanisms involved during activation of CD40.

Finally, we have shown that mini-CD40Ls are efficient on B lymphocytes in the presence of an anti-CD40 mAb. Two mechanisms may explain this phenomenon. Anti-CD40 mAb binds to an epitope different from the mini-CD40L-binding region on CD40. First, one can thus hypothesize that it induces some conformational changes within the CD40 protein that enhance binding and/or activation by mini-CD40Ls. Second, anti-CD40 mAb may induce oligomerization and clustering of the CD40 within membrane microdomains, what would potentiate the activity of mini-CD40Ls. The threshold of CD40 oligomerization required for activation of some cellular signaling could probably not be reached by our small CD40L mimetics.

To test this hypothesis, we have generated a dimeric form of mini-CD40L, consisting of two trimeric mini-CD40Ls covalently linked by a spacer arm. Preliminary results suggest that these hexameric mini-CD40Ls are more potent than the trimeric corresponding form. They induced significant proliferation of murine B cells without costimulation. Further investigations will also assess the efficiency of mini-CD40Ls presented on liposomes. Because mini-CD40Ls offer the advantage to be constructed and modulated as a Lego, they represent highly versatile unique tools for the elucidation of complex physicochemical mechanisms of CD40 activation that are not yet fully understood.

Optimization of mini-CD40Ls obtained from the structure/activity study has led to a better understanding of the molecular determinants that contribute to effector functions of mini-CD40Ls. Topology, structural folding, and presentation of the CD40-binding motif were improved, and we identified a second functional CD40-binding motif derived from the E

CONCLUSION AND PERSPECTIVES

β -strand of CD40L. This strategy is likely to be extended to other members of the TNF-R family. The next step of this project will be to propose mimetics of TRAIL (mini-TRAILS), a promising molecule to mediate powerful and selective anti-tumor responses.

The important question about the real binding stoichiometry of mini-CD40L to CD40 can be partially addressed with finding that monomeric, dimeric and tetrameric mini-CD40Ls are not or significantly less biologically active than the trimeric mini-CD40L. Surface plasmon resonance experiments gave some clues about the number of CD40 receptors bound per mini-CD40L molecule. It will be crucial to obtain consistent data on the interaction of mini-CD40Ls with membrane-bound CD40. We could use for example fluorescence correlation spectroscopy (FCS) to characterize the precise binding process of mini-CD40Ls to surface CD40 on living cells at the level of individual molecules.

The loss of cooperativity observed during interaction of some mimetics, containing a point mutation in the CD40-binding motif, with recombinant CD40 has been related to differential cellular effects. We propose to exploit such mutated CD40L mimetics to determine the steps required for a proper bioactivity. In particular, we will describe the requirement of raft microdomains, and the intracellular partners implicated in cell signaling induced by normal and such "non-cooperative" mini-CD40Ls. Further investigations will be required to document the non-cooperative effects of some mini-CD40Ls in various cellular systems and animal models. Since such molecules bind to CD40 but can not induce all biological effects of mini-CD40Ls based on native sequences, they may be used as inhibitors of the CD40-CD40L interaction and eventually for the treatment of autoimmune diseases or during transplantation.

Mini-CD40Ls are certainly very useful tools for dissecting the intracellular pathways initiated by CD40 activation in various cell types. The description of the engaged pathways is far from being completed and we will look for known pathways and search for unidentified signaling intermediates. To this end, the proteomic tools available in the institute, like 2D gel electrophoresis coupled to mass spectrometry, might prove useful. We will also try to identify by co-immunoprecipitation proteins localized in the activated signalosome, and transcription factors activated by mRNA microarrays and real-time PCR techniques.

CD40-transfected cells could serve to study the complex interactions taking place under the plasma membrane. For example, one could investigate differential TRAF

CONCLUSION AND PERSPECTIVES

recruitment to the cytoplasmic domain of CD40 and the downstream signaling pathways induced upon binding of mini-CD40Ls versus recombinant soluble CD40L, membrane-bound CD40L and anti-CD40 mAb. Interplay between pathways engaged by different receptors will be described to explain, for example, the synergy between mini-CD40Ls and IL-4 in proliferation of B cells.

Finally, we have demonstrated the efficiency of mini-CD40Ls *in vivo*. We provided evidences that our CD40L mimetics act on the immune system to counteract the immunosuppression induced by *Trypanosoma cruzi* parasite in mice. Direct cytotoxicity against malignant cells and activation of immune system suggest that mini-CD40L may have an important application in cancer immunotherapy. We are now developing two main models of cancer in mice (lymphoma and solid tumor models) to test and characterize any effects induced by mini-CD40Ls. These experiments are currently undertaken by a new PhD student in our team.

Should we identify mini-TRAILs, we could thus imagine the preparation of heterodimeric mini-ligands consisting of one mini-CD40L unit linked to a mini-TRAIL unit for a synergistic anti-tumor immunotherapy. The discovery of an inhibitory mini-CD40L will no doubt find an application in lupus therapy. Mini-CD40Ls might also have beneficial effects in many other diseases, and we are opened to any proposition for testing our molecules in diverse models. All fundamental experiments proposed here, and experiments in various other animal models will be necessary to increase our knowledge on mini-CD40Ls mode of action prior to their applications in primate models and hopefully in treatments of human diseases, in particular cancer, one of the principal causes of death in developed countries.

The CD40–CD40L interaction plays a central role in development of both humoral and cellular immune responses. CD40 belongs to the tumor necrosis factor receptor (TNF-R) family, and is constitutively expressed on B lymphocytes, dendritic cells and monocytes/macrophages. CD40L belongs to the TNF family, and is mainly expressed transiently on activated T lymphocytes. Proteins from the TNF-R/TNF superfamily assemble in a C_3 symmetry, forming hexavalent complexes that are important for transduction of intracellular cell signaling.

Many groups have used antibodies directed against CD40 and CD40L as therapeutics, to either inhibit or activate the immune system. Research on synthetic multivalent molecules that could act as ligands in complex biological systems is an innovating field in medicinal chemistry. On the basis of crystallographic data and directed mutagenesis experiments, we have developed synthetic molecules (mini-CD40Ls) built on synthetic C_3 platforms linked to the residues essential for interaction with CD40 via spacer arms.

The results obtained with mini-CD40Ls in various molecular and cellular systems suggested for the first time that small synthetic molecules could act as functional CD40L mimetics. A complete structure–activity study was performed on mini-CD40Ls to get detailed informations on their mechanisms of action and to optimize them. In particular, we found an interesting mini-CD40L mutant that has lost its cooperative effect in the interaction with CD40. Our data suggested that CD40 binding properties are important for effector functions. We then used mini-CD40Ls as valuable tool to dissect complex signaling pathways activated by CD40 in different cell systems. Finally, we demonstrated that mini-CD40Ls induce an efficient T immune response during experimental infection with *Trypanosoma cruzi* in mice.

Le couple CD40/CD40L joue un rôle central dans le système immunitaire. CD40 appartient à la famille des récepteurs au TNF (tumor necrosis factor), et est constitutivement exprimé par les lymphocytes B, les cellules dendritiques et les monocytes/macrophages. Son ligand, CD40L, est un membre de la famille du TNF qui est exprimé transitoirement sur les cellules T activées. Les protéines de la superfamille des TNF-R/TNF s'assemblent selon une symétrie C_3 , formant des complexes hexavalents importants pour la transduction des signaux intracellulaires.

Différents groupes ont utilisé des anticorps dirigés contre CD40 et CD40L à des fins thérapeutiques, dans le but d'inhiber ou d'activer la réponse immunitaire. La recherche de molécules multivalentes synthétiques agissant comme ligands dans des systèmes biologiques complexes représente aujourd'hui un domaine novateur de la chimie médicinale. Nous avons développé des molécules synthétiques, sur la base des données de cristallographie et d'expériences de mutagenèse dirigée, construites sur des plateformes synthétiques de symétrie C_3 sur lesquelles, par l'intermédiaire de bras espaceurs de longueur optimale, ont été greffés les résidus de CD40L essentiels à l'interaction avec son récepteur.

Les résultats que nous avons obtenus avec les mini-CD40Ls dans divers systèmes moléculaires et cellulaires suggèrent que de petites molécules synthétiques peuvent reproduire les effets biologiques de la protéine CD40L naturelle. Nous avons réalisé une étude complète de structure-fonction sur les mini-CD40Ls afin de préciser leurs mécanismes d'action et de les optimiser. En particulier, nous avons généré un mini-CD40L qui a perdu sa capacité d'interagir de manière coopérative avec CD40. Nos données suggèrent l'existence d'une relation entre les propriétés d'interaction au CD40 et les effets biologiques induits par les mini-CD40Ls. Nous avons utilisé les mini-CD40Ls pour décrire les voies de signalisation activées par CD40 dans différents systèmes cellulaires. Enfin, nous avons démontré que les mini-CD40Ls induisent une réponse T efficace dans un modèle d'infection expérimentale par *Trypanosoma cruzi* chez la souris.